Volume 55 September - October 1960 Number 6

Economic Geology

and the

Bulletin of the Society of Economic Geologists

CONTENTS

Supergene Alteration of Zinc and Lead Deposits in Limestone ..... *Taro Takahashi* 1083

The Chief Oxide-Burgin Area Discoveries, East Tintic District, Utah; A Case History. Pt. I. U. S. Geological Survey Studies and Exploration ..... *T. S. Lovering and H. T. Morris* 1116

Synthetic and Natural Phases in the System Au-Ag-Te. Pt. I ..... *N. L. Markham* 1148

Genetic Aspects of the Monazite and Columbium-Bearing Rutile Deposits in Northern Lemhi County, Idaho ..... *Alfred L. Anderson* 1179

Oxidation of Sulfide Ore Bodies. II. Oxidation Mechanisms of Sulfide Minerals at 25° C. ..... *Motoaki Sato* 1202

A New Geochemical Method for the Determination of Molybdenum in Soil and Rock ..... *J. Kent Perry* 1232

Intrusion and Ore Deposition in New Mexico ..... *Charles Banks Belt, Jr.* 1244

Residual Characteristics of Crystallates Genetically Associated with Ore Deposits ..... *J. H. Rattigan* 1272

A Bauxite Deposit in the Paleozoic of Leon, Spain ..... *M. Font-Altaba and J. Closas M.* 1285

Relationship Between the Stratigraphy and Petrography of Pottsville Sandstones and the Occurrence of High-Alumina Mercer Clay ..... *E. G. Williams* 1291

Scientific Communications:

Contact Printing of Drill Cores ..... *William C. Kelly* 1303

Reflectivity Measurements With a Hallimond Visual Microphotometer ..... *B. F. Leonard* 1306

Discussions:

Titanium Mineralogy of Certain Bauxites and Their Parent Materials ..... *James A. Hartman* 1313

The System Cu-Fe-S-O ..... *Hugh McKinstry* 1314

Reviews:

Short Reviews of New Russian Books ..... *C. F. Davidson* 1315

Geotektonische Forschungen, Heft 13. Die Kleintektonische Arbeitsweise unter besonderer Berücksichtigung ihrer Anwendung im deutschen Paläozoikum (Bruno Engels) 1316

The Sea Off Southern California (K. O. Emery) 1317

Subsurface Mapping (M. S. Bishop) 1317

Application de la Géologie aux Travaux de l'Ingénieur (J. Goguel) 1318

New Observations on the Ores of the Witwatersrand and Their Genetic Significance (P. Ramdohr) 1318

Books Received ..... *Roger L. Ames and John E. Cotton* 1319

Society of Economic Geologists 1323

Scientific Notes and News 1343

PUBLISHED SEMI-QUARTERLY

Eight Dollars Fifty Cents a Year, One Dollar Fifty Cents a Copy

THE ECONOMIC GEOLOGY PUBLISHING COMPANY

Printed by Lancaster Press, Inc., Prince and Lemon Streets, Lancaster, Pa.

Second-class postage paid at Lancaster, Pa.

Economic Geology

and the

Bulletin of the Society of Economic Geologists

Issued Semi-Quarterly (Jan.-Feb., Mar.-Apr., May, June-July, Aug., Sept.-Oct., Nov. and Dec.) and sent to subscribers on or about the following dates: February 1, March 15, May 1, June 15, August 1, September 15, November 1, December 15.

Manuscripts for publication should be sent to the Editor, **ALAN M. BATEMAN, at Yale University, Yale Station, New Haven, Conn.** It is requested that contributors exercise care in writing *scientific* and *proper names*. References to other publications should be in accordance with the forms used in the pages of this journal. The manuscript should be typewritten with double space lines and must be preceded by *a brief abstract*. Galley proof will be sent authors only where a request to this effect accompanies the manuscript, or when, in the editor's opinion, the subject matter is such as will require correction by the author.

Reviews should conform to the journal usage. Review Committee: The Editor, C. H. Behre, L. C. Graton, J. T. Singewald, Jr., J. Gilluly, A. F. Buddington, W. H. Newhouse.

Books and Pamphlets for review should be sent to the Editor.

Reprints. Contributors desiring reprints of their papers may obtain them by filling out the order slip which will be attached to the galley proof when it is sent to the author. Provided the order slip is received by the editor, *with the return of the proof*, 50 reprints without covers will be furnished without charge. Reprints of discussions and informal communications are not furnished free of charge except when they exceed four pages in length when 50 will be supplied without charge. Reprints of reviews are not supplied. Additional reprints will be furnished at approximately the rates given in the table below (effective with No. 5) when ordered *in advance of publication*. The rates apply only to plain text, with line engravings. Papers containing folded maps or plates will be more expensive.

The following rates do not include free carriage. *Postage or express must be paid by the author.*

	4 pp. 1–4	8 pp. 5–8	12 pp. 9–12	16 pp. 13–16	20 pp. 17–20	24 pp. 21–24	28 pp. 25–28	32 pp. 29–32	Covers
50 copies.....	$4.20	$6.65	$10.40	$10.85	$14.15	$16.25	$18.70	$19.95	$5.75
100 "	5.00	7.95	12.00	13.30	17.00	19.95	23.30	25.00	7.80
Additional copies per C.	1.70	2.55	4.20	5.00	5.85	7.50	9.15	10.00	3.75

For 500 copies deduct 5%; for 1000 copies or more deduct 10%. For more than 32 pages add cost per schedule to make total. Example: For 44 pages add cost for 32 pages and 12 pages. The 50 copy price is the minimum charge.

Covers: Standard covers are of the same style of type and paper as the cover of the journal, and bear the title of the article and name of its author. Special printing on cover is charged for at the cost of composition.

Plates are $4.20 for the first 50 if printed on one side, and $3.15 per "C" for additional's; printed on both sides, $6.30 for the first 50, and $4.70 per "C" for additional's.

Collotype plates are 8 cents each for each additional reprint over the 50 copies furnished free. Example: An extra 50 reprints containing one collotype plate would cost $4.00; 2 collotype plates, $8.00.

Note: For any reprints requiring additional composition or changes, either in text or cover, an extra charge will be made.

The retail prices of single reprints when available from the office of the Business Manager are as follows:

1–4 pp.	5–8 pp.	9–12 pp.	13–20 pp.	21–28 pp.
15c	20c	25c	30c	35c
29–36 pp.	**37–44 pp.**	**45–52 pp.**	**53–60 pp.**	**61–68 pp.**
40c	45c	50c	55c	60c

Subscriptions. The price of the journal to subscribers in the United States and its dependencies is $1.50 for a single copy, or $8.50 a year for eight numbers effective Jan. 1, 1960. To subscribers in Canada, Cuba, Mexico, Spain, and countries in Central and South America, except Dutch and French Guiana, the annual rate is $8.80; to other countries, $9.25. Students, U. S., $5.00; Canada, $5.30.

Forwarding. Subscribers wishing their journal to be forwarded to a new address should leave postage for that purpose with the Postmaster at their old address.

Missing numbers will be replaced without charge if claim is made within four weeks after the date of issue of the following number, provided that the neglect to receive them is not due to neglect to arrange for their forwarding.

Remittances should be made payable to the **ECONOMIC GEOLOGY PUBLISHING COMPANY**, and should be mailed to **M. M. LEIGHTON**, Business Manager, Urbana, Illinois, to whom also all **Business Communications** should be addressed.

Foreign Agents. The Technical Bookshop, Salisbury House, London Wall, London, E. C. 2, England, British Agents.

Indexed in the Industrial Arts Series.

LANCASTER PRESS, INC., LANCASTER, PA.

ECONOMIC GEOLOGY

AND THE

BULLETIN OF THE SOCIETY OF ECONOMIC GEOLOGISTS

EDITOR: ALAN MARA BATEMAN
Yale University, New Haven, Connecticut

BUSINESS EDITOR: MORRIS M. LEIGHTON
Illinois Geological Survey, Urbana, Illinois

ASSISTANT EDITORS

H. E. MCKINSTRY, *Harvard University*
M. LEROY JENSEN, *Yale University*
JOE W. PEOPLES, *Wesleyan University*
J. D. BATEMAN, Toronto, Ont.
R. H. JAHNS, *Pennsylvania State University, University Park*

ASSOCIATE EDITORS

D. F. HEWETT
U. S. Geological Survey, Menlo Park, Calif.

A. I. LEVORSEN
Tulsa, Okla.

B. S. BUTLER
University of Arizona, Tucson, Ariz.

W. E. WRATHER
Washington, D. C.

A. N. SAYRE
U. S. Geological Survey, Washington, D. C.

L. C. GRATON
Orange, Connecticut

E. S. MOORE
University of Toronto, Toronto, Can.

GEORGE W. MOREY
U. S. Geological Survey, Washington, D. C.

PER GEIJER
Djursholm, Sweden

P. F. FOURMARIER
Liège University, Liège, Belgium

M. S. KRISHNAN
Andhra University, Waltair, India

T. W. GEVERS
University of the Witwatersrand, Johannesburg, S. Africa

C. F. DAVIDSON
St. Andrews University, Fife, Scotland

J. A. BROGGI
Instituto Geologica, Lima, Peru

TAKEO WATANABE
University of Tokyo, Tokyo, Japan

KONRAD B. KRAUSKOPF
Stanford University, California

PAUL RAMDOHR
University of Heidelberg, Heidelberg, Germany

A SEMI-QUARTERLY JOURNAL PUBLISHED BY
THE ECONOMIC GEOLOGY PUBLISHING COMPANY

SOCIETY OF ECONOMIC GEOLOGISTS

THE PUBLICATIONS OF WHICH CONSTITUTE
A PART OF THIS JOURNAL

OFFICERS FOR 1960

DUNCAN R. DERRY, *President*
CHARLES F. PARK, *Vice President*

PHILIP J. SHENON, *President-Elect*
JOHN K. GUSTAFSON,
Vice President-Elect

HAROLD M. BANNERMAN, *Secretary*, U. S. Geological Survey, Washington 25, D. C.

JOSEPH T. SINGEWALD, JR., *Treasurer*, Johns Hopkins University, Baltimore 18, Maryland

Councilors

1960	*1961*	*1962*
PHILIP W. CHASE	VINCENT D. PERRY	S. WARREN HOBBS
ROBERT M. GARRELS	STANLEY DAVIDSON	LYMAN H. HART
EDWARD H. WISSER	DESMOND F. KIDD	VINCENT C. KELLEY

Regional Vice Presidents

A. PAUL GERHARD SOHNGE, Africa.....KINGSLEY CHARLES DUNHAM, Europe
LUIS SANTOS-YÑIGO, Asia.....J. RUBEN VELASCO, North America
HADDON F. KING, Australia.....ALBERTO BENAVIDES Q., South America

Executive Committee

DUNCAN R. DERBY, *Chmn.* JOSEPH L. GILLSON HAROLD M. BANNERMAN
CHARLES F. PARK PHILIP J. SHENON JOSEPH T. SINGEWALD, JR.

Standing Committees for 1960–61

Finance Committee

JOSEPH T. SINGEWALD, JR., *Chairman* OLAF N. ROVE J. K. GUSTAFSON

Program Policy Committee

CHARLES A. ANDERSON, *Chairman* CHARLES F. PARK, JR. J. K. GUSTAFSON
J. P. POLLOCK WESTON BOURRET

Program Committee

M. L. JENSEN, *Chairman* PAUL AVERITT F. G. SNYDER
JAMES P. POLLOCK H. E. HAWKES, JR. H. M. BANNERMAN, *ex officio*

Committee on Publications

DUNCAN R. DERRY, *Chairman* CHARLES A. ANDERSON R. H. JAHNS

Nominating Committee

D. F. KIDD, *Chairman* JAMES BOYD CARL TOLMAN

Admissions Committee

J. E. THOMSON, *Chairman* J. C. FRYE R. B. FULTON, III
CHARLES F. PARK, JR. ROBERT M. GARRELS

Auditing Committee

A. N. SAYRE, *Chairman* THOR KIILSGAARD

ECONOMIC GEOLOGY

AND THE

BULLETIN OF THE SOCIETY OF
ECONOMIC GEOLOGISTS

VOL. 55 SEPTEMBER–OCTOBER, 1960 NO. 6

SUPERGENE ALTERATION OF ZINC AND LEAD DEPOSITS IN LIMESTONE

TARO TAKAHASHI*

CONTENTS

	PAGE
Abstract	1084
Introduction	1084
Previous work	1085
Acknowledgments	1085
Field studies	1085
Goodsprings district, Nevada	1086
Upper Mississippi Valley district	1087
Southern Appalachian district	1088
Theoretical and experimental studies of the supergene zinc minerals	1089
Introduction	1089
Experimental study of the solubility curves	1090
Theoretical study of the solubility curves	1091
Solubility curve of smithsonite	1091
Solubility curve of hydrozincite	1093
Solubility curve of zinc hydroxide	1093
Solubility curves of the zinc silicates	1095
Application of the solubility curves	1095
Paragenesis	1095
Relation between smithsonite and hydrozincite in an arid environment	1096
Smithsonite, hydrozincite and zinc hydroxide in a humid environment	1097
Hemimorphite in a humid environment	1098
Willemite problem	1099
Theoretical study of the supergene lead minerals	1099
Cerussite	1100
Galena and anglesite	1101

* Present address: Department of Ceramic Research, College of Ceramics, State University of New York at Alfred University, Alfred, N. Y.

PAGE
Massicot ... 1101
Minium ... 1103
Plattnerite ... 1104
Wulfenite ... 1105
Wulfenite-Galena-Molybdenite ... 1105
Wulfenite-Cerussite-Molybdenite ... 1106
Cadmium minerals ... 1108
Sources of the minor elements in supergene facies ... 1112
Molybdenum ... 1112
Arsenic ... 1112
Vanadium ... 1112
Phosphorus ... 1113
Conclusions ... 1113
References ... 1114

ABSTRACT

An attempt is made here to describe occurrences and paragenetic sequences of the supergene zinc and lead minerals in three districts representing varying mean temperatures and humidities. The facts observed in field and laboratory are interpreted in the light of physical chemistry, assuming equilibrium conditions. The stability relationships between smithsonite, hydrozincite and zinc hydroxide are defined in terms of pH and total carbon dioxide concentrations in the aqueous solution system, or of the partial pressure of carbon dioxide in the dry system. The stability fields of hemimorphite and willemite are also discussed. The study explains the common occurrence of hydrozincite in arid regions, and the scarcity of this mineral in humid regions. The common occurrences of smithsonite and hemimorphite in the Southern Appalachian district, and the predominance of smithsonite over hydrozincite and hemimorphite in the Upper Mississippi Valley district can be explained by the pH of the ground waters and soils. The stability fields of supergene lead oxide minerals, wulfenite, cerussite, anglesite, and cadmium minerals are calculated in terms of pH, Eh and total sulfur concentration or total carbon dioxide concentration in solution. The paragenesis of the lead minerals and the mobilization of molybdate and cadmium ions are discussed. The results of the spectrochemical analyses indicate that molybdenum and arsenic in the supergene facies were derived from galena, whereas vanadium and phosphorus were derived from the limestones and shales.

INTRODUCTION

MANY studies of the oxidation products of primary sulfide deposits have been published, but relatively little has been said except on the basis of deductive reasoning to explain the observed features. The present study is an attempt to contrast different kinds of supergene alteration of primary zinc and lead minerals and to explain the observed contrasts on the basis of geochemical and physico-chemical grounds.

The field studies that serve as practical basis of this paper were made during the summers of 1954 and 1955 in the Goodsprings mining district of Nevada, the Upper Mississippi Valley zinc and lead district, and the Southern Appalachian zinc and lead district. More than seven hundred

specimens, collected from seventy-seven mines and prospects, were studied in the field and laboratory with special attention to paragenesis.

Most of the fundamental physico-chemical data measured at room temperature and pressure, such as free energies of formation and standard oxidation-reduction potentials, can be applied to such geological phenomena as weathering and sedimentation, assuming a state of equilibrium. In the present study, an attempt was made to explain the supergene processes by assuming such a state. It is hoped that ultimately such a theoretical approach, when combined with careful field studies, may make possible the detection of primary ore bodies below the surface and will also permit inferences as to the nature and grade of the primary ore.

Previous Work.—The supergene features produced by oxidation of sulfide ores have been considered by Blanchard, Boswell, Emmons, Locke and others, but their approaches have been mainly descriptive. The results have been applied especially to ores of copper, zinc, and lead. Recently, Garrels and his co-workers applied physico-chemical reasoning to the interpretation of the supergene minerals of copper, zinc, lead, and uranium; they defined stability fields of various supergene minerals in terms of Eh (oxidation-reduction potential) and pH. The present study is intended to extend this pioneering work to the supergene minerals of zinc, lead, and other associated minor elements in order to account for observations made by the author and others.

Acknowledgments.—The writer is greatly indebted to Professor C. H. Behre, Jr., of Columbia University for valuable and stimulating supervision in the field and laboratory. Thanks are also due to Professors P. F. Kerr and J. Lawrence Kulp of Columbia University, and to Dr. P. B. Barton, Jr., of the United States Geological Survey for their criticisms and suggestions in various phases of this study, Professor T. I. Taylor of the Chemistry Department, Columbia University on the techniques of chemical analyses. Messrs. J. J. Durek, A. J. Silverman and B. E. Felber were of much assistance to the writer in the field and laboratory.

The advice and counsel of Dr. C. R. L. Oder of the American Zinc Company; Dr. W. Horatio Brown, Messrs. R. W. Metsger and Howard Miller of the New Jersey Zinc Company; Dr. A. F. Agnew of the United States Geological Survey, then at Platteville, Wis.; and Mr. Edward Jennings of the Universal Exploration Company are deeply appreciated.

Field and laboratory work were financed from the Higgins Fund, a Lamont Geological Grant, and funds from the Ore Genesis Laboratory of Columbia University. The writer is especially grateful to the late Mr. J. P. Royston and to Mrs. Royston of Bridgeport, Conn., for their financial support and kind encouragement.

FIELD STUDIES

A significant difference in mineralogy between the oxidized zinc and lead deposits in the western United States and those in the eastern United States

has been noted by many earlier workers. In the present study, the Goodsprings mining district, Nevada, was studied as a source of typical cases of supergene alteration in an arid climate. In contrast, the Southern Appalachian and Upper Mississippi Valley districts were studied as representatives of more humid climate—the first warm, the second much cooler.

The Goodsprings District, Nevada

The Goodsprings district is about 30 miles west of Las Vegas, Nevada. The mean annual precipitation and temperature recorded at Las Vegas during the years between 1921 and 1950 are 4.35 inches and 66.8° F respectively.

The ore deposits in this district were mined for gold, copper, zinc, and lead, with accessory vanadium. The zinc and lead deposits on which this study is focussed occur in lower Mississippian limestones and dolomites. The detailed descriptions of geology and mineralogy have been published elsewhere (3, 4, 5, 17, 30).

The following twenty-two zinc-lead mines were investigated: Accident, Anchor, Bullion, Frederickson, Green Monster, Hoodoo, Hoosier, Kirby, Milford No. 1, Milford No. 3, Mobile, Monte Cristo, Potosi, Root, Ruth, Shenandoah, Singer-Tiffin, Smithsonite, Sultan, South Whale, Whale and Yellow Pine mines. About two hundred specimens from those mines were studied. The following minerals were identified by means of optical, chemical, X-ray, and differential thermal methods: smithsonite, hydrozincite, hemimorphite, willemite, sphalerite, anglesite, cerussite, plattnerite, wulfenite, mimetite, pyromorphite, galena, plumbojarosite, descloizite, vanadinite, greenockite, jarosite, alunite, limonite, gypsum, calcite and quartz. The paragenetic sequence of the supergene minerals was studied under the petrographic and binocular microscopes with the aid of microchemical analysis and ultra-violet light. The results of the field and laboratory studies are summarized as follows:

1) With the exception of galena, the sulfide minerals of all but a few deposits have been completely altered to secondary minerals, down to the greatest depths so far explored. Galena has been entirely oxidized to cerussite in the zone of most intense weathering, but is generally stable at depth;

2) The most abundant minerals of economic importance are probably hydrozincite, smithsonite, and galena;

3) The paragenetic sequence of the supergene minerals of zinc, lead and other elements is schematically shown in Table 1. It, however, must be noted that the diagram for the zinc minerals bears no relation to that for the lead minerals, the greenockite, or the gangue minerals. Among the zinc minerals, smithsonite is earliest, hydrozincite is next, and hemimorphite is latest;

4) Hydrozincite is the most abundant zinc mineral in most of the mines, and tends to decrease with depth;

5) Smithsonite and hemimorphite are distributed widely, and appear to increase with depth;

TABLE 1

PARAGENETIC SEQUENCE OF THE SUPERGENE MINERALS IN THE GOODSPRINGS DISTRICT, NEVADA

6) Willemite occurs in the Singer-Tiffin mine. It was first detected by ultra-violet light in the mine, and was identified by X-ray and optical methods. Its origin appears to be supergene because of (a) its close association with hemimorphite and limonite, (b) its occurrences in the faults which are probably post-sulfide, and (c) its uncorroded hexagonal prisms;

7) Cerussite is the most abundant lead mineral, whereas anglesite is rare;

8) The occurrence of plattnerite indicates a highly oxidizing environment. It was identified by X-ray and micro-chemical methods;

9) Wulfenite occurs in two ways: as inclusions in oxidizing galena crystals, and as fracture fillings in the country rocks near ore bodies;

10) Greenockite occurs in a few mines such as the Potosi and Green Monster, where sphalerite has still resisted oxidation.

The Upper Mississippi Valley District

The Upper Mississippi Valley zinc and lead mining district comprises southern Wisconsin and adjacent parts of Iowa and Illinois. The mean annual precipitation and temperature during the period 1921–1950 are 32.85 inches and 47.0° F respectively.

Most of the ore bodies are in the Middle Ordovician Platteville, Decorah, and Galena formations, which are limestones, dolomites, and shales with local cherty beds. The detailed descriptions of geology and mineralogy have been published elsewhere (1, 2, 6, 7, 8, 18, 30).

The following twenty-seven major zinc-lead mines and prospects were investigated; Beadle, Brugh, East and West Locky, Hill and 8th Street, Ewing (Dubuque Co., Iowa); Boyle-Hardy, De Rocher, James, Little Giant, Helena-Roachdale, Champion, Old and New Ida Blends, Big Dick, Frontier (Lafayette Co., Wisconsin); Barreltown, B. Pierson, Clarke, Eberle, Centerville, Imhoff, Linden, Williams (Iowa Co., Wisconsin); Piquette, and McBerney (Grant Co., Wisconsin). At a majority of the mines and prospects visited, the underground workings were not accessible. The results of the

study of more than three hundred specimens of oxidized ores are summarized as follows:

1) Smithsonite is the predominant supergene zinc mineral throughout the district and is the earliest supergene zinc mineral in the paragenetic sequence, as schematically shown in Table 2.

TABLE 2

PARAGENETIC SEQUENCE OF THE SUPERGENE MINERALS IN THE UPPER MISSISSIPPI VALLEY DISTRICT

	Early ← → Late
Anglesite	
Cerussite	
Pyromorphite	
Smithsonite	
Hydrozincite	
Hemimorphite	
Greenockite	

2) Smithsonite is in many instances deposited on sphalerite, and smithsonite pseudomorphous after sphalerite is observed. These facts indicate that smithsonite may be formed in the acid environment that may prevail around oxidizing sphalerite because of the formation of sulfuric acid;

3) Hydrozincite and hemimorphite are scarce throughout the district;

4) Cerussite is the most common supergene lead mineral;

5) The following supergene minerals were identified by optical, chemical and X-ray methods: smithsonite, hydrozincite, hemimorphite, cerussite, pyromorphite, greenockite, erythrite, aurichalcite, gypsum, and limonite. It is readily recognized that the mineral associations are much simpler than those in the Goodsprings district. No molybdenum, arsenic, and vanadium minerals have been reported.

The Southern Appalachian District

The Southern Appalachian zinc-lead mining district includes eastern Tennessee and adjacent part of Virginia in the Great Valley region. The primary ores of zinc and lead of commercial importance are almost wholly confined to the Shady dolomite, Maynardville limestone, and Kingsport formation of the Knox group. Detailed studies of the geology and mineralogy are published elsewhere (9, 10, 11, 12, 23, 25, 26, 28, 30).

Weathering in this district is characterized by the formation of bright red soil because of oxidation and hydration of iron, and by the strong leaching of carbonate and other soluble materials from the soil because of the heavy rainfall and relatively high temperatures. The mean annual precipitation and temperature recorded at Knoxville, Tenn., during the period 1921–1950 are 45.5 inches and 59.3° F respectively.

The following thirty major zinc-lead mines and prospects were visited: Austinville, Bertha, Ivanhoe (Wythe Co., Va.); Allisonia, McAllister (Allisona Co., Va.); Arcadia (Scott Co., Va.); Davis, Grasselli, Jarnigan, Mossey Creek (Jefferson Co., Tenn.); Mascot (Knox Co., Tenn.); Brown-Tipton (Greene Co., Tenn.); Straight Creek, Bunch Hollow, Ritchie (Claiborne

Co., Tenn.); New Prospect, Eli Goin (Union Co., Tenn.); Shilo (Hancock Co., Tenn.); Scott Burton (Carter Co., Tenn.); Sweetwater (Monroe Co., Tenn.); and Embreeville (Washington and Unicoi Co., Tenn.). More than two hundred and fifty specimens were collected, and their mineralogy and paragenesis were studied in the field and laboratory. In most of the mines, the deposits have been mined out, and the once prominent high grade supergene ores are rarely seen. This unfortunately made it impossible to estimate the relative abundances of smithsonite and hemimorphite. The results of the study are summarized as follows:

1) Smithsonite and hemimorphite are the principal supergene zinc minerals, and hydrozincite is rare.

2) The paragenetic sequence of the oxidized zinc minerals from oldest to youngest is smithsonite-hydrozincite-hemimorphite. However, a few specimens indicated the earliest formation of hemimorphite. The generalized sequence is schematically shown in Table 3.

TABLE 3

PARAGENETIC SEQUENCE OF THE SUPERGENE MINERALS IN THE SOUTHERN APPALACHIAN DISTRICT

3) Cerussite is widely distributed, but is insignificant in its amount, except in the Embreeville area. Anglesite is rare.

4) Greenockite is widely distributed, being closely associated with oxidizing sphalerite.

5) The assemblage of the supergene minerals is simple; smithsonite, hydrozincite, hemimorphite, cerussite, anglesite, greenockite and gypsum were identified by optical, chemical, and X-ray methods. No molybdenum, arsenic, and vanadium minerals have been reported.

THEORETICAL AND EXPERIMENTAL STUDIES OF THE SUPERGENE ZINC MINERALS

Introduction

The stability fields for sphalerite and smithsonite in terms of pH and Eh were previously calculated by Garrels (15), who assumed the total carbon dioxide concentration in solution to be 0.03 mole/l (saturation with the atmospheric carbon dioxide under 1 atm at 25° C in distilled water) and the total sulfur in solution to be 0.1 mole/l at 25° C under one atmosphere. The purpose of the present study is to explore more details of the stability fields of supergene zinc minerals within the smithsonite field calculated by Garrels. The factors involved in the formation of the most common supergene zinc minerals, smithsonite, hemimorphite, and hydrozincite, are pH,

total carbon dioxide in solution (or partial pressure of carbon dioxide), concentration of silica, temperature, and pressure. Eh (oxidation-reduction potential) is not related to the stability boundaries between these minerals, since there is no change in the valence of the elements involved during the formation of these minerals. In supergene conditions, temperature and pressure may be assumed to be constant, 25° C and 1 atm., and therefore the pH, carbon dioxide concentration, partial pressure of carbon dioxide, and silica concentration in solution are considered to be the most important factors. The absence of the thermodynamic data of the various forms of Si-O radical made it impossible to determine the stability fields of zinc silicate minerals. However, the stability fields of smithsonite and hydrozincite, and the probable maximum field of hemimorphite were determined in terms of pH and total carbon dioxide in solution.

Experimental Procedure.—The solubilities of smithsonite, hydrozincite, hemimorphite, and willemite were measured in solutions with different pH and under one atmosphere of total pressure. The samples used for the study were as follows:

Smithsonite,	creamy color,	Morning Star mine,	Rush, Arkansas.
Hydrozincite,	snow white,	Yellow Pine mine,	Goodsprings, Nevada.
Hemimorphite,	transparent,	Sterling Hill mine,	New Jersey.
Willemite,	pale green,	Franklin mine,	New Jersey.

Two grams of powdered mineral were ground in a porcelain mortar, and put in a 200 ml buffer solution. Sodium acetate-acetic acid buffer solutions (0.01–0.03 mole/l) were used as solvent in a pH range between 4 and 6.5, and sodium bicarbonate-sodium carbonate buffer solutions (0.005–0.02mole/l) were used in a range of pH above 6.5. During the solubility measurement of smithsonite and hydrozincite, the partial pressure of carbon dioxide over the solution was controlled to maintain the concentration of total carbon dioxide in solution constant. At pH 5.5, the partial pressure of carbon dioxide over the solution is to be 1.0 atm. to maintain the total carbon dioxide in solution at 0.03 mole/l. This condition can be satisfied by flushing pure carbon dioxide gas over the solution under one atmosphere pressure. At pH above 5.5, the partial pressure of carbon dioxide is to be less than one atmosphere (at pH = 7, P_{CO_2} = 0.05 atm.; at pH = 8, P_{CO_2} = 0.005 atm.) to maintain the total carbon dioxide in solution at 0.03 mole/l. To control the partial pressure of carbon dioxide in this range of pressure, several nitrogen-carbon dioxide mixtures which have desired partial pressures of carbon dioxide were prepared and flushed over the solution. For the silicate minerals, a solution that was saturated with silica by immersing powdered silica gel for a week previous to the solubility measurement was used as solvent.

To examine an equilibrium between a powdered mineral and solution, 2 ml samples were taken for zinc analysis at regular time intervals. The zinc concentration in the 2 ml samples was analyzed by means of the polarograph. A Sargent-Heyrovsky photographic recording unit was used, and calibrated for zinc concentrations between 10^{-1} and $10^{-5.5}$ mole/l with

an accuracy of ±5%. The pH of the solutions was measured with a Beckman Model G pH meter, whenever the 2 ml samples were taken. Smithsonite attained equilibrium with the solutions within two or three weeks, and hydrozincite reached equilibrium within a few days. About three weeks were necessary for hemimorphite and willemite to attain equilibrium. Precipitation and dissolution curves were established for smithsonite and hydrozincite to demonstrate the equilibrium (30). The precipitation curves for hemimorphite and willemite could not be obtained because of the slow rate of reaction of silica. The results of the solubility measurement are listed in Table 4, and are plotted in a pH-zinc concentration diagram (Fig. 1).

TABLE 4

SOLUBILITIES OF SMITHSONITE, HYDROZINCITE, HEMIMORPHITE AND WILLEMITE

pH	Solubility (Zn mole/l)
Solubility of Smithsonite in Solutions Containing 0.03 mole/l CO_3 at 25° C, 1 atm.	
5.9	1.47×10^{-3}
6.4	2.8×10^{-4}
7.3	2.0×10^{-5}
8.3	2×10^{-6}
Solubility of Hydrozincite in Solutions Containing 0.03 mole/l CO_3 at 25° C, 1 atm.	
5.5	2.40×10^{-2}
6.4	1.75×10^{-3}
6.7	5.3×10^{-4}
6.9	3.0×10^{-4}
8.1	6×10^{-6}
Solubility of Hemimorphite in Solutions at 25° C, 1 atm.	
4.70	2.60×10^{-2}
5.25	4.40×10^{-3}
6.30	5.1×10^{-4}
6.85	1.8×10^{-4}
6.98	1.6×10^{-4}
Solubility of Willemite in Solution at 25° C, 1 atm.	
4.05	3.50×10^{-2}
4.80	5.70×10^{-3}
4.95	5.10×10^{-3}
5.60	1.10×10^{-3}
6.50	1.2×10^{-4}
7.05	6.8×10^{-5}

Theoretical Study of the Solubility Curves

Solubility Curve of Smithsonite.—Among the supergene zinc minerals, smithsonite is the only mineral of which the thermodynamic data are known in detail. When smithsonite is dissolved in solution, the total zinc concentration in solution is not only a function of the simple zinc ion, but also of undissociated zinc carbonate and various zinc complex ions. However, of these only $Zn(OH)^+$ is significant, and the concentrations of the undissociated carbonate and other complex ions are negligibly small compared with the concentration of Zn^{++} in a pH range between 5 and 10.

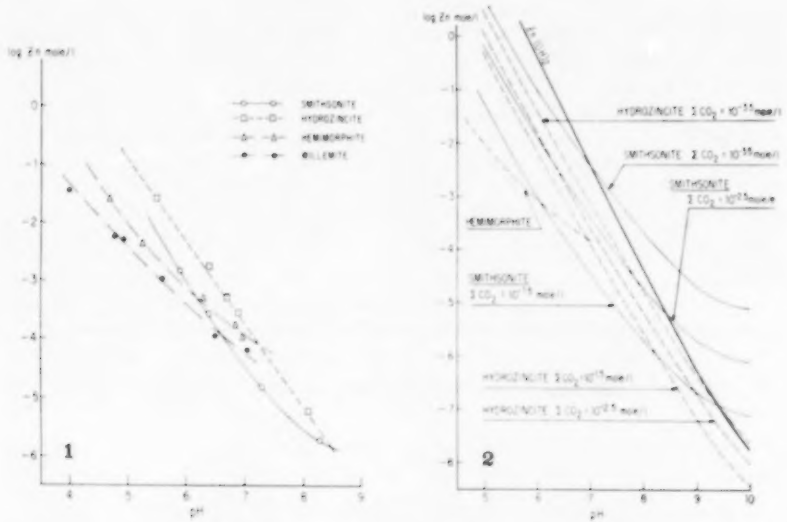

FIG. 1. Solubility curves of smithsonite, hydrozincite, hemimorphite and willemite in solutions containing 0.03 mole/l carbon dioxide, at 25° C and 1 atm.

FIG. 2. Solubility curves of smithsonite, hydrozincite, and zinc hydroxide as calculated from the thermodynamic data.

The dissociation of smithsonite is (21, p. 171):

$$ZnCO_3 = Zn^{++} + CO_3^{=}, \quad K = a_{Zn^{++}} \cdot a_{CO_3^{=}} = 10^{-9.7}. \tag{1}$$

If the activity of carbonate ion is known, the activity of the zinc ion can be calculated by use of Equation (1).

Let the total carbon dioxide content in solution be 10^p mole/l. In a dilute solution, the total carbon dioxide in solution is approximately equal to summation of the activities of undissociated carbonic acid, bicarbonate ion and carbonate ion:

$$a_{H_2CO_3} + a_{HCO_3^-} + a_{CO_3^{=}} = 10^p. \tag{2}$$

The first and second dissociation constants are (21, p. 135):

$$a_{HCO_3^-} \cdot a_{H^+} / a_{H_2CO_3} = 10^{-6.5}, \tag{3}$$

$$a_{CO_3^{=}} \cdot a_{H^+} / a_{HCO_3^-} = 10^{-10.5}. \tag{4}$$

Substituting Equations (3) and (4) in Equation (2), the activity of the carbonate ion can be calculated:

$$a_{CO_3^{=}} = 10^p / (1 + a_{H^+} \cdot 10^{10.5} + a^2_{H^+} \cdot 10^{17}). \tag{5}$$

Substituting Equation (5) in Equation (1), the activities of zinc ion in solutions at different pH and total carbon dioxide concentrations can be calculated:

$$\log a_{Zn^{++}} = -(9.7 + p) + \log (1 + a_{H^+} \cdot 10^{10.6} + a^2_{H^+} \cdot 10^{17}). \quad (6)$$

The relation between zinc ion and the most important zinc complex, $Zn(OH)^+$, is (Latimer, p. 170):

$$\begin{gathered} Zn(OH)^+ + H^+ = Zn^{++} + H_2O, \quad K = 10^{9.61}, \\ \log a_{Zn(OH)^+} = -9.61 + \log a_{Zn^{++}} + pH. \end{gathered} \quad (7)$$

In dilute solutions, a summation of the activities of zinc ion and the complex ion is considered to be approximately equal to the solubility of smithsonite. When a solution is saturated with carbon dioxide at 25° C under one atmosphere, the p in Equation (6) is equal to -1.5. The solubilities thus calculated at different pH values are plotted in Figure 2. The theoretical solubilities agree with the measured solubilities within tolerance of experimental errors and activity coefficient which has been assumed to be unity. This agreement indicates that an extrapolation of the solubility curves for different total carbon dioxide concentrations in solutions can be safely made by the similar calculations. The results of the calculations for the solubilities in solutions with $p = -2.5$, and -3.5 (0.03 and 0.003 mole/l CO_2 respectively) are plotted in Figure 2.

Solubility of Zinc Hydroxide.—The solubility curve of zinc hydroxide can be calculated by a similar method employed in the smithsonite solubilities. Although no solubility measurement was made in the present study, the calculated values are considered to be reliable within the accuracy required. The dissociation of zinc hydroxide is expressed as (21, p. 168):

$$Zn(OH)_2 = Zn^{++} + 2OH^-, \quad K = 10^{-16.35}.$$

Assuming the activity of zinc hydroxide to be unity,

$$\log a_{Zn^{++}} = 11.65 - 2pH. \quad (8)$$

The activity of $Zn(OH)^+$ complex can be calculated by Equation (7). In dilute solutions, ignoring undissociated zinc hydroxide, the summation of these activities is considered to be approximately equal to the solubility of zinc hydroxide. The results of the calculation are plotted in Figure 2. It is obvious that the solubility of zinc hydroxide is not related to the total carbon dioxide in solution, but is a function of pH.

Solubility Curve of Hydrozincite.—Based on the solubility curve in Figure 4, the free energy of formation of hydrozincite can be calculated, and then the solubility curves of hydrozincite in solutions containing different amounts of carbon dioxide can be calculated. The dissociation of hydrozincite in solution may be expressed by the following formula:

$$2ZnCO_3 \cdot 3Zn(OH)_2 = 5Zn^{++} + 2CO_3^{=} + 6OH^-,$$

$$K = \frac{a^5_{Zn^{++}} \cdot a^2_{CO_3^{=}} \cdot a^6_{OH^-}}{a_{\text{hydrozincite}}}.$$

Assuming the activity of hydrozincite to be unity,

$$K = a^5_{Zn^{++}} \cdot a^2_{CO_3^{--}} \cdot a^6_{OH^-}. \quad (9)$$

Assuming that the activities of zinc and its complex ions are approximately the same as to concentration, the relation between the total zinc concentration and the activities is expressed by Equation (10):

$$\tfrac{1}{5} C_{Zn} = a_{Zn^{++}} + a_{Zn(OH)^+}. \quad (10)$$

Substituting (7) in (10), the activity of zinc ions can be calculated by Equation (11) by measuring the total zinc concentration and hydrogen ion activity:

$$a_{Zn^{++}} = \frac{C_{Zn}}{5} (1 + 10^{-9.61} \cdot a^{-1}_{H^+}). \quad (11)$$

The activity of hydrogen ion can be measured by a pH meter. The total zinc concentration can be measured by means of the polarograph. Therefore, the activity of zinc ion can be calculated, and the results are listed in Table 4. Further, the activity of carbonate ions can be calculated by Equation (5) at 25° C and under 1 atm. as $p = -1.5$. Thus, all of the three activities which are necessary for calculating the equilibrium constant for the dissociation of hydrozincite can be obtained. Substituting these activities in Equation (9), the equilibrium constant is calculated by assuming the activity of hydrozincite is unity. The average value of three measurements at different pH is $10^{-75.8}$ (Table 5):

TABLE 5

EQUILIBRIUM CONSTANT FOR DISSOCIATION OF HYDROZINCITE

pH	log aZn^{++}	log K	
5.5	−2.2	−76.9	Ave.
6.0	−2.8	−75.4	−75.8
7.0	−4.5	−75.0	

The free energy of formation of hydrozincite can also be calculated out by using this equilibrium constant. For the dissociation of hydrozincite,

$$\Delta f^0 = -1.364 \log K,$$
$$= 103.4 \text{ kcal/mole};$$

therefore, the free energy of formation of hydrozincite is,

$$\Delta F^0_{hyz} = 5\Delta F^0_{Zn^{++}} + 2\Delta F^0_{CO_3^{--}} + 6\Delta F^0_{OH^-} - 103.4$$
$$= -757.3 \pm 1 \text{ kcal/mole}.$$

Substituting for the activity of carbonate ion and the equilibrium constant in Equation (9), the activity of zinc ion can be calculated by knowing pH:

$$\log a_{Zn^{++}} = \tfrac{1}{5}\{8 - 6\,pH + 2 \log 10^{-p}(1 + a_{H^+} \cdot 10^{10.5} + a^2_{H^+} \cdot 10^{17})\}. \quad (12)$$

Substituting Equation (12) in Equation (11), the solubilities of hydrozincite in solutions with different pH and total carbon dioxide concentrations can be calculated. The results of the calculations are plotted in Figure 2.

Solubility Curves of the Zinc Silicates.—The dissociation of hemimorphite and willemite in solution may be expressed by the following formulae:

$$Zn_4(Si_2O_7)(OH)_2 \cdot H_2O = 4Zn^{++} + Si_2O_7^{-6} + 2OH^- + H_2O,$$
$$\log K = 4 \log a_{Zn^{++}} + \log a_{Si_2O_7^{-6}} + 2 \log a_{OH^-} + \log a_{H_2O};$$

and

$$Zn_2SiO_4 = 2Zn^{++} + SiO_4^{-4},$$
$$\log K = 2 \log a_{Zn^{++}} + \log a_{SiO_4^{-4}}.$$

It is unfortunate that the thermodynamic data for these Si-O radicals and a reliable analytical technique for these have not been known. This absence of the basic data made it impossible to calculate the equilibrium constants for those reactions. Accordingly, the solubility curves in terms of pH and the concentration of a Si-O radical cannot be determined. The determination of the thermodynamic data for the Si-O radicals is greatly needed for the study of the silicate minerals.

Applications of the Solubility Curves

Paragenesis.—It is well known that, under equilibrium conditions, the least soluble mineral starts to precipitate from solution first and the most soluble mineral last, when a solution is gradually concentrated.

As shown in Figure 2, in solutions saturated with atmospheric carbon dioxide at 25° C, hemimorphite is least soluble in a pH range of less than 6.2. In a few specimens from the Grasselli and Mossy Creek mines, Tenn., hemimorphite was found to be the earliest supergene mineral, being coated with smithsonite. This hemimorphite is interpreted to have been formed in a pH range of less than 6.2. Although hemimorphite is not commonly observed as the earliest supergene zinc mineral in the paragenetic sequence, it may be explained in three ways:

1) In a limestone region, acid solutions that were formed by the oxidation of sulfide minerals may be readily neutralized, and solutions with a pH of less than 6.2 may be uncommon.

2) When ground water circulates sufficiently well, the zinc sulfate concentration in the water may be so low that it may not have a pH less than 6.2, recalling that the pH of 0.1 mole/l $ZnSO_4$ is about 5, and that of 0.01 mole/l $ZnSO_4$ is about 5.8. If sphalerite alone is being oxidized slowly, a pH of less than 6.2 may not be actually attained around the sphalerite.

3) In strongly acid solutions, hemimorphite is relatively soluble. Thus, at pH = 3, the solubility is about 0.1 mole/l Zn. The mineral may therefore readily be leached away.

In solutions with a pH between 6.2 and 8.1, smithsonite is the least soluble mineral. In most of natural waters that have a pH between 6 and 8,

therefore, smithsonite is least soluble. Thus, its first formation in the paragenetic sequence and also its common occurrences are explained.

Hemimorphite is more soluble than smithsonite in this pH range, 6.2–6.8, but is less soluble than hydrozincite. Although hemimorphite should start to precipitate earlier than hydrozincite in this pH range, only a few specimens clearly indicating this sequence were observed. This is probably due to the slow rate of reaction of silica and zinc ions. Intimate mixtures of hemimorphite and hydrozincite, while relatively commonly observed in the specimens from the Goodsprings district were probably formed in this pH range.

In solutions with a pH of more than 6.8, hydrozincite is less soluble than hemimorphite, and is more soluble than smithsonite. This sequence of solubilities coincides with the most common paragenetic sequence of the three minerals observed in the districts investigated. Considering that the ground water in limestone regions has a pH between 7 and 8, this sequence in the solubilities appears to explain the most common paragenetic sequence of the zinc minerals.

Relation between Smithsonite and Hydrozincite in an Arid Environment.— In the arid climate of the Goodsprings district, Nevada, hydrozincite is the most common supergene zinc mineral. The present water table is very deep and has not been reached by mining. In such a dry environment, the following formula may be valid:

$$5ZnCO_3 + 3H_2O(g) \rightleftharpoons 2ZnCO_3 \cdot 3Zn(OH)_2 + 3CO_2(g).$$

The equilibrium constant for this reaction can be calculated from the free energies of formation of the individuals:

$$\Delta F^0 = -2.2 \text{ kcal},$$
$$\log K = \Delta F^0/1.364 = 1.61.$$

Assuming that (fugacity of smithsonite)^5/(fugacity of hydrozincite) is unity, the partial pressure of carbon dioxide at equilibrium can be calculated by knowing the partial pressure of water vapor:

$$\log P_{CO_2} = \tfrac{1}{3}(\log K + 3 \log P_{H_2O}).$$

At 25° C, the partial pressure of water is 0.0313 ($10^{-1.51}$) atm.; therefore,

$$P_{CO_2} = 10^{-0.99} \text{ atm.}$$

In the same way,

at 15° C, $\log P_{H_2O} = -1.78$; $P_{CO_2} = 10^{-1.24}$ atm.:
at 40° C, $\log P_{H_2O} = -1.14$; $P_{CO_2} = 10^{-0.60}$ atm.

If the partial pressure of carbon dioxide is lower than these values at the respective temperatures, the reaction would be driven to the right. The partial pressure of carbon dioxide in air is in a range of 10^{-3} to 10^{-4} atm. Considering the minimum humidity in the Goodsprings district to be 10%

at 40° C, this range is far below the partial pressure of carbon dioxide at equilibrium. Therefore, the reaction is driven to the right, and hydrozincite is more stable than smithsonite. In depth, carbon dioxide gas may less easily escape because of the slow rate of diffusion and its entrapment in the interstices between minerals. Under such conditions, the carbon dioxide partial pressure may exceed the equilibrium value, and consequently, the reaction is driven to the left, and the smithsonite becomes more stable. Thus, the increase of smithsonite with depth, so common in the Goodsprings district, is explained.

In humid regions, hydrozincite occurs as thin coating on rock surfaces exposed to the air, but it does not occur as masses under the ground water table. This also indicates that hydrozincite is formed when carbon dioxide can freely escape.

In contrast to hydrozincite, zinc hydroxide has never been reported in the Goodsprings district or elsewhere. The explanation of its absence can be obtained by studying the following equation:

$$2ZnCO_3 \cdot 3Zn(OH)_2 + 2H_2O(g) = 5Zn(OH)_2 + 2CO_2(g).$$

The equilibrium constant for this reaction can be calculated from the free energies of formation of the reactants and products:

$$\Delta F^0 = 15.1 \text{ kcal}, \quad \log K = -15.1/1.364 = 11.1.$$

Assuming (fugacity of hydrozincite)/(fugacity of zinc hydroxide)^5, to be unity, the partial pressures of carbon dioxide at the equilibrium can be calculated at given temperatures. At 15°, 25° and 40° C, the partial pressures of carbon dioxide at the equilibrium are $10^{-7.3}$, $10^{-7.0}$ and $10^{-6.6}$ atm. respectively. These carbon dioxide partial pressures are below the atmospheric carbon dioxide partial pressure. Consequently, in air this reaction is driven to the left in favor of hydrozincite, and zinc hydroxide is thermodynamically unstable. Thus the absence of zinc hydroxide in nature is explained.

Smithsonite, Hydrozincite and Zinc Hydroxide in a Humid Environment.— Of two minerals that are chemically similar and can be precipitated from the same solution, the more soluble mineral is dissolved and precipitated from a solution in the less soluble form. Put differently, the least soluble mineral is the most stable one. Based on this principle, the stability relationship between smithsonite, hydrozincite, and zinc hydroxide can be determined. The solubility curves shown in Figure 2 are used to determine the least soluble mineral in respect to the pH and total carbon dioxide concentrations in solution. The stability fields thus determined are illustrated in Figure 3.

The scarcity of hydrozincite in humid regions where sufficient water is available may be explained by the stability field. Hydrozincite is the stable mineral in solutions which are in equilibrium with air ($P_{CO_2} = 3 \times 10^{-4}$ atm.) and which have a pH higher than 8.1. Scarcity of such an alkaline water in nature explains the rarity of hydrozincite in humid regions.

The absence of zinc hydroxide can be readily understood by its stability field as shown in Figure 3. When the total carbon dioxide concentration in solution is one-thousandth of its saturation under 1 atm. air and 25° C, it becomes the stable mineral in a range of pH above 8.3; when the concentration is one-hundredth of the saturation, it becomes the stable mineral in a range of pH above 9.5. In nature, such conditions are extremely rare, and consequently zinc hydroxide is unstable in humid as in dry regions.

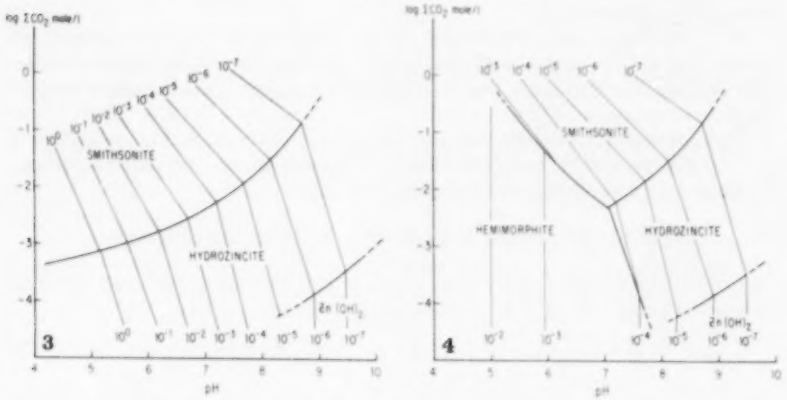

FIG. 3. Stability fields of smithsonite, hydrozincite and zinc hydroxide in solutions free from silica at 25° C as determined from the solubilities. (The numbers indicate the concentrations of Zn mole/l in solution.)

FIG. 4. Possible maximum field of hemimorphite as determined from the solubilities at 25° C. (The numbers indicate the concentrations of Zn mole/l in solution.)

Hemimorphite in a Humid Environment.—Because of the absence of the fundamental thermodynamic data of Si-O radicals such as $Si_2O_7^{-6}$ and SiO_4^{-4}, the stability field of hemimorphite in terms of the concentration of the Si-O radicals cannot be determined. Nevertheless, the possible maximum field of hemimorphite can be determined with the available data. Since the solubility curve of hemimorphite represents its minimum solubility in silica saturated solutions, the stability field which may be determined from this curve should indicate the possible maximum stability field of hemimorphite (Fig. 4). In the solutions that are undersaturated with silica, the boundary curves of the hemimorphite field must be shifted to the left (the more acid side), and its area will be reduced.

The scarcity of hemimorphite in the Upper Mississippi Valley district may be explained by the pH of the ground water. The average pH of seventeen springs and the waters from drill holes through the mineralized zones in the Potosi area, Wis., is 7.5 (19). The average pH of two water samples from old mines is 7.0 (19). When the ground waters are in equilibrium with the atmospheric carbon dioxide or contain more carbon dioxide

than the equilibrium concentration being supplied by the carbonate country rocks, this pH range falls within the stability field of smithsonite (Fig. 4).

In contrast to the Upper Mississippi Valley district, hemimorphite is common in the Southern Appalachian district. Fulton (14) studied the acidity of about 1,500 soil samples from the Austinville area, Va., and concluded that the pH of most of the soil samples ranged between 4.0 and 5.0. The results of his study indicate that, if the ground water attained an equilibrium with the soil, the pH of the ground water would be within this range. Masses of secondary zinc ores occur mostly in soil at the outcrops of ore deposits (28). Therefore, the pH of soil is considered to be an important factor in the formation of the secondary zinc minerals. This pH range falls within the stability field of hemimorphite (Fig. 4) regardless of the carbon dioxide concentrations in solution. The common occurrences of massive hemimorphite in the red soils thus can be explained. On the other hand, it is reported (28) that masses of smithsonite had been mostly found in the basins between limestone pinnacles and at the contact between the red soil and the limestone bed rock. In such environments, a higher pH may be expected because of the neutralization of the acid ground water by limestones. Consequently, smithsonite becomes a stable mineral in or near the limestones.

The Willemite Problem.—In looking for an answer as to whether the willemite discovered in the Goodsprings district is of supergene origin or is residual from a hypogene origin, the solubility curve of willemite was measured. In Figure 1, it is shown that willemite is less soluble than hemimorphite in the pH range studied at 25° C. In experimental conditions at 25° C and under 1 atm., willemite appears more stable than hemimorphite, and may be formed preferentially. If so, why does not willemite occur more commonly than hemimorphite in supergene facies? In the Sterling Hill mine, N. J., hypogene willemite has been altered to hemimorphite. This occurrence indicates that willemite is thermodynamically less stable than hemimorphite under supergene conditions and seems to contradict the result of the experiment. The hydrothermal study of Roy and Mumpton (27) indicates that willemite is more stable than hemimorphite at higher temperatures. Therefore, it is suspected that the willemite-hemimorphite solubility relationship observed at 25° C may be reversed at the lower temperatures. The theoretical interpretation for this relationship cannot be made because of the lack of the thermodynamic constants of various Si-O radicals. The study of the solubilities at lower temperatures is planned as future work.

THEORETICAL STUDY OF SECONDARY LEAD MINERALS

The stability fields of galena, anglesite and cerussite have been calculated by Garrels (15) in terms of pH and Eh. In the study here described, the stability fields of those minerals were recalculated as a function of pH, Eh and carbon dioxide partial pressure with the additional consideration of $Pb(OH)^+$ complex ions. The stability fields of massicot, PbO, minium Pb_3PbO_4, and plattnerite, PbO_2 were calculated in a similar manner looking

for an explanation for the formation of plattnerite in the Goodsprings district, Nevada. The stability fields of molybdenite and wulfenite were also calculated for explaining the occurrences and paragenesis of wulfenite.

In the geological literature published previously, it was found that the definition of oxidation-reduction potential, Eh, was diverse.[3] In the present study, the definition of oxidation-reduction potential that appears in standard physical chemistry textbooks is employed. Otherwise, an oxidation-reduction potential cannot be converted to a free energy of formation without confusion. Consequently, an oxidizing condition is expressed by a negative potential, and a reducing condition is expressed by a positive potential.

Cerussite

The stability field of cerussite that had been studied by Garrels (15) was reinvestigated with the additional consideration of the most important plumbous complex ion, $Pb(OH)^+$. The stability field will be determined as a function of pH, Eh, and partial pressure of carbon dioxide.

The equations used for the calculation of the stability field of cerussite are as follows:

$$PbCO_3 = Pb^{++} + CO_3^{--}: \quad K = 10^{-12.82},$$

$$Pb(OH)^+ = Pb^{++} + OH^-: \quad K = 10^{-7.82},$$

$$a_{CO_3^{--}} = \frac{\alpha_0 \cdot P_{CO_2} \cdot K_1 \cdot K_2}{a^2_{H^+}},$$

where $K_1 = 0.44 \times 10^{-6}$ (the first dissociation constant of carbonic acid).

$K_2 = 0.47 \times 10^{-10}$ (the second dissociation constant of carbonic acid).

$\alpha_0 = 341 \times 10^{-4}$ mole/l.

P_{CO_2} = partial pressure of carbon dioxide.

Assuming that, in a dilute solution, activities of ions are approximately equal to the concentrations, the solubility of cerussite may be calculated by the following equation when pH and the partial pressure of carbon dioxide are defined in the system:

$$Pb\ (\text{cerussite}) = C_{Pb^{++}} + C_{Pb(OH)^+}$$

where

$$\log C_{Pb^{++}} = -12.82 - \log a_{CO_3^{--}} \tag{13}$$

$$\log C_{Pb(OH)^+} = -6.12 + pH + \log C_{Pb^{++}}.$$

The stability field of cerussite can be defined as such that its solubility is smaller than the other minerals under varying Eh, pH and P_{CO_2} conditions. Figure 5 shows the stability field of cerussite when the system is in equilibrium with the air, which exerts a carbon dioxide partial pressure of $10^{-3.5}$ atm. It is noted that the cerussite field extends above the line of water decomposition and occupies the whole area between the galena and

plattnerite fields in neutral and alkaline solutions. Figure 7 shows the cerussite field as a function of Eh, pH and carbon dioxide partial pressure. The cerussite field increases as carbon dioxide partial pressure increases.

Galena and Anglesite

The stability fields of galena and anglesite were calculated in the way used by Garrels (15), except for the additional consideration of the $Pb(OH)^+$ complex ion, which resulted in the curved boundary in alkaline solutions.

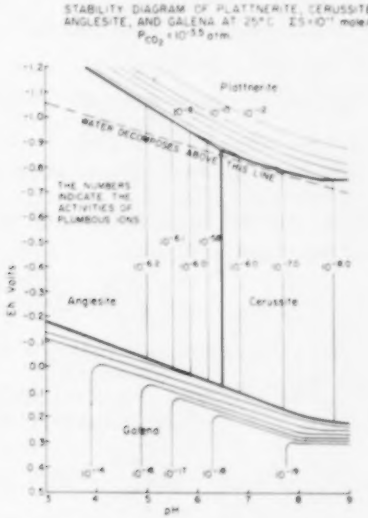

FIG. 5. Stability fields of galena, anglesite, cerussite, and plattnerite. (The numbers indicate the concentrations of lead in mole/l.)

Massicot

The dissociation of massicot in an aqueous solution is expressed by the following equations:

$$PbO + H_2O = Pb^{++} + 2OH^-, \quad K = 10^{-15.37},$$
$$Pb(OH)^+ = Pb^{++} + OH^-, \quad K = 10^{-7.82}.$$

In a dilute solution, the activity of sparingly soluble massicot and of water may be assumed to be unity. Therefore the activity of plumbous ions can be calculated by the following equation:

$$\log a_{Pb^{++}} = \log K - 2 \log a_{OH^-}$$
$$= 12.63 - 2pH.$$

Assuming that the activities are approximately equal to the concentrations in such a dilute solution, the solubility of massicot can be calculated by the following equations as a summation of the simple and complex ions:

$$\text{Pb (massicot)} = C_{Pb^{++}} + C_{Pb(OH)^{+}},$$

where Pb (massicot) denotes the solubility of massicot, and

$$\log C_{Pb^{++}} = \log a_{Pb^{++}},$$
$$\log C_{Pb(OH)^{+}} = -6.12 + \text{pH} + \log C_{Pb^{++}}.$$

The stability field of massicot may be defined as the least soluble mineral in a solution:

Pb (massicot) $\leq$ Pb (galena); Pb (anglesite); Pb (cerussite);
Pb (minium); and Pb (plattnerite)

The calculations were made in the solutions containing various carbon dioxide and sulfur concentrations (Figs. 5, 6 and 7). When solutions are free from carbon dioxide, massicot becomes stable in an oxidizing alkaline

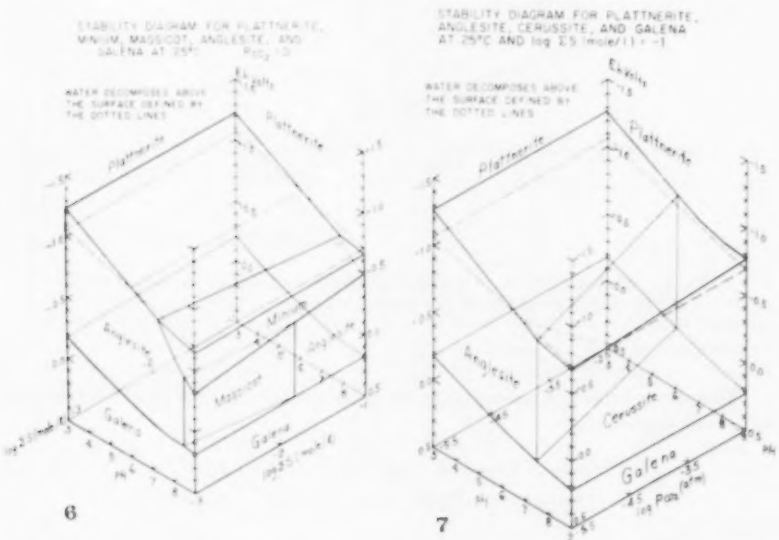
STABILITY DIAGRAM FOR PLATTNERITE, MINIUM, MASSICOT, ANGLESITE, AND GALENA AT 25°C
WATER DECOMPOSES ABOVE THE SURFACE DEFINED BY THE DOTTED LINES
Plattnerite
Anglesite
Galena
STABILITY DIAGRAM FOR PLATTNERITE, ANGLESITE, CERUSSITE, AND GALENA AT 25°C AND log ΣS (mole/l) = -1
WATER DECOMPOSES ABOVE THE SURFACE DEFINED BY THE DOTTED LINES
Plattnerite
Anglesite
Cerussite
Galena

6 7

FIG. 6. Stability diagram of galena, cerussite, anglesite, massicot, minium and plattnerite as a function of Eh, pH, and total sulfur concentration in solution at 25° C, assuming no carbon dioxide.

FIG. 7. Stability diagram of galena, cerussite, anglesite, minium and plattnerite as a function of Eh, pH, and partial pressure of carbon dioxide in solution at 25° C, assuming total sulfur in solution to be 10^{-1} mole/l.

solution which contains less than 10^{-2} mole/l of sulfur. However, the stability field of massicot disappears if a small amount of carbon dioxide is present in the system. Therefore, massicot cannot be the stable phase in the carbonated ground waters which may prevail in limestone regions such as the three districts investigated, but can be formed in a strongly alkaline and non-carbonated ground water.

Minium

The following formula may be written for the dissociation of minium, and its equilibrium constant can be calculated from the available thermodynamic data:

$$Pb_2PbO_4 + 8H^+ = Pb^{+4} + 2Pb^{++} + 4H_2O,$$
$$\log K = 13.55.$$

Assuming that the activity of minium is unity as it is sparingly soluble, and that the activity of water is unity,

$$\log K = \log a_{Pb^{+4}} + 2 \log a_{Pb^{++}} + 8pH. \tag{14}$$

On the other hand, the relationship between plumbous and plumbic ions is as follows:

$$Pb^{++} = Pb^{+4} + 2e; \quad E^0 = -1.7 \text{ volts};$$
$$Eh = -1.7 - 0.03 (\log a_{Pb^{+4}} - \log a_{Pb^{++}}). \tag{15}$$

Substituting Equation (14) in Equation (15), the activity of plumbous ions can be obtained in terms of pH and Eh:

$$\log a_{Pb^{++}} = \frac{1}{3}\left\{70.3 - 8pH + \frac{100}{3} Eh\right\}. \tag{16}$$

Assuming that the activities are approximately equal to the concentrations in dilute solutions, the solubility of minium may be calculated by the following equations:

$$Pb \text{ (minium)} = C_{Pb^{++}} + C_{Pb(OH)^+},$$
$$\log C_{Pb^{++}} = \log a_{Pb^{++}},$$
$$\log C_{Pb(OH)^+} = -6.12 + pH + \log C_{Pb^{++}}.$$

When the solubility of minium was exceeded by the solubilities of other minerals, minium becomes the stable mineral in the system. Thus, the stability field of minium was determined in terms of pH, Eh and the total sulfur concentration (Fig. 6). In solutions with a pH above 7 and containing no carbon dioxide, minium is the stable mineral in a moderately oxidizing environment, whereas, in solutions containing carbon dioxide, the stability field of minium, as well as massicot, is replaced by the cerussite field (Fig. 5 and 7).

Plattnerite

The dissociation of plattnerite, PbO_2, is expressed by the following formula:

$$PbO_2 + 4H^+ = Pb^{++} + 2H_2O, \quad \log K = -7.95,$$
$$Pb^{++} = Pb^{++++} + 2e, \quad E^0 = -1.7 \text{ volts.}$$

Assuming that the activities of sparingly soluble plattnerite is unity and also that the activity of water is unity, the activity of the plumbous ions which are in equilibrium with plattnerite can be calculated in terms of pH and Eh:

$$\log a_{Pb^{++}} = \frac{100}{3}(Eh + 1.7) - 4pH - 7.95$$

Assuming that the activity of plumbous ions is approximately equal to the concentration in dilute solutions, the solubility of plattnerite can be calculated by the following equations:

$$Pb \text{ (plattnerite)} = C_{Pb^{++}} + C_{Pb(OH)^+},$$
$$\log C_{Pb^{++}} = \log a_{Pb^{++}},$$
$$\log C_{Pb(OH)^+} = -6.12 + pH + \log C_{Pb^{++}}.$$

The stability field of plattnerite is defined as such that its solubility is least of the minerals in consideration, and is shown in Figures 8, 9 and 10. It is noted that the plattnerite field exists mostly within the environment in which water is decomposed. However, in solutions with a P_{CO_2} less than $10^{-4.7}$ atm., it extends into the region where water is stable. If the plattnerite discovered in the Goodsprings district was precipitated from an aqueous solution in an equilibrium condition, it would be predicted that the plattnerite was formed in the limited environment which is represented by a thin wedge (below the surface of the decomposition of water, but within the plattnerite field) in Figure 7. However, considering the effect of overvoltage, water may be stable above the theoretical voltage for the decomposition of water, and consequently the possible environment for the formation of plattnerite would be broadened, if such a highly oxidizing environment might exist in nature. The disappearance of the massicot and minium fields in carbonated solutions is of geological interest. One wonders why minium and massicot, which have striking yellow and red colors, have never been reported from the Goodsprings district where a highly oxidizing environment has prevailed, being indicated by the occurrences of plattnerite. As shown in Figure 7, the minium and massicot fields do not exist in carbonated solution. Instead, the cerussite and anglesite fields occupy the entire space between the galena and plattnerite field. Therefore, the absence of minium and massicot in the Goodsprings district can be explained by the instability of these minerals in a carbonated solution.

Wulfenite

The source of molybdenum in supergene facies in the Goodsprings district is galena as indicated by the spectrographic analysis, which will be discussed in a later section. During the oxidation, molydenum was liberated from galena and was precipitated in its supergene minerals. However, the state of molybdenum in galena crystals is still an unsettled problem. Goldschmidt (16) doubts if molybdenum would enter the galena lattice, and believes that molybdenum is more likely to be in the form of molybdenite as small inclusions in galena. In the present study, the stability relationships between molybdenite, wulfenite, galena, and cerussite are discussed.

Wulfenite-Galena-Molybdenite.—Since information on the complex ions of molybdenum in acid solutions is not available, the present discussion is limited to alkaline solutions in which molybdenum exists mostly as molybdate ions. The dissociation of molybdenite (MoS_2) in an alkaline solution may be expressed by the following equation, and its standard oxidation-reduction potential can be calculated from the free energies of formation of the reactants and products.

$$MoS_2 + 8OH^- = MoO_4^{=} + 2S^{=} + 4H_2O + 2e,$$

$$\Delta F^0 = -46.8 \text{ kcal/mole}, \quad E^0_R = 1.02 \text{ volt},$$

$$Eh = 1.02 - 0.03 \log (a_{MoO_4^{=}} \cdot a^2_{S^{=}} / a_{MoS_2} \cdot a^8_{OH^-}).$$

Assuming that the activity of sparingly soluble molybdenite is unity,

$$\log a_{MoO_4^{=}} = 8 \log a_{OH^-} - 2 \log a_{S^{=}} - \frac{100}{3} (Eh - 1.02). \qquad (17)$$

On the other hand, the activity of ionic sulfur can be calculated by Equation (18):

$$S^{=} + 4H_2O = SO_4^{=} + 8H^+ + 8e, \quad E^0 = -0.14 \text{ volt},$$

$$Eh = -0.14 - \frac{0.06}{8} \log (a_{SO_4^{=}} a^8_{H^+} / a_{S^{=}}). \qquad (18)$$

Assuming that the total soluble sulfur in solution is ΣS mole/l, that the summation of the activities of various forms of sulfur is approximately equal to the concentration of the total sulfur in solution, and that the activities of various complexed sulfur ions are negligibly small,

$$\Sigma S = a_{H_2S} + a_{HS^-} + a_{S^{=}} + a_{SO_4^{=}}, \qquad (19)$$

$$a_{HS^-} \cdot a_{H^+} / a_{H_2S} = 1.1 \times 10^{-7},$$

$$a_{S^{=}} \cdot a_{H^+} / a_{HS^-} = 10^{-14}.$$

From these three equations, the activity of sulfur ions can be obtained:

$$a_{S^{=}} = \Sigma S \{1 + a_{H^+}{}^{-8} \cdot 10^{-122(Eh+0.14)} + a_{H^+} \cdot 10^{14} + a^2_{H^+} \cdot 10^{21}\}. \qquad (20)$$

Substituting Equation (20) in Equation (18), the activity of molybdate ions which are in equilibrium with molybdenite can be obtained:

$$\log a_{MoO_4^{=}} = -\frac{100}{3}\,Eh + 8pH - 78 - 2\log \Sigma S + 2\log \{1 + a^{8}_{H^+} \cdot 10^{-122(Eh+0.14)} + a_{H^+} \cdot 10^{14} + a^{2}_{H^+} \cdot 10^{21}\}. \quad (21)$$

On the other hand, the activity of lead ions which are in equilibrium with wulfenite can be calculated when the activities of molybdate ions are known:

$$PbMoO_4 = Pb^{++} + MoO_4^{=}, \quad K = 10^{-5.4},$$
$$\log a_{Pb^{++}} = -5.4 - \log a_{MoO_4^{=}}, \quad (22)$$

and substituting Equation (21) in Equation (22),

$$\log a_{Pb^{++}} = 72.6 + 2\log \Sigma S + \frac{100}{3}\,Eh - 8\,pH - 2\log \{1 + a^{-8}_{H^+} \cdot 10^{-122(Eh+0.14)} + a_{H^+} \cdot 10^{14} + a^{2}_{H^+} \cdot 10^{21}\}. \quad (23)$$

The activities of lead ions which are in equilibrium with galena can be calculated by a similar method:

$$PbS = Pb^{++} + S^{=}, \quad K = 10^{-28.15};$$
$$\log a_{Pb^{++}} = \log K - \log S^{=} = -28.15 - \log \Sigma S + \log \{1 + a^{-8}_{H^+} \cdot 10^{-122(Eh+0.14)} + a_{H^+} \cdot 10^{14} + a^{2}_{H^+} \cdot 10^{21}\}. \quad (24)$$

The boundary surface between the wulfenite and the galena stability fields is obtained by equating Equation (23) and (24):

$$3\log \Sigma S + \frac{100}{3}\,Eh - 8pH - 3\log \{1 + a^{-8}_{H^+} \cdot 10^{-122(Eh+0.14)} + a_{H^+} \cdot 10^{14} + a^{2}_{H^+} \cdot 10^{21}\} + 100.75 = 0.$$

This is a function of Eh, pH and ΣS, and is indicated by the surface (ABCD) in Figure 8. In an environment with a higher Eh than this boundary surface, wulfenite is more stable than galena in the presence of molybdenite whereas galena is more stable than wulfenite in the presence of molybdenite in an environment with a lower Eh than the boundary surface.

Wulfenite-Cerussite-Molybdenite.—In a higher oxidizing environment, galena will be altered to cerussite. The boundary between the stability fields of wulfenite and cerussite in presence of molybdenite will be investigated in this section. Assuming the total carbon dioxide in solution to be 0.03 mole/l, the activity of lead ions which are in equilibrium with cerussite is calculated by Equation (13). Substituting Equation (5) in Equation (13),

$$\log a_{Pb^{++}} = -11.3 + \log \{1 + a_{H^+} \cdot 10^{10.5} + a^{2}_{H^+} \cdot 10^{17}\}. \quad (25)$$

The boundary between the stability fields of wulfenite and cerussite is obtained by equating Equation (23) and (25):

$$2 \log \Sigma S + \frac{100}{3} Eh - 8pH$$
$$- 2 \log \{1 + a^{-8}_{H^+} \cdot 10^{-132(Eh+0.14)} + a_{H^+} \cdot 10^{14} + a^2_{H^+} \cdot 10^{21}\}$$
$$- \log \{1 + a_{H^+} \cdot 10^{10.5} + a^2_{H^+} \cdot 10^{17}\} + 72.6 = 0.$$

This boundary, below which cerussite is more stable than wulfenite, is found to fall in a reducing environment where galena is more stable than cerussite.

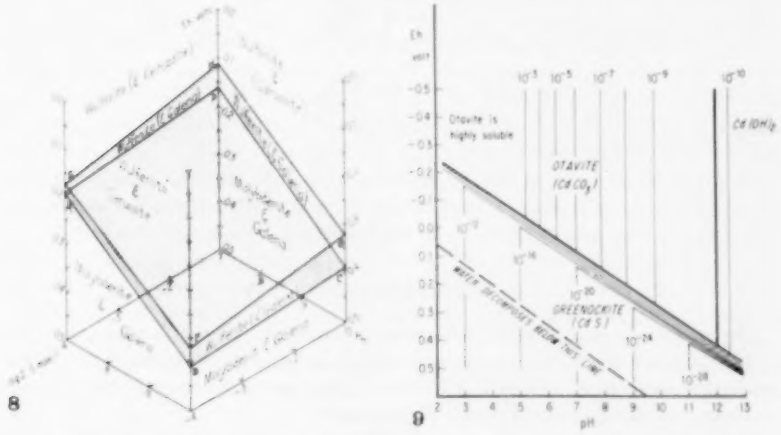

FIG. 8. Stability diagram of molybdenite, galena, wulfenite, and cerussite at 25° C as a function of Eh, pH, and total sulfur in solution, assuming the total carbon dioxide in solution to be 0.03 mole/l. (The minerals in parenthese are the species which may appear in excess of plumbous ion.)

FIG. 9. Stability fields of greenockite, otavite and cadmium hydroxide, assuming the total carbon dioxide in solution to be $10^{-1.5}$ (0.03) mole/l, and the total sulfur in solution to be 10^{-1} (0.1) mole/l at 25° C. (The numbers indicate the activity of cadmium ion.)

This means that, in the presence of molybdenite, wulfenite is always more stable than cerussite in the environments investigated. However, after the molybdenite was all weathered and removed from the system, cerussite could be more stable than wulfenite.

A hypothetical case may be taken, in which a galena crystal that includes a small crystal of molybdenite is assumed to be altered by supergene process. During this process, when the environment becomes more oxidizing and reaches a condition on the stability boundary (ABCD), wulfenite comes into existence. In a condition within the space between the boundary surfaces (ABCD) and (EFGH), galena is continuously converted to wulfenite in presence of molybdenite. Here, the boundary surface (EFGH) is the

galena-cerussite boundary. The wulfenite inclusions in an oxidizing galena, which were commonly observed in the specimens from the Goodsprings, district, may represent this condition.

As long as molybdenite exists, wulfenite is more stable than cerussite and galena in a field above (ABCD). When the environment becomes more oxidizing above the boundary between galena and cerussite, (EFGH), molybdenite and galena will still be altered to wulfenite, as long as molybdenite exists. Eventually, molybdenite will be all dissipated and removed from the system. Thereafter, wulfenite cannot be the stable mineral, because molybdate ions are no longer supplied by molybdenite. Galena is altered to cerussite instead of wulfenite, and further, wulfenite is taken into solution and migrates or is transported away. The molybdate ions may be reprecipitated when the solubility product of wulfenite is exceeded because the solution evaporates or because the molybdate ions encounter a solution rich in lead ions. The study of the paragenesis of wulfenite indicates two stages of formation: the earlier is represented by the wulfenite inclusions in galena, and the later is represented by the wulfenite found in fractures in the country rocks away from the ore bodies and evidencing the migration of the ions. This paragenesis agrees with the course of the supergene alteration discussed above, and appears to be explained by the present study.

CADMIUM MINERALS

In a zone of supergene alteration, greenockite (CdS) is generally the most common mineral of cadmium and is in many cases associated with oxidizing sphalerite. Otavite ($CdCO_3$) is a rare supergene mineral and cadmium oxide is extremely rare in nature.

The dissociations of these minerals in solution are expressed by the following formulae (21):

$$CdS = Cd^{++} + S^{=}; \qquad K = 1.0 \times 10^{-28},$$

$$CdCO_3 = Cd^{++} + CO_3^{=}; \qquad K = 5.2 \times 10^{-12},$$

$$CdO + 2H^{+} = Cd^{++} + H_2O; \qquad K = 5.6 \times 10^{15},$$

$$Cd(OH)_2 = Cd^{++} + 2OH^{-}; \qquad K = 2.0 \times 10^{-14}.$$

Assuming that the total sulfur in solution is 0.1 mole/l at 25° C under 1 atm., and the total carbon dioxide in solutions is 0.03 mole/l under the same conditions, the activities of cadmium ions which are in equilibrium with greenockite and with otavite can be calculated by the following equations:

$$\log a_{Cd^{++}} = -27 + \log \{1 + a^{-8}_{H^{+}} \cdot 10^{-133(Eh+0.14)} + a_{H^{+}} \cdot 10^{14} + a^{2}_{H^{+}} \cdot 10^{21}\}$$

for greenockite, and

$$\log a_{Cd^{++}} = -9.8 + \log (1 + a_{H^{+}} \cdot 10^{10.5} + a^{2}_{H^{+}} \cdot 10^{17})$$ for otavite.

The activities of cadmium ions for the dissociation of cadmium oxide and of cadmium hydroxide are calculated by:

$$\log a_{Cd^{++}} = 15.8 - 2pH, \text{ and}$$
$$\log a_{Cd^{++}} = 14.3 - 2pH \text{ respectively.}$$

Assuming that the activity of the cadmium ion is approximately equal to its concentration in dilute solutions, of the four minerals the one which has the least activities of cadmium ions should be the most stable mineral in an environment. Therefore, the boundary lines between those stability fields can be calculated by equating those four equations with each other. The results are shown on a pH-Eh diagram (Fig. 9) with the activities of cadmium ions.

The greenockite stability field extends into oxidizing environments when a solution is acid. This explains the close association of greenockite in a zone of oxidation with oxidizing sphalerite around which an acid environment may prevail through the formation of sulfate ions.

The scarcity of greenockite in the Goodsprings district is probably due to the highly oxidizing and alkaline environment prevailing in that locality in which greenockite is no longer stable, and, instead, otavite becomes the more stable mineral. In sphalerite from the Potosi mine, Goodsprings, 0.5–1.0% of cadmium was reported, and 0.05–0.1% of cadmium was also reported in a snow white hydrozincite specimen from the Singer-Tiffin mine, Goodsprings, by Barton and Behre (4, p. 96). The result of the analysis indicates that cadmium was present in the sphalerite in the Singer-Tiffin mine, which later altered to hydrozincite, and that the cadmium liberated from the sphalerite was precipitated with hydrozincite as otavite or as a trace element in divalent metal carbonates by ionic substitution. A difficulty was encountered in the search for otavite because of its similarity in physical characteristics with smithsonite and other carbonates. Although the writer failed to discover otavite, a further study might find a common occurrence of otavite in the Goodsprings district.

Cadmium hydroxide becomes stable in extremely alkaline solutions with a pH above 12.0. On the other hand, the stability field for cadmium oxide in solutions does not exist in the assumed solutions. However, in a dry environment, cadmium oxide may become more stable than the hydroxide, depending upon the partial pressure of water vapor. In a dry environment, the following formula may be valid:

$$CdO + H_2O(g) = Cd(OH)_2, \quad K = 10^{2.95}.$$

Assuming that the fugacity of the solid phases is unity and the fugacity of water vapor is approximately equal to its partial pressure:

$$P_{H_2O} = 10^{-2.95} \text{ atm. at } 25^\circ \text{ C in an equilibrium condition.}$$

If the system was saturated with water at 25° C, the reaction would be driven to the right in favor of cadmium hydroxide as the water vapor

pressure ($10^{-1.52}$ atm. at 25° C) exceeds the equilibrium pressure. On the other hand, if the partial pressure of water vapor was 5% of its saturation, the reaction would be driven to the left in favor of cadmium oxide. Therefore, cadmium oxide formed in nature might have been precipitated as the hydroxide from an unusually strong alkaline solution, and then converted to the oxide under a dry environment.

TABLE 6

SPECTROCHEMICAL ANALYSES OF MINERALS AND ROCKS FROM THE GOODSPRINGS DISTRICT, NEVADA

Minerals	Mines	Specimen No.	Sb	Bi	As	Ge	Mo	P	V	Ag	Co	Zn
Galena	Potosi	T-186	P	—	tr	—	A	—	—	—	—	A
Galena	South Whale	T-42	P	—	P	—	P	—	—	A	—	A
Galena	Frederickson	T-174	P	—	A	—	tr	—	—	P	—	P
Galena (oxidizing)	Ruth	T-114	P	—	tr	—	P	P	A	tr	—	A
Cerussite	Yellow Pine	T-8	—	—	—	—	P	—	—	—	—	P
Sphalerite (with some shale)	Potosi	PB-67-54	P	—	—	P	—	—	P	P	—	A
Black shale	Potosi	T-144	—	—	—	—	—	A	A	P	—	P
Gray shale	Frederickson	T-113	—	—	—	—	—	—	A	A	—	P
Limestone	South Whale	T-34-1	—	—	—	—	—	P	—	—	—	P
Limestone	South Whale	T-34-3	—	—	—	—	—	tr	—	—	—	tr
Limestone	South Whale	T-34-4	—	—	—	—	—	—	—	—	—	P
Limestone	Hoodoo	T-184	—	—	—	—	—	P	tr	—	—	P
Limestone	South Whale	T-185	—	—	—	—	—	P	—	—	—	P
Limestone	Ruth	T-109	—	—	—	—	—	P	P	—	—	P

A = abundant, P = present, tr = trace, and — = absent. Analysis by Taro Takahashi.

TABLE 7

SPECTROCHEMICAL ANALYSES OF MINERALS AND ROCKS FROM THE UPPER MISSISSIPPI VALLEY DISTRICT

Minerals	Mines	Specimen No.	Ag	As	Bi	Co	Ge	Mo	P	Sb	V	Zn
Sphalerite*	Piquette	PQ-149	P	—	—	—	P	—	—		—	A
Galena	Piquette	TW-4-P	P	—	—	—	—	—	—	tr	—	—
Galena	Barreltown	TW-1-B	P	—	—	—	—	—	—	P	—	P
Limestone	Piquette	TW-1-P	—	—	—	—	—	—	P	—	—	P
Limestone	Piquette	TW-2-P	—	—	—	—	—	—	P	—	—	P
Limestone	Piquette	TW-3-P	—	—	—	—	—	—	P	—	—	P
Limestone	Barreltown	TW-2-B	—	—	—	—	—	—	P	—	—	P
Limestone	Barreltown	TW-3-B	—	—	—	—	—	—	P	—	P	P
Soil	Road cut 5 miles southwest of Mineral Point		—	—	—	—	P	—	P	—	P	P

A = abundant, P = present, tr = trace, — = absent.

* Analysis by J. J. Durek. In addition to the elements indicated above, the following were determined:

1) Present in some quantity = Mg, Ca, Fe, Mn, and Si.
2) Trace = Al and Gu.
3) Absent = Be, B, Cr, In, K, La, Hg, Ni, Rb, Sn and Ti.

TABLE 8

SPECTROCHEMICAL ANALYSES OF MINERALS AND ROCKS FROM THE SOUTHERN APPALACHIAN DISTRICT

Mineral	Mine	Specimen No.	As	Bi	Cd	Co	Ga	Ge	Mn	Mo	Ni	P	Sb	Sn	V	Zn	Analyst
Sphalerite	Grasselli, Tenn.	DT-37-55	—	—	P	—		P		—		—	—		—	A	T. T.
Sphalerite	New Prospect, Tenn.		—	—	b	—	c	d	d	—	tr			—			R. E. S.
Sphalerite	Mascot, Tenn.		—	—	a	—	d	d	—	—	—			—			R. E. S.
Sphalerite	Austinville, Va.		—	—	b	—	—	d	d	—	tr			—			R. E. S.
Galena	Austinville, Va.	DT-13-55	—	—		—		—		—		—	—		—	—	T. T.
Hemimorphite	Austinville, Va.	DT-10-55	—	—		—		P		—		P	—		—	A	T. T.
Hemimorphite	Mascot, Tenn.	12-L	—	—		—		P		—		P	—		—	A	T. T.
Limestone	Grasselli, Tenn.	DT-25-55	—	—		—		—		—		P	—		P	tr	T. T.
Red soil at outcrop of ore body	Mascot, Tenn.	DT-79-55	—	—		—		tr		—		P	—		P	A	T. T.

A = abundant, P = present, tr = trace, — = absent.
a = over 1%, b = 1–0.1%, c = 0.1–0.01%, d = below 0.01%.
R. E. S. = R. E. Stoiber, T. T. = T. Takahashi.

SOURCES OF THE MINOR ELEMENTS IN SUPERGENE FACIES

The ore minerals and country rocks were analyzed by the (qualitative) emission spectrographic method to account for the sources of the minor elements such as Mo, As, V, and P in the supergene facies, and also for the mineralogic contrasts observed in the three districts investigated. The results of the analyses are shown in Tables 6, 7, and 8. The sensitivities of the spectrograph were 0.01–0.001% for Mo, 1.0–0.1% for As, 0.01–0.001% for V, and 1.0–0.1% for P.

Molybdenum.—In the Goodsprings district, molybdenum was detected in galena and cerussite, but could not be recognized in sphalerite and the country rocks. The results of the analyses and the close association of wulfenite with galena indicate that molybdenum, a major constituent of wulfenite, was derived from galena during supergene alteration. In contrast to the Goodsprings district, no molybdenum mineral has been reported in the supergene zones of the Upper Mississippi Valley and the Southern Appalachian districts. In accordance with this field observation, no molybdenum was found in the ore minerals and the country rocks. Therefore, it appears that the absence of molybdenum minerals in the supergene facies is due to its complete absence or to its extremely low concentration in these districts.

Arsenic.—In the specimens from the Goodsprings district, arsenic was detectable only in galena, but was present in sphalerite and in the country rocks in quantities below the sensitivity of the present technique. In view of the close association of mimetite with galena, it appears that galena was the source of arsenic in the supergene facies.

In the Upper Mississippi Valley and the Southern Appalachian districts, arsenic could be detected neither in the ore minerals nor in the country rocks. The absence of supergene arsenic minerals in these districts is probably the result of its low concentration or its absence in the supergene zone.

Vanadium.—Vanadium was found in the shales, but failed to appear in unaltered galena from the Goodsprings district. The occurrences of the supergene vanadium minerals also indicate the shales as the source of the vanadium ions in the supergene facies. In the South Whale and Mobile mines in this district, the occurrences of the supergene vanadium minerals, descloizite and cupro-descloizite, are restricted to the brecciated fault zones which cut through the ore bodies. These occurrences can be explained by three factors: 1) the prevailing environment must be high enough to convert the tetravalent vanadium to the pentavalent vanadium (13) (the tetravalent vanadium, which is probably the state in shales, is relatively immobile due to the formation of the sparingly soluble VO_2, whereas pentavalent vanadium is soluble as VO_4^{-3} and will be precipitated by reacting with heavy metal ions); 2) the geologic structures must be favorable for guiding the ground water, which is loaded with vanadate ions, to the oxidizing ore bodies, where a sufficient concentration of heavy metal ions are present to form insoluble vanadate minerals; and 3) a quick evaporation

rate of the ground water may be necessary to concentrate vanadate and heavy metal ions and thus to cause the precipitation.

In the Upper Mississippi Valley and the Southern Appalachian districts, vanadium was detected in the country rocks and soils. However, no vanadium mineral has ever been reported in these districts. The absence of vanadium minerals in the supergene facies of these districts may be because 1) in the humid climate the vanadate and heavy metal ions in the ground water are not sufficiently concentrated to cause precipitation, or because 2) the environments are not oxidizing enough to convert tetravalent vanadium to the pentavalent state.

Phosphorus.—Phosphorus was detected in the country rocks in the three districts studied, whereas it was not found in the primary ore minerals. Therefore, the source of phosphorus is attributed to the country rocks. The wide distribution of pyromorphite can be explained by 1) the widespread presence of phosphorus in the rocks, and by 2) the stability of the pentavalent phosphorus (PO_4^{-3}) in the entire supergene environment (30).

It is noted that two hemimorphite specimens from the Southern Appalachian district contain phosphorus. Neither X-ray study nor microscopic observation uncovered a distinct zinc phosphate mineral. Therefore, phosphorus is probably in the hemimorphite lattice substituting for silicon ions.

CONCLUSIONS

1) Hydrozincite is the most abundant supergene zinc mineral in the Goodsprings district, Nevada. This was caused by the dry environment in which carbon dioxide gas could freely escape into the air, maintaining its partial pressures at less than the equilibrium value in the smithsonite-hydrozincite reaction. The carbon dioxide partial pressure at equilibrium was calculated to be $10^{-1.4}$ atm. at 15° C; $10^{-1.2}$ atm. at 25° C; and $10^{-0.8}$ atm. at 40° C. If the partial pressure were higher than those values at the respective temperatures, smithsonite would be more stable than hydrozincite. An increase of smithsonite with depth may have been caused by a slow rate of diffusion and entrapment of carbon dioxide in rocks, which in turn resulted in a locally high partial pressure of carbon dioxide.

2) Smithsonite is the predominant supergene zinc mineral in the Upper Mississippi Valley district. This is probably attributable to the nature of the ground water, with its average pH of 7.5 and a probable carbon dioxide content close to saturation. In solutions which are saturated with atmospheric carbon dioxide under 1 atm., at 25° C and in a pH range of 7–8, smithsonite is from ten to fifty times less soluble than hemimorphite, and is the most stable supergene zinc mineral.

3) Smithsonite and hemimorphite are the chief supergene zinc minerals in the Southern Appalachian district. The occurrences of hemimorphite masses in red soil are probably attributed to the acid soil, which has a pH between 4.0 and 5.0. In such solutions, it was experimentally proved that hemimorphite is more stable than smithsonite or hydrozincite. Masses of smithsonite near the limestone bed rock may be explained by the neutralization of acid by limestone which also supplies carbon dioxide.

4) The general paragenetic sequence of the supergene zinc minerals was established to be 1) smithsonite, 2) hydrozincite, and 3) hemimorphite. This sequence coincides with the sequence of the solubilities of these minerals in solutions containing the total carbon dioxide of 0.03 mole/l with a pH range of 7–8.

5) The occurrence of plattnerite in the Goodsprings district indicates a highly oxidizing environment during its formation. Based on a solubility study that assumes an equilibrium condition at 25° C, it was postulated that plattnerite was probably formed in a solution with an Eh over − 0.7 volts in a weakly alkaline environment.

6) Massicot and minium can only be stable in a carbonate free solution, whereas cerussite becomes more stable than either in a carbonated solution. Therefore, the absence of massicot and minium in the Goodsprings district is probably because of its carbonated (limestone) environment.

7) In the presence of molybdenite, wulfenite is more stable than cerussite in a supergene environment. This explains the common occurrences of wulfenite as inclusions in oxidizing galena. However, wulfenite becomes less stable than cerussite when molybdenite is removed from the system. Migration of molybdate ions in a later stage of the supergene alteration in the Goodsprings district is evidenced by the occurrence of wulfenite as fracture-fillings away from the ore bodies.

8) Greenockite may readily be dissolved in an oxidizing alkaline solution, but is stable in acid solution under weakly oxidizing or reducing conditions.

9) The results of spectrochemical analyses indicate that, in the supergene facies studied, molybdenum and arsenic originated from galena and that vanadium and phosphorus were derived from the country rocks.

ORE GENESIS LABORATORY,
DEPARTMENT OF GEOLOGY,
COLUMBIA UNIVERSITY, NEW YORK,
Sept. 15, 1959

REFERENCES

1. Agnew, A. F., 1955, Application of geology to the discovery of zinc lead ore in the Wisconsin-Illinois-Iowa district: Min. Engineering, v. 7, p. 781–795.
2. Agnew, A. F., Heyl, A. V., Jr., Behre, C. H., Jr., and Lyons, E. J., 1956, Stratigraphy of middle Ordovician rocks in the zinc-lead district of Wisconsin, Illinois and Iowa: U. S. Geol. Survey Prof. Paper 274-K, p. 251–309.
3. Albritton, C. C., Jr., Richards, A., Brokaw, A. L., and Reinemund, J. A., 1954, Geologic controls of lead and zinc deposits in the Goodsprings district, Nevada: U. S. Geol. Survey Bull. 1010, p. 1–111.
4. Barton, P. B., Jr., and Behre, C. H., Jr., 1954, Interpretation and evaluation of the uranium occurrences near Goodsprings, Nevada: U. S. Atomic Energy Comm. RME-3119, p. 1–105.
5. Barton, P. B., Jr., 1956, Fixation of uranium in the oxidized base metal ores of the Goodsprings district, Clark Co., Nevada: ECON. GEOL., v. 51, p. 178–191.
6. Bastin, E. S., Editor, 1939, Contributions to a knowledge of the lead and zinc deposits of the Mississippi Valley region: Geol. Soc. America Spec. Paper 24, p. 1–156.
7. Behre, C. H., Jr., Scott, E. R., and Banfield, A. F., 1937, The Wisconsin lead-zinc district, preliminary paper: ECON. GEOL., v. 32, p. 738–809.
8. Behre, C. H., Jr., Heyl, A. U. and McKnight, E. T., 1948, Zinc and lead deposits of the Mississippi Valley region: Symposium on the geology, paragenesis and reserves of ores of lead and zinc, 18th Intern'l. Geol. Congress, London, p. 46–61.
9. Bridge, John, 1945, Geologic map and structure sections of the Mascot-Jefferson City zinc mining district, Tennessee: Division of Geology, Dept. of Conservation, State of Tennessee.

10. Brokaw, A. L., 1948, Geology and mineralogy of the East Tennessee zinc district: 18th Intern'l. Geol. Congress, London, p. 46–61.
11. Currier, L. W., 1935, Zinc and lead region of southwestern Virginia: Virginia Geol. Survey Bull. 43, p. 1–122.
12. ——, 1935, Structural relations of Southern Appalachian zinc deposits: Econ. Geol., v. 30, p. 260–286.
13. Evans, H. T. and Garrels, R. M., 1958, Thermodynamic equilibria of vanadium in aqueous systems as applied to the interpretation of the Colorado Plateau ore deposits: Geoch. at Cosmoch. Acta, v. 15, p. 131–149.
14. Fulton, R. B., 1950, Prospecting for zinc using semiquantitative chemical analyses of soils: Econ. Geol., v. 45, p. 645–670.
15. Garrels, R. M., 1954, Mineral species as function of pH and oxidation potentials, with special reference to the zone of oxidation and secondary enrichment of sulfide ore deposits: Geoch. et Cosmoch. Acta, v. 5, p. 158–159.
16. Goldschmidt, V. M., 1954, Geochemistry: Oxford Univ. Press, London, p. 407.
17. Hewett, D. F., 1931, Geology and ore deposits of the Goodsprings quadrangle, Nevada: U. S. Geol. Survey Prof. Paper 162, p. 1–172.
18. Heyl, A. U., Lyons, E. J., Agnew, A. F., and Behre, C. H., Jr., 1955, Zinc-lead-copper resources and general geology of the Upper Mississippi Valley district: U. S. Geol. Survey Bull. 1015–6, p. 227–245.
19. Kennedy, V. C., 1956, Geochemical studies in the southwestern Wisconsin zinc-lead area: U. S. Geol. Survey Bull. 1000-E, p. 187–223.
20. Krumbein, W. C., and Garrels, R. M., 1950, Origin and classification of chemical sediments in terms of pH and oxidation-reduction potential: Jour. Geology, v. 60, p. 1–33.
21. Latimer, W. M., 1952, Oxidation potentials (2nd Ed.): Prentice-Hall, Inc., New York, p. 1–392.
22. Mason, Brian, 1947, Oxidation and reduction in geochemistry: Jour. Geology, v. 57, p. 67–72.
23. Oder, C. R. L., and Hood, J. W., 1949, Zinc deposits of the southeastern states: Symposium on mineral resources of the southeastern United States, p. 72–87, Univ. Tenn. Press.
24. Pough, F. H., 1941, Occurrence of willemite: Am. Mineralogist, v. 26, p. 92–102.
25. Purdue, A. H., 1912, The zinc deposits of northeastern Tennessee: Tennessee Geol. Survey Bull. 14, p. 5–69.
26. Rogers, John, 1953, Geologic map of East Tennessee with explanatory text: Tennessee Geol. Survey Bull. 58, p. 1–168.
27. Roy, Della M. and Mumpton, F. A., 1956, Stability of minerals in the system ZnO-SiO_2-H_2O: Econ. Geol., v. 51, p. 432–443.
28. Secrist, M. H., 1924, Zinc deposits of East Tennessee: Tennessee Geol. Survey Bull. 31, p. 1–165.
29. Stoiber, R. E., 1940, Minor elements in sphalerite: Econ. Geol., v. 35, p. 501–519.
30. Takahashi, Taro, 1957, Supergene alteration of zinc and lead deposits: Ph.D. Thesis, Columbia University, New York, p. 1–163.

Economic Geology
Vol. 55, 1960, pp. 1116–1147

THE CHIEF OXIDE-BURGIN AREA DISCOVERIES, EAST TINTIC DISTRICT, UTAH: A CASE HISTORY

J. B. BUSH, D. R. COOK, T. S. LOVERING, AND H. T. MORRIS

PART I

U. S. GEOLOGICAL SURVEY STUDIES AND EXPLORATION[1]

T. S. LOVERING AND H. T. MORRIS

CONTENTS

	PAGE
Abstract	1116
Introduction	1117
Acknowledgments	1118
Historical summary	1119
Work prior to 1943	1119
U. S. Geological Survey studies—1943–1955	1123
Geology	1125
Regional setting	1125
Igneous and sedimentary rocks	1126
Structural history of the East Tintic district	1128
Alteration and ore deposits	1134
Ore guides	1136
Exploration by Geological Survey	1140
Chief Oxide area	1141
References	1146

ABSTRACT

The Burgin Shaft is in the Chief Oxide area of the East Tintic district, Utah, and is about a mile east of any previously known ore bodies; workings from it are currently developing a substantial amount of commercial lead-zinc ore in several blind ore bodies that lie in folded Paleozoic carbonate rock concealed beneath a blanket of Eocene lava. This area was mapped by Tower and Smith of the Geological Survey in 1897 and again by Lindgren and Loughlin in 1911, but no detailed work was done until after 1943 when a field party headed by T. S. Lovering began a study of the entire East Tintic district. The history of the development of exploration concepts is summarized under Historical Summary.

The East Tintic mining district is in the east-central part of a north-trending fault-block mountain range near the eastern margin of the Great Basin; dominant structures of the range are a north-trending syncline on the west and a less well exposed anticline on the east. Both folds are cut by an intersecting system of transcurrent strike-slip faults and by minor thrust faults and normal faults of moderate displacement. A strong west-

[1] Publication authorized by the Director, U. S. Geological Survey.

dipping thrust fault cuts the anticline a short distance east of the fold axis, but is hidden by Eocene lava throughout the East Tintic district. The pre-Tertiary rocks range from Lower Cambrian to Upper Mississippian and exceed 7,000 feet in total thickness; they are dominantly marine limestone and dolomite except for a thick basal Cambrian quartzite. The Tertiary rocks are chiefly dacitic lavas and pyroclastic deposits that are intruded by moderately persistent dikes and irregular bodies of monzonite and quartz porphyry. Nearly all the faulting and folding took place before the extrusion of the lavas on a rugged Eocene erosion surface. At about the time of the intrusion of monzonitic magma, many of the faults in the Paleozoic rock were re-opened and in the overlying lava some fracturing took place which was later accented by hydrothermal alteration.

Most of the ore mined in the East Tintic district has come from lead-zinc-silver replacement bodies in shattered jasperoidized hydrothermal dolomite at the intersection of low angle faults and steep mineralized northeast-trending cross fractures.

The U. S. Geological Survey studies of 1943 to 1957 concentrated on detailed mapping of geology and alteration in the East Tintic district, together with field and laboratory studies of the relation of alteration to stages of mineralization and ore deposition. Trenching and core drilling were carried on after World War II to aid in interpreting the sub-rhyolite geology and the Chief Oxide area was one of four localities tested by drilling. Study of the fossils, lithology, and alteration shown here in a deep drill core, together with the knowledge of the regional geology led to an essentially correct interpretation of sub-rhyolite structure in the strongly discordant underlying Paleozoic rocks in which a mineralized tear fault cuts a strong thrust fault, and to the conclusion that ore stage mineralization was present in substantial amounts in the Paleozoic rocks below the Chief Oxide alteration patch in the quartz latite lava. Subsequent geothermal and geochemical work strengthened this conclusion, and the recent development work of the Bear Creek Mining Company, which sank the Burgin Shaft, has shown the presence of lead-zinc-silver ore of commercial grade in substantial amount in blind ore bodies below the lava blanket in the Chief Oxide area.

INTRODUCTION

THE Burgin Shaft in the Chief Oxide area of the East Tintic district, Utah, (Fig. 1) promises to add another important blind ore body to the small but select list of the district's productive blind ore shoots—which have furnished virtually all of the $110,000,000 worth of ore ($75,000,000 net from smelter) credited to the East Tintic district. It and the adjoining main Tintic mining district are officially defined as two districts, but are often referred to as the Tintic mining district; total production of the combined districts is approximately $430,000,000 (gross), of which more than 22 percent has been paid out in dividends. The background and some of the details of the work that resulted in the discovery of the ore body opened by the Burgin Shaft exploration should be relevant to the search for ore in other areas, and we believe they serve to illustrate the effective utilization by private enterprise of investigations appropriate to a government Geological Survey. The Chief Oxide discovery not only opens up an entirely new area of the East Tintic district for deep exploration, but also establishes the value of certain discovery techniques, which may be successful in areas far removed from the Burgin Shaft.

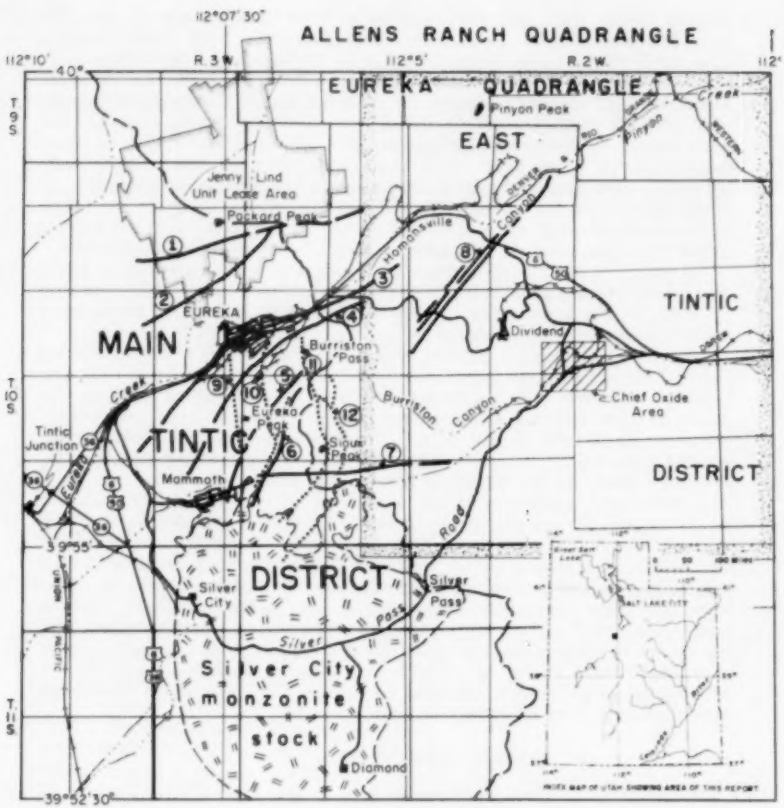

FIG. 1. Index map of the East Tintic district, Utah.

ACKNOWLEDGMENTS

The geologic studies of the U. S. Geological Survey preceding the Chief Oxide discovery were conducted in an environment of close and friendly cooperation with the mining companies active in the East Tintic mining district. Every facility required in examining underground workings and surface

exposures was freely extended to us by the principal property holders in the Chief Oxide area, i.e., the Chief Consolidated Mining Company and the Tintic Standard Mining Company. Although limitations of space make it impossible to list all who have facilitated our work we wish to make special mention of the courtesies and assistance received from C. A. Fitch, Sr., and C. A. Fitch, Jr., technical consultant and president respectively of the Chief Consolidated Mining Company; from M. D. Paine, vice-president of the Tintic Standard Mining Company; and from Mayer G. Hansen and John K. Gustafson of the Newmont Mining Company (in 1947–48).

Many geologists and engineers who have been associated with these companies, and others who are or have been associated with other companies in the district have made tangible and intangible contributions to our work by their interest and suggestions. Special mention should be made of the many stimulating discussions with R. C. Gebhardt of the E. J. Longyear Drilling Company, who maintained a most friendly, continuing, albeit a somewhat skeptical, interest in the alteration studies of the Survey.

HISTORICAL SUMMARY

Work Prior to 1943.—Ore in the Tintic district was first found late in 1869 and within a few years most of the major ore bodies that cropped out were being mined. As the ore bodies were developed, it soon became evident that they were in zones that had a northerly trend, but that the individual shoots were very irregular and formed pockets, chimneys, or pipes, which range from nearly horizontal to nearly vertical. Most of the ore bodies were found along three major "ore channels" that trend nearly north–south, and are known as the Eureka (or Gemini), the Mammoth, and the Godiva-Sioux Mountain ore zones (Fig. 1).

The first systematic study of the district was made by Tower and Smith (*27*) during the latter half of 1897. At this time they mapped the Tintic quadrangle of 234 square miles and also studied most of the accessible mines in the district. There was abundant proof even then that some large elongate bodies of ore were present that had little or no surface indication, and much fruitful prospecting was done on the basis of ore trends. In their suggestions for exploration, Tower and Smith (*27*, p. 711) say, "when an ore body is found, the safest method is to follow it with levels, winzes, or upraises and subsequently to extend workings from the mine shaft to the ore bodies thus developed. When an ore-bearing fissure ceases to carry ore it is safest to look for a cross fissure for the continuation of the ore before following the barren fissure or if this method fails crosscuts should be extended frequently to find other fissures."

One of the most popular—and successful—methods of finding ore at this time, and a technique that is still valid, was the projection of the long axes of stopes into the unexplored areas ahead, followed by underground exploration in the favorable areas thus located. A map, a straight edge, and a bold spirit led to the discovery of many of the major ore bodies in the Tintic district. It was essentially this method that in 1912 led to the last discovery of a major

ore body in the main Tintic district. Mr. Walter Fitch, Sr., a Michigan iron miner, projected the Mammoth ore zone north far beyond any known ore, sank a shaft some 1200 feet deep under "Poverty Flat" just south of the town of Eureka, and proved that his judgment was shrewd. Several years earlier in 1905, the fourth—and last—major ore channel of the main district, the Iron Blossom ore zone, had been found in quite a different fashion by Jesse Knight. This discovery is generally ascribed to a dream he had in which he saw a "ribbon of silver ore" under the mountain, but Knight no doubt had carefully observed the mines near Eureka and had come to recognize the altered appearance of the country rock near ore bodies.

The importance of stratigraphic and structural controls of ore in the main district emphasized the need for more detailed geologic information than that contained in the Tower and Smith report (27); this need led to a restudy of the district by Lindgren and Loughlin (17) who spent two months in the field in 1911 and Loughlin briefly revisited the district in 1913, 1914, and 1916. Both the revision of the Tower and Smith quadrangle map and of their detailed map of the main Tintic district at 1:9600 (28) were completed by Loughlin in 1911. The four stratigraphic units into which the entire Paleozoic section had been divided by Tower and Smith were further subdivided by Lindgren and Loughlin into essentially the same major units that are recognized today in this area, numbering 16 readily distinguishable formations from the Cambrian Tintic quartzite to the Mississippian Humbug formation. The detailed work of the Survey since 1943 has caused only minor changes in the nomenclature and subdivisions of the section, which now comprise 18 formations (Table 1). Loughlin's revisions (17) of the maps in the Tintic Special Folio (28) added much useful structural, stratigraphic, and petrologic information, and Loughlin's map showed for the first time the general areas of pyrometasomatic alteration in the carbonate sedimentary rocks on the north side of the Silver City monzonite stock.

G. W. Crane was taken on as geologist in 1915 at the Chief Consolidated mine, and soon began an intensive study of the sedimentary rocks and subdivided many of the formations into several units (9), most of which are now recognized as members of the formations as designated today. This work was quickly utilized by mining geologists as an indispensible aid in deciphering the details of geologic structure throughout the district.

The discovery by Jesse Knight in 1905 of the essentially blind ore run of the Beck Tunnel-Iron Blossom some distance east of the nearest developed ore run suggested the possibility of additional ore bodies and ore runs still farther east. But it was not until 1916 that any real strike was made in the previously unproductive area known as the East Tintic district.

In the continuing search for new ore, desultory exploration was carried on by a few stubborn and unreasonable optimists in the region north and east of the main Tintic district in an unproductive terrain dominated by volcanic rocks and generally considered hopeless. Although there were many patches of much altered ground within the lava terrane, a few of which were in the islands of sedimentary rocks that projected through the lava cap, only a very

few weak showings of oxidized ore rewarded the earliest ventures in the East Tintic district.

Many claims were staked in the East Tintic district before the turn of the century, but the only locality where anything approaching an outcrop of ore had been found was in the vicinity of the present Eureka Lilly shaft (Fig. 2), and it was from this area that the first recorded shipments of the East Tintic district were made in 1909. Near the Eureka Lilly shaft oxidized ore followed a small fault in the easily recognized Dagmar dolomite only a few hundred yards west of the jasperoidized outcrop of a bedding plane fault breccia between the Dagmar dolomite and the overlying Herkimer limestone.

E. J. Raddatz, who became interested in the area about 1906, believed that the Dagmar dolomite was an inhospitable host rock and reasoned that if it contained even a "showing" of lead and silver there was an excellent chance of finding a good ore body in the limestones of the Ophir formation below it. His reasoning was excellent, but he reckoned without knowledge of the complex of steep and low angle faults that localized ore and bewildered the miner. Finally, in 1916, after sinking two shafts, driving thousands of feet of drifts and crosscuts, and sinking hundreds of feet of winzes, the dogged persistence of Raddatz was rewarded by the discovery of the great Tintic Standard ore body. It was not, however, until a year later when the Tintic Standard No. 2 shaft (Fig. 2, no. 7) cut ore averaging 20 percent lead at a depth of 1174 feet and remained in ore for nearly 200 feet, that the full magnitude of the Tintic Standard find was appreciated. The excitement caused by this discovery led to a wave of prospecting by both major and minor companies throughout the East Tintic district and within a few years several other properties were in production—all from blind ore bodies.

Largely because the Tintic Standard No. 2 shaft was sunk in an area of pyritized lava or "bleached rhyolite," much of the prospecting stimulated by the discovery of the Tintic Standard ore body took the form of shaft sinking in various areas of altered Packard quartz latite lava. Within a year, shafts were being sunk at the Eureka Bullion, the Iron King, the Copper Leaf, the Eureka Lilly, the Zuma, and the Apex Standard, but with the exception of the Eureka Lilly, none of them proved especially productive.

When it became clear that the Tintic Standard ore body was to be one of the great lead-silver deposits of the world, the district was studied by many mining geologists, among them Paul Billingsley, who was able to deduce by purely geological reasoning the probable presence of ore in the North Lily ground. He found that the lava cap was pre-mineral and hence had been exposed to alteration by mineralizing solutions coeval with the ore, that certain persistent dikes and fissures are continuous through the rhyolite and into the limestone below, and he was able to utilize the extensive underground workings of the Tintic Standard mine to study the structure in the sub-rhyolite Paleozoic rocks and the occurrence of ore. The results of this work (3) led to the discovery of the North Lily ore bodies. A long crosscut from the Tintic Standard 700-foot level was driven to cut the intersection of the persistent North Lily pebble dike zone with the strong fault that brought beds of the Ophir formation in the hanging wall against the Tintic quartzite in the

footwall; an excellent blind ore body was found here, and the rapid development of the North Lily mine into the second major producer of the area followed.

The discovery of gold ore in the Eureka Standard mine in 1928 added another profitable group of blind ore bodies to those already exploited. Although Raddatz began active development work in the Eureka Standard in 1923, the poor quality of the mineralization found in the hanging wall of the Eureka Standard fault discouraged exploration. After Billingsley's discovery of the North Lily ore, however, geological methods were utilized in the Tintic Standard mine. This geologic work is credited not only with the discovery of substantial new and better grade ore bodies in the Tintic Standard mine but also with the exploration that led to the discovery of the rich gold ores in the quartzite footwall of the Eureka Standard fault late in 1928 (14, p. 18).

In spite of much shaft sinking and geological work supplemented by diamond drilling, no further discoveries of importance were made in the district until that of the Burgin shaft in 1958.

Billingsley's studies of the geology, ore controls, and the relation of ore to alteration are reported very incompletely in print (3, 5) but were the subject of many detailed private reports to some of the major mining companies of the district. According to Howd (13), many of the conclusions later reached by the present writers (19) concerning alteration were anticipated by Billingsley in his private reports. These reports, unfortunately, were not seen by the writers. Earlier geologists, however, had already made substantial contributions to the subject of alteration within the district. Tower and Smith (27, p. 658–664) recognized that chlorite, epidote, sericite, serpentine, talc, magnetite, pyrite, and quartz were formed by the hydrothermal alteration of monzonite and lavas. Contrary to opinion widely held at that time, they stated that silicification or the introduction of pyrite is characteristic of hydrothermal alteration rather than of weathering. They also noted that much of the pyrite was formed by sulfidization of magnetite or other iron-rich minerals of the rock.

Lindgren and Loughlin also studied the hydrothermal alteration and the apparent zonation outward from ore-bearing veins in igneous rocks. The inner zone, according to them (17, p. 98), was completely replaced by quartz and pyrite accompanied locally by barite and a minor amount of sericite. Ore, they noted, is confined to the completely silicified zones. The margins of these zones grade outward into a quartz-sericite-pyrite rock where the original texture of the host is well preserved. Farther from a vein, strongly altered rock, which is bleached white on the weathered surface, grades laterally into a gray or greenish-gray rock incompletely replaced by sericite, chlorite, epidote, calcite, and a minor amount of pyrite and silica. In jasperoidized limestones and dolomites the passage from quartz into unreplaced rock was described as abrupt, although some dolomite and calcite spar were observed near the margins of the jasperoid. Carbonate veins were observed at a considerable distance from commercial ore and their distribution seemed comparable to that of the less intensely altered chloritized igneous rock.

The conclusions of Billingsley that were generally accepted in the district,

as well as those of Survey geologists and other mining geologists, were summarized by Kildale in his section "Guides to ore deposits in the Tintic district" in his unpublished but available thesis (14, p. 141–143). Favorable beds were universally regarded as the most reliable guides to ore deposits if in the neighborhood of mineralized fissures or where strike fissuring had been localized along such beds. The fracture system regarded as most closely associated with ore deposition was the northeastward-trending system in which the general strike averages about N. 30° E. Where sedimentary rocks are steep and strike in a northerly direction, strike fissuring seemed an effective substitute for northeast fissures. "Crease" folds and minor thrust faults associated with intrusive breccias, strong mineralizing fissures, or intrusive breccias that are mineralized, were recognized as being closely associated with ore bodies in some localities.

Guides to ore less direct than those listed above, but commonly used in outlining a general target area, were: 1) Major fault zones, known to be intimately associated with loci of mineralization—suggesting further search along the strike of such zones. 2) "Bleached" volcanic rocks, in which the sequence of alteration moving outward from centers of intrusion, as noted by Kildale (14), is silicification, sericitization, and chloritization. 3) Both pebble dikes and intrusive igneous rocks were regarded as favorable, but intrusive igneous rocks were not believed to be as closely associated with mineralization as were the pebble dikes or the alteration halos in the volcanic rocks. Billingsley was probably the first to recognize hydrothermal dolomitization of the limestones and to note that in the overlying lavas there was an allied alteration—unspecified in the printed article but presumably magnesian and therefore chloritic (5, p. 117).

U. S. Geological Survey Studies—1943–1955.—In 1942 and 1943, during World War II, the temporary success of the German submarine campaign against Allied shipping had reached such proportions that grave concern was felt for the continuing supplies of ores and other raw materials from foreign sources. It seemed quite possible that in the event of a long war, the United States would require many new sources of ore within her own boundaries to augment those currently in use. As part of the long range program designed to prepare for such contingencies, a detailed and comprehensive study of known blind ore bodies was decided upon, and the East Tintic district was chosen for an intensive study of the chemical, physical, and geologic expression of blind ore bodies at the surface. A field party worked continuously in the district from early in 1943 until 1946; field work and office work were carried on with many interruptions from that time until 1955 when the project was temporarily recessed.

At the start of the work it seemed probable that spectrographic examination of altered rocks above blind ore bodies might indicate the presence of underlying ores, but spectrographic analyses of ore minerals, gangue minerals, fresh and altered lava both above and remote from ore bodies yielded no correlation that could be relied upon. In many places the altered lava above the ore bodies carried perceptibly smaller amounts of the ore metals than did fresh unaltered rock. This proved to be the result of both hydrothermal

and supergene leaching of the metals originally present in the unaltered lava in areas where little if any metal had been added to the altered rhyolite during the formation of the blind ore bodies at depth. No correlation between minor elements and blind ore was found. After the apparent failure of the geochemical prospecting method, attention was centered for several years on petrographic and geologic studies. As this work proceeded, it became evident that certain types of alteration were much more common than other types near blind ore bodies, and that a study of alteration in conjunction with other geologic techniques promised a chance of materially increasing the discovery rate. As the area of detailed mapping (1:4,800 and 1:9,600) was enlarged, several places where blind ore bodies might be present in the rocks underlying the lava cap became apparent. Following World War II attention was given to the possibility of further localizing target areas by means of geophysics and geochemistry. Geophysical work in the complex structure of the Tintic mining district has been relatively unsuccessful to date, however, and it seems probable that substantial advances must be made in this technique before it can be used profitably to find deep-lying blind ore bodies under the adverse geological conditions that characterize many of our western mining districts.

In the second attempt to use geochemical methods, newly developed rapid colorimetric techniques for determining traces of metals were used with considerable success. Geochemical work and the study of alteration, when carried on in conjunction with detailed geological work, promised to greatly facilitate the search for blind ore bodies in this and other districts. Three areas in the East Tintic district were selected for study: one up-rake from the large, known blind ore shoots of the Tintic Standard mine, the tops of which were some 700 feet below the surface, and two other areas—the Greyhound and Chief Oxide areas—where strong pyritic alteration in the lava cap suggested possible target areas at depth. This work, which was reported in 1948 (18), encouraged the belief that geochemical work could pick up anomalously high heavy metal content in altered lava up-rake from blind ore bodies, especially where the cap rock was fissured. The geochemical tests in the Greyhound area, which is a half mile southeast of the Tintic Standard mine, showed little evidence of heavy metals, and later drilling and underground openings indicate that no replacement ore is associated with this alteration zone immediately below the lava. In the Chief Oxide area, however, the geochemical tests were definitely encouraging, as was reported in the paper by Lovering, Sokoloff, and Morris (18).

During 1948 Almond and Morris (1) carried on additional geochemical studies, which showed that anomalous amounts of zinc and lead are concentrated in altered extrusive rocks 300 to 500 feet above the horizontal north–south, pipe-like Iron Blossom ore zone of the main Tintic mining district, but only where it crosses the east-west pre-mineral Sioux-Ajax fault zone (Fig. 1). To the north and south of this fault zone no geochemical anomaly was perceptible above the Iron Blossom ore zone. Evidently a leakage channel to short circuit some of the ore solution is essential if the "metalized smoke" of the blind ore body is to ascend into the altered lava about it.

At the conclusion of this work, Morris made a hasty reconnaissance along the easterly projection of the Sioux-Ajax fault to sample in the altered lavas between the Iron Blossom zone and the Trixie ground. Two of the samples, one from the altered lava and one from altered limestone adjacent to the Silver Pass road (Fig. 1), were anomalously high in zinc and called attention to this area as worthy of further study. Later drilling here for the Geological Survey established the presence of ore minerals at depth.

Additional geochemical work on the mobility of the heavy metals in ground water and on the primary dispersion pattern of heavy metals in carbonate and in quartz-monzonite wallrocks was carried on in the years following 1948 (22). This study together with the earlier work firmly established the value of geochemical exploration in the search for blind ore bodies in the area, and suggested some of the limitations as well as the possibilities of such methods.

By 1950 the mapping of the district and the study of alteration had proceeded far enough to focus interest on certain areas where drilling beneath the lava cap promised to reveal information of major importance in appraising the value of the various geological and geochemical techniques utilized by the Survey. Four target areas were chosen and three of them were drilled during 1950–51. The fourth was drilled in 1952 when a substantial amount of additional drilling was done in the Chief Oxide area. Two of the four "wildcats" proved the presence of lead-zinc minerals, and one of the two was in the Chief Oxide area—the subject of this paper.

The major contributions of the work of the Geological Survey towards delineating target areas in the East Tintic district were the detailed geologic mapping of formations, structure, and alteration (21), the better understanding achieved of the relation of hydrothermal alteration to intrusions and to ore (19), and the development of geochemical techniques suited to the study of bedrock geochemical anomalies related to blind ore bodies.

The major conclusions regarding the structure, alteration, and mineralization in the Chief Oxide area were announced at the Salt Lake City meeting of the Mining Congress in 1950, after the U.S.G.S. No. 1 drill hole had been completed. It has long been a practice for Survey geologists to discuss orally with owners of mining properties, when requested, the results of the geologic work within their property boundaries. We were therefore able to make pertinent information available orally to individual owners and to mining companies on the properties that they owned. This led to some privately supported drilling and exploration both before and after the Survey drilling program of 1950–51, including the work carried on by the Bear Creek Mining Company, which ultimately resulted in the Chief Oxide discovery. Details of the work relating to the Chief Oxide area are given further on.

GEOLOGY

Regional Setting.—The East Tintic mining district is in the east-central part of the East Tintic Mountains, a north-trending fault-block mountain range near the east-central margin of the Great Basin. The range is aligned

with the Oquirrh Range to the north and the Gilson and Canyon Ranges to the south, and is separated from the mountain ranges that are parallel to it on the east and west by structural valleys that are deeply filled with lacustrine and alluvial deposits.

During Cretaceous time the rocks of this part of the Great Basin were strongly compressed, resulting in the development of great overthrust faults, some of which are many miles in length and breadth. Associated with these large thrust sheets are tear faults, broad folds, and other structures. Although the only thrusts exposed in the East Tintic Mountains have stratigraphic displacements of a few hundred to a few thousand feet, regional geologic studies and stratigraphic correlations indicate that the Paleozoic and Precambrian rocks of the range are characteristic of those found in the upper plate of the great Charleston-Nebo thrust fault exposed in the Wasatch Range about 20 miles to the east (2, 11) and of rocks found in the lower plate of the Sheeprock thrust fault exposed 15 miles to the west in the Sheeprock and West Tintic Ranges (6, 26). These relations suggest that the range is part of an allochthonous mass of rock that is underlain at depth by a low-angle fault with a displacement of tens or even scores of miles, and may at one time have been overlain by another great thrust sheet, probably of similar magnitude.

The dominant structures recognized in the East Tintic Mountains in the latitude of the East Tintic district are two great folds, a north-trending asymmetric syncline on the west and a less well exposed anticline on the east. These folds are cut by an intersecting system of transcurrent strike-slip faults, and by thrust faults and normal faults of moderate displacement. The axis of the syncline, which coincides with the west boundary of the East Tintic district, lies about two miles west of Dividend and follows the east flank of Sioux Peak and Godiva Mountain where the youngest Paleozoic formations in the district are exposed. The beds in the western limb of the syncline are nearly vertical and comprise a prominently exposed section extending from the Lower Cambrian Tintic quartzite at the base to the Upper Mississippian Humbug formation. The more gently dipping beds in the eastern limb are, in large part, covered by volcanic rocks, but drill holes and mine workings show the axis of the anticline to be about ½ mile east of Dividend. The structure of the Paleozoic rocks in the area underlain by the common limb of the syncline and anticline is shown in Figure 2.

Igneous and Sedimentary Rocks.—The pre-Tertiary rocks exposed in the East Tintic district range in age from Early Cambrian to Late Mississippian and exceed 7,000 feet in total thickness. Except for a thick basal Cambrian quartzite, these rocks are dominantly marine limestones and dolomites that were deposited in relatively shallow water near the margins of a large geosynclinal basin.

The Tertiary and post-Tertiary rocks include pyroclastic deposits, lavas, and porphyritic intrusive rocks of middle Eocene age, and various unconsolidated deposits of Pleistocene and Recent age. Steep contacts between the extrusive rocks and the underlying Paleozoic formations, marked lateral variations in thickness of the volcanic deposits, and irregular distribution of

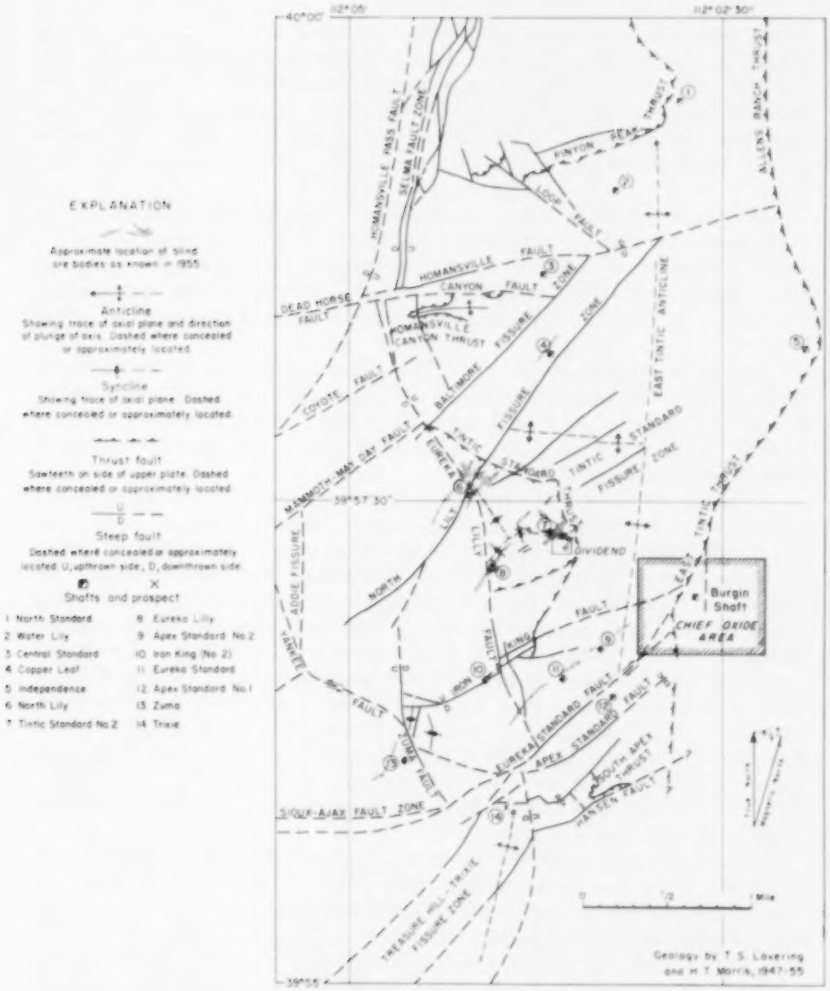

FIG. 2. Subsurface structure map of the East Tintic mining district.

the basal members of the volcanic rocks all indicate that the East Tintic district was an area of moderately high relief at the beginning of volcanic activity. The absence of major folds, thrusts, and tear faults in the lavas indicates that the principal compressive structural deformation of the area took place before the lavas were erupted.

Intrusive bodies are numerous in the East Tintic district but none is large; they comprise many moderately persistent dikes, many irregularly shaped to cylindrical bodies ranging from fingers of intrusive rock less than ten feet in diameter to stocks more than a thousand feet in diameter, and severals sills and diatremes. The largest pluton in the East Tintic Mountains lies just southwest of the East Tintic district near Silver City, and is a stock of monzonite porphyry with a total surface area of about seven square miles.

The unconsolidated and semiconsolidated deposits are thickest and of greatest variety in the larger gulches and in the broad valleys that border the range. They are all post-ore and are unimportant in exploration except as they totally conceal the underlying bedrock. Details of the stratigraphy, thickness, lithology, and current nomenclature of the rocks are summarized in Table 1.

Structural History of the East Tintic district.—As shown in Figure 2, even a generalized map of the major elements of the Tintic structure shows a complex pattern of steep- and low-angle faults. The interrelations of these features can perhaps be pictured best by following the probable course of their development.

Although the East Tintic area may have been uplifted in a broad gentle, east–west fold at an early time, perhaps at the end of the Jurassic, most of its structural features are related to regional east–west compression during Cretaceous time. The first effect of this compression was probably the gradual uplift of the East Tintic anticline, and as it developed, minor folding crumpled the longer more gently sloping west limb between the crest of the anticline and the trough of the Tintic syncline to the west. The minor crumpling was accompanied by small tear faults and locally by minor thrust faults such as the Pinyon Peak thrust fault, the Tintic Standard thrust fault, the South Apex thrust fault, and the Homansville Canyon thrust fault. Eventually, when the East Tintic anticline had risen to a critical elevation above the syncline that bordered it on the east, a major thrust developed—the Allens Ranch-East Tintic thrust fault—and much of the compressive stress in the anticline was relieved.

Contemporaneous with the formation of the Allens Ranch-East Tintic thrust are many tear faults, which strike from northeast to east-northeast. These faults include several in the Allens Ranch quadrangle as well as some that are well exposed in the East Tintic district. The most impressive of the tear faults is probably the Eureka Standard fault of the East Tintic district, but it is believed that the nearby Apex Standard and Hansen faults are also tear faults related to the development of the East Tintic thrust fault.

The next major event in the structural history was probably the development of the North Tintic anticline, which lies west of the Tintic syncline. In this asymmetric anticline, which faces to the east, folding and faulting were concentrated north of the steep northeasterly Paxman fault, which crosses the main Tintic district about 4,000 feet northwest of Eureka (Fig. 1). Much of the compression resulted in northeasterly tear faults and a general extension of the range in a north–south direction. Some of these tear faults

TABLE 1

GENERALIZED SECTION OF IGNEOUS AND SEDIMENTARY ROCKS IN THE EAST TINTIC DISTRICT

Series	Formation (Member or constituent units shown in parentheses)	Thickness (in feet) in or near East Tintic district	Character
Recent	Alluvium	<100	Alluvium: gravel, sand, silt, and clay.
	Colluvium	<200	Colluvium: creep mantle, slope wash mantle, and talus.
		Unconformity	
Pleistocene	Upland deposits younger than Lake Bonneville	<200	Talus, creep mantle, slopewash, fanglomerate, and alluvium.
	Lake Bonneville deposits	<200	Gravel, sand, silt, and clay deposited near the shore of glacial Lake Bonneville.
	Upland deposits older than Lake Bonneville	<200	Talus, slopewash, fanglomerate, terrace and pediment gravels, and stream-channel alluvium.
		Unconformity	
Eocene	Stocks, plugs, dikes, and sills.		In approximate order of abundance: 1) biotite-hornblende monzonite porphyry and locally quartz monzonite porphyry, 2) biotite-augite monzonite porphyry, 3) hornblende-biotite latite porphyry, 4) biotite-augite latite porphyry, and 5) biotite-augite andesite.
	Pebble dikes		Dike-like bodies (commonly silicified) of injection breccia consisting chiefly of angular to rounded fragments of quartzite, with minor fragments of shale and rare limestone in a matrix of comminuted quartz, carbonate rock, or monzonite.
	Laguna Springs latite	0–+3,000	In sequence: 1) a basal tuff, 2) a lower flow series, 3) an intermediate tuff and agglomerate, 4) an upper flow series, and 5) a thick agglomerate, all with the general composition of biotite-hornblende-augite latite; however, hypersthene is present instead of hornblende in some flows.
	Packard quartz latite	0–+2,300	In sequence: 1) a basal tuff, 2) a thin lower vitrophyre, 3) a massive flow unit, and 4) an upper vitrophyre, all with the general composition of biotite quartz latite.
		Unconformity	
Eocene(?)	Apex conglomerate	<300	Angular fragments of quartzite, limestone, and shale in a brick-red claystone matrix; unit is medium to coarse-grained, and displays virtually no bedding.

[1] Thickness in East Tintic district.
[2] Thickness in central part of main Tintic district.
[3] Thickness in southern part of North Tintic district.

TABLE 1—*Continued*

Series	Formation (Member or constituent units shown in parentheses)	Thickness (in feet) in or near East Tintic district	Character
	Unconformity		
Upper Mississippian	Humbug formation	650[2]	Alternating beds of brown cross-bedded sandstone and light-gray locally cherty limestone with some thin units of dolomite and shale. In the northern and southern parts of the East Tintic Mountains the Humbug is overlain by a thick succession of Upper Mississippian, Pennsylvanian, and Permian strata.
	Deseret limestone	1,100[2]	
	(Uncle Joe member)	(535[2])	Chiefly medium- to light-gray, medium-bedded highly fossiliferous limestone, but includes some beds of fine-grained silty limestone that contain few fossils, and some medium-grained brown-weathering sandstones. Many of the limestone layers contain nodules and stringers of chert.
	(Tetro member)	(475[2])	Medium- to fine-grained, medium- and poorly-bedded blue-gray sandy or silty limestone containing abundant chert.
	(Basal phosphatic shale)	(90[2])	Sooty black phosphatic shale interlayered with dark-gray to black cherty limestone; includes near base one or more beds of carbonaceous, pelletal phosphorite. Ranges in thickness from 10 to 160 feet.
Lower Mississippian	Gardison limestone	500[2]	Upper one-third is medium blue-gray medium-bedded fine-grained fossiliferous limestone containing much nodular and layered chert. Lower two-thirds is medium to dark blue-gray prominently bedded fossiliferous limestone that is fine grained near base, but somewhat coarser grained in middle and upper parts.
	Fitchville formation	280[2]	
	(Curly limestone)	(1.5[2])	Distinctive bed of dense medium- and dark-gray crenulated limestone of algal origin.
	(Pink lithographic limestone)	(7[2])	Dense pinkish-gray limestone of high purity.
	(Sugary dolomite)	(58[2])	Medium- to dark-gray, medium-grained dolomite with one or more beds of novaculitic quartzite, or locally green chert, 10 to 20 feet below top.
	(Black dolomite)	(65[2])	Dusky blue-gray to black coarse-grained cherty dolomite with conspicuous almond-shaped pods of white calcite and dolomite 2 to 4 inches long replacing some of the chert nodules.
	(Blue shaly limestone)	(46[2])	Blue-gray thin-bedded fossiliferous limestone.
	(White limestone)	(50[2])	Massive coarse-grained light-gray to white limestone.
	(Blue flaky limestone)	(52[2])	Blue-gray thin-bedded argillaceous limestone containing numerous small round flakes with dark centers that are probably fossil fragments.
	(Sand-grain marker bed)	(.5[2])	Dull blue-gray sand-streaked limestone or brownish-weathering calcareous quartzite containing rounded to ovoid grains of frosted quartz from less than a millimeter to 5 mm in diameter.
Lower Mississippian and Upper Devonian	Pinyon Peak limestone	70[3]–76[2]	Medium- to light-blue fine-grained argillaceous limestone streaked with wispy veinlets and partings of brown-weathering mudstone; lower part massive, upper part thin-bedded.

TABLE 1—*Continued*

Series	Formation (Member or constituent units shown in parentheses)	Thickness (in feet) in or near East Tintic district	Character
		Unconformity (?)	
Upper Devonian	Victoria formation	280[2, 3]	Upper 70 or 80 feet is light-gray massive dolomite with irregular patches of coarsely crystalline dolomite which grades into the finer-grained dolomite matrix. Lower 200 feet consists of wood-ash gray medium- to fine-grained dolomite interlayered with brown-weathering dolomitic sandstone and quartzite, some of which was converted to a breccia shortly after deposition.
Upper and Middle (?) Devonian, Middle Silurian, and Upper Ordovician	Bluebell dolomite	490[2]	
	(Upper member)	(205[2])	Medium- to dark-gray, medium- to thick-bedded, medium- to coarse-grained dolomite, the upper third of which contains almond-shaped pods of white dolomite 1 to 2 inches long and ½ to 1 inch thick.
	(Colorado Chief marker bed)	(10[2])	Medium- and light-gray crenulated dolomite of algal origin.
	(Lower member)	(275[2])	Upper two-thirds is chiefly medium- to dark-gray, medium- to coarse-grained, thick-bedded dolomite; lower third is light-gray fine-grained dolomite in thin to medium beds, some of which are laminated.
Upper Ordovician	Fish Haven dolomite	285[2]–345[3]	Dark- and light-gray, thin- and massive-bedded, medium- to coarse-grained dolomite with nodules of chert sparsely distributed near the base and fairly abundant in the upper third; top marked by a massive bed of conspicuously mottled dolomite 30 to 100 feet thick known locally as the "leopardskin" marker bed.
		Unconformity	
Lower Ordovician	Opohonga limestone	850[2, 3] (Thins to 300 feet in southern part of North Tintic district.)	Light blue-gray, medium- to fine-grained, thin-bedded limestone with seams and layers of yellow-, pink-, and red-weathering mudstone which in cross section divide and rejoin in pattern resembling flattened hexagons. The lower 50 feet contains large nodules of white chert, and the base is marked by a bed of brown-weathering limy sandstone.
Upper Cambrian	Ajax dolomite	560[2]	
	(Upper member)	(350[2])	Medium to dusky blue-gray, medium grained prominently bedded dolomite containing much nodular white, pink, brown, and black chert.
	(Emerald member)	(30[2])	A massive bed of creamy- or grayish-white medium-grained dolomite mottled by irregular layers from 1 to 2 inches thick consisting of light-gray to white coarse-grained dolomite.
	(Lower member)	(180[2])	Medium to dusky blue-gray medium- to coarse-grained faintly mottled dolomite containing many pods and lenses of black and brown chert.
	Opex formation	245[3]	Alternating thin and thick beds of bluish-gray argillaceous limestone, calcareous oolite, flat-pebble conglomerate, and medium- and coarse-grained dolomite. One or more beds of red and green shale 5 to 20 feet thick occur at the top of the Opex in some places but locally are missing.

TABLE 1—*Continued*

Series	Formation (Member or constituent units shown in parentheses)	Thickness (in feet) in or near East Tintic district	Character
Middle Cambrian	Cole Canyon dolomite	820[2]	The upper 200 feet or so consists chiefly of dusky blue-gray medium-grained dolomite; some beds mottled, some contain small white twig-shaped bodies similar to those in the Bluebird dolomite. The lower 600 feet consists of alternating beds of light gray laminated dolomite resembling the Dagmar dolomite, and massive dusky blue-gray, locally "twiggy," dolomite of the Bluebird type. The light-gray beds weather creamy-white and the thickest creamy white weathering unit is 60 to 90 feet thick. The dark-colored beds are 10 to 30 feet thick.
	Bluebird dolomite	180–200[2]	Dusky blue-gray medium-grained thick-bedded dolomite, obscurely mottled on weathered surface; contains many white twig-shaped bodies $\frac{1}{8}$ to $\frac{3}{4}$ inches long and $\frac{1}{4}$ inch in diameter that appear to be of organic origin.
	Herkimer limestone (Upper member)	375–425[1] (175–225[1])	Medium blue-gray thin-bedded limestone, flat-pebble conglomerate and calcareous oolite; most beds separated by shale partings an inch or less to several inches thick.
	(Shale member)	(20[1])	Buff to greenish-gray, fissle, limy shale similar to shales in Ophir formation.
	(Lower member)	(180[1])	Blue-gray medium-bedded argillaceous limestone mottled by thin discontinuous layers and irregular masses of gray to yellowish-brown mudstone.
	Dagmar dolomite	80[1]	Medium- to light-gray fine-grained laminated dolomitic limestone that weathers creamy-white; it is medium to thin bedded, and characteristically breaks into small straight-sided blocks. Best marker in the Cambrian section.
	Teutonic limestone	420[1]	Upper part blue-gray medium- to fine-grained thin-bedded limestone with a few beds of pisolitic limestone; meddle part similar to upper part, but contains many more pisolitic beds; lower part blue-gray medium- to fine-grained medium-bedded limestone containing $\frac{1}{2}$- to 2-inch bands of gray- to yellowish-brown-weathering mudstone; basal bed contains globular structures, which are $\frac{1}{4}$ to $\frac{1}{2}$ inch in diameter, probably of algal origin.
	Ophir formation (Upper shale member)	410[1] (90[1])	Buff to greenish-gray, splintery-fracturing shale with numerous lenses of limy sandstone and sandy shale.
	(Middle limestone member)	(145[1])	Consists of 2 to 5 or more beds of blue-gray medium- to fine-grained mudstone-streaked limestone interlayered with olive-green shale in beds 3 to about 40 feet thick. The lowest of the limestone beds—the Ophir No. 1 limestone—is characterized by many fossilized fragments of trilobite tests and brachiopod shells.
	(Lower shale member)	(175[1])	Base marked by a bed of dark-brown sandy shale 1 to 10 feet thick which is overlain by a bed of brown-weathering medium-grained porous sandstone, but the lower 90 feet is mostly brownish-green fissile calcareous shale containing some thin sandstone in the lower part; a persistent brown shaly dolomite 10 feet thick occurs 90 feet above the base, and the upper 75 feet is a gray- to olive-green non-calcareous shale
Lower Cambrian	Tintic quartzite	2,300–3,200[2]	Dominantly light-colored prominantly-bedded medium-grained quartzite, but quartzite conglomerate beds are common throughout lower half of the formation and are the dominant rock within 300 feet of the base; beds of gray-green micaceous shale are common in upper 500 feet. Average thickness of Tintic is 2,800 feet, including a 2- to 30-foot bed of chloritized amydaloidal basalt about 980 feet above base. Only the uppermost beds are exposed in East Tintic district.

merely separate folds of different magnitude, whereas others pass into thrust faults of substantial displacement. The major northeasterly faults, which caused a northerly elongation of the range, are right lateral faults, whereas a conjugate set of northwesterly faults, so evident on the western side of the range, are left lateral faults in which the movement was a natural response to the east–west forces that raised the North Tintic anticline.

South of the Paxman fault the severe east–west compression that resulted in the conjugate fractures of the North Tintic anticline apparently induced a secondary southeasterly directed compression that caused left lateral movement along northeasterly fissures in the main Tintic district, and caused many minor folds and faults typical of a northwesterly compressive force. We thus find, between the Paxman fault on the northwest and the Hansen fault on the southeast, evidence of northwest to southeast compression, which is not apparent in the rest of the East Tintic Mountains. Such a stress would result if the area to the south of the Hansen fault acted as a stable buttress against which the block of ground south of the Paxman fault was pushed during the east–west compression noted above. The effects of the southerly compression are evident in the left lateral movement on the Beck, Centennial and Grand Central faults (Fig. 1) in the main Tintic district, in the folding of minor thrusts in the upper plate of the Chief Oxide thrust, as well as in the development of minor imbricate thrusting in the upper plate of the Tintic Standard thrust fault. Folding of the Homansville Canyon thrust probably occurred at this time and the minor folding of the South Apex thrust just north of the Hansen fault also reflects these forces. The intermittent and changing character of the forces along the northeasterly fractures is probably responsible for the alteration of thrusting and normal faulting in the Tintic Standard area.

With the completion of the major folding of the North Tintic anticline and the relaxation of the east–west compressive forces, major north–south faults that are later than the structures described above came into being. The first breaking along the Selma fault, the Eureka Lilly, and other northerly trending normal faults took place, and was followed at a somewhat later date by north–south tension and the development of large and persistent east–west faults such as those in the Burriston Pass area.

The beginning of volcanic activity in Eocene time was accompanied by much local movement concentrated chiefly along pre-existing faults—especially near centers of vulcanism—and by the development of northeasterly compressive stress. The intrusion of monzonite porphyries during the volcanic episode quite apparently was contemporaneous with the appearance of several northeasterly tension fissures, many of which became major avenues of escape for hydrothermal fluids emanating from the monzonitic intrusions at depth. Comparatively little of the post-lava and post-mineral faulting is later than the period of mineralization, but movement along Basin and Range type faults, which began locally as early as the volcanic activity, continued intermittently through the Tertiary and Pleistocene, and some activity is quite recent. The cumulative effect of the Basin and Range type of faulting has been to drop the valley floor more than a mile beneath the top of the valley

fill in the areas just west of the East Tintic Mountains, but so far as is known, bounding faults to the east of the mountains are either lacking or of small displacement.

Alteration and Ore Deposits.—Most of the ore mined in the East Tintic district has come from lead-zinc-silver replacement bodies in calcareous Paleozoic formations, but pyritic copper-gold veins and argentiferous gray copper-gold telluride veins in the noncalcareous Tintic quartzite have contributed several million dollars to the total production of the district. As the water level is more than 1,000 feet below the surface in the areas thus far exploited, vadose water and oxidation have greatly changed the character of the primary ores and have yielded a wide variety of oxidized ore minerals. The primary ores in the base metal replacement deposits are made up chiefly of sphalerite, galena, pyrite, and minor ruby silver in a quartz-barite gangue; gold, enargite, tetrahedrite, and pyrite are the chief primary minerals of the auriferous copper veins in the Tintic quartzite; and various gold and silver tellurides, tetrahedrite, and pyrite are the chief primary minerals in the gold telluride veins of the Tintic quartzite.

The replacement deposits are commonly in shattered jasperoidized limestone at the intersection of low-angle faults and steep mineralized northeasterly-trending cross fractures. Where the walls of the northeasterly fissures are quartzite they very commonly carry barren pyrite or pyritic copper ore below or on strike with lead-zinc replacement deposits in carbonate host rocks. The gold-copper ores rarely occur within formations younger than the Tintic quartzite; bodies of lead-zinc ore are just as unusual in veins having quartzite walls—although such ores may occur in carbonate rocks at the same elevation within a very short distance and on strike with an auriferous vein. Most of the replacement ore bodies have a casing of pyritic jasperoid around them ranging from a few feet to 250 feet in thickness. This siliceous casing is in turn generally surrounded by an envelope of hydrothermal dolomite, and in many places small bodies of strongly argillized dolomite intervene between the jasperoid and the hydrothermal dolomite. Above or at the end of elongate replacement ore bodies, the dolomite may be replaced by manganiferous carbonates. These carbonates are represented by secondary manganese oxides above the water table. This somewhat zonal arrangement, although partly fortuitous, is helpful in exploration. Locally the ores may be found against unaltered limestone walls or any of the alteration facies noted above. This fact strongly suggests that the zonal arrangement, in part at least, is the result of alteration performed by solutions that followed the same general path at different times, and that it is not contemporaneous with the ore stage.

In the work reported on by Lovering and others (19), five stages of alteration are recognized, and each stage is thought to be separated from the next by a time interval: (1) the early barren stage; (2) the mid-barren stage; (3) the late barren stage; (4) the early productive stage; and (5) the productive (ore) stage. In the early barren stage, the limestone was altered to dolomite, and in the basal part of the volcanic series some chlorite, zeolite, and quartz were introduced. The solutions causing this alteration followed

more routes to the surface and penetrated farther than those of the later alteration stages, but in about nine areas out of ten the later ore solutions followed a conduit previously used by the early dolomitizing solutions. The chloritic and dolomitic alterations therefore outline virtually the entire hydrothermal plumbing system, only a small part of which was used by ore-stage solutions. No pyrite or other sulfides accompanied the early barren stage.

The mid-barren stage is characterized by argillic alteration, and it is most extensive in volcanic rocks, but as noted earlier it is also locally prominent in calcareous rocks near hydrothermal conduits. Argillization is concentrated around centers of intrusion, and in many of the resulting alteration halos a zonation within the mid-barren stage is recognized. This zoning, where complete outward from a conduit, is characterized by the following dominant minerals in dolomite: (1) hematite and quartz, with or without hypogene manganese oxides; (2) dickite, kaolinite, or halloysite; (3) kaolin minerals and fluorite, or alunite; (4) diaspore, fluorite, and kaolin minerals with some mica and mixed-layer chlorite-montmorillonite, or alunite and kaolinite; (5) "sanded" (granular) dolomite with minor kaolinite; (6) massive dolomite. In igneous rocks the zonation is similar except that fluorite, hematite, and manganese oxides are rare; hydromica and mixer-layer clays are common; the outer zone is generally marked by quartz and inconspicuous alunite, or rarely by zunyite; and beyond it there is commonly a montmorillonitic transition zone between the kaolin group clays and the slightly sericitized and chloritized fringe zone of alteration. In many places, especially in the lavas near centers of intrusion, barite, alunite, and cubic pyrite indicate the presence of sulfur acids during the time of argillic alteration, but in other localities the development of fluorite and the lack of sulfides or sulfates suggest that halogen acids were dominant. This alteration stage was characterized by substantial leaching of nearly all the constituents of the rock and by corresponding increase in porosity. This is especially evident in the carbonate sediments where the partial disintegration of dolomite gives it a granular appearance and a sandy feel that justifies the use of them term "sanded dolomite."

The late barren stage is characterized chiefly by jasperoid, cubic pyrite, some barite, and sparse chlorite in the sediments; and by barite, cubic pyrite, calcite, allophane-bearing quartz, and minor delessite in the overlying volcanic rocks. Late barren stage alteration is localized near major channels of mineralization and is more closely related to ore than to visible intrusives. The late-barren stage jasperoids seldom extend far beyond the levels of ore deposition, but pyrite and calcite of this stage travelled much farther. Cubic pyrite is generally disseminated in the lava directly above or somewhat up-dip from fractures that have guided pre-ore alteration in the underlying Paleozoic rocks. Calcite of replacement origin may be present in the lavas for hundreds of feet laterally beyond the pyritic zone; it is commonly up-rake from fissures in underlying Paleozoic rocks and spreads out on the footwall side. This probably represents calcium displaced during silicification of nearby dolomite underlying the lava, and although spread through a relatively large volume of rock, such calcite suggests jasperoid in concealed carbonate rocks and therefore is an important alteration guide to concealed ore bodies.

The early productive stage is indicated by sericite, minor clear quartz, and some pyritohedral pyrite. Although this stage is earlier than the ore stage, pyritohedral pyrite is in large part contemporaneous with ore. The alteration may follow fissures above an ore body for several hundred feet but does not extend into the wall rocks more than a very short distance.

The productive stage is, of course, distinguished by the presence of sulfides of the base metals and by sulfantimonides and sulfarsenides of copper and silver and by gold and tellurides, all accompanied by very little gangue.

Weathering has masked the hydrothermal alteration effects in many areas. The disseminated pyrite of the mid-barren and late-barren stages is generally indicated by limonite-stained areas in the lava and rarely does one find even a pseudomorph of pyrite in the oxidized pyritic halo at the surface. Oxidation of pyrite, however, generates sulfuric acid, which is an argillizing agent of moderate intensity itself, and which quite commonly has caused the brown iron-stained cap of the pyritic zone to be surrounded by bleached, slightly argillized rock. In many places there is a band of manganese oxides between the limonite-stained cap rock and the supergene bleached zone, where the outward moving acids were neutralized beyond the pyritized zone.

Recognition of the alteration products of the various stages of hypogene alteration and appreciation of supergene effects are indispensible in mapping the altered rocks of the district and in appraising their significance.

Ore Guides.—Because a favorable combination of structure and lithology is essential to localization of ore bodies of commercial size, any information on these vital ore controls that is available will be used when searching for blind ore bodies beneath an unconformable cap of lava; unfortunately, the exploration geologist may have to depend largely on other information. Underground workings, drill holes, and information as to lithology and structure of the bedrock in nearby or in pertinent areas not covered by lava must be appraised most carefully. In the East Tintic district, the intrusive pebble dikes, which consist largely of pebbles of the underlying Tintic quartzite, but which also contain fragments of other rocks where they underlie the lava, may be a source of valuable information. Limestone and shale counts of pebble dikes helped us distinguish areas where the lava is underlain by Tintic quartzite from those where the more hospitable host rocks were present.

Of chief importance in localizing ore are fractures that were opened or reopened after the Packard quartz latite blanketed the area. Minor movements along old fractures in the Paleozoic rocks were sufficient to open avenues of escape for mineralizing solutions, and although the minor movement or breaking in the lava might escape detection, the trail left by mineralizing solutions as they followed the fissures into the lava and altered them is readily discernible in many places. Despite the failure of the alteration and fracture pattern in the lava to reflect completely the complex structure of the underlying Paleozoic rocks, this pattern usually does focus attention on those areas in which mineralizing solutions moved below the lava. It is, of course, important to realize that the alteration halo in the lava may be offset—and generally is—from a position vertically over ore; all that may be said with

confidence is that such halos are on the upward projection of hydrothermal conduits that may or may not carry ore.

Chloritic alteration products associated with hydrothermal dolomite are generally confined to the lower 200 or 300 feet of the lava, and like the underlying hydrothermal dolomite, they indicate, only in a very broad way, areas that may be of interest. Argillic alteration is especially common near certain of the intrusive bodies, most of which are not closely associated with ore, however. A map that shows a halo of argillized lava surrounding a cluster of monzonite porphyries indicates an area that was marked by intense intrusive activity and by the exhalation of acid emanations that did not themselves give rise to ore deposits. In fact quite commonly a "dead space" within which ore deposits are lacking or of minor importance surrounds such intrusive centers. Argillic alteration not obviously associated with intrusions, however, suggests hydrothermal conduits that later may have been the site of ore deposition.

The most favorable combination of alteration zones in the lava is a large pyritized zone (marked by heavy limonite stain to a depth of 30 to 100 feet but usually called "bleached areas" by the local geologists); calcitized lava adjoining the pyritized zone on one side, which suggests that the footwall side of a mineralized fracture is present at depth; and weakly argillized lava on the other side of the pyritized zone. If, in addition, *silicified* pebble dikes cut the altered rocks, the area should be carefully studied for its possible value as a drilling target. A good correlation seems to exist between jasperoidized dolomite or limestone at depth and the calcitized lava at the surface. Although this relationship cannot be established everywhere—partly because the concentration of jasperoid in the dolomite tends to be local, whereas the calcitic alteration above is much more widespread—nevertheless the presence of calcitic alteration strongly suggests the presence of jasperoid at depth; conversely, its lack is discouraging. Calcitic alteration, however, does not have as great a vertical range in the lava cap as does pyritic alteration.

Geochemical exploration rapidly diminishes in effectiveness as the thickness of the lava cover increases; nevertheless it should always be used, as positive results greatly strengthen the case for drilling or other types of physical exploration. As with the alteration halos, the geochemical anomalies are commonly up-rake from ore rather than directly over ore, and the drilling program should be planned accordingly.

Where mineralized ground has been found beneath the lava or where altered carbonate rocks below the lava have been cored by drills, the common zoning that is found around ore deposits should be considered in interpreting the ground penetrated. First it is important to recognize the presence of "prepared ground" and to interpret structures as possible ore controls. However, structure alone is not attractive to the miner—a commercially-minded gentleman intent on profits—as "structure" devoid of alteration or mineralization is rarely productive of dividends. Attention, therefore, should be centered on the mineralogy as well as the structure of carbonate rocks.

Proceeding from above downward or from the outside inward towards ore the following changes are apt to take place: cubic pyrite in otherwise

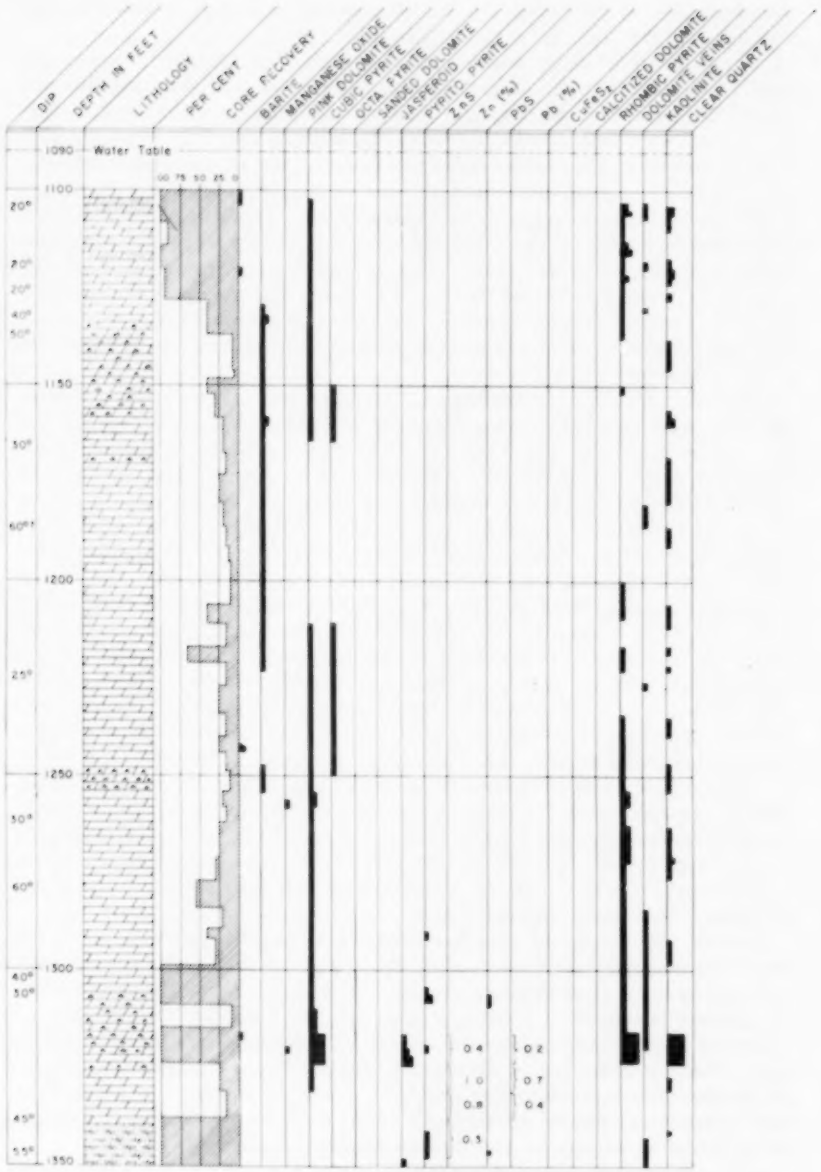

FIG. 3. Graphic log of U.S.G.S. diamond drill hole OX 1.

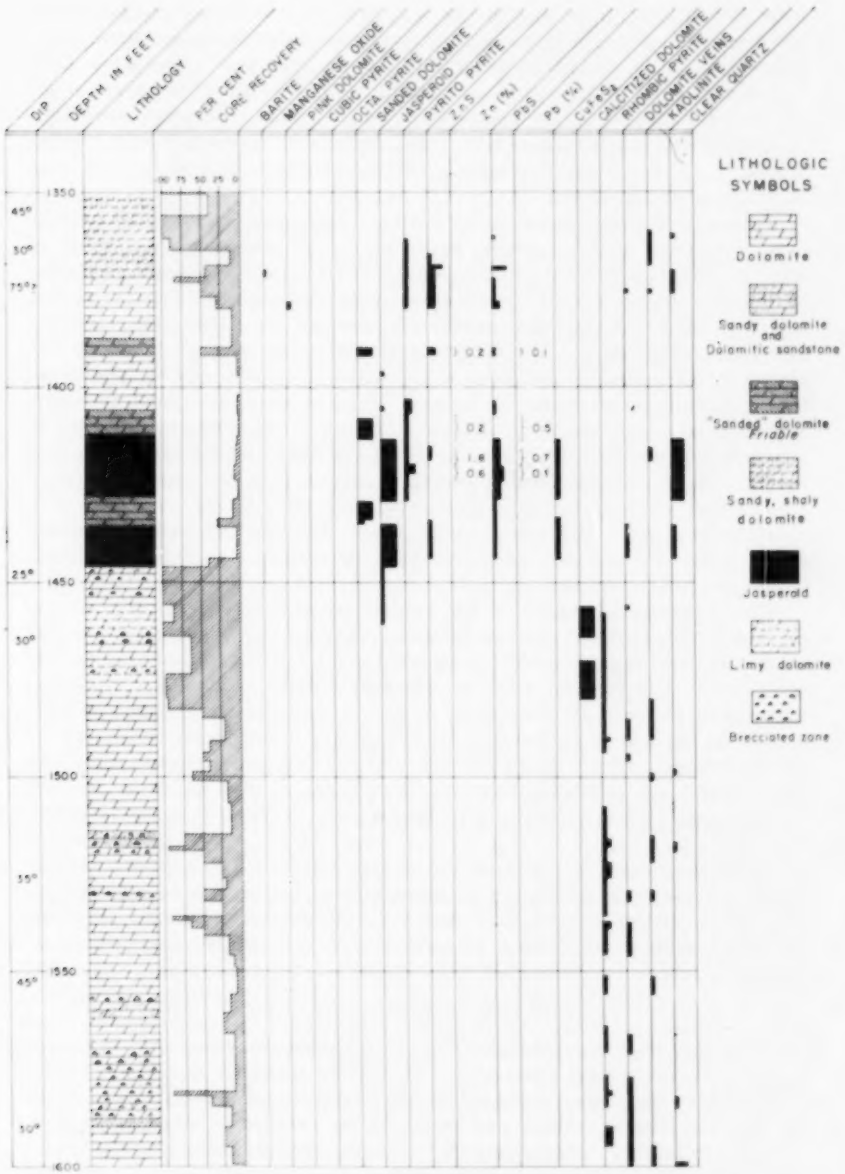

FIG. 3. Graphic log of U.S.G.S. diamond drill hole OX 1. *(Continued.)*

little altered rock gives way to—or is intermingled with—octahedral pyrite and late light-colored dolomite or manganiferous ankerite seams; small veinlets of clay with or without quartz crystals are common. The small clear well-terminated quartz crystals associated with dolomite rhombs are commonly in the outer zone of mineralization, and as ore is approached these may be intermixed with barrite or with small crystals of fluorescent light-colored sphalerite (or its oxidation product) which constitutes the first real evidence of ore stage mineralization.

Although manganiferous carbonates are intergrown with some sulfide ores, manganese is very common in the outermost zones and may travel as much as 1500 feet above the locus of base-metal sulfide deposition. Generally pyritohedral pyrite is found before or at approximately the same spot as the first tiny specks of clear fluorescent sphalerite—if the rocks penetrated are below the water table. The limestone country rock in most places is replaced by hydrothermal dolomite well beyond the limits of the base-metal sulfide deposition and it may be "sanded" in many areas, as a result of either hypogene or supergene acid solutions. Hydrothermally sanded dolomite is generally a precursor of kaolinite, halloysite, or other argillic minerals. The sanded dolomite and the argillic alteration zone in turn are commonly found surrounding a silicic shell of jasperoid, which is likely to be metalized or a casing around ore. However in many places the jasperoid does not extend as far as does the ore, and this is especially true where a manganiferous carbonate gangue is present.

The supergene alteration of the primary minerals produces suites above the water table that are appropriate to the oxidized zone, but in general the change in mineralogy is readily interpreted if the primary zonal relations are understood. Geochemical work is especially helpful in the oxidized zone, where small amounts of oxidized ore minerals escape the eye, especially where masked by manganese or iron oxides. Oxidation of sulfides in the permeable ore zones underlying the less permeable lava cap, which may contain relatively unoxidized pyrite, gives rise to temperature gradients of 5 to 10° F per 100 feet of depth, and therefore a steep temperature gradient is to be expected over ore.

These then were the guides to ore used in the East Tintic district by the Geological Survey in its attempt to choose target areas worthy of exploration. The fewer of the "guides" that were available the more hesitant we were in picking a place for drilling but nowhere did we find all the indications desired.

EXPLORATION BY GEOLOGICAL SURVEY

Prior to 1945, the quartz-latite flows that blanket the area north, east, and south of the North Lily, Tintic Standard, Eureka Standard, and Apex Standard workings had been penetrated by drill holes or mine workings in very few places. Almost nothing was known of the subrhyolite stratigraphy and structure throughout this moderately extensive terrane, although there were many areas where the rocks at the surface were strongly altered. As the detailed mapping of the Geological Survey progressed and the character and

extent of the alteration became known, some plausible conjectures as to subrhyolite structures took form. It became evident that a few well-placed drill holes might yield invaluable information as to stratigraphy, structure, and mineralization below the rhyolite, as well as data on the thickness of the lava cover that would be of vital importance to the mining industry if the rocks below it were metallized. A half dozen of the most critical areas were proposed by us for exploration by the Geological Survey, but because of the limitation of funds only four of them were drilled. The reasons for selecting the Chief Oxide area for drilling, the objectives of the drilling, and the concomitant geologic and petrographic studies together with the conclusions reached are briefly summarized in the following pages. Information on the results of exploration in the other areas is planned for a separate paper.

Chief Oxide Area.—Shortly after World War II ended, Mr. M. G. Hansen, then geologist for the Newmont Mining Company, became interested in the Geological Survey's work on alteration and structure in the Chief Oxide and Apex Standard areas of the East Tintic district. The surface geology of this part of the district is shown in Figure 4. As a result of Hansen's recommendations, Newmont Mining Company reopened part of the Apex Standard mine in an effort to explore the area to the east of the mine. The drive toward the Chief Oxide alteration patch was abandoned because of some heavy ground on the 1,000-foot level and instead two churn drill holes were put down to water level. The cuttings from these drill holes established the presence of a limestone section several hundred feet thick beneath the Packard quartz latite, and small amounts of lead and zinc were found through some fifty feet of the section in the western (Newmont No. 1) drill hole. The lack of commercial ore, however, discouraged the Newmont Company, and exploration stopped when the second hole failed to cut metallized rock above the water table at 1,100 feet.

Geochemical work at the surface indicated an apparent anomaly not unlike that up-rake from the Tintic Standard ore body (18). This, together with the low-grade mineralization in the No. 1 Newmont hole, the inability of anyone to identify satisfactorily the formation from the churn drill cuttings, the abundance of fine-grained pyrite in chips of what appeared to be hydrothermal dolomite, and finally the presence of chips of jasperoidized dolomite in the No. 1, hole, all combined to suggest the desirability of core drilling. With some difficulty, a hole was drilled for the Geological Survey from the bottom of the Newmont No. 2 hole, from a depth of 1,100 feet to a depth of 1,600 feet. The core from this hole, designated the OX 1 drill hole (Fig. 4), yielded the definitive information required for an interpretation of the structure, alteration, and mineralization. The section cored was hydrothermal dolomite with some sandstone, and prior to cutting lead and zinc sulfides between depths of 1,310 and 1,445 feet, it showed alteration effects typical of the changes to be expected when approaching an ore body from the exit side of the solutions.

Fortunately some of the core contained identifiable fossils which established the age of the rocks as Late Devonian or Early Mississippian. The presence of sandstone in the section made it possible to identify these beds

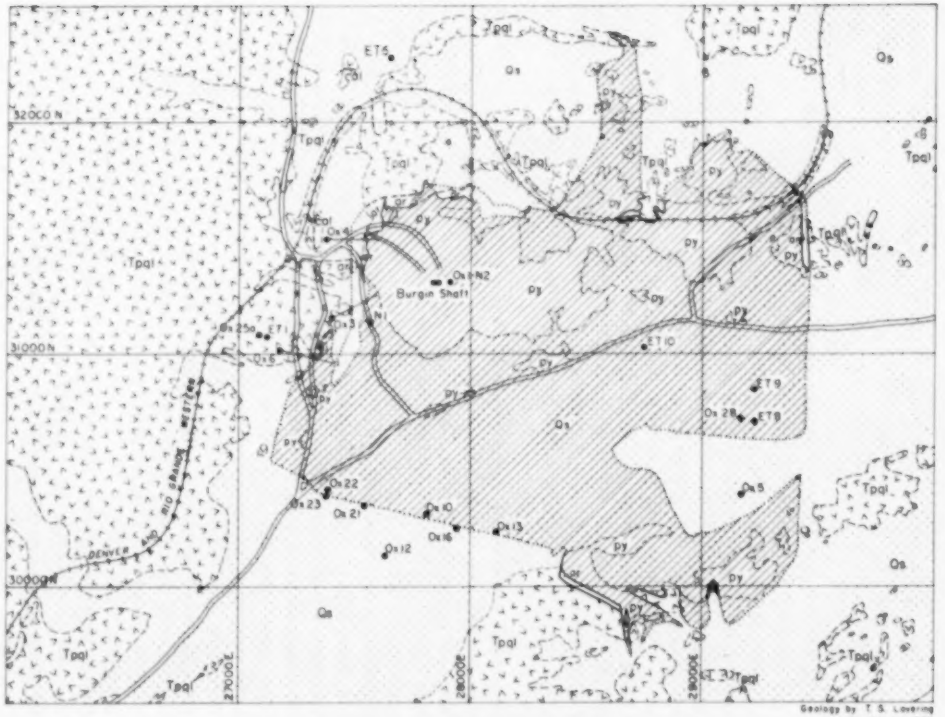
Tpql
Qs
Qs
ET5
32000 N
Tpql
Tpql
Tpql

as either the Humbug formation or the fossiliferous Pinyon Peak limestone and unfossiliferous Victoria formation; the presence of the Cambrian Ophir formation on the 1,000-foot level of the Apex Standard mine only 1,300 feet to the west of the drill hole established conclusively the presence of a large fault between this hole and the Apex Standard workings. It was inferred that the western edge of the alteration zone, which lies some distance west of the Newmont No. 1 hole, was controlled by this fault zone.

At this time (1952) the work by Proctor and others (25) in the Allens Ranch quadrangle to the north was almost completed and the Allens Ranch thrust fault, which had a stratigraphic displacement of about 3,500 feet, had been mapped to the point where it disappeared under the northern edge of the lava 4½ miles north of the Chief Oxide area. The persistence of this thrust in the Paleozoic rocks to the north of the volcanic field suggested that the thrust fault or related deformation probably extended under the lava well to the south. Reports on the geology of the Silver Shield Mining Company's Independence shaft located midway between the Allens Ranch quadrangle and the Chief Oxide area together with the records of a few churn drill holes indicated the persistence of this structure several miles south of the southernmost exposure of the thrust (Fig. 2). Fragments of limy drill core on the dump of the caved Independence shaft lent weight to the report that a substantial thickness of limestone lay below the shales of the Ophir formation and Tintic quartzite under the lava in this locality. It was concluded, therefore, that the large fault between the U.S.G.S. OX 1 drill hole and the easternmost Apex Standard workings was a reverse fault and presumably a thrust fault of displacement comparable to the Allens Ranch thrust. The known change in attitude of low-angle faults, where they pass from Paleozoic rocks into volcanic rocks above, allowed us to project the position of the fault—the East Tintic thrust (Fig. 2)—with a fair degree of accuracy, as was proved later by the underground exploration described in Part II of this paper.

The size of the brown altered areas in the Chief Oxide locality and the knowledge that they represented an outcrop of pyritized lava, showed that hundreds of thousands of tons of sulfur had been introduced into this lava cap and indicated the presence of a major hydrothermal conduit at depth. As the Chief Oxide alteration area was at the intersection of a major north-trending thrust fault with one or more of series of mineralized northeasterly striking faults, there seemed little doubt but that a huge amount of "prepared ground" existed in this locality, and therefore that the pyritic mineralization probably pressaged the presence of more valuable sulfides at depth.

The log of the U.S.G.S. diamond drill hole OX 1, (Fig. 3) illustrates graphically the changes in mineralogy and lithology on the exit and inlet side of the metallized jasperoid. Some of the more obvious alteration effects in the rocks persist throughout the drill core and are not diagnostic of proximity to ore. In this class of "far travellers" we place the numerous white dolomite veins cutting hydrothermal dolomite, the kaolinite lining small vugs, and the small clear quartz crystals that occur in vugs throughout the section of hydrothermal dolomite. Minerals that seemed to be far ranging on the

exit side but that did not persist below the point where the galena and sphalerite-bearing jasperoid was found include barite, cubic pyrite, octahedral pyrite, manganese oxides, and pink "dolomite"—probably a manganiferous ankerite. Alteration minerals that are generally more closely associated with ore than the above include jasperoid and sanded dolomite, i.e., a somewhat friable dolomite. Pyritohedral pyrite is very intimately associated with ore, but a few crystals were observed high in the section. The first of the ore-stage sulfides to appear is a very light-colored sphalerite that shows a strong orange fluorescence. This fluorescence gradually diminishes in the sphalerite at greater depth, especially that associated with galena and chalcopyrite. The ore sulfides first appeared in small nearly vertical veinlets associated with clear quartz and pyritohedral pyrite, and in light-colored vuggy dolomite veins and veinlets some of which contained small crystals of barite. The greatest concentration of ore sulfides, however, is in jasperoid gangue.

Beneath the strongly jasperoidized zone at 1,412 to 1,445 feet the rock is strongly calcitized—an alteration of hydrothermal dolomite. Calcitized dolomite most commonly reflects outlet side alteration of pre-ore pyrometasomatism at depth, but the explanation of its occurrence under the jasperoid here is best deferred until more information is available. Sparse sulfides continue below the jasperoid to the bottom of the hole at 1,600 feet, but the pyrite is completely different in crystal form from any found at higher levels, the faces of the rare euhedral crystals are diamond shaped, and the six-sided crystals are rhombehedral in appearance. These crystals appear to be identical with an unusual distortion of a pyritohedral pyrite from the Ural Mountains that is figured by Palache, Berman, and Frondel (23, p. 283).

The data provided by the drill core strengthened the earlier picture of alteration derived from the regional study and also added interesting suggestive details that should be checked by further observation. Tentative inferences made earlier seemed adequately substantiated. It was believed that a much more satisfactory appraisal of the situation would be possible after additional short-hole exploration had been carried on to outline the main pyritic alteration zone in the lava and to establish, if possible, the third dimension of this zone and of the weak geochemical anomalies, which had been found earlier. To this end, the Geological Survey contracted for the bulldozing of many trenches across the contact and for the drilling of 60 drill holes ranging in length from 25 to 700 feet; the suboutcrop of the pyritized lava, as shown on Figure 4, was determined with confidence. Cores from the moderately deep inclined drill holes at the western side of the pyritic alteration area showed that much more widespread calcitic alteration was present at depth in the lava than was apparent at the surface. This find further increased our confidence that substantial bodies of jasperoid were present in the carbonate rock below.

An intrusive breccia was uncovered in several of the bulldozer pits at the west margin of the alteration zone. In some places the breccia contained much visible barite and assayed 200 ppm in lead. Efforts to obtain the rake of the anomaly by drilling were unsuccessful however, largely because of poor core recovery in critical areas.

Temperature measurements made in all drill holes reaching a depth of more than 100 feet indicated a substantial "oxidation gradient" (about 4° to 5° F/100 feet), but the highest temperature gradient was found in unpyritized lava 200 feet southwest of the Chief Oxide alteration zone in the U.S.G.S. OX 12 hole where a gradient of 10° F/100 feet was registered. This hole is on strike with the zone where oxidized lead ore was found in the subsequent Burgin shaft exploration, and is over ground not yet explored.

During this drilling campaign we attempted to cut the East Tintic thrust fault by drilling OX 25A, a hole between Newmont No. 1 and the eastern end of the Apex Standard workings. Unfortunately the hole was lost at a depth of 891 feet in bad ground which was probably in the thrust fault zone. The lava was 602 feet thick here, and the lower 100 feet was chloritized, pyritized, and strongly calcitized tuff. The section below the tuff comprised 30 feet of limy shale, a foot of pyritic, siliceous breccia, 40 feet of dark-gray dolomite (Herkimer formation), 45 feet of dominantly cream-colored, thin-bedded limy dolomite (Dagmar dolomite ?), and 176 feet of gray dolomite and dolomitic limestone (Teutonic limestone ?). Near the bottom of the hole low-angle carbonate and breccia seams were common and the rock was broken and vuggy. Clear quartz, rhodochrosite, calcite, kaolinite, cubic pyrite, and manganese and iron oxides were moderately abundant. Lead and zinc anomalies were locally present and barium was high in the lower part of the hole.

Several geophysical techniques were tried in the Chief Oxide area, but with the exception of our own geothermal work, results have not proved helpful in locating mineralized ground. Preliminary resistivity traverses showed an area of low resistivity at an estimated depth of about 370 feet below the surface in the southeastern part of the alteration area and in a locality where there was a heavy gravel cover. The results were interpreted by the geophysicists as indicating the presence of a sulfide body at this relatively shallow depth, but a drill hole (U.S.G.S. OX 5) penetrated a section of fresh tuffs of the Laguna Springs latite and then cut alternating zones of argillized and fresh Packard quartz latite. The most argillized rock was at a depth of about 370 to 390 feet but from a depth of 400 to 430 feet, where the hole was stopped, the rock was almost entirely fresh. The low resistivity apparently reflected damp clay in the altered rock. Inhole electrical resistivity surveys showed appreciable differences in different octants and quadrants of the compass, but little confidence was expressed in the geological interpretation of the results.

An effort to check the boundaries of the disseminated pyrite in the lava by use of the pulse method was unsatisfactory; apparently the pyrite was too fine grained or too meager to provide workable conditions for the method. The only locality where the inferred boundaries coincided with those known was where a traverse crossed a bulldozer pit in which the colluvium covering the contact had been scraped off. In the gravel-covered areas where the contact was well established by shorthole drilling and lay beneath 20 to 50 feet of gravel, the pulse method indicated the presence of the contact hundreds

of feet, and in one instance more than a thousand feet, from the actual position of the contact.

Magnetic surveys of the area, by a private consultant, that purported to show the depth of the quartz latite, failed completely to check drilling and underground information. No appreciable gravity anomaly was found in the area, and no effort was made to determine the thickness of the lava or the depth to the basement by seismic methods, as the opinion of a consulting geophysicist was adverse to the use of this method here.

This, then was the positive information assembled by the Geological Survey at the close of 1954: a reasonably accurate alteration map of the bedrock in the area of pyritic alteration had been made; an anomalously high geothermal gradient had been found in the brown pyritized alteration zone and to the southwest of it; a fault with a displacement of several thousand feet was known to exist beneath the lava less than 700 feet west of the alteration zone, and strong but indirect evidence indicated that it was a low-angle thrust fault dipping to the west; the Chief Oxide alteration zone was known to be on strike with northeast-trending mineralized faults, and hence there was good reason to believe the "prepared ground" existed in the carbonate rocks at the intersection of these major structural trends; an altered zone typical of the outlet side of a hydrothermal conduit had been found; and finally, ore stage mineralization was found to have introduced lead and zinc sulfides of submarginal grade through at least 50 feet of section cut in two holes collared 400 feet apart in the oxidized pyritic lava. At this point in the development of the geologic picture the Geological Survey withdrew from further exploration, with the hope that the area would be investigated further by private industry.

Bear Creek Mining Company, Dividend, Utah.
Bear Creek Mining Company, Salt Lake City, Utah.
U. S. Geological Survey, Denver, Colorado.
U. S. Geological Survey, Menlo Park, California.
April 2, 1960

REFERENCES

1. Almond, Hy, and Morris, H. T., 1951, Geochemical techniques as applied in recent investigations in the Tintic district, Utah: Econ. Geol., v. 46, p. 608–625.
2. Baker, A. A., and others, 1947, Stratigraphy of the Wasatch Mountains in the vicinity of Provo, Utah: U. S. Geol. Survey Oil and Gas Inv. Prelim. Chart, no. 30, chart with text, index map.
3. Billingsley, Paul, 1927, North Lily development in East Tintic: Mining and Metallurgy, v. 8, p. 182–183.
4. —— and Smith, N., 1927, Rhyolite alteration in the East Tintic district: Unpublished manuscript.
5. Billingsley, Paul, and Crane, G. W., 1933, Tintic mining district, the Salt Lake region: 16th Internat. Geol. Cong. Guide Book 17, p. 101–124.
6. Butler, B. S., Loughlin, G. F., and others, 1920, The ore deposits of Utah: U. S. Geol. Survey Prof. Paper 111, 672 p.
7. Cook, D. R., Editor, 1957, Geology of the East Tintic Mountains and ore deposits of the Tintic mining district: Utah Geol. Soc. Guidebook to the Geology of Utah, No. 12.
8. Cook, D. R., 1959, Bonanza project, Bear Creek Mining Company: Am. Inst. Min. Met. Eng. Trans., (in press).
9. Crane, G. W., 1917, Geology of the ore deposits of the Tintic mining district, Utah: Am. Inst. Min. Met. Eng. Trans., v. 54, p. 342–355.
10. Duke, D. A., 1959, Jasperoids and ore deposits in the East Tintic mining district: Unpublished thesis, Utah Univ.

11. Eardley, A. J., 1944, Geology of the north-central Wasatch Mountains, Utah: Geol. Soc. America Bull., v. 55, p. 819–894.
12. Havenor, H. E., 1924, Mining camps of North America, Tintic Utah; active since 1870: Eng. Mining Jour. Press, v. 117, p. 355–361.
13. Howd, F. H., 1957, Hydrothermal alteration in the East Tintic district, *in* Geology of the East Tintic Mountains and ore deposits of the Tintic mining district [1957]: Utah Geol. Soc. Guidebook to the geology of Utah, no. 12, p. 124–134.
14. Kildale, M. B., 1938, Structure and ore deposits of the Tintic district, Utah: Unpublished thesis, Stanford Univ., Stanford, California.
15. Kransdorff, D., 1934, The geology of the Eureka Standard mine, Tintic, Utah: Unpublished thesis, Harvard Univ., Cambridge, Massachusetts.
16. Lindgren, W., 1915, Processes of mineralization and enrichment in the Tintic mining district: Econ. Geol., v. 10, p. 225–240.
17. —— and Loughlin, G. F., 1919, Geology and ore deposits of the Tintic mining district, Utah: U. S. Geol. Survey Prof. Paper 107, 282 p.
18. Lovering, T. S., Sokoloff, V. P., and Morris, H. T., 1948, Heavy metals in altered rock over blind ore bodies, East Tintic district, Utah: Econ. Geol., v. 43, p. 384–399.
19. Lovering, T. S., and others, 1949, Alteration as related to ore deposits in the East Tintic district, Utah: Econ. Geol. Mon. 1.
20. Lovering, T. S., Morris, H. T., and others, 1960, Geologic map of the East Tintic district, Utah: U. S. Geol. Survey Mineral Inv. Map, MF 230, sheet 1.
21. Lovering, T. S., Morris, H. T., and others, 1960, Alteration map of the East Tintic district, Utah: U. S. Geol. Survey Mineral Inv. Map, MF 230, sheet 2.
22. Morris, H. T., and Lovering, T. S., 1952, Supergene and hydrothermal dispersion of heavy metals in wall rocks near ore bodies, Tintic district, Utah: Econ. Geol., v. 47, p. 685–716.
23. Palache, Charles, Berman, Harry, and Frondel, Clifford, 1944, Dana's system of mineralogy, v. 1, p. 283: New York, John Wiley and Sons.
24. Parsons, A. B., 1925, The Tintic Standard mine: Eng. Mining Jour. Press, v. 120, p. 645–652.
25. Proctor, P. D., and others, 1956, Preliminary geologic map of the Allens Ranch quadrangle, Utah: U. S. Geol. Survey Mineral Inv. Map, MF 45.
26. Stringham, Bronson, 1942, Mineralization in the West Tintic mining district, Utah: Geol. Soc. America Bull., v. 53, no. 2, p. 267–290.
27. Tower, G. W., Jr., and Smith, G. O., 1899, Geology and mining industry of the Tintic district, Utah: U. S. Geol. Survey 19th Ann. Rept., pt. 3, p. 601–767.
28. —— and Emmons, S. F., 1900, Tintic special folio, Utah: U. S. Geol. Survey Geol. Atlas, Folio 65.

Economic Geology
Vol. 55, 1960, pp. 1148–1178

SYNTHETIC AND NATURAL PHASES IN THE SYSTEM Au-Ag-Te

N. L. MARKHAM

PART I

CONTENTS

PAGE

Abstract 1148
Introduction 1148
The system gold-silver-tellurium 1149
  Previous work 1149
  Present study 1152
  Experimental procedure 1153
  Duration of runs 1153
  Experimental results 1153
  Discussion of phase diagram 1159
  Geological applications 1161
Kalgoorlie 1162
  General geology 1162
  Previous mineralogical work 1163
  Present study 1163
  Descriptive mineralogy 1163

ABSTRACT

The subsolidus phase relationships in the ternary system gold-silver-tellurium have been investigated experimentally. From the results obtained an isothermal section at 300° C has been drawn showing compatible phases and approximate limits of solid solution. All natural gold-silver telluride minerals, with the exception of krennerite and montbrayite, have been synthesized. It is concluded that krennerite is the low-temperature, low-pressure polymorph of $AuTe_2$ and that higher temperatures and pressures favor the development of calaverite.

A detailed mineralogical description is given of the telluride deposits of Kalgoorlie, Western Australia and Vatukoula, Fijian Islands. The assemblages observed are compared with those obtained experimentally and there is found to be good agreement between the two sets of data. The natural assemblages have also been analysed in terms of the phase rule. It is concluded that experimental data are still insufficient to indicate a meaningfull range of temperatures over which any given telluride deposit could have formed but that the calaverite-krennerite transition, when experimentally determined, should provide a most useful geological thermometer.

INTRODUCTION

PHASE equilibrium studies, so successfully applied to rock-forming silicates, have recently been extended to include metallic sulfides, sulfosalts and related

minerals. Such studies, when coupled with an examination of natural mineral occurrences, may be expected to yield valuable data on the temperature and pressure conditions under which many mineral deposits form. In addition they may help to explain why certain mineral assemblages and textural features are so frequently observed. The present investigation is concerned with the telluride minerals, in particular, with the subsolidus phase relations in the ternary system gold-silver-tellurium. It also deals with the application of this data to the telluride deposits of Kalgoorlie, Western Australia, and Vatukoula, Fijian Islands.

Previous work on telluride minerals is varied and extensive. Amongst the most important contributions and those most pertinent to the present study may be mentioned those of Tunell and co-workers (42, 43, 44, 45, 46) on the crystal structures of the gold-silver ditellurides, Pellini and Quercigh (23, 24, 25) and Kracek and Ksanda (14, 15) on the phase relations in the ternary system, Thompson (39) on the descriptive mineralogy of the tellurides and Stillwell (32, 33) on the telluride mineralogy of Kalgoorlie and Vatukoula. Their work and that of other writers will be discussed in the following sections.

THE SYSTEM GOLD-SILVER-TELLURIUM

Previous Work

Previous work on the ternary system deals largely with the nature of the liquidus surface. It will be convenient to first consider the three limiting binary joins Au-Te, Ag-Te and Au-Ag and finally, the ternary system itself.

Au-Te.—This system was investigated by Rose (27), Pélabon (22), and Pellini and Quercigh (25) with results that are in essential agreement. The phase diagram of Figure 1 shows one binary phase of composition $AuTe_2$ with eutectic points existing between Au-$AuTe_2$ and $AuTe_2$-Te. No solid solution was observed nor was there any indication of a phase of composition Au_2Te_3. Peacock and Thompson (20) attempted, unsuccessfully, to synthesize a phase of composition Au_2Te_3 corresponding to the mineral montbrayite while Thompson (38) showed that synthetic $AuTe_2$ has the same crystal structure as natural calaverite.

Ag-Te.—The system silver-tellurium has been investigated by Pélabon (21), Pellini and Quercigh (24), Chikashige and Saito (5), Koern (12), Kracek and Ksanda (14) and Kracek and Rowland (16). All investigators found two binary phases, the first of composition Ag_2Te and the second whose composition has been variously listed as AgTe, Ag_7Te_4, $Ag_{12}Te_7$, Ag_3Te_2, Ag_5Te_3, $Ag_{2-x}Te_{1+x}$ and $Ag_{5-x}Te_3$. These phases correspond to the minerals hessite and empressite.

The phase diagram of Figure 2 has been drawn up utilizing the most recent data of Kracek and Rowland. It shows that hessite melts congruently at 959° C and empressite melts incongruently at 460° C to hessite plus liquid. Other salient points include the presence of a liquid immiscibility field between the compositions 69–91 atomic percent silver and the presence of eutectic points between Ag-Ag_2Te and $Ag_{5-x}Te_3$-Te. Kracek and Row-

land further showed that hessite and empressite both undergo two solid state transitions, the temperatures of which are markedly sensitive to composition.

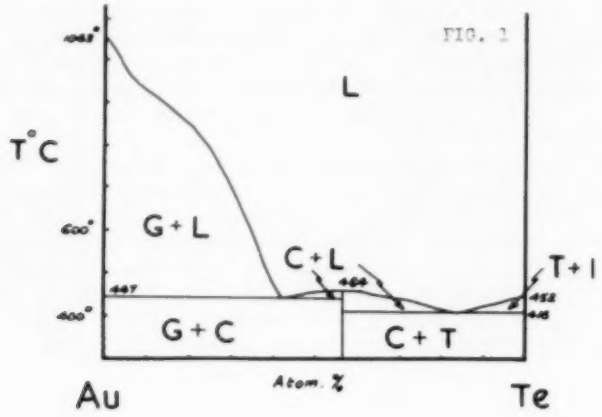

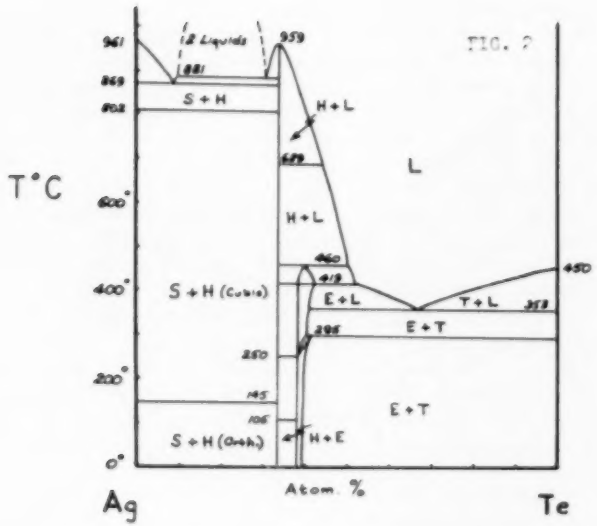

FIG. 1. (upper) The binary system gold-tellurium after Rose, Pélabon and Pellini and Quercigh.

FIG. 2. (lower) The binary system silver-tellurium after Kracek and Ksanda and Kracek and Rowland.

Ag_2Te.—Lower Transition, Orthorhombic → Cubic
105° ± 25° C in the presence of a slight excess of tellurium.
145° ± 2° C in the presence of a slight excess of silver.
Upper Transition
Corresponding temperatures are 689° ± 5° C and 802 ± 2° C.

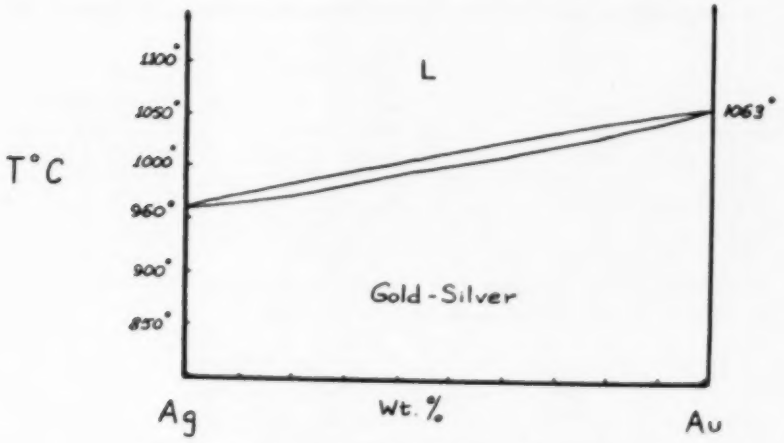

FIG. 3. The binary system gold-silver after Hansen.

$Ag_{5-x}Te_3$.—Lower Transition, probably heat capacity anomaly
295° in the presence of excess tellurium.
250° in the presence of excess silver.
Upper Transition, Hexagonal → Unknown structure
419° ± 5° in the presence of excess tellurium.
417° ± 2° in the presence of excess silver.

Thompson, Peacock, Rowland and Berry (40) synthesized empressite with a mixture corresponding to the composition $AgTe_3$. They suggested that a structural formula for both synthetic and natural material would be $Ag_{2-x}Te_{1+x}$, implying substitutional solid solution. More recently, Donnay, Kracek and Rowland (6) have shown that a more correct structural formula is $Ag_{5-x}Te_3$, implying omission of silver atoms.

Au-Ag.—The binary system gold-silver has been investigated by many workers. The phase diagram of Figure 3 is that given by Hansen (9) and shows complete solid solution over the whole composition range.

Au-Ag-Te.—Pellini (23) and Kracek and Ksanda (15) have investigated the ternary system, both studies being concerned with the nature of the liquidus surface. Pellini studied in detail the partial system Ag_2Te-$AuTe_2$-Te and deduced four invariant points, including a ternary eutectic at 335° C ($Au_5Ag_{35}Te_{60}$ atomic %). Pellini was unable to find any indication of a ternary phase corresponding to the mineral sylvanite ($AuAgTe_4$) but tenta-

tively correlated a phase of approximate composition $(AgAu)_3Te_2$ with the mineral petzite $(AuAg_3Te_2)$.

Kracek and Ksanda synthesized sylvanite and petzite and noted that both minerals melt incongruently, the first to calaverite plus liquid and the second to a gold-silver alloy plus liquid. The position of the ternary eutectic was found to be at 330° C with the solid phases tellurium, empressite and sylvanite coexisting with a liquid of approximate composition $Au_4Ag_{35}Te_{61}$ atomic %.

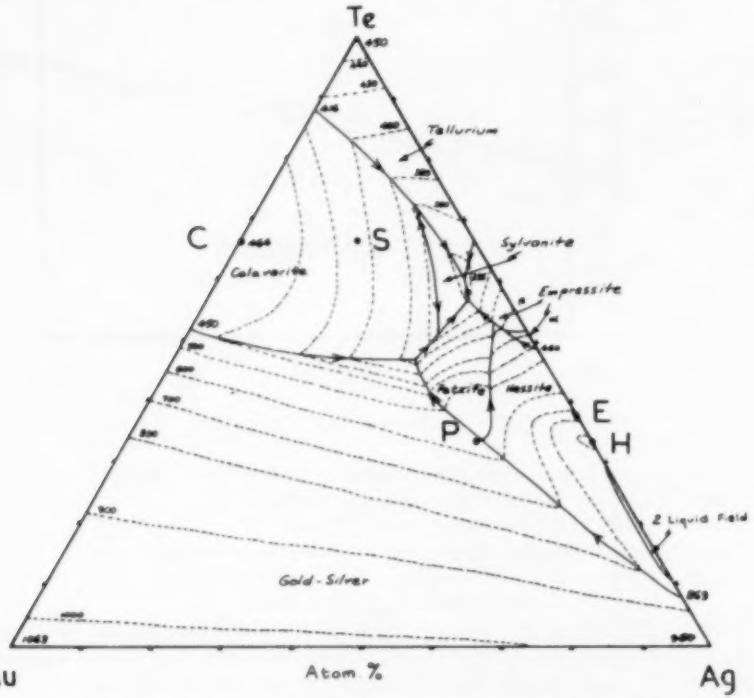

FIG. 4. The ternary system gold-silver-tellurium after Pellini and Kracek and Ksanda.

Unfortunately, Kracek and Ksanda published no phase diagram so that Figure 4 is that necessarily drawn up by the present writer from all available data. Uncertainty still exists regarding the precise nature and location of some of the phase boundaries but the general features of the diagram are consistent with what is at present known.

Present Study

The aim of the present investigation has been to investigate subsolidus equilibrium relationships in the ternary system gold-silver-tellurium. In

the absence of a complete subsolidus study, a fruitful method of approach is to establish an isothermal section whose temperature, ideally, is chosen so as to fall within the range of temperatures thought to exist in a natural mineral system. The 300° C isotherm was selected because it represents a temperature high enough to permit a sufficiently rapid rate of reaction, yet low enough to allow correlation with natural mineral assemblages. Additional runs have been carried out at temperatures of 150°, 250°, 330°, 400° and 430° C.

Experimental Procedure

Finely powdered tellurium, silver and gold of 99.9 percent purity have been utilized. Each run, totalling 0.1 gms in weight, was mixed in the desired proportions and sealed in evacuated pyrex glass tubes. After heating in a tube furnace (temperature control ± 4° C), the products were identified by X-ray diffraction methods using the reference patterns as published by Thompson (39), Swanson and Tatge (36), Tunell et al. (42, 43, 45), Rowland and Berry (28) and Thompson, Peacock, Rowland and Berry (40). Examination of the products by reflected light methods did not prove satisfactory because of their extremely fine grain size and very similar optical properties.

Duration of Runs

Preliminary experimental work had indicated a fairly rapid rate of reaction in the charges. Thus runs corresponding to the composition of calaverite were heated at 300° C for intervals of two, four and six days. Complete reaction had occurred after two days and the remaining runs showed no differences in their X-ray powder patterns. Identical results were obtained in the case of hessite, empressite, sylvanite and petzite (Runs M1–M27). The ternary system was then explored by a series of runs, of duration four days, in order to map out roughly the phase boundaries. Compositions numbered M28–M75 represent these exploratory runs. More precise location of the phase boundaries and limits of solid solution have been determined by a series of runs, numbered M76–M188, heated for periods of seven to eleven days. A close approach to equilibrium has been achieved in the majority of these runs, but certain runs have yielded four phases instead of the three as permitted by the phase rule. However, as will be indicated in the next section, the extremely narrow compositional range over which four phases could be detected, coupled with the limited mutual solubility of the phases, have allowed the phase boundaries to be drawn with an uncertainty not exceeding ± 1–2 wt. % of any given element.

At temperatures of 400° C and 430° C, the equivalent reactions proceed very rapidly and those runs numbered M200–M215 represent a close approach to equilibrium.

Experimental Results

The results of all experimental work on the 300° isotherm are listed in Table 1 and the phase diagrams of Figure 5 (Wt. %) and Figure 6 (Atom

TABLE 1

No.	Composition, wt. %			Time in days	Products*
	Au	Ag	Te		
Temperature: 300° C					
M1–3	43.59	—	56.41	2, 4, 6	C
M4–8	90.0–47.0	—	10.0–53.0	2	C+G
M9–11	30.0–10.0	—	70.0–90.0	2	C+T
M12–13	—	62.86	37.14	2, 4	H
M14–15	—	58.5	41.5	2, 4	E
M16–17	25.42	41.71	32.87	2, 4	P
M18–19	24.19	13.22	62.59	2, 4	S
M20–23	—	10.0–50.0	90.0–50.0	4	T+E
M24	—	60.0	40.0	4	E+H
M25–27	—	70.0–90.0	30.0–10.0	4	H+Si
M28	32.5	7.5	60.0	4	C+S
M29	25.0	5.0	70.0	4	C+S+T
M30	13.0	7.0	80.0	4	S+T
M31	10.0	25.0	65.0	4	S+T+E
M32	10.0	40.0	50.0	4	S+E
M33	15.0	42.0	43.0	4	S+P+H
M34	13.0	52.0	35.0	4	P+H
M35	25.0	30.0	45.0	4	P+S
M36	80.0	10.0	10.0	4	GS+P+C
M37	70.0	20.0	10.0	4	GS+P+H(?)
M38	60.0	30.0	10.0	4	GS+H+P(?)
M39–43	50.0–10.0	40.0–80.0	10.0	4	GS+H
M44–45	70.0–60.0	10.0–20.0	20.0	4	GS+P+C
M46–47	50.0–40.0	30.0–40.0	20.0	4	GS+P+H
M48–51	30.0–10.0	50.0–70.0	20.0–30.0	4	GS+H
M52–56	60.0–40.0	10.0–30.0	30.0–40.0	4	GS+C+P
M57–58	30.0–40.0	30.0–10.0	40.0–50.0	4	C+P
M59	30.0	20.0	50.0	4	C+P+S
M60–62	10.0	15.0–35.0	75.0–55.0	4	S+T+E
M63–66	20.0–10.0	30.0–52.0	50.0–38.0	4	S+P+H
M67	8.0	55.0	37.0	4	P+H
M68–69	35.0–30.0	10.0–15.0	55.0	4	C+P+S
M70	25.0	20.0	55.0	4	P+S
M71–73	16.0–8.0	30.0–45.0	54.0–47.0	4	S+E
M74	6.5	50.0	43.5	4	S+E+P
M75	3.2	56.3	40.5	4	E+H+P
M76–79	42.5–39.5	0.8–2.8	56.7–57.7	11	C
M80–83	38.5–35.5	3.5–5.5	58.0–59.0	11	C+S
M85–86	22.0–23.0	14.7–14.0	63.0–63.3	15	S+T+E
M87	25.0	12.7	62.3	15	S+T
M88–90	26.0–28.0	12.0–10.6	62.0–61.4	15	S
M91	29.0	10.0	61.0	15	S+C
M92	1.0	62.0	37.0	14	H
M93–99	2.0–8.0	61.2–56.2	36.8–35.8	14	H+P
M102–105	21.0–24.0	45.4–42.9	33.6–33.1	14	P+H
M106	27.0	40.3	32.7	14	P
M107	28.0	39.5	32.5	14	P+C+GS
M108–110	35.0	34.0–36.0	31.0–29.0	12	C+P+GS
M111	35.0	37.0	28.0	12	G+P+GS+H
M112–114	35.0	27.0–25.0	27.0–25.0	12	P+GS+H
M115–118	35.0	41.0–44.0	24.0–21.0	14	H+GS+P
M119	35.0	45.0	20.0	14	H+GS
M120–123	20.0	42.0–48.0	28.0–32.0	14	H+GS+P
M124	63.0	2.0	35.0	14	C+GS

TABLE 1—(*Continued*)

No.	Composition, wt. %			Time in days	Products*
	Au	Ag	Te		
Temperature: 300° C					
M125–127	62.0–60.0	3.0–5.0	35.0	14	G+GS+P
M128–129	24.0–23.0	1.0–2.0	75.0	14	C+T
M130–131	22.0–21.0	3.0–4.0	75.0	14	C+T+S
M132–134	40.0–38.0	15.0	45.0–47.0	21	C+P+GS
M135–137	37.0–35.0	15.0	48.0–50.0	21	C+P
M138–139	34.0–33.0	15.0	51.0–52.0	21	C+P+S
M140–141	28.0–27.0	25.0–26.0	47.0	14	C+P+S
M142–143	26.0–25.0	27.0–28.0	47.0	14	C+P+S+H
M144–147	24.0–21.0	29.0–32.0	47.0	14	P+S+H
M148–149	11.0–10.0	48.0	41.0–42.0	21	P+S+H
M150–151	9.0–8.0	48.0	43.0–44.0	21	P+S+H+E
M152–153	7.0–6.0	48.0	45.0–46.0	21	S+E
M154–155	5.0–4.0	48.0	47.0–48.0	21	S+E+T
M164–167	99.0–96.0	—	1.0–4.0	8	G+C
M168–171	1.0–4.0	—	99.0–96.0	8	T+C
M172–175	39.6–42.6	—	60.4–57.4	8	C+T
M176–179	44.6–47.6	—	55.4–52.4	8	C+G
M180–182	—	54.0–56.0	46.0–44.0	7	E+T
M183–186	—	59.0–62.0	41.0–38.0	7	E+H
M187–188	—	65.0–66.0	35.0–34.0	7	H+Si
Temperature: 330° C					
M189–190	10.0–7.0	50.0–55.0	40.0–38.0	14	P+S+E
Temperature: 430° C					
M200–201	35.5–37.0	5.5–4.5	59.0–58.5	7	C
M202		Natural calaverite		7	C
M203		Natural krennerite		7	C+K (trace)
Temperature: 400° C					
M204–205	38.5–37.0	3.5–4.5	58.0–58.5	7	C
M206–207	35.5–34.0	5.5–6.5	59.0–59.5	7	C+S
M208–210	38.0–34.0	2.0–5.0	60.0–61.0	7	C+T
M211		Natural krennerite		14	C
M213	40.0	4.0	56.0	7	C
M214–215	38.0–37.0	6.0–8.0	56.0–55.0	7	C+P

* C = Calaverite, P = Petzite, S = Sylvanite, H = Hessite, E = Empressite, T = Tellurium, G = Gold, Si = Silver, GS = Goldsilver, K = Krennerite.

%) are drawn up from this data. Figure 5 (Wt. %) also shows the compositions studied.

In discussing the results obtained, each mineral phase will be described in turn together with details of its crystal structure, range of chemical composition and the nature of the three phase fields it forms within the ternary system.

Calaverite $AuTe_2$.—Calaverite is monoclinic with space group C2/m. As elucidated by Tunell (43), the gold atoms in the structure are in 6-fold co-ordination but the neighboring atoms are not all at equal distances. Thus each gold atom has two tellurium neighbors distant 2.68 A° and four at 2.97 A° while each tellurium atom is surrounded by three gold atoms at 2.68 A° and 2.97 A° (2) and three tellurium atoms at 3.19 A° (2) and

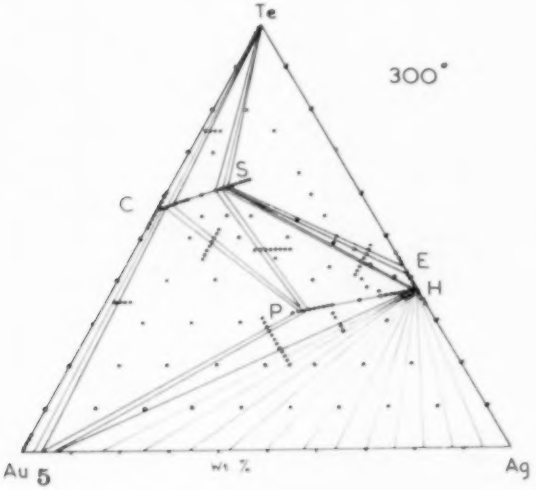

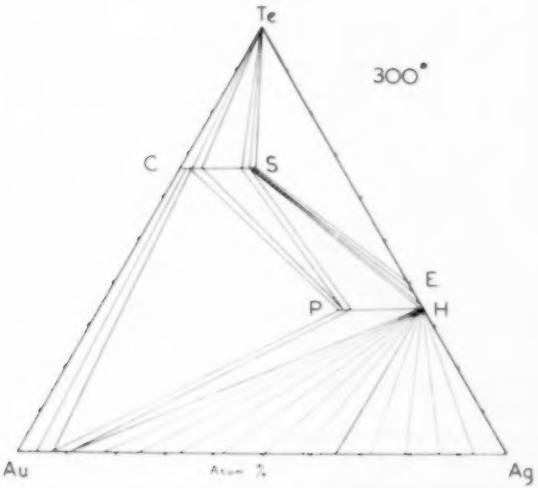

FIGS. 5 and 6. The 300° C isotherm in the ternary system gold-silver-tellurium.

3.47 A°. The structure can be derived by small distortions from a simple cubic arrangement, with an atom of gold, silver or tellurium at each lattice point. Silver atoms substitute for gold to a minor extent (a maximum of 3.2 wt. % in natural material) but it is not known for certain whether the substitution is entirely random.

Experimentally, the maximum solubility of silver in calaverite was determined to be 3 ± 1 wt. % at 300° C, a figure in good agreement with the composition of natural material. Along the joins Au-$AuTe_2$ and $AuTe_2$-Te there is no detectable solid solution and calaverite is essentially stoichiometric in composition.

At 300° C calaverite is compatible with petzite, sylvanite, tellurium and a gold-rich alloy. It is not compatible with hessite or empressite nor a gold-silver alloy more silver-rich than $Au_{83}Ag_7$ (Atom %).

Sylvanite $AuAgTe_4$.—Sylvanite is monoclinic with space group P2/c. The structure of sylvanite is basically similar to that of calaverite. Tunell and Pauling (46) point out that if a silver atom is substituted for the gold atom at co-ordinates $\frac{1}{2}\frac{1}{2}0$ in the calaverite structure, and slight changes made in the parameters of the silver and tellurium atoms, the structure of sylvanite can be produced.

Theoretically, sylvanite should have the composition

$$\left.\begin{array}{ll} \text{Au} & 24.19 \\ \text{Ag} & 13.22 \\ \text{Te} & 62.59 \end{array}\right\} \text{Wt. \%.}$$

corresponding to a Au : Ag atomic ratio of 1 : 1. Most analyses of natural material, however, reveal a Au : Ag ratio somewhat in excess of this figure. A series of eight analyses of Kalgoorlie material and a further one from Vatukoula, show atomic ratios ranging from 1.21–1.78 : 1. Likewise, the analyses reported by Palache, Berman and Frondel (19) show gold to be well in excess of that demanded by the ideal formula. Experimentally it has been found that, at compositions corresponding to the ideal formula of sylvanite, the three phase assemblage sylvanite-tellurium-empressite was produced. The one-phase sylvanite field was obtained from compositions whose atomic ratios ranged from 1.18–1.44 : 1. These results suggest that sylvanite could well be non-stoichiometric with a not inconsiderable excess of gold atoms over that demanded by the theoretical formula.

At 300° C sylvanite is compatible with all phases in the ternary system, with the exception of a gold silver alloy (regardless of its composition).

Petzite $Au_2Ag_3Te_2$.—The mineral petzite shows neither cleavage nor crystalline form, consequently its symmetry and crystal structure remain unknown.

Theoretically, petzite should have the composition

$$\left.\begin{array}{ll} \text{Au} & = 25.4 \\ \text{Ag} & = 41.8 \\ \text{Te} & = 32.8 \end{array}\right\} \text{Wt. \%.}$$

and analyses of natural material show very little deviation from these figures. Thus, a series of six analyses of Kalgoorlie petzite reveal a variation in gold content from 24.33–25.3% with corresponding changes in the amount of silver.

Experimentally, the one-phase petzite field was found to occur in the range 24–27 wt. % Au. There is thus a very wide miscibility gap between petzite and hessite at 300° C and there seems no justification, as has been done, in regarding petzite as gold-bearing hessite. With respect to its tellurium content, petzite is essentially stoichiometric.

At 300° C, petzite is compatible with calaverite, sylvanite, hessite and a gold-silver alloy of composition $Au_{93}Ag_7$ to $Au_{89}Ag_{11}$ atom %. Petzite is not compatible with tellurium or empressite.

Hessite Ag_2Te.—Hessite is orthorhombic at low temperatures but inverts to the cubic form between 105°–145° C, the actual transition temperature being markedly dependent on whether tellurium or silver be present in excess. This transition is also an extremely rapid one and the high temperature form cannot be quenched by rapid cooling through the inversion interval.

The structure of orthorhombic hessite is not known, but that of cubic hessite has been described by Rahlfs (*26*). Of the eight silver atoms in the unit cell, four of these occupy the coordinate positions $\frac{1}{4}\cdot\frac{1}{4}\cdot\frac{1}{4}\cdot$ so that together with the anions they form the zincblende structure. The remaining four silver atoms are statistically distributed over a large number of vacant lattice positions. Cubic Ag_2Te is not isostructural with Ag_2S, as might be expected, rather it has close similarities to berzelianite (Cu_2Se).

The few reliable analyses of natural hessite from Kalgoorlie contain 0.1 and 0.8 wt. % Au while the analyses quoted by Palache, Berman and Frondel (19) are, with one doubtful exception, quite similar. Most natural hessites show evidence (anomalous anisotropism in polished section) of having passed through the polymorphic inversion and it is perhaps legitimate, therefore, to regard these analyses as representative of the composition of the high-temperature form.

The experimental results are in good agreement with this data. The maximum solubility of gold in hessite was found to be 1 wt. % while along the joins Ag_2Te-Ag and Ag_2Te-$Ag_{5-x}Te_3$, there was no evidence of any deviation from stoichiometric composition.

At 300° C, hessite is compatible with empressite, sylvanite, petzite and a gold silver alloy of widely varying composition. It is not compatible with either calaverite or tellurium.

Empressite $Ag_{5-x}Te_3$.—The structure and range in chemical composition of empressite have been investigated by Thompson, Peacock, Rowland and Berry (40) and Donnay, Kracek and Rowland (6).

Donnay et al. determined $Ag_{5-x}Te_3$ to be the ideal structural formula for natural empressite, with the structure permitting omission of silver atoms to a considerable extent. Thus they determined synthetic empressite to be a homogeneous phase between Ag_5Te_3-$Ag_{4.5}Te_3$, and a careful analysis of natural material, as listed by Thompson et al., gives a formula of $Ag_{4.29}Te_3$.

The present experimental work is in fair agreement with this data. Along the join Ag_5Te_3-Ag_2Te there is no detectable solid solution, but Ag_5Te_3 was found to be a homogeneous phase as far as the composition $Ag_{4.8}Te_3$.

At 300° C, empressite is compatible with hessite, sylvanite and tellurium but not with calaverite, petzite or a gold silver alloy.

Tellurium Te.—Tellurium is hexagonal with space group $C3_12$ on $C3_22$. The structure is made up of spiral chains of tellurium atoms. Within any one chain, each tellurium atom has two nearest neighbors. The bonding is of the covalent type, with each tellurium atom sharing two electrons with its two neighboring atoms. It might be predicted that gold and silver atoms could not enter into this structure to any great extent without disrupting the tellurium chains, and, experimentally, this is found to be the case ($< \frac{1}{2}$ wt. %).

At 300° C, tellurium is compatible with calaverite, sylvanite and empressite but not with hessite, petzite or a gold silver alloy.

Gold Silver Au Ag.—Gold and silver have identical crystal structures and a complete solid solution series exists between the two elements.

Gold silver alloys are compatible with calaverite, petzite and hessite but not with empressite, sylvanite or tellurium. The appropriate compositions are as follows:

Gold Silver—Calaverite Au_{100} to $Au_{93}Ag_7$ (Atom. %)
Gold Silver—Petzite $Au_{93}Ag_7$ to $A_{89}Ag_{11}$
Gold Silver—Hessite $Au_{89}Ag_{11}$ to Ag_{100}

These compositions are subject to an uncertainty of $\pm 2\%$ although along the gold silver-petzite join the uncertainty is somewhat greater owing to a lack of complete equilibrium being reached. The compositions have been determined by the appearance or disappearance of a phase across the binary joins and not by unit cell measurements of the resultant gold silver alloy. The unit cell edges of gold and silver are so similar (4.0786 A° and 4.0862 A° respectively) that precise determinations of composition are not practicable with the methods used.

Solubility of tellurium in a gold silver alloy could not be detected.

Discussion of Phase Diagram

1. Neither krennerite $(AuAg)Te_2$ nor montbrayite (Au_2Te_3) have been synthesized in the present investigation. Inasmuch as krennerite is a common telluride at Kalgoorlie, Cripple Creek, Nagyag, and Fiji, a knowledge of its field of stability is of considerable importance.

Borchert (4), after examination of a suite of ore specimens from Cripple Creek (Colorado) and Nagyag, concluded that orthorhombic krennerite was the low-temperature polymorph of $AuTe_2$ and that above a temperature of 184° C, calaverite was the stable form. This conclusion was based on certain heating experiments in which Borchert noted a change in the lamellar structure of natural krennerite when heated above 184° C. Borchert further concluded that natural calaverite crystals were essentially paramorphs, possessing calaverite morphology but having the internal structure of krennerite. Tunell and Ksanda (44), after completing their structural study of calaverite crystals, demonstrated that the morphological axes and axial ratios of calaverite, as measured on the reflection goniometer, were in complete agreement with the structural axes, as determined by the rotation and Weissenberg

methods. They concluded that the calaverite crystals did not possess the krennerite structure and could not have passed through a polymorphic inversion. In the same way they demonstrated that the external faces of krennerite were in perfect accord with its internal structure. The question of a field of stability for krennerite was thus left in abeyance.

When it became apparent, in the present study, that krennerite could not be synthesized at 300° C an attempt was made to form it at other temperatures. It was reasoned that, as krennerite contained consistently more Ag than calaverite (natural material contains in excess of 5 wt. %), the former mineral might well be a high temperature phase stable at the liquidus surface. A series of runs were then made at 400° and 430° C yielding results as follows:

430°C Natural krennerite largely transformed to calaverite.
Natural calaverite remained unchanged.
Runs of the krennerite composition produced calaverite.

400°C Natural krennerite transformed to calaverite.
Runs of krennerite composition, runs deficient in and containing excess tellurium, all produced calaverite.

These results clearly indicate that calaverite and not krennerite is the stable form at elevated temperatures. It may also be noted that the molar volume of calaverite (160.4 $A^{\circ 3}$) is significantly less than that of krennerite (162.6 $A^{\circ 3}$), hence the latter mineral cannot be a high-pressure phase.

The following alternative hypotheses seem to be quite compatible with what is at present known of the phase relationships:

(a) Krennerite is the low-temperature, low-pressure polymorph of $AuTe_2$. This explanation seems to be the most reasonable one. It is also the original hypothesis of Borchert, though his notion that all calaverite has passed through the inversion is erroneous. Geological evidence clearly indicates that if calaverite and krennerite are indeed polymorphs the transition between them must be a very sluggish one. Figure 7 is a schematic diagram of the phase relationships along the composition join $AuTe_2$-$AgTe_2$ on the assumption that krennerite is the stable phase at lower temperatures.

(b) Krennerite is always metastable with respect to calaverite. This would imply that the stability field of krennerite lies somewhere above the melting curve.

Additional experimental runs designed to throw light on the above problem have been carried out:

300°C Natural krennerite heated for a period of 7 days. No change in the mineral was observed.

250°C Results identical to those at 300° C.

150°C Natural krennerite remained unchanged after heating for 7 days. Runs of krennerite composition heated for a period of 7 days—reaction incomplete but calaverite starting to form.

These results are again inconclusive and further work is required to elucidate the relationship between the two minerals.

The mineral montbrayite has been reported from only one locality (20), with an analysis corresponding approximately to the composition Au_2Te_3. The mineral is triclinic with a structure similar (43) to that of calaverite, krennerite, and sylvanite. Neither Peacock and Thompson nor the present writer were able to synthesize montbrayite and its field of stability thus remains unknown.

2. The 300° isotherm shows very limited mutual solubility between the phases. With the exception of the pure elements, gold and silver atoms do not readily substitute for one another. This feature was commented upon earlier by Kracek and Ksanda (15) and Tunell and Pauling (46) and is borne out by analyses of natural material. Tunell and Pauling have equated the very limited solubility of silver in calaverite and krennerite and gold in sylvanite with slight differences in oxidation number of the gold and silver atoms.

3. The phase diagram of Figure 5 shows the various two and three-phase fields stable at 300° C. There is, of course, no reason why these fields should not change at lower temperatures. It is possible, for example, that calaverite and petzite could react to form gold and sylvanite, the reaction taking place somewhere in the temperature range 0–300° C. As will be indicated later, however, there is no geological evidence for such reactions ever having occurred and it is most probable that with the exception of krennerite in lieu of calaverite, the phase relations at 300° C are similar to those at lower temperatures.

A serious discrepancy arose regarding the assemblages to be expected at temperatures in excess of 300° C. A glance at Figure 4 shows that the liquidus fields of petzite and empressite imply a subsolidus tie line between those two phases. At 300°, however, we find them incompatible. This discrepancy suggested that either the liquidus or subsolidus experimental work was at fault or that between 300°–340° C, petzite and empressite had reacted to form sylvanite-hessite. Two runs, whose compositions lay within the petzite-hessite-sylvanite field, were heated at 330° C for a period of 14 days to test the possibility of such a reaction. These runs indicate that the hessite-sylvanite join at 300° C changes to that of petzite-empressite at a temperature of 315 ± 10° C. There can be little doubt that hessite and sylvanite are compatible at lower temperatures for they are consistently found together in many natural telluride deposits.

Geological Applications

The experimental work that has been carried out so far has two important geological applications.

1. For a given bulk composition in the ternary system, the mineral assemblages to be expected in a natural telluride deposit have been specifically defined. The phase diagram in its present form, therefore, is essentially a compatibility diagram.
2. The phase diagram gives the approximate limits of solid solution to be expected in naturally occurring telluride minerals.

Both these applications are dependent, of course, on the extent to which the phase relations at 300° C approximate those at other temperatures.

It is obvious that the phase equilibrium work is of little value as a geological thermometer. It would seem that the temperatures of transition from orthorhombic to cubic hessite and from krennerite to calaverite (assuming that these two minerals bear a dimorphous relationship to one another and that the transition temperature can be experimentally determined) would be more useful in this regard.

The presence of sulfur and selenium in a natural mineral system, together with more highly mobile components such as water and carbon dioxide, could conceivably alter the equilibrium relationships if they were able to substitute for gold, silver or tellurium in the solid phases. Chemical analyses of natural telluride minerals suggest, however, that there is no basis for this supposition and we may conclude that the presence or absence of water and other components has no effect on the subsolidus equilibrium relationships.

The results obtained will now be applied to two important telluride localities of the world, that of Kalgoorlie, Western Australia and Vatukoula, Fiji. The geological environment of Kalgoorlie is distinct from Vatukoula and the two localities span what has generally been regarded as the range of P-T conditions under which telluride deposits have formed.

It is proposed to show that the mineral assemblages observed in these two localities are in excellent agreement with those determined experimentally.

KALGOORLIE

General Geology

The rocks at Kalgoorlie are of Precambrian age and consist essentially of two series of mafic igneous rocks known as the Older and Younger Greenstone Series. The Older Greenstones are made up of mafic lavas and tuffs with some thin bands of sediment, while the Younger Greenstones consist of an intrusive sill or sills of highly altered quartz dolerite. The Greenstone Series and overlying sediments have been tightly folded, the dominant structure in the region of Kalgoorlie being the south plunging Kalgoorlie syncline. Gold mineralization is largely restricted to the Younger Greenstone horizon on either side of the sheared synclinal axis although the Older Greenstones or "calc schists" may locally become an important ore-bearing horizon.

The Younger Greenstones are highly altered igneous rocks containing chlorite, quartz, epidote, albite and carbonate minerals. Adjacent to the lodes, which occupy shear zones or fractures, the rock becomes enriched in dolomite, sericite and pyrite. The lodes are characterized by their schistose appearance, abundance of fine-grained pyrite and lack of large quartz masses. In type, they resemble many gold veins in the greenstones of the Canadian shield. The auriferous zone at Kalgoorlie is about 6 miles long and one mile wide, but mineralization is most intense at the South end or Golden Mile.

For a more detailed description of Kalgoorlie geology, reference may be made to the volume entitled "Geology of Australian Ore Deposits" (7).

Previous Mineralogical Work

In a recent paper on the occurrence of tellurides at Kalgoorlie Stillwell (34) has reviewed all previous mineralogical work. Of these contributions, the most important are by Simpson (29) who published the first detailed description of Kalgoorlie rocks and minerals, incorporating these and many subsequent observations in his three-volume summary of West Australian mineralogy (30), and Stillwell (32) who carried out an excellent mineragraphic study of Kalgoorlie ores. Stillwell identified at least ten telluride minerals and described their textural relationships. These observations were later summarized by Stillwell (34). More detailed reference to the above works will be made in the following sections.

Present Study

Approximately 110 telluride-bearing samples from the Kalgoorlie goldfields have been studied during the present investigation. The samples were obtained from the Geology Department of the University of Adelaide, the South Australian Museum, the Kalgoorlie School of Mines and operating companies of the Golden Mile, Kalgoorlie. All samples have been polished and examined under the reflecting microscope. Mineral identification has been exclusively by X-ray diffraction methods.

The present suite of samples represents rich telluride ore whose locations range widely over the Kalgoorlie field. Although much of the material is not accurately located the samples are believed to be quite representative of the ore as a whole. The close agreement in results between the present writer and the earlier work of Stillwell and Simpson lends support to this view.

The main object of the present investigation has been to record the various telluride-sulfide mineral assemblages at Kalgoorlie, to ascertain whether these assemblages represent an approach to chemical equilibrium and to compare observed assemblages with those found experimentally in the system Au-Ag-Te. Accordingly, the relevant mineral descriptions will deal only with observed mineral assemblages and not physical properties. An attempt will be made to indicate which minerals appear to be in stable contact. Chemical analyses are quoted where available.

Descriptive Mineralogy

The following metallic minerals have been observed in the samples studied:

Tellurides
- Calaverite
- Coloradoite
- Petzite
- Krennerite
- Sylvanite
- Hessite
- Empressite
- Native Tellurium
- Altaite
- Tetradymite
- Nagyagite
- Melonite
- Weissite

which are accompanied by:

Gold	Galena
Tetrahedrite-Tennantite	Sphalerite
Chalcopyrite	Bournonite-Seligmannite
Pyrite	Native Arsenic
Pyrrhotite	Magnetite
Arsenopyrite	Haematite

These metallic minerals occur in a gangue of quartz, mixed carbonates of iron, magnesium and calcium, sericite, chlorite and occasional tourmaline. The list of telluride minerals includes all those recorded by Stillwell but with the addition of empressite (recorded for the first time at Kalgoorlie), native tellurium, tetradymite and weissite.

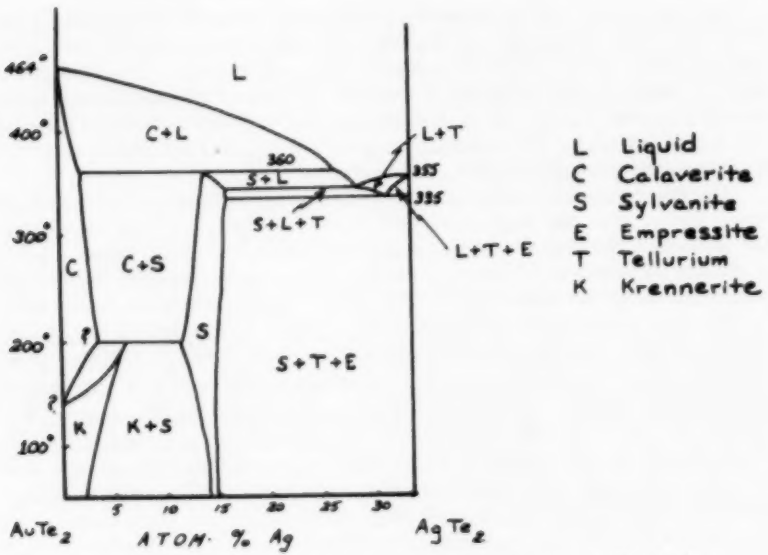

FIG. 7. Phase relations along the composition join $AuTe_2$-$AgTe_2$ (hypothetical only).

Calaverite $AuTe_2$.—Calaverite is the most abundant telluride of the Kalgoorlie field and with the exception of the Hidden Secret mine, has been reported from all mines of the Boulder Belt. Calaverite has been recorded in masses up to 40 × 15 cm, but it is more commonly of fine grain size and shows little or no trace of crystal form. It thus differs markedly from the calaverite of Cripple Creek.

In the present study, the following minerals have been observed in actual contact with calaverite: coloradoite, petzite, sylvanite, gold, krennerite, nagya-

gite, altaite, melonite, chalcopyrite, pyrite, and tetrahedrite, a list essentially identical to that given by Simpson (30). Calaverite has not been found in contact with empressite, hessite, or native tellurium. The most common mineral assemblages are as follows:

Calaverite-coloradoite
Calaverite-coloradoite-petzite
Calaverite-coloradoite-gold
Calaverite-petzite (Fig. 8)
Calaverite-coloradoite-tetrahedrite (Fig. 9)

while rarer assemblages are:

Calaverite-gold
Calaverite-sylvanite
Calaverite-krennerite

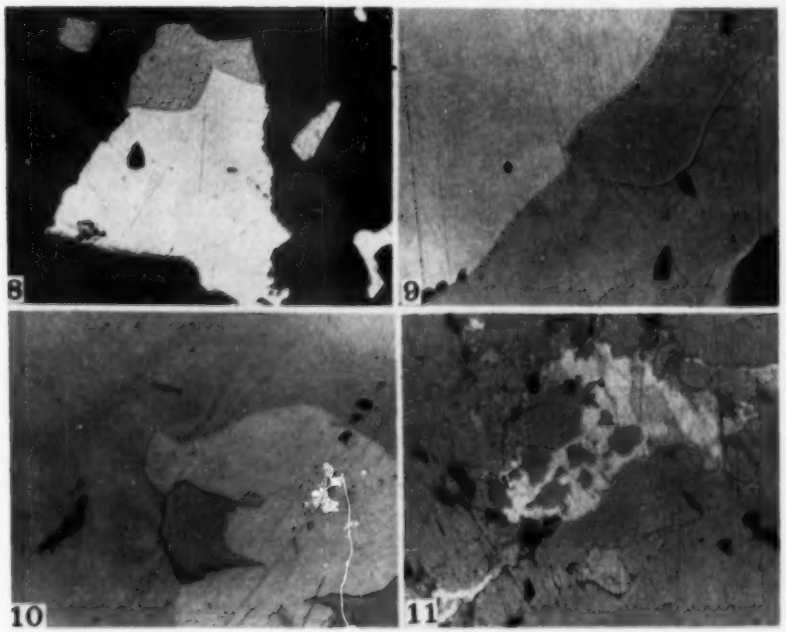

FIG. 8. The association calaverite (white)-petzite (light gray), Kalgoorlie. × 170.

FIG. 9. The association calaverite (white)-coloradoite (light gray) and tetrahedrite (medium gray), Kalgoorlie. × 170.

FIG. 10. The association calaverite (white)-coloradoite (light gray)-petzite (medium gray)-tetrahedrite (high relief), Kalgoorlie. × 65.

FIG. 11. Tetrahedrite (medium gray) showing inclusions of and partial replacement by sylvanite (white) and hessite (light gray), Kalgoorlie. × 250.

Altaite, melonite, nagyagite, and tetradymite may occur with calaverite but are generally present in only trace or accessory amounts.

Coloradoite is by far the commonest associate of calaverite; numerous specimens show the two minerals present as discrete masses with a broad contact or as intimate admixtures. The association is common enough to infer that it is a stable assemblage under the conditions of its formation. Petzite behaves in a similar way and the three-phase assemblage calaverite-coloradoite-petzite is not infrequent. In certain cases these three minerals may be accompanied by tetrahedrite and chalcopyrite (Fig. 10). Calaverite-coloradoite-gold is also common, but where the assemblage occurs the gold particles are never found in contact with calaverite but are always distributed in coloradoite. Likewise the discrete assemblage calaverite-gold has been found in only two specimens (Stillwell reports similar findings). Possible reasons for the failure of calaverite and gold to occur together will be given in a later section. The assemblages calaverite-sylvanite and calaverite-krennerite are rare, the first being found on two occasions and the second in five specimens. In all of the associations described, altaite, melonite, nagyagite and tetradymite may be present as accessory minerals. Tetrahedrite and chalcopyrite are widely distributed minerals and are often observed in contact with calaverite. The three minerals appear to be quite compatible even though calaverite may vein and partially replace the earlier tetrahedrite grains. In contact with calaverite, pyrite crystals frequently show corroded outlines and replacement of the sulfide mineral is clearly indicated. A feature of the telluride minerals from Kalgoorlie, however, is that they only rarely occur in the presence of pyrite.

Chemical Composition of Calaverite.—Many specimens of Kalgoorlie calaverite have been analyzed. The results are listed by Spencer (31) and Simpson (30). A number of these analyses appear unreliable, however, either because evidence of homogeneity of the sample was lacking or because the mineral has been confused with krennerite and sylvanite. In certain instances tellurium has not been determined so that there has been no check as to the accuracy of the gold and silver determinations.

The following results, of varying reliability, indicate that Kalgoorlie calaverite may contain up to 2.3% Ag but that its silver content is generally less than 1 percent. The figures for gold and tellurium range over rather wide limits. This may be due partly to inaccuracies of analysis and partly to slight variations in the stoichiometric ratios of gold and tellurium.

	1	2	3	4	5	6	7	8	9	
Au	43.59	41.37	41.76	42.15	41.54	38.6	41.64	40.0	40.75	
Ag	—	0.58	0.80	0.60	0.89	2.3	0.25	1.5	0.86	Wt. %
Te	56.41	57.27	56.64	57.00	56.48	—	—	—	—	
Total	100.00	99.22	99.20	99.84	98.91	—	—	—	—	

1. $AuTe_2$ theoretical composition.
2–4. Listed by Simpson.
5. Analyst: Wright, Perseverance G. M.
6–9. Analyst: Hooker.

Analyses 5, 6, 7, 8 and 9 have recently been carried out for Gold Mines of Kalgoorlie at the request of Mr. G. S. Compton.

Coloradoite HgTe.—Coloradoite is also an extremely common telluride throughout the Kalgoorlie field and has been reported in masses up to several pounds in weight. Like calaverite, it shows no trace of crystal form.

Calaverite, gold, petzite, sylvanite, hessite, altaite, galena, tetradymite, nagyagite, tetrahedrite and chalcopyrite have all been observed in contact with coloradoite and the most common mineral assemblages are listed below:

Coloradoite-gold	Coloradoite-petzite-tetrahedrite-chalcopyrite
Coloradoite-gold-petzite	Coloradoite-gold-tetrahedrite
Coloradoite-petzite-calaverite	Coloradoite-krennerite
Coloradoite-calaverite	Coloradoite-altaite

The association of coloradoite with hessite, sylvanite, nagyagite, galena and tetradymite is uncommon.

One of the most interesting features of Kalgoorlie mineralogy is the constant association of gold and coloradoite. It is rare to find a piece of coloradoite that does not contain some gold; moreover, many of the spectacular gold specimens on display at the Kalgoorlie mines consist of masses of bright yellow gold set in equally abundant masses of coloradoite. In this association, altaite is commonly present as an accessory telluride, and galena has been observed in two such specimens. Other characteristic associations are with calaverite and petzite. Tetrahedrite-chalcopyrite may accompany these assemblages.

Coloradoite tends to occur preferentially with gold and those tellurides rich in gold, though this may be merely a function of the commonness of occurrence of gold-rich as opposed to silver-rich tellurides, than to any chemical preference for the former.

Chemical Composition of Coloradoite.—Available analyses of Kalgoorlie coloradoite (29) agree well with the theoretical formula HgTe.

	1	2	3
Hg	61.14	60.95	61.62
Te	38.86	39.38	38.43
Total	100.00	100.33	100.05

1. HgTe.
2. Analyst: Spencer (1903)
3. Analyst: Simpson (1912).

Recently, two partial analyses have been carried out at the request of Gold Mines of Kalgoorlie. These yield gold contents of 0.1 and 0.56%, the gold being present either as a discrete phase or in solid solution.

Petzite $AuAg_3Te_2$.—Petzite, though subordinate to calaverite and coloradoite, is a common telluride at Kalgoorlie. It has been reported in large quantities from the Hidden Secret mine at the north end of the field and in smaller masses from the Golden Mile. Stillwell (32) regarded it as somewhat rare, especially in the deeper levels, and suggested that some of the Kalgoorlie petzite was of secondary origin.

In the present suite, petzite is generally present in most specimens containing calaverite and coloradoite but petzite is found, along with hessite

and sylvanite, in the more silver-rich telluride ores. The most common mineral associations are as follows:

Petzite-Calaverite-Coloradoite	Petzite-Coloradoite-Gold
Petzite-Calaverite	Petzite-Coloradoite-Tetrahedrite-Chalcopyrite
Petzite-Calaverite-Altaite	Petzite-Sylvanite-Hessite

Coloradoite and calaverite are the commonest associates of petzite and the three minerals may be found together in varying proportions. In the assemblage petzite-coloradoite-gold, the host mineral for native gold is generally coloradoite, but the preference of gold for coloradoite in this assemblage is not nearly so marked as in the corresponding calaverite-coloradoite-gold association.

Large grains of petzite commonly contain a little altaite and in some cases, ex solution-type intergrowths with sylvanite. However, petzite is more commonly an associate of sylvanite when the latter occurs as an intergrowth with hessite. The assemblage petzite-sylvanite-hessite, the former mineral occurring as discrete grains, the latter two as a fine intergrowth, is typical of Kalgoorlie and is well shown in ore from the Hidden Secret and Gt. Boulder Perseverance mines. This association was first described by Stillwell (32).

Petzite is often found with tetrahedrite and chalcopyrite.

Chemical Composition of Petzite.—Simpson (30) lists six complete and three partial analyses of petzite from Kalgoorlie. Of these, three are mixtures of petzite and coloradoite. The remainder show:

	1	2	3	4	5	6	7
Au	25.4	24.33	24.64	24.62	25.3	25.2	25.2
Ag	41.8	40.70	40.47	40.45	42.0	41.8	41.7
Te	32.8	32.60	34.60	—	—	—	—
Total	100.0	97.63	99.71	—	—	—	—

1. $AuAg_3Te_2$.
2–7. Quoted from Simpson.

Available analyses suggest that there is very little deviation from the stoichiometric formula, though silver does substitute for gold to a minor extent.

Krennerite $AuTe_2$.—Simpson and Stillwell, in their earlier studies of Kalgoorlie tellurides, clearly recognized that much of their supposed "sylvanite" might well be krennerite, but in the absence of recognizable crystal form and lack of knowledge of the true chemical composition and crystal structure of krennerite, they were unable to make the distinction. X-ray identification of samples has clearly shown that krennerite is not only an exceedingly common mineral at Kalgoorlie, but that much of what was previously regarded as sylvanite is, in fact, krennerite. This conclusion was anticipated by Stillwell in 1953 when he reported that the main gold-bearing mineral on the 300-foot level of the Lake View Consols lode was probably krennerite and not sylvanite as previously thought.

Krennerite occurs in large masses up to several inches in dimension and is commonly observed free from inclusions of other minerals. Where mineral associations do occur, the following are the most common:

Krennerite-coloradoite
Krennerite-tetrahedrite
Krennerite-tetrahedrite-chalcopyrite
Krennerite-coloradoite-calaverite
Krennerite-calaverite

Large masses of krennerite may contain small marginal areas rich in coloradoite, in some places in the presence of relict corroded crystals of pyrite. Tetrahedrite and chalcopyrite, the former generally well crystallized, are also characteristic associated minerals.

The association of krennerite with calaverite is most interesting in the light of experimental work so far carried out though, unfortunately, the textural relationships do not allow any conclusions to be drawn regarding stable mineral assemblages. Two specimens do suggest veining and replacement of calaverite by krennerite but the evidence is not clear-cut in polished section.

Krennerite appears to be a common telluride mineral on the 2,200-foot level (Phantom S. Lode) of the Gt. Boulder G. M., where it has been reported by Baker (1) associated with petzite, sylvanite, tetrahedrite, chalcopyrite and coloradoite.

Krennerite was also observed in polished section associated with weissite and gold. The weissite, containing many filaments of free gold, has penetrated along the cleavage directions of krennerite and partly replaced that mineral. This association was described earlier by Stillwell, who considered the copper tellurides to be of secondary origin, its formation being analogous to the development of secondary chalcocite in the zone of secondary enrichment.

Chemical Composition of Krennerite.—Simpson (30) lists fifteen chemical analyses of sylvanite of which six appear to belong to the mineral krennerite. Two partial analyses of known krennerite have recently been carried out for Gold Mines of Kalgoorlie.

	1	2	3	4	5	6	7	8
Au	36.60	36.6	36.1	36.1	32.58	33.4	33.07	39.2
Ag	3.82	3.5	4.4	2.0	6.64	6.0	6.46	3.2
Te	58.63	—	—	—	—	—	—	—
Total	101.05							

1–3. Simpson.
4. Analyst: Hooker. Perseverance G. M. 1,300-foot level.
5–7. Simpson.
8. Analyst: Canning: Perseverance G. M.

Although these analyses are of varying reliability, they clearly indicate a much higher silver content than the corresponding figures for calaverite.

Sylvanite $AuAgTe_4$.—Sylvanite was previously regarded as a common telluride at Kalgoorlie, but many of the occurrences must now be ascribed to krennerite. The known associations of sylvanite are largely made up of silver-rich as opposed to gold-rich telluride ores.

Sylvanite-petzite	Sylvanite-hessite-petzite-altaite-tetrahedrite
Sylvanite-petzite-hessite	Sylvanite-calaverite
Sylvanite-hessite	Sylvanite-empressite
Sylvanite-hessite-coloradoite	Sylvanite-tellurium

The sylvanite-hessite intergrowths are a feature of Kalgoorlie mineralogy (cf. Stillwell, 32). Commonly the intergrowths are accompanied by petzite or by petzite and altaite, and in one specimen from the Gt. Boulder G. M., by petzite and tetradymite. On the 2,200-foot level of the same mine, hessite-sylvanite veinlets are associated with chalcopyrite and tetrahedrite (Fig. 11). Sylvanite and petzite may also occur together without hessite. These intergrowths may be interpreted as due to exsolution of an original homogeneous phase.

The associations sylvanite-empressite and sylvanite-tellurium have been found in only one specimen viz. the Tetley lode of the Associated G. M. The assemblage calaverite-sylvanite is also rare.

Chemical Composition of Sylvanite.—The following analyses of Kalgoorlie sylvanite are essentially those reported by Simpson (30) but with krennerite analyses deleted. It will be noted that the range in silver content is from 9.18–11.77 percent, figures somewhat lower than that demanded by the theoretical formula.

	1	2	3	4	5	6	7	8	9
Au	24.19	28.55	29.85	25.98	25.5	26.1	29.2	29.2	29.4
Ag	13.22	9.76	9.18	11.77	11.2	11.4	10.6	9.4	9.3
Te	62.59	60.83	60.45	61.90	—	—	—	—	—
Total	100.00	99.14	99.48	99.65	—	—	—	—	—

1. $AuAgTe_4$.
2–9. Simpson.

Hessite Ag_2Te.—Hessite has previously been described by Simpson and Stillwell as a common mineral in ore from the Hidden Secret G. M., where it occurred with sylvanite, petzite and coloradoite, but that it was of more sporadic occurrence along the Golden Mile. Stillwell regarded some Kalgoorlie hessite as being of secondary origin. In the present investigation, hessite was found in most localities where sylvanite occurred. On the deeper levels it occurs extensively on the 2,200-foot level of the Gt. Boulder G. M.

The mineral associations with hessite are largely those already indicated; it will be noted that the assemblages invariably include sylvanite.

Hessite-sylvanite	Hessite-sylvanite-coloradoite
Hessite-sylvanite-petzite	Hessite-sylvanite-petzite-altaite
Hessite-sylvanite-petzite-tetradymite	

Although the hessite-sylvanite intergrowths are characteristic, hessite may also occur as discrete grains.

Under crossed nicols, hessite usually shows anomalous anisotropism, suggesting that it has passed through the low temperature inversion point.

Chemical Composition of Hessite.—Two specimens of hessite from the Hidden Secret G. M. were collected by Simpson and analyzed. Both analyses show very minor substitution of silver by gold.

	1	2	3
Ag	62.86	61.0	61.7
Au	—	0.8	0.1
Te	37.14	—	—
Total	100.00	—	—

1. Ag_2Te.
2–3. Simpson.

. . . Empressite $Ag_{5-x}Te_3$.—Empressite had not previously been recorded from Kalgoorlie but in one specimen from the Tetley Lode, Associated G. M., was found to occur with sylvanite. On the reverse side of the specimen tellurium and sylvanite are associated.

Kalgoorlie empressite yields an X-ray powder pattern identical to that given by Thompson, Peacock, Rowland and Berry (40) for both their natural and synthetic material. Insufficient material was available for a chemical analysis.

Tellurium Te.—Native tellurium was recorded by MacIvor (17) in the early history of Kalgoorlie but was never observed by any later workers. In the present specimen from the Associated G. M. (Tetley lode) a crystal of tellurium, approximately 1.5 × 0.5 cms, was observed in contact with a smaller mass of sylvanite. The assemblages recorded in this specimen, tellurium-sylvanite and empressite-sylvanite, are quite distinct and are not in juxta position.

An analysis carried out by MacIvor yielded 96.94% Te and 2.4% Au. Traces of iron and sulfur were noted but no selenium.

Altaite PbTe.—Altaite has been recorded in small amounts from eight of the one hundred or so specimens studied and is to be regarded as an accessory mineral only.

Mineral associations recorded are as follows:

Altaite-sylvanite-petzite
Altaite-sylvanite-petzite-hessite
Altaite-coloradoite-calaverite
(Figs. 12, 13)
Altaite-petzite-coloradoite
Altaite-coloradoite-tetrahedrite
Altaite-galena-gold
Altaite-coloradoite-petzite-gold

The data suggest that altaite is an associate of most of the common telluride assemblages at Kalgoorlie but is present in accessory form only. One specimen of altaite contained numerous oriented blebs of seligmannite-bournonite together with minor coloradoite and tetrahedrite.

Chemical Composition of Altaite.—Simpson lists an analysis of impure material collected from the Hidden Secret G. M.

	Pb	Ag	Au	Cu	Fe	Te	Se	Total
1.	61.91	—	—	—	—	38.09	—	100.0
2.	61.33	0.43	0.02	0.01	0.13	38.43	0.08	100.4

1. PbTe.
2. Simpson.

The relatively high content of silver, together with traces of selenium, have been taken by Stillwell (32) as evidence for the possible existence of the silver selenides aguilarite and naumannite. These he equates with a number of small inclusions within altaite. In the present suite, however, no inclusions similar to those observed by Stillwell have been noted.

Tetradymite Bi_2Te_2S.—Tetradymite has previously been reported by Simpson (29) but was not observed by Stillwell (32). In the present study

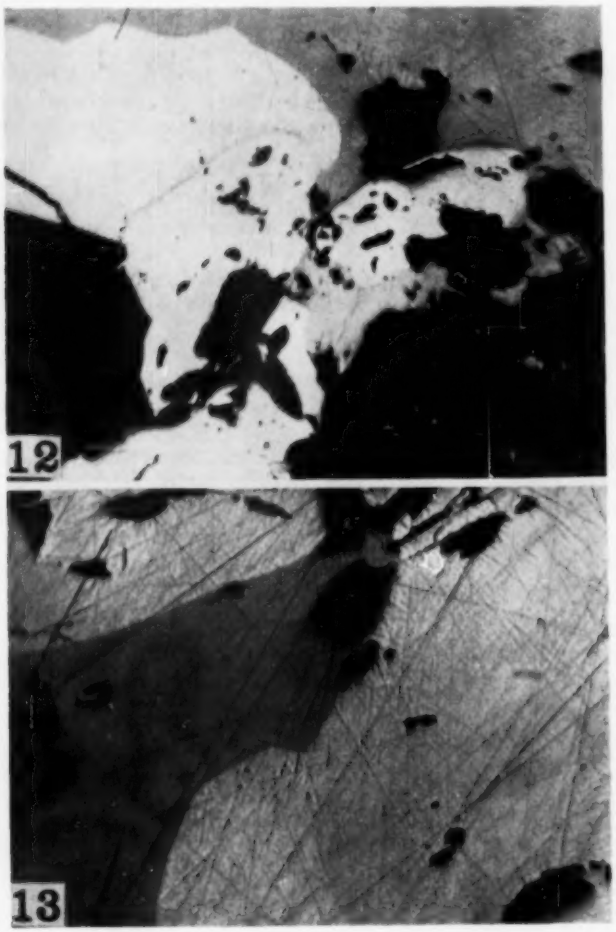

FIG. 12. The association calaverite (creamy white)-coloradoite (light gray)-altaite (white), Kalgoorlie. × 75.

FIG. 13. Same as Fig. 12 but with magnification × 350.

it has been found in samples from the Gt. Boulder and Lake View and Star mines and in a third specimen whose locality remains unknown. Bismuth, however, appears to be generally absent from the Kalgoorlie ores. Observed mineral associations include:

Grt. Boulder	Tetradymite-petzite
	Tetradymite-petzite-sylvanite-hessite
Lake View and Star	Tetradymite-calaverite
	Tetradymite-coloradoite
	Tetradymite-coloradoite-petzite-chalcopyrite
Kalgoorlie	Tetradymite-coloradoite
	Tetradymite-coloradoite-gold

Mr. H. Jensen (pers. communication) reports that tetradymite is a not uncommon telluride on the 2,400-foot level of the Lake View and Star mine. No chemical analyses are available.

Nagyagite $AuPb\,Sb(TeS)_{11}$.—Nagyagite was first recorded from the Oroya-Brownhill mine by Mezrett (18), but no further material was located until Stillwell's mineragraphic work. He found nagyagite in a specimen from the Gt. Boulder G. M. and from two other unknown localities.

In the present study, a relatively large mass of nagyagite was found on a specimen from the 600-foot level, Gt. Boulder G. M. The predominant minerals are nagyagite and calaverite, but within the nagyagite are many small inclusions of gold, coloradoite and altaite. In a second occurrence, locality unknown, nagyagite occurs as minute grains associated with calaverite, coloradoite and petzite. Within these three tellurides are found many relict crystals of arsenopyrite.

The assemblages described by Stillwell are complex but include the following minerals:

Nagyagite-krennerite-coloradoite-petzite
Nagyagite-petzite-seligmannite
Nagyagite-coloradoite-krennerite-tetrahedrite

Chemical Composition of Nagyagite.—Simpson (30) lists an analysis of material collected from the Oroya-Brownhill mine.

	Au	Pb	Ag	S	Te	Sb	Fe	Total
1.	10.16	52.55	1.12	8.62	18.80	7.00	—	98.25
2.	8.34	55.56	—	10.51	17.54	7.47	0.47	99.89

Analysis 2 represents the "ideal" composition of nagyagite as given by Berry (2).

Melonite $NiTe_2$.—Melonite was first reported by Thompson (37) from the Hidden Secret G. M. Stillwell (32) observed it in specimens from the Associated Northern, Kalgurli, South Kalgurli and Lake View mines. In all of these cases, melonite occurred in microscopical amounts, the largest particles not exceeding 1 mm in diameter.

Melonite was again recorded in the present study as minute grains within larger masses of calaverite, altaite and petzite. The grains were too small to be identified by X-ray methods. The percentage of nickel in the Kalgoorlie ores is extremely low.

Weissite Cu_2Te.—In a specimen from the Gt. Boulder G. M. (500-foot level, Robb South lode), abundant weissite was observed. In polished section, grains of calaverite and krennerite are intersected by narrow veinlets of weissite which in turn, enclose smaller filaments of gold. Weissite-gold veinlets penetrate along the cleavage directions of krennerite while the lack of cleavage in calaverite has resulted in that mineral being randomly veined.

A completely analogous occurrence was recorded earlier by Stillwell (32) in a specimen from the Kalgurli mine (420-foot level). Stillwell then expressed the view that the copper telluride (he called it rickardite) was of secondary origin and formed in the zone of secondary enrichment of copper. The present writer agrees with this interpretation. It seems likely that copper-bearing solutions descending from the oxidized zone have reacted with gold tellurides to form copper telluride plus gold. A possible reaction would be

$$4\ Cu^{++} + AuTe_2 = 2\ Cu_2Te + Au$$

An X-ray powder photograph shows the mineral to be definitely weissite and not rickardite, a fact anticipated by Stillwell (34). The probable secondary origin of weissite is supported by the fact that secondary chalcocite and covellite may often be observed replacing tetrahedrite and chalcopyrite.

Gold.—The percentage of free gold in the Kalgoorlie ore differs widely from place to place, both along the line of lode and within any one vein. The gold is generally in minute grains disseminated throughout the ore and only in the spectacular gold-coloradoite associations is the gold massive in appearance. Simpson (29) has well summarized the crystallographic and physical forms in which the gold occurs. Emphasis is here placed on its mineral associations.

As already indicated, the predominant association is gold-coloradoite, but gold-petzite may also occur quite frequently. On the other hand, gold may be absent from the telluride veinlets and occur in the adjacent wall rock or siliceous gangue. The following associations of gold were recorded in the present study; they are largely in order of abundance:

Gold-coloradoite
Gold-petzite
Gold-coloradoite-petzite-tetrahedrite
Gold-coloradoite-petzite-altaite
Gold-pyrite
Gold-calaverite
Gold-calaverite-chalcopyrite
Gold-altaite-galena
Gold-coloradoite-nagyagite
Gold-magnetite

Gold occurs most commonly with coloradoite, less commonly with petzite and only rarely with calaverite. It has not been observed in contact with sylvanite, krennerite, or hessite. The gold-coloradoite assemblage may be

accompanied by tetrahedrite, by calaverite (but not in contact with the gold), by altaite and by petzite. Gold-chalcopyrite has been observed on three occasions, gold-magnetite once. Gold occurs with pyrite in the more siliceous pyritic ores and in those veins lacking telluride minerals. Such gold may be isolated in quartz, occur interstitially between pyrite grains or, more rarely, within the pyrite itself. These observations on the associations of native gold are in good agreement with those made earlier by Stillwell (32).

Chemical Composition of Gold.—Only two analyses of Kalgoorlie gold are available. Simpson (29) reports 93.93% Au and 5.85% Ag in a specimen of primary "rough" gold from the Oroya G. M., while gold from a gold-coloradoite assemblage (N. Kalgurli G. M.) as analyzed at N. Kalgurli G. M., yielded the approximate figures of 92% Au, 5% Ag and 2% "base" metal.

The color of primary gold in polished section is bright yellow and no obvious variation in color has been detected. In the absence of any further data, it seems reasonable to assume that Kalgoorlie gold is of the above order of composition though variations from these values doubtless occur.

Tetrahedrite-Tennantite.—This complex sulfosalt is most abundant at Kalgoorlie. Its prominent associations are with the telluride minerals on the one hand and chalcopyrite on the other. In the present description, the term tetrahedrite implies a member of the tetrahedrite-tennantite series.

Simpson (29) and Stillwell (32) report that tetrahedrite is most commonly found in irregular quartz veins cutting across the general trend of the lodes. This feature may be readily observed but it does not imply any lack of intimate association with the telluride minerals themselves.

The following common associations with tetrahedrite have been recorded. It is important to note that the telluride assemblages containing tetrahedrite and chalcopyrite are the same regardless of the presence of these two sulfide minerals.

Tetrahedrite-coloradoite
Tetrahedrite-coloradoite-petzite
Tetrahedrite-coloradoite-gold
Tetrahedrite-coloradoite-calaverite
Tetrahedrite-coloradoite-calaverite-petzite
Tetrahedrite-krennerite
Tetrahedrite-petzite-gold
Tetrahedrite-calaverite
Tetrahedrite-petzite
Tetrahedrite-sylvanite-hessite

In all of the above assemblages, chalcopyrite may accompany the tetrahedrite. Altaite is commonly present as small rounded inclusions in tetrahedrite and associated with calaverite, coloradoite, and gold. Tetrahedrite, with or without chalcopyrite, is common in contact with pyrite. In such cases the pyrite grains may show evidence of replacement.

It may be noted that the association of tetrahedrite with the telluride minerals is both complex and varied. Under conditions existing during the formation of the telluride minerals, tetrahedrite appears to have been a common and stable mineral.

Chemical Composition of Tetrahedrite.—Simpson (*29*) lists three complete and one partial analyses of Kalgoorlie material. The results indicate, as might be expected, a varying Sb: As ratio.

	1	2	3	4
Gangue	0.26	—	1.1	—
Au	0.12	—	0.015	—
Ag	0.22	—	0.68	—
Cu	41.69	38.96	37.8	—
Fe	4.76	3.94	3.1	—
Ni	0.15	—	—	—
Pb	0.10	0.43	Nil	—
Zn	2.68	5.12	5.6	—
As	16.87	10.01	11.0	5.58
Sb	4.30	9.57	14.6	21.36
Bi	—	—	Nil	—
S	28.43	30.17	26.6	—
Te	0.05	—	N.D.	—
Total	99.63	98.20	100.495	—

Analyses 1–4: Simpson.

Considerable substitution of copper by iron and zinc is evident, but silver and lead are conspicuously low. Analyses 1 and 2 show sulfur to be well in excess of that demanded by the formula.

Chalcopyrite.—The mineral chalcopyrite is not as widespread as tetrahedrite but may locally predominate. It occurs with both the telluride minerals and with pyrite. Chalcopyrite has been noted in this study with all of the common telluride assemblages so far described and detailed associations need not be repeated. Commonly the chalcopyrite-telluride assemblages contain tetrahedrite. In contact with pyrite, chalcopyrite generally shows evidence of having replaced the earlier iron sulfide. In the zone of secondary enrichment chalcopyrite, like tetrahedrite, may be veined by a mixture of chalcocite and covellite.

Chemical Composition of Chalcopyrite.—Simpson (*29*) reports an analysis of chalcopyrite collected from the Hidden Secret G. M.

	1	2
Cu	34.84	34.64
Fe	30.04	30.42
S	35.75	34.94
Total	100.63	100.00

1. Simpson.
2. $CuFeS_2$.

Pyrite.—Pyrite is a ubiquitous mineral occurring throughout the Kalgoorlie mineralized zone. Its abundance appears to bear no relationship to the amount of gold or telluride minerals present in the lode, though where tellurides do occur, the pyrite is rarely in contact with them.

Pyrite is present most commonly as small euhedral crystals disseminated throughout the adjacent greenstone wallrock. The pyritic wallrock is generally segregated from the telluride minerals by a zone rich in silica, so that there may be little or no contact between the sulfide, as distinct from the

telluride zone of mineralization. Where pyrite does occur in contact with telluride minerals, the crystals are generally corroded and appear as residual grains.

Simpson (*29*) estimated the average content of pyrite in the ore to be of the order of 7 percent, while away from the lode channels the amount decreased to about 1 percent. Simpson also pointed out that many pyrite grains have developed by the conversion of magnetite and hematite to iron sulfide, the iron oxides having formed largely through retrograde metamorphism of the original igneous rock. The changes described by Simpson, namely iron-silicates → iron oxides and iron oxides → pyrite were observed also by Stillwell and the present writer.

Much of the pyrite is fine grained and shows well developed cubic crystal forms. Inclusions of other minerals are rare and although gold has been observed within pyrite, it generally occurs interstitially. Pyrite may be veined and replaced by chalcopyrite, tetrahedrite, and by many telluride minerals.

Pyrrhotite.—Pyrrhotite is a rare constituent of the Kalgoorlie ores. It was observed by Simpson (*30*), Feldtmann (*8*) and the present writer in a specimen from the 2,570-foot level of the Ivanhoe G. M. Pyrrhotite is here associated with chalcopyrite and pyrite.

Arsenopyrite.—Arsenopyrite is also rare at Kalgoorlie. It has been noted in greenstone country rock as slender prismatic crystals and occasionally is present within the telluride veins. In a specimen from the Associated G. M. (900-foot level) arsenopyrite crystals occur within tetrahedrite, coloradoite, and calaverite. The arsenopyrite is locally almost completely replaced by calaverite.

Galena.—Simpson (*29*) and Stillwell (*32*) both report galena in minor amounts. Two associations recorded in the present suite include:

Oroya G. M.	Galena-altaite-gold
N. Kalgurli G. M.	Galena-coloradoite-gold

Sphalerite.—Sphalerite was noted by Stillwell (*32*) associated with chalcopyrite and jamesonite, and the present writer observed it in the presence of coloradoite and a little chalcopyrite.

Bournonite-Seligmannite.—Stillwell (*32*) reports both bournonite and seligmannite from Kalgoorlie, one specimen of seligmannite forming an intimate intergrowth with petzite. In the present study, bournonite-seligmannite was found as oriented blebs within altaite, together with associated coloradoite, tetrahedrite and petzite. No other occurrences of these minerals were noted.

Native Arsenic.—Native arsenic occurs in a specimen from the Chaffers G. M., 1,500-foot level where it was first described by Simpson (*29*). No associated metallic minerals occur.

Magnetite-Hematite.—As previously pointed out by Simpson (*29*) and Stillwell (*32*), magnetite and hematite readily form during the alteration of quartz dolerite to greenstone. In the vicinity of the lode, much of this

ferric oxide has been converted to pyrite though a few quartz-magnetite and quartz-hematite masses have been preserved. Rarely, such magnetite may be veined by calaverite, chalcopyrite, and gold.

Other Metallic Minerals.—Stillwell (*32*) reports the presence of enargite, jamesonite, and stibnite from Kalgoorlie but these were not observed in the present suite. They are, presumably of rare occurrence.

Gangue Minerals.—The predominant gangue minerals at Kalgoorlie are quartz, dolomite-ankerite, siderite-magnesite, chlorite, sericite, and some tourmaline. These minerals have previously been described by Simpson (*29*) in some detail and need not be here reviewed. An important feature of Kalgoorlie mineralogy, however, is the general absence of large masses of vein quartz. Much of the silica in the veins appears the result of alteration from a silicate to carbonate-rich wallrock and the quartz is to be regarded as a metamorphic rather than an introduced vein mineral.

To be Concluded in Next Number.

Economic Geology
Vol. 55, 1960, pp. 1179–1201

GENETIC ASPECTS OF THE MONAZITE AND COLUMBIUM-BEARING RUTILE DEPOSITS IN NORTHERN LEMHI COUNTY, IDAHO *

ALFRED L. ANDERSON

CONTENTS

	PAGE
Abstract	1179
Introduction	1180
Geographic setting	1180
Geologic setting	1181
Stratigraphic and structural relationships of the deposits	1182
Size of the deposits	1183
Mineralogy	1184
Summation	1184
Descriptive features	1184
Silicates	1184
Phosphates	1188
Carbonates	1189
Sulfates	1191
Oxides	1191
Sulfides	1193
Paragenesis	1193
Textural and structural characteristics	1196
Regional zoning	1198
Origin of the deposits	1198
Previously proposed concepts of origin	1198
Objections to the previous concepts	1199
Discussion and conclusions	1200
References	1201

ABSTRACT

Deposits of monazite and columbium-bearing rutile in a belt more than 10 miles long in northern Lemhi County, Idaho, are distinguished by their notable concentrations of such elements as thorium, titanium, columbium, barium, calcium, iron, phosphorus, sulfur and the rare earths, and by their abundance of carbonates, chiefly calcite. These deposits occur as structurally controlled replacements of crystalline limestones, amphibolites, and porphyroblastic gneisses which form part of the complex metamorphic border zone of the Idaho batholith. Most of the deposits, which are small and tabular, show a sporadic and irregular distribution of minerals, the most abundant of which are actinolite, allanite, apatite, monazite, calcite, barite, ilmenorutile (columbium-bearing rutile), ilmenite, and magnetite. Other minerals, some of them sparse, include biotite, phlogopite, garnet,

* Published with the approval of the Director of the Idaho Bureau of Mines and Geology. Presented before the Society of Economic Geologists, St. Louis, 1958.

epidote, glaucophane, ancylite, bastnaesite, sphene, rutile, chlorite, pyrite, pyrrhotite, chalcopyrite, and quartz. Silicates, except sphene, were deposited first and were followed successively by phosphates, carbonates, sulfates, oxides, and sulfides. Most of the thorium entered the allanite instead of the somewhat later monazite.

The deposits possess all the compositional characteristics of the carbonatites, but differ from the type carbonatites in their seemingly lack of association with alkalic igneous rocks. Although the deposits were regarded by others as replacements of marble beds and as products of metamorphic differentiation, the unique association and concentration of elements so characteristic of the carbonatites, coupled with the paragenetic development, suggests that they, like the carbonatites, are of magmatic rather than of metamorphic origin.

INTRODUCTION

In northern Lemhi County, Idaho, are some unique carbonatic deposits with notable concentrations of such elements as thorium, columbium, titanium, calcium, barium, iron, phosphorus, sulfur and rare earths, an association of elements characteristic of the carbonatites found with alkalic igneous rocks. These elements find expression locally in monazite, allanite, columbium-bearing rutile (ilmenorutile), apatite, ilmenite, magnetite, barite, calcite, and in many other minerals. The mineral assemblage resembles that of the carbonatites, but the mineral deposits appear to differ from the normal carbonatites in their apparent lack of association with alkalic intrusives.

These deposits have been described as replacements of marble lenses in the complexly metamorphosed rocks of the Belt series marginal to the Idaho batholith, and have been explained as products of metamorphic differentiation (1, p. 22) and metamorphic segregation (7), in which the enclosing sediments rather than fluids of magmatic origin supplied the essential constituents of the deposits.

On visiting some of these deposits in 1954, the writer became interested in the compositional and genetic aspects of the mineralization. As a result of detailed microscopic investigation then and after a more comprehensive examination of the deposits in 1957 (2, pp. 21–44), a metamorphic genesis was found to be unacceptable, for the paragenesis and other factors lend support to a magmatic source as the most satisfactory explanation of the origin of the deposits. The present study discloses that not all the deposits are replacements of marble lenses and that much of the calcite so abundantly associated with the mineralization is introduced or vein calcite and is younger than the silicate and phosphatic minerals. The paragenetic relationships thus play an important role in the interpretation of the genetic history of the deposits and afford a compelling argument for a magmatic rather than a metamorphic source.

GEOGRAPHIC SETTING

These carbonatic deposits are in the rugged canyon country carved by the Salmon River and its tributaries about 30 miles northwest of Salmon, the county seat (Fig. 1). Most of them are aligned along a belt from 1½ to 2½

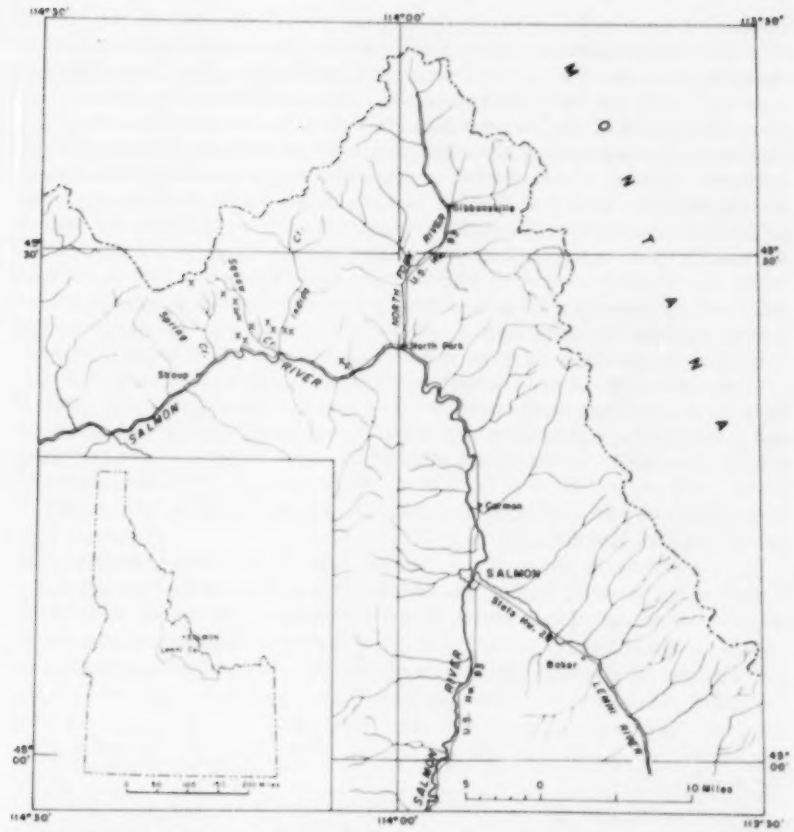
114°30'
114°00'
113°30'
45° 30'
45° 00'
SALMON RIVER
North Fork
SALMON
Salmon
Lemhi
Lemhi River
Spring Cr.
Spring Cr.
Indian Cr.
Indian Cr.
Williams Cr.
Williams Cr.
Sheep Cr.
Sheep Cr.
Big Deer Cr.
Big Deer Cr.
Deer Cr.
Deer Cr.
Hughes Cr.
Hughes Cr.
Panther Cr.
Panther Cr.
Lemhi Cr.
Lemhi Cr.
Lemhi Mts.
Lemhi Mts.
Beaver Cr.
Beaver Cr.
Big Timber Cr.
Big Timber Cr.
Big Timber

metamorphic rocks are regarded by Abbott (1, p 5–10) and Kaiser (7) as originally sedimentary, probably Beltian rocks, transformed by metasomatic metamorphism into their present form, supposedly by agencies and processes associated with the emplacement of the Idaho batholith. The gneisses are most widespread of the metamorphic rocks, but the amphibolites are almost as abundantly represented along the main belt of mineralization as are the gneisses. Instead of sedimentary origin, as intimated by Abbott and Kaiser, the amphibolites were found to be derived from igneous rocks of originally gabbroic composition. Where the metamorphism has not been so intense, the amphibolitic schist and gneisses show transition into massive gabbro which has retained most of its original minerals. Where the gabbro has been deformed by shearing, it has been changed to hornblendic schist and where, further modified by additions of potash feldspar during metasomatic metamorphism, to gneiss or in many places, to porphyroblastic "augen" gneiss.

Some thin beds of fine- to medium-grained crystalline limestone of bluish-gray color (buff on weathered surfaces) are intercalated with the gneisses and schists of original sedimentary origin; but some of the reported limestone, occurring as lenses in the foliate amphibolites and in some of the porphyroblastic and other gneisses, is vein calcite associated with the carbonatic mineralization. This vein calcite, generally of coarse grain, also occurs in the mineralized limestone lenses.

The rocks along the mineralized zone show complicated structural relationships. Abbott (1, p. 12) has described these relationships in terms of a large synclinorium of northwesterly trend with much crumpling of the beds, especially of the limestone beds which are approximately astride the synclinorium axis. Kaiser (7) likewise interprets the structure as a large complexly crumpled, overturned fold, more specifically a synclinorium made up of many small to large isoclinally folded structures, with the complex crumpling particularly pronounced in the amphibolite zone along the central part of the synclinorium.

Recognizing that the amphibolites are derived from igneous rather than from sedimentary rocks, the writer regards the central part of the synclinorium as constituting a zone of special structural weakness that facilitated intrusion of gabbroic magma and later the metasomatic metamorphism associated with the emplacement of the Idaho batholith. The metasomatic metamorphism apparently spread through the sheared and crumpled rocks converting the gabbro to the various amphibolites and in considerable part also into porphyroblastic rocks. Later still this zone of structural weakness localized and directed the movement of the carbonatic fluids that gave rise to the monazite and columbium-bearing rutile deposits.

STATIGRAPHIC AND STRUCTURAL RELATIONSHIPS OF THE DEPOSITS

The monazite and columbium-bearing rutile deposits are mainly within the zone of amphibolitic rocks and are contained in massive and schistose amphi-

bolites, in the porphyroblastic gneisses derived from the amphibolites and enclosing sedimentary rocks, and in thin beds of crystalline limestone.

The zone of mineralization tends to conform with the belt of amphibolized rock and hence with the inferred zone of structural weakness, which, prior to metamorphism, had directed the intrusion of gabbroic rocks. Within the zone of mineralization the individual deposits, which have broadly tabular and lenticular shapes, trend in northwesterly directions, in part approximately coinciding with regional structural trends. Individual bodies strike N 80° W, N 60° W, N 30° W, and N 10° W. Deposits on the southwest side of the synclinorium dip northeast and those on the northeast side dip steeply southwest.

The deposits are structurally controlled, but the control is not always readily apparent. Some occur along well-defined zones of shearing, parallel to or conformable with the folding or banding of the enclosing rock and are bordered by sharply defined walls, unmarked by gouge. Some cut the non-foliated amphibolites and appear to be fissure rather than shear-controlled. In many deposits the structural guidance has been almost obliterated by the mineralization, which, through replacement, has removed directive shears or fractures.

The relations of the deposits have been explained by Abbott (1, p. 8–9) and Kaiser (7) on the basis of both stratigraphic and structural controls. Both believe that the beds of crystalline limestone have been instrumental in localizing the mineralization, with the deposits assuming the structural characteristics of the folded limestone beds. Kaiser suggests that the deposits are particularly localized in crests and troughs of small folds, the actual location depending on a combination of a fault, a fold, and a bed of limestone.

SIZE OF THE DEPOSITS

Deposits uncovered so far are small, rarely more than a foot or two across, exceptionally as much as 8 feet; and, because of insufficient development, cannot be traced for more than a few tens of feet. One more fully explored than the others has been traced for more than 300 feet, ranging in thickness from 1½ to 6 feet. Another, from scattered exposures, may be more than 1,000 feet long; but in this deposit as well as in the others the important minerals show an irregular distribution and are largely confined to small shoots, exceptionally more than 40 or 50 feet long.

In some places the mineralization is spread sparingly through relatively broad zones of schistic rock, with the greatest concentration of minerals in small, irregularly distributed veins mostly less than a foot thick. Several of these veins may lie along the schistic zone, one vein parallel to the other, none extending more than a few tens of feet on strike and dip. Small, sporadically distributed bunches or pockets of vein minerals may also appear along these broad schistic zones. These may possibly be regarded as large, low-grade lode deposits, perhaps as much as 40 feet across.

MINERALOGY

Summation

The deposits contain a mineral assemblage characteristic of the carbonatites, deposits noted for their concentration of minerals containing thorium, titanium, columbium, barium, calcium, phosphorus, iron, and rare-earth elements, in association with abundant carbonates, chiefly calcite. The minerals containing these elements are conspicuously developed in the Lemhi County deposits and are represented by monazite, allanite, apatite, ilmenorutile, rutile, ilmenite, magnetite, barite, and calcite, along with biotite, phlogopite, actinolite, garnet, glaucophane, epidote, bastnaesite, ancylite, sphene, pyrite, pyrrhotite, chalcopyrite, and sparse quartz. Other minerals reported but not observed include specularite, zoisite, serpentine, molybdenite, and siderite. All of the minerals, except the glaucophane, epidote, sphene, garnet, rare-earth carbonates (ancylite and bastnaesite), quartz, and sulfides, are relatively though not uniformly abundant; and all, except the garnet, epidote, sphene, apatite, and rare-earth carbonates, are recognizable without the microscope. The most distinctive or diagnostic minerals in the deposits are the actinolite, biotite, phlogopite, allanite, monazite, apatite, calcite, barite, ilmenite, ilmenorutile, and magnetite.

Descriptive Features

For a more orderly presentation, the minerals are grouped and described separately as silicates, phosphates, carbonates, sulfates, oxides, and sulfides. Particular attention is given to mineral characteristics and relationships.

To provide easy reference, the groups and their minerals are listed below.

Silicates	Phosphates	Oxides
Biotite	Apatite	Ilmenorutile
Actinolite	Monazite	Rutile
Phlogopite		Ilmenite
Garnet	Carbonates	Magnetite
Glaucophane	Ancylite	Quartz
Epidote	Bastnaesite	
Allanite	Calcite	Sulfides
Chlorite		Pyrite
Sphene	Sulfates	Pyrrhotite
	Barite	Chalcopyrite

Silicates.—Biotite, although visible in all the deposits, is one of the lesser minerals and is relatively inconspicuous, except in the deposits near the Montana line. Most of the grains are small, comparable in size with those in bordering schists; but some grains in the deposits near the State line are considerably larger and measure up to half an inch in diameter. Much of the biotite shows a preference for the border zone of the deposits.

The biotite is black but in thin section the grains are not deeply colored and are not strongly pleochroic. Colors are mostly brown, less commonly green; and grains show only moderate absorption.

Some of the biotite in the deposits is obviously an inheritance from the schistic country rock, but a part of it may have been introduced into the rock

during early stages of mineralization. In either case the biotite is penetrated and replaced by crystals of actinolite and other minerals (Fig. 2). On the other hand, considerable of the biotite and especially that tending toward coarser grain growth penetrates into and through the actinolite crystals, commonly retaining oriented remnant inclusions of the actinolite. Such biotite is itself embayed or otherwise penetrated by other minerals and has been observed as shadowy, ghost-like inclusions in the calcite. This biotite approaches phlogopite in composition.

Actinolite is one of the most abundant minerals and in some desposits is the leading mineral. It occurs in all deposits but is not so conspicuously developed along the southeastern part of the belt as toward the northwest, possibly because its grains are smaller and not so darkly colored. Where unweathered, the actinolite is dark green and highly lustrous, but in some deposits it is pale green and rather dull in appearance. Because of its color and textural habit, the actinolite is one of the most striking minerals in the deposits.

The actinolite possesses rather distinctive characteristics. Much of it shows a tendency to occur as complete to incomplete radial aggregates of long, slender crystals or needles; as bundles of needles in divergent and sheaflike forms; and as felted, essentially fibrous masses. The radial- or divergent-like aggregates are generally of small size, less than one half inch in diameter; but in some deposits on upper Squaw Creek the aggregates are composed of slender rods as much as four inches long. The tendency for radial or rosette development is well displayed in thin section. Thin sections also reveal that the actinolite lacks uniformity of composition and has a higher iron content in some places than in others. Where relatively rich in iron, the actinolite is distinctly greenish and notably pleochroic; otherwise the actinolite is pale green to nearly colorless and shows but feeble pleochroism or none at all. Such actinolite shows transition to tremolite.

The actinolite has an irregular distribution and may occur anywhere through the deposit, but in some places it shows preference for marginal areas and may appear in greater abundance along one or both walls or along one wall and then the other. In such areas the radial and felted aggregates may penetrate outward into the host rock (Fig. 2). Irregular masses, however, may occupy central parts of the deposits, their erratic distribution fixed by the sporadic distribution of the calcite, which has permeated unevenly through the deposits, disrupting what otherwise would have been a continuous and essentially uniform body of actinolite (Fig. 12).

The actinolite, regardless of its distribution, penetrates and replaces all minerals inherited from the host rock, including also the biotite introduced into the rock during the initial stages of mineralization (Fig. 2). It then in turn serves as a host for all the other minerals of the deposits and shows penetration and more or less extensive replacement by calcite (Fig. 3), magnetite (Fig. 2), rutile (Figs. 10, 11), and the remainder of the minerals. It is particularly "soaked" through by the calcite, its radial group and felted masses commonly occurring as irregular remnants or as ghost-like inclusions,

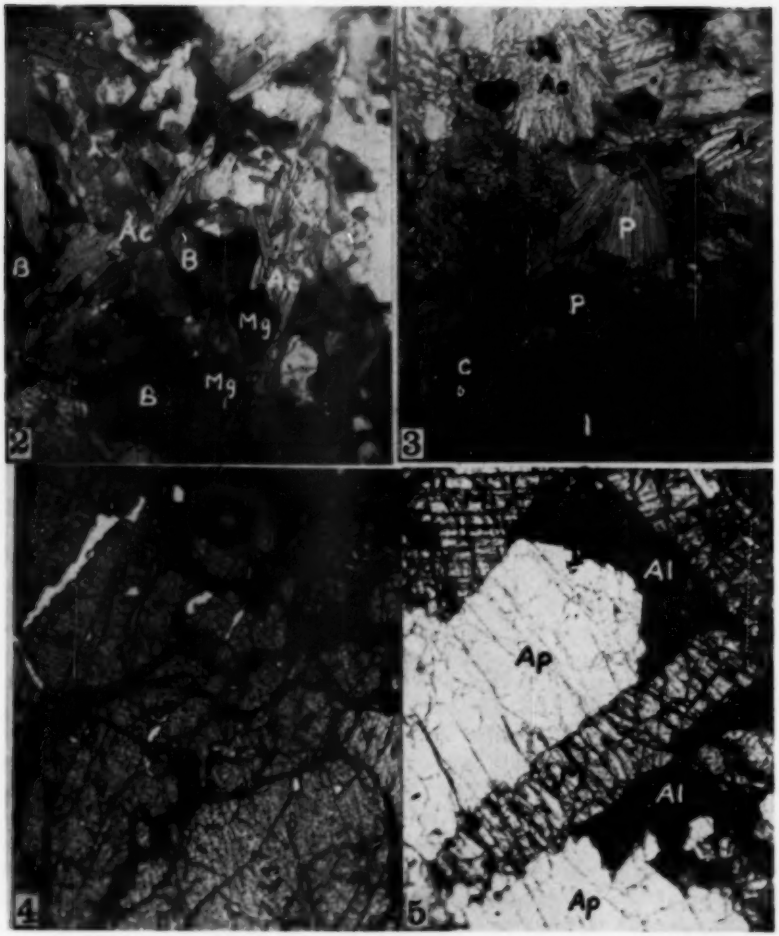

FIG. 2. Biotite-enriched siliceous wall rock penetrated by actinolite and magnetite. The actinolite laths (Ac) cut through and replace the aggregate biotite (B) and the quartz-feldspar host, whereas the magnetite grains (Mg) impregnate and replace both the biotite and actinolite. Inward the deposit contains much allanite, coarse calcite, and ilmenorutile. Uncrossed nicols. × 40.

FIG. 3. Needle aggregates of actinolite (Ac) and divergent sheafs of phlogopite (P) unevenly penetrated and corroded by calcite (C) and then by a large crystal of ilmenite (I) and smaller, scattered grains of magnetite (also black). The ilmenite has irregular penetrative borders. Uncrossed nichols. × 40.

FIG. 4. Large grain of epidote veined by irregular, ramifying seams of allanite (dark). Uncrossed nicols. × 40.

recognized in the larger grains and aggregates of calcite as shadowy outlines or as scattered oriented remnants.

Phlogopite cannot be safely distinguished from the biotite, except microscopically; but it appears in most thin sections and may be the principal mica in the deposits characterized by the presence of pale-green or lighter-colored actinolite. The phlogopite is pale brown to colorless in thin section and is much less absorptive than the biotite. The phlogopite shows a marked tendency for a divergent, sheaf-like development (Fig. 3). These grains, like those of the post-actinolite biotite, penetrate into and across the actinolitic aggregates with retention here and there of remnant inclusions of the actinolite. Like the biotite, the phlogopite is in turn penetrated and corroded by the other minerals, with the corrosive effects most strongly manifested by the calcite (Fig. 3).

Garnet is a scarce mineral and was observed in a single thin section from one of the deposits on upper Spring Creek. It occurs as yellowish-green grains in which are distributed a few minor remnants of biotite and actinolite. These grains are contained within and are irregularly corroded by calcite.

Glaucophane occurs in one of the deposits on the east side of Indian Creek where it forms coarse, black needle aggregates along a few fractures in the highly silicated part of the filling. The needles tend to lie along the fractures, but some of them penetrate into or pierce the bordering aggregates of actinolite. As the directing fractures were not observed in the carbonate areas, the relations of the glaucophane to the calcite and other minerals cannot be directly established. Thin section study suggests local invasion of some of the glaucophane by calcite.

Epidote is another of the lesser minerals revealed by microscopic study. It forms relatively large grains in several of the deposits, closely associated with allanite in the actinolite areas. Some of the epidote is mantled and some is veined by allanite (Fig. 4). The epidote appears to transect the aggregates of actinolite and biotite.

Allanite is one of the most persistent minerals along the mineral belt and may be observed in most, if not all, deposits, in some as microscopic grains and in others as coarse grains easily discernible by the unaided eye. It may be regarded as one of the more abundant minerals in the deposits. Where visible, it has a rather dull, grayish-black color, showing marked resemblance to a blackish amphibole, its somewhat flattened grains measuring up to half an inch long. Where especially abundant, it forms granular pods up to an inch thick and several inches long. It may also occur as scattered nests, small bunches, and more widely scattered grains, generally closely associated with actinolite. The allanite is strongly radioactive and may contain much of the thorium in the deposits.

In thin section the allanite is distinguished by its pronounced pale- to dark-brown, in places nearly reddish pleochroism, and by its tendency to

FIG. 5. Crystal of allanite (Al) deeply and unevenly penetrated by apatite (Ap) with both then penetrated and replaced by euhedral crystals of monazite (M). Uncrossed nicols. × 40.

occur as well-shaped crystals, many of which are zoned and some of which are twinned. Generally the crystals are unaltered, but in some places they show minor breakdown, especially near margins, to a reddish metamict. Locally the allanite veins and mantles the epidote (Fig. 4), but most of it forms crystals that penetrate into and through the actinolite and biotite. Much of the allanite is free of included minerals; but it may itself appear as inclusions in other minerals, especially as remnants in monazite and calcite. In places its borders are penetrated by monazite and apatite (Fig. 7) and locally the penetration by monazite crystals may be so complete that the allanite appears as irregular, interrupted mantles on the monazite crystals.

Chlorite is present in nearly every thin section, mostly as an alteration product of the biotite. In some sections, the alteration is slight or incomplete; but in others the chlorite may form complete pseudomorphs of the mica, with preservation of sheaf-like structures. Such pseudomorphs as well as the partly altered biotite grains may occur in remnant form engulfed in the carbonates.

Sphene is another of the scanty minerals, occurring as microscopic grains in some of the ilmenite-rich deposits near the Salmon River below the mouth of Squaw Creek. Some of the grains penetrate the actinolite near ilmenite-grain margins, but much of the sphene lies against or occurs as included remnants within the larger grains of ilmenite.

Phosphates.—Apatite is a notably abundant mineral in the deposits, but its presence is revealed only by the microscope. It may occur as small, barrel-shaped crystals scattered irregularly and relatively abundantly through the deposit and bordering crystalline limestone or, more generally, as groups of crystals packed into large granular aggregates, which remain entirely within the deposit. The individual crystals and aggregates penetrate into and locally engulf the silicate minerals or their remnant (Fig. 5) and are in turn penetrated and held as remnant inclusions in the monazite (Fig. 5), calcite, and other non-silicate minerals.

Monazite has been observed in every deposit, more abundantly in some than in others. It occurs as crystals and small crystal aggregates which have a highly irregular distribution, with local concentrations into pods as much as 1 foot thick and 10 to 20 feet long. It is discernible in most deposits without the microscope. Its grains and crystals range from microscopic sizes to half an inch, exceptionally 2 inches, long. Most of the monazite has a honey-brown color; but in some deposits the grains are reddish brown, and in others decidedly reddish.

Most of the monazite is only weakly radioactive and in general contains less than 1 percent thoria, if any at all. Only a little of it shows alteration to reddish decomposition products and the extent of alteration is generally slight, a reflection of its low thorium content. Most of the thorium in the deposits was apparently taken up by the allanite.

Like the allanite, the monazite tends to develop as well-shaped crystals that penetrate the silicate minerals and the aggregate apatite without loss or change of shape (Fig. 5). It seems to possess to a high degree the ability to take its own crystal form in replacing other minerals. In extending

across grains and crystals of allanite it may give the impression that it is irregularly mantled by allanite. The monazite tends to clear itself of other minerals, but some of its crystals contain minor remnant inclusions or shadowy outlines of the allanite and actinolite. It generally presents good crystal outlines against the calcite, but some crystals are rounded and some are held as remnant inclusions in the calcite (Fig. 6).

Carbonates.—Ancylite [$(Ce, La)_4(Sr, Ca)_3(CO_3)_7(OH)_4 \cdot 3H_2O$] was at first mistaken for impure carbonate grains inherited from the crystalline limestone, but later, more detailed studies disclosed that it was not an inherited mineral but that it and the closely associated bastnaesite and calcite are younger than the silicates and phosphates. The ancylite is not abundantly represented in the deposits and is not discernible, except microscopically, and even then in only a few thin sections made of the materials collected from the deposits near the Montana line. The ancylite has a tendency to form octahedral grains, which are generally somewhat rounded as though corroded by enveloping calcite.

Bastnaesite [$(Ce, La)(CO_3)F$] is closely associated with the ancylite and in the thin sections examined is more abundant than the ancylite, though still a minor mineral. It may be distinguished from the calcite by its higher relief, its indistinct cleavage or parting, its clouded appearance, its weak pleochroism, and its decidedly tabular habit. Its pleochroism and tabular habit also separate it from the ancylite. The bastnaesite grains are generally somewhat rounded or corroded by the calcite. Monazite in contact with the bastnaesite shows some effects of corrosion.

Calcite, one of the most essential minerals, occurs in variable quantities in every deposit, generally as one of the most abundant minerals. The calcite is generally coarsely granular, its grain in places measuring up to one-half inch long. It is not to be confused with the fine- to medium-grained, bluish-gray calcite composing the crystalline limestone commonly present in or along the deposits. The contrast between the two calcites is particularly marked where the coarse calcite forms irregular seams cutting or penetrating the limestone. The contrast is even more enhanced by the white to pale-buff color of the coarse calcite on fresh surfaces. Some of the pale-buff calcite resembles siderite superficially, but unlike siderite, it reacts vigorously with cold acid.

The calcite is distributed sporadically through the deposits as small, irregular seams, pods, and bunches, which ordinarily are without sharp boundaries, the calcite diffusing into the bordering minerals, commonly preserving shadow outlines of the minerals, visible even to the unaided eye. Thin sections reveal that the calcite penetrates the silicate minerals, commonly holding remnants of them in undisturbed orientation and also as irregularly corroded grains. The calcite also penetrates and corrodes the phosphates, in places wiping out all except minor remnants of former large masses of aggregate apatite and locally showing strong corrosion or replacement of the monazite (Fig. 6). This relation applies just to the silicates and phosphates and not to the sulfates, oxides, and sulfides, which show much the same relation to the calcite as the calcite does to these other minerals.

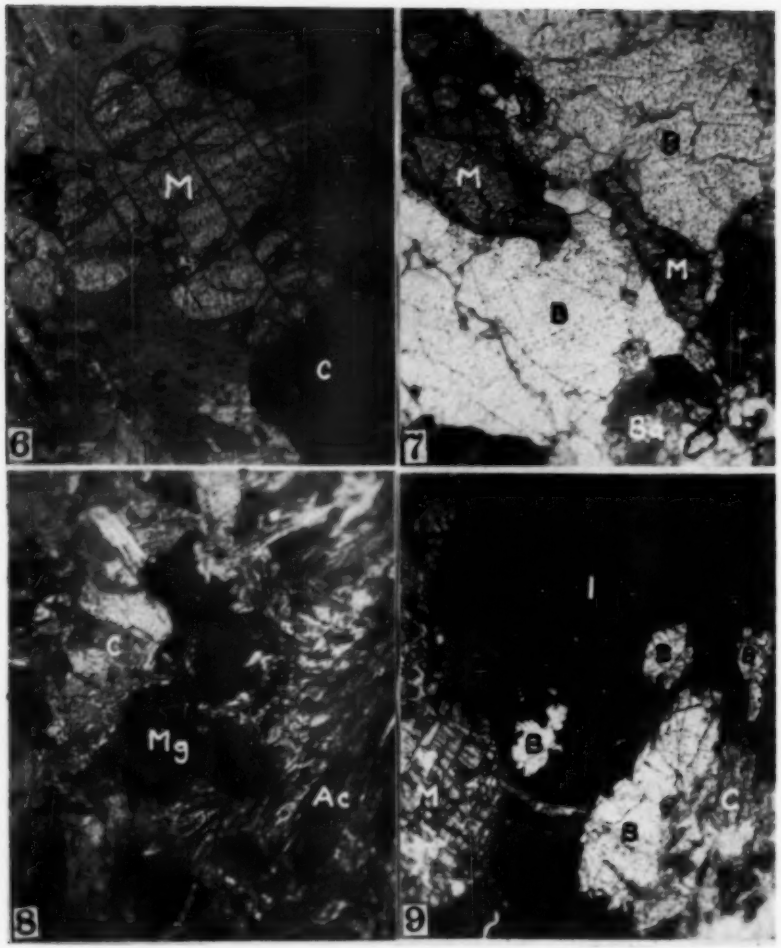

FIG. 6. Large grain of monazite (M) rounded or corroded by calcite (C)—evidence that the calcite is younger than the monazite. Generally the monazite tends to resist replacement by the calcite and retains its euhedral shape. X-nicols. × 40.

FIG. 7. Two corroded remnants (M) of a monazite crystal included within a replacing aggregate of barite (B). The barite also encloses a grain of bastnaesite (Ba). Some dark remnants of allanite remain in the section. Uncrossed nicols. × 40.

FIG. 8. Irregular grain aggregates of magnetite (Mg) penetrating into and across groups of actinolite needles (Ac) and extending into calcite (C), locally holding included remnants of the calcite. X-nicols. × 40.

Sulfates.—Barite is another of the distinctive minerals, but is not so abundant nor so readily detected as are the calcite and some of the other minerals. In some places its grains or crystals may be seen by the unaided eye, especially where it forms white, coarsely crystalline aggregates; in other places its presence may be inferred from the heavier-than-to-be expected weight of the specimen material. In most places, unless exceptionally abundant, its presence is best revealed by the microscope. The barite shows some tendency to occur as pods and irregular masses within the bodies of calcite, but its distribution is irregular and somewhat sporadic and is not restricted exclusively to calcite.

The barite grains penetrate and embay other minerals, particularly the silicates, phosphates, and calcite. Most of the grains are free of included materials but some of them do retain remnant inclusions of the silicate minerals and corroded and engulfed crystals of apatite and monazite (Fig. 7). The grains rather commonly hold irregular, island-like remnants of the calcite grains. Its relations to the oxides and sulfides are like those of the calcite, though it is not penetrated so extensively by these minerals as is the calcite. Figure 9 shows its inclusion within a large grain of ilmenite.

Oxides.—Magnetite is present in variable but generally small amounts in all deposits, but is rarely a conspicuous mineral. Its grains and crystals are generally small and occur as disseminations, less commonly as small irregular veinlets or as fine, granular streaks. The magnetite seems to be more closely associated with and more abundantly disseminated through the carbonates than with and through other minerals. The disseminated grains show a preferential distribution along borders of the calcite grains whereas the veinlets are found along minor fractures. Some grains are very irregular in outline and suggest included remnants, perhaps as in inheritance from the crystalline limestone. Many of the grains, especially the larger ones, enclose irregular remnants of calcite and barite, and here and there also of actinolite and biotite (Fig. 8). The grains of magnetite may lie in contact with but were not observed within the ilmenite. Some of its more isolated crystals are cut or penetrated by tiny veinlets of ilmenite.

Ilmenite is conspicuously abundant in some of the deposits along the Salmon River below the mouth of Squaw Creek, but elsewhere it is a minor mineral. It shows a tendency to develop its own platy, crystal form; but lumps or grains do occur. Its grains are generally rather small; but in one deposit along the Salmon River, the crystals approach giant size, measuring up to 8 inches long and 4 inches wide. Its color is black but its luster is not so bright nor shiny as that of the ilmenorutile, and in contrast appears rather dull. The ilmenite contains a small amount of columbium, less than 1 percent.

The ilmenite displays a preference for the carbonate-rich parts of the deposits, but is not excluded from the silicate areas. Its crystals and grains

FIG. 9. Large black grain of ilmenite (I) locally bordered by the containing oriented-island inclusions of barite (B). The bordering barite shows invasion of calcite (C). The monazite (M) is unevenly corroded by ilmenite but tends to resist replacement by it. Uncrossed nicols. × 40.

contain a few remnants of sphene, chlorite, and actinolite, and somewhat more abundant remnants of calcite and barite (Fig. 9). ,The larger crystals and grains in and near the outcrop are generally much fractured with the fractures healed by supergene calcite.

Ilmenorutile or columbium-bearing rutile (Ti, Cb)O_2 has a somewhat restricted distribution and has been observed only in the deposits from Indian Creek northwestward to the Montana line, reaching its greatest development in the Squaw Creek area. Where present, it is generally a conspicuous mineral, much of it occurring as lumps and granules measuring up to an inch or two in diameter and as pods, up to several inches long. Although the microscope reveals long prismatic or tabular crystals (Figs. 10, 11), the ilmenorutile otherwise occurs as dark, steel-gray, granular masses, which are much more lustrous in appearance than either the magnetite or ilmenite.

The striking metallic appearance of the ilmenorutile reflects its high but somewhat variable columbium content, reported by Kaiser (7) to range from 4 to 10 percent columbium metal and by Heinrich et al. (5, p. 1581), up to 13 percent columbium with less than 0.1 percent tantalum. According to Russell Wood(oral communication), chemists of the Molybdenum Corporation of America reported that some of the ilmenorutile contained from 45 to 48 percent columbium expressed as columbic oxide. Because of its high columbium content, the ilmenorutile is generally opaque in thin section and, unless it shows its crystal form, is difficult to distinguish from the magnetite and ilmenite. As the columbium content decreases, the crystals and grains of ilmenorutile become weakly translucent. In polished sections with polarized reflected light, the ilmenorutile is readily distinguished from the ilmenite by its rather distinctive grayish polarization colors.

The ilmenorutile generally occurs in the more central parts of the deposits, generally with the calcite, although granules or masses may extend into the actinolite and other silicates. Viewed in thin section the grains and crystals penetrate into and through the calcite and silicate minerals (Figs. 10, 11), but rarely retain them as inclusions. Its crystals also penetrate and replace ilmenite, commonly retaining small oriented remnants of the ilmenite. In places unreplaced ilmenite appears to wrap around or fill in between the ilmenorutile crystals.

Rutile is one of the lesser minerals and has been postively identified only at the far southeast end of the mineral belt. It is free of columbium and has a distinctly reddish color and the adamantine luster generally characteristic of the mineral. It occurs as small grains and granules, mostly less than a half inch in diameter, scattered sporadically through the more carbonatic parts of the deposits. Its relations to other minerals seems to be the same as for the ilmenorutile.

Quartz is a rare mineral and has been observed sparingly in only a few deposits, mostly as microscopic pods and irregular masses in the interstices between calcite and barite crystals. Some of it occurs as a cleft filling and borders well-shaped crystals of calcite and barite. It is a primary metal of the deposits and not a secondary mineral introduced along post-mineralization fractures. In places the quartz corrodes the barite and locally holds small

oriented remnants of bordering grains of calcite and barite. Its relations to the oxide and sulfide minerals were not established.

Sulfides.—The sulfides are scantily represented in the deposits but are visible to the unaided eye, mostly as widely disseminated grains, exceptionally as coarse aggregates. They occur irregularly through the deposits but are most abundant in the areas of carbonate mineralization, where their distribution shows some dependence on the boundaries of the calcite grains.

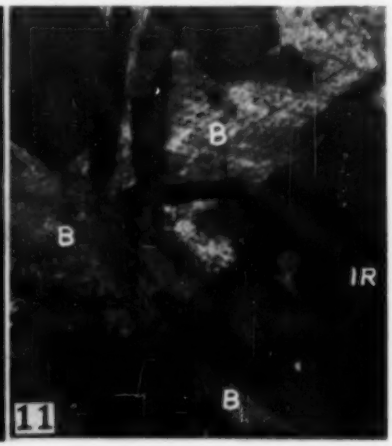

FIG. 10. Tabular ilmenorutile crystals (IR) penetrating allanite (Al), actinolite (Ac), and calcite (C). The ilmenorutile shows a marked tendency for euhedral replacements. Uncrossed nicols. × 40.

FIG. 11. Black euhedral crystals of ilmenorutile (IR) penetrating and replacing barite (B), some of which is retained as included remnants in the ilmenorutile. Uncrossed nicols. × 40.

The most abundant and most widely represented sulfide is *pyrite*, which occurs in part as cubic crystals up to one-eighth inch square. Some of these crystals hold minor inclusions of calcite and other minerals, including, locally, remnants of ilmenite and ilmenorutile. *Pyrrhotite* and *chalcopyrite* are not so abundantly nor so widely distributed and more difficult to detect. In one deposit on upper Squaw Creek, exploratory work uncovered a small pocket of sulfides containing coarse grains of pyrite, pyrrhotite, and chalcopyrite. This pocket formed in and against calcite and actinolite, the sulfides transecting the actinolite needles and calcite grains. The pyrite shows cubic crystallization, but its large grains are partly enclosed and somewhat penetrated by pyrrhotite and in part by chalcopyrite.

Paragenesis

Because of its bearing on the origin of the deposits, the mineral paragenesis is of especially pertinent interest. On cursory observation the mineral rela-

tionships seem baffling and contradictory. The baffling relationships stem from the fact that so many of the minerals tend to assume their own euhedral forms during replacements and thus penetrate extensively into neighboring minerals. That the penetration is by replacement is indicated by the retention of oriented-island remnants of the host mineral and also by preservation of shadowy or phantom-like outlines of the host, especially if the replacing mineral is calcite. Some minerals also show corrosive effects where engulfed in other minerals. Embayments and other evidence of transection of the minerals are also common. Evidences such as these make it possible to establish the paragenesis with a high degree of accuracy.

Biotite is the only mineral with contradictory relationships, but this contradiction exists only because the biotite is not all the same age. Inasmuch as some of the biotite is penetrated and replaced by actinolite and more or less directly by all the minerals that follow, it can be definitely established as the earliest mineral. Part of it and perhaps most of it may be an inheritance from the country rock, but some is so closely associated with the actinolite that it must have been formed by the mineralizing fluids just ahead of the actinolite. Such biotite is penetrated by and in part replaced by the actinolite (Fig. 2). On the other hand, the biotite, which penetrates and contains remnant inclusions of the actinolite, indicates that there are two generations of biotite, one older and one younger than the actinolite. As the younger biotite is also penetrated and corroded by all the other minerals, it had to form just after the actinolitte.

The phlogopite has exactly the same relations as the younger biotite and the two may be essentially contemporaneous, the presence of one or the other reflecting local variations in the composition of the mineralizing solutions.

The only minerals penetrated by the actinolite are those of the country rock and the early biotite (Fig. 2). As the actinolite is in one way or another affected by all the other minerals, its position as the second mineral in the sequence is definitely established.

The position of some of the minor silicates is not so well known. The garnet in part replaces biotite and actinolite. The same is true of the epidote. Both are corroded by and are older than the calcite; but, as the two were not observed in contact with each other, the age of one with respect to the other remains unknown. The epidote, however, is mantled and veined by allanite and its position in the sequence, therefore, is somewhat more restricted than that of the garnet. The position of the other silicates is less easily ascertained. The chlorite is largely pseudomorphous after biotite and phlogopite and has been observed as engulfed remnants in the calcite, but there seems to be no way of telling whether the change to chlorite preceded or followed the introduction of calcite or whether it formed much later. The glaucophane also poses a problem. It is the only mineral whose distribution is related to more or less well-defined fractures, all of which are in the heavily silicated parts of the deposit. Inasmuch as it penetrates and replaces actinolite and biotite or phlogopite, it may have formed late during the silication. The sphene does not occur with the other silicates, except in close association with the ilmenite. It is, therefore, probably somewhat younger than the other silicates.

The position of the allanite is established as one of the youngest of the silicates. It shows prominent euhedral replacement of the actinolite and biotite and, locally, some mantling and veining of the epidote (Fig. 4). In turn it is penetrated and replaced by euhedral crystals of monazite (Fig. 5), some with retained remnants of the allanite, and is penetrated and veined by aggregates of apatite (Fig. 5). Thus the allanite as well as the actinolite and biotite are older than the phosphates.

The penetration of the silicates by euhedral monazite and by the apatite (Fig. 5) is one of the striking features of the deposits. The apatite takes the lead in the penetration of the silicates, for inclusions of the apatite have been observed with the crystals of monazite, and euhedral replacements of the aggregate apatite by the monazite crystals are not uncommon (Fig. 5). The occurrence of both as corroded inclusions in the carbonates imposes further limitation on age development (Fig. 6).

As the carbonates, especially the calcite, contain actual or shadowy-like inclusions of the phosphatic minerals and most of the silicates, they cannot be construed as remnants of an originally limestone or marble host, but on the contrary are, like the other minerals, depositional products formed later than the silicates and phosphates. The ancylite and bastnaesite retain their outlines against and in part seem somewhat corroded by the calcite, but there is no evidence to indicate which of these two rare-earth carbonates is the earlier. All carbonates, however, are older than the barite, oxides (Figs. 8, 10, 11), and sulfides, for in each of these calcite has been observed as incompletely replaced inclusions.

Because of its remnant calcite inclusions, commonly in oriented position, the barite is known to be the younger of the two minerals. It is not so young, however, as the oxides, for occasional remnants of the barite have been found within the magnetite and ilmenite (Fig. 9).

Because of remnant inclusions of barite and calcite and euhedral replacements of phosphates and silicates, the position of the oxides is well-established. Study of polished sections reveals age differences among the oxides. Although the magnetite and ilmenite lack good contact relationships, the veining of a few grains of magnetite by ilmenite indicates that the magnetite is the earlier of the two minerals. It is likely that some of the magnetite is older than the carbonatic mineralization and is an inheritance from the marble. In its large crystal development the ilmenite has converted all incorporated magnetite grains entirely to its own composition without remnant inclusions. This explains why the large ilmenite crystals may be surrounded by much smaller, abundantly disseminated, magnetite grains. As the ilmenorutile shows euhedral replacement of ilmenite with some retention of oriented inclusions of the ilmenite, its position as the latest of the three oxides is fixed. The sphene, which probably formed during the oxide stage just ahead of the ilmenite, occurs as sparsely distributed remnants within the ilmenite crystals.

Since remnant oxides have been found within the pyrite, the sulfides are dated as the last minerals to form. Where the three sulfides are in contact, their relations indicate that the pyrite was the first to form, the pyrrhotite next, and the chalcopyrite last.

The quartz is not associated with the oxides, but it is known to be younger than the calcite and barite. Its exact position in the mineral sequence is in doubt.

The paragenetic sequence is tabulated below. The sequence demonstrates that silicates, except sphene, formed ahead of the phosphates; the phosphates, ahead of the carbonates; the carbonates, ahead of the sulfates; the sulfates, ahead of the oxides; and the oxides, ahead of the sulfides.

MINERAL SUCCESSION

TEXTURAL AND STRUCTURAL CHARACTERISTICS

Although some of the minerals, unless crowded into aggregates, are microscopic in size, most and especially those of most pertinent economic interest are rather coarse grained and impose on the deposits a notably coarse granular texture. The texture, however, is not uniformly coarse and may be more aptly described as variable but generally coarse with grains and crystals in some places ranging upward to several inches long.

The variable texture results largely from the highly irregular and unsystematic distribution of the minerals, particularly of such persistently and abundantly distributed minerals as the actinolite and calcite and, locally also, of the monazite and ilmenorutile. In addition to their irregular bunchy or spotty distribution, the minerals also display considerable range in grain size, individually and in aggregates. In some places the distribution of the minerals may suggest a rude zonal development with the silicates mainly at the borders and the carbonates and the other minerals toward the center; but within a few inches bunches or pods of the carbonates and the minerals that tend to

accompany the carbonates may appear along one or both walls, with the silicates or remnants of the silicates confined to the interior. Actually, irregular bunches of the carbonates may occur anywhere within the deposit and spread irregularly into the enclosing silicated areas (Fig. 12).

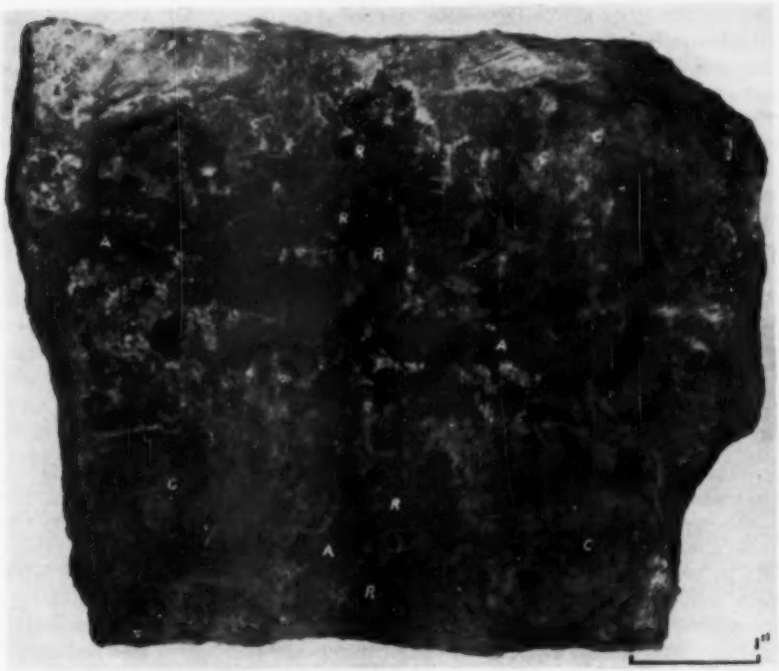

FIG. 12. Vein specimen from upper Squaw Creek showing erratic distribution of the dark gray actinolite (A) and the lighter-colored but somewhat mottled calcite (C), cut by podlike granules of ilmenorutile (R). The irregular outlines of the divergent actinolite aggregates have resulted from the uneven penetration of the actinolite by the invading and replacing calcite and associated carbonates.

The irregular and seemingly haphazard distribution of the minerals is simply a reflection of their replacement origin. The distributional pattern of the early silicates suggests rather uniform silicate development through the deposits. This pattern was then disrupted where the silicated bodies were irregularly permeated or soaked by the ensuing fluids and thus irregularly and sporadically replaced by the successive groups of phosphates, carbonates, sulfates, oxides, and sulfides. Hence, local erratic introduction and replacement has been responsible for the somewhat erratic appearance of the deposits.

REGIONAL ZONING

Although not strikingly developed, the deposits do show some regional variation in composition and mineralogy. Such minerals as the actinolite, allanite, apatite, monazite, and calcite are distributed through the entire mineral belt, whereas other minerals are more limited in their distribution. Among the latter are the minerals containing titanium and columbium. The titanium minerals occur along the southeast half of the mineral belt and are represented by ilmenite, ilmenorutile, and rutile. These minerals are not known to be present in the Montana deposits (5, p.1580–1581). In Idaho the columbium has entered into the rutile to form the ilmenorutile. This mineral occurs in the deposits from Indian Creek to Spring Creek and attains its greatest abundance in the deposits on upper Squaw Creek. It does not reach the southeast end of the belt nor is it present in the Montana deposits, where, because of the lack of titanium, the columbium was deposited as columbite (5, p. 1580). The rare earth carbonates increase in abundance toward the Montana line and are reported as important minerals in the Montana deposits (5, p. 1580). The biotite also shows some increase toward the State line, but the most notable regional variation in the mineralization is reflected in the distribution of the titanium and columbium.

ORIGIN OF THE DEPOSITS

Previously Proposed Concepts

The deposits are regarded by both Abbott (1, p. 8–9; 12–22) and Kaiser as replacements of thin lenses of crystalline limestone or marble in the metamorphosed Belt series. In discussing their origin Abbott discounts the possibility that the mineralization may have any relation to magmatic processes and turns to metamorphic differentiation as the process that best accords with field and laboratory observations. He proposes that during regional metamorphism migrating ions released by dissociation of original, rare-earth-bearing clastic grains in the nearby argillaceous and arenaceous Belt sediments found a compatible environment for reconstruction into monazite and other minerals in the chemically favorable phosphatic limestones. He accounts for the local, sporadic concentration of the monazite in the deposits to nearness of the marble to pockets of the clastic, rare-earth-bearing minerals or else to channelizing of the migrating rare-earth ions along structural zones in the metamorphic complex into intercepted beds of marble, where the most extensive replacement of the carbonate rock took place (p. 22).

Kaiser offers a somewhat modified version of the metamorphic differentiation concept advanced by Abbott. He postulates that during metamorphism solutions permeated the rocks and carried appreciable though small proportions of the rare elements, either introduced with the solutions from an unknown source or taken up selectively from the rocks themselves, and that these elements were concentrated under favorable environmental conditions involving a combination of a limestone and a certain structural setting with stratigraphic and structural controls restricting the deposits to their present position.

Objections to the Metamorphic Concepts

The writer does not agree with Abbott and Kaiser that the facts obtained from field and laboratory observations favor an origin through metamorphic differentiation. The chief argument for the metamorphic concept seems to be the introduction of the rare elements into the beds of crystalline limestone; but this argument loses much of its force when these elements are also found in the siliceous rocks, though not to the same extent as in the more reactive and therefore more favorable marble beds. Some of the deposits regarded by Abbott as occurring in marble may not be in marble, for his criterion (p. 9) that marble may be recognized by its associated actinolite, barite, monazite, ilmenite, etc. is faulty and not applicable, inasmuch as the carbonate may be entirely of mineralization rather than meta-sedimentary origin. Such is the case of the deposits contained in the amphibolites derived from the gabbro. The laboratory evidence also cannot be depended upon as a support for the metamorphic concept, for the paragenesis presented by Abbott, without revealing his supporting evidence, does not accord with that obtained during the present investigation. His sequence (p. 21) of calcite, barite, apatite, siderite, magnetite and ilmenite?, actinolite, monazite, and then more ilmenite and magnetite is without systematic order and does not accord with any known metamorphic or hydrothermal sequence.

Other aspects of the mineralization do not support a metamorphic origin. The textural and structural characteristics are not those expected of deposits formed during regional metamorphism. If formed during regional metamorphism, the deposits, like the bordering rocks, should possess structures indicative of stress conditions; but, unlike the bordering rocks, the deposits show no foliation or mineral alignments. On the contrary the minerals were formed in already foliated rocks and therefore were introduced and the deposits formed after regional metamorphism had come to an end.

There are also other obstacles in the way of accepting metamorphic differentiation as the origin of the deposits. It is hard to conceive that the nearby Belt sediments should happen to have clastic concentrations of heavy minerals containing all the elements: rare earths, phosphorus, titanium, columbium, barium, sulfur, or iron, needed to form the present deposits and that the deposits resulting through metamorphic differentiation processes should have all the compositional and mineralogical characteristics of the carbonatites, which so far are known only as products of alkalic magmatic activity.

Another objection to the metamorphic concept is the mineral paragenesis that fixes the essential carbonate as one of the younger minerals, younger than the silicates and phosphates, but not so young as the barite and the oxides and sulfides. The mineral sequence accords with that expected of formation from cooling magmatic or hydrothermal fluids and not with one involving increasing and decreasing intensities of metamorphism. The presence of the typical assemblage of the silicates actinolite, garnet, zoisite, of the oxides magnetite, specularite and ilmenorutile, and also pyrite and barite has prompted Heinrich

(4, p. 249) to regard the deposits as more likely of metasomatic than of metamorphic origin and as veins similar to some to the north in Montana.

Discussion and Conclusions

Inasmuch as the association and concentration of elements in these deposits are so much like those found in and characteristic of carbonatites (9, p. 1537–1556), any origin other than through igneous agencies seems most improbable. The local field and laboratory evidence indicates that these deposits were formed by highly mobile, carbonatic fluids charged with silicon, rare-earth constituents, phosphorus, calcium, barium, titanium, columbium, iron, and sulfur and that mineral formation proceeded in an orderly manner, controlled by declining temperatures and changing chemical composition. As in the high-temperature hydrothermal deposits, the silicates were the first to form, presumably when the temperatures were highest; whereas the carbonates, oxides, and sulfides were the last to form, after temperatures had declined to more moderate levels. The sequence can be regarded as more or less typically hydrothermal, although the same mineral succession should be obtained in a carbonatic magma containing like concentrations of the rarer elements.

Whether the carbonatic fluids were hot aqueous solutions or represented actual carbonatic magmas cannot be told. Recent experimental work on synthetic carbonatite magma by Wyllie and Tuttle (11) suggests that carbonatic magmas can exist at moderate temperatures through a wide range of pressure. From the characteristics of the mineralization, it may be inferred that the deposition was from a highly fluid medium, which favored relatively coarse grain growth, and that changing physical and chemical equilibria permitted reaction between earlier-formed minerals and the later permeating fluids, with replacement of earlier minerals by later ones. Similar phenomena should exist were the medium a highly fluid carbonatite magma. A carbonatic magma, however, is not essential to the formation of the carbonatite-type of deposit. Pecora (9, p. 15) has extended the carbonatite to include all carbonate-rich deposits formed from hot fluids, but has taken the position (p. 1541) that the term carbonatite should be restricted to those special carbonate-rich rocks in alkalic provinces that can be shown to be intrusive and to be former by precipitation from hot solutions of any temperature and concentration.

The local deposits possess all the attributes of the carbonatites, except the association of alkalic igneous rocks. No such intrusives have been recognized in the vicinity of the deposits, but this lack of association with the alkalic rocks may be more apparent than real, for in Montana E. W. Heinrich (written communication) reports that the alkaline nature of the mineralization is hinted at by the presence of numerous barite veins, by a number of fluorite deposits, and by at least one small intrusion of syenitic and alkaline peridotitic rocks.

Recent lead-alpha age determinations made on the monazite give the deposits an average age of 95 million years (6, p. 96), some 13 million years

less than the 108 million years assigned the Idaho batholith (8). Despite this appreciable age difference, the deposits may still be related to the batholith or to younger, probably late Cretaceous components of the batholith. Until relationships are better established, it is sufficient to state that these unique monazite and columbium-bearing rutile deposits in Lemhi County, Idaho, are replacements, chiefly in crystalline limestone, and should be classed as carbonatites formed by carbonatic fluids later than the metamorphism associated with the emplacement of the Idaho batholith.

LABORATORY OF ECONOMIC GEOLOGY,
CORNELL UNIVERSITY,
ITHACA, NEW YORK.
January 24, 1960

REFERENCES

1. Abbott, A. T., 1954, Monazite deposits in calcareous rocks, northern Lemi County, Idaho: Idaho Bureau of Mines and Geology Pamph. 99, 24 p.
2. Anderson, A. L., 1958, Uranium, thorium, columbium, and rare earth deposits in the Salmon River region, Lemhi County, Idaho: Idaho Bureau of Mines and Geology Pamph. 115, p. 21–44.
3. Anderson, A. L., 1958, Genetic aspects of the monazite and columbium-bearing rutile deposits in northern Lemhi County, Idaho: Abst., Geol. Soc. America Bull. v. 69, No. 12, Pt. 2, p. 1530.
4. Heinrich, E. Wm., 1958, Mineralogy and geology of radioactive raw materials. McGraw-Hill Book Company, 654 p.
5. Heinrich, E. Wm., Levenson, A. A., Axelrod, J. M., and Milton, Charles, 1958, Niobium-titanium-rare earth minerals of Ravalli County, Montana, and Lemhi County, Idaho: Abst., Geol. Soc. America Bull., v. 69, No. 12, Pt. 2, p. 1580–1581.
6. Jaffe, H. W., Gottfried, D., Waring, C. L., and Worthing, H. W., 1959, Lead-alpha age determinations of accessory minerals of igneous rocks (1953–1957): U. S. Geol. Survey Bull. 1097-B, p. 65–148.
7. Kaiser, E. P., 1956, Preliminary report on the geology and deposits of monazite, thorite, and niobium-bearing rutile of the Mineral Hill district, Lemhi County, Idaho: U. S. Geol. Survey Open File Report, Spokane, Washington.
8. Larsen, E. S., Jr., and Schmidt, G. R., 1958, A reconnaissance of the Idaho batholith and comparison with the Southern California batholith: U. S. Geol. Survey Bull. 1070-A, 32 p.
9. Pecora, W. T., 1956, Carbonatites, a review: Geol. Soc. America Bull., v. 67, No. 11, p. 1537–1556.
10. Weis, P. L., Armstrong, F. C., and Rosenblum, S., 1958, Reconnaissance for radioactive minerals in Washington, Idaho, and Western Montana 1952-1955: U. S. Geol. Survey Bull. 1074-B, p. 39–40.
11. Wyllie, P. J., and Tuttle, O. F., 1959, Synthetic carbonatite magma: Nature, v. 183, p. 770.

Economic Geology
Vol. 55, 1960, pp. 1202–1231

OXIDATION OF SULFIDE ORE BODIES, II. OXIDATION MECHANISMS OF SULFIDE MINERALS AT 25° C

MOTOAKI SATO

CONTENTS

	PAGE
Introduction	1203
Previous work	1203
Analytical approach	1204
Mineralogical approach	1204
Kinetic approach	1205
Electochemical approach	1205
Method of investigation	1207
Apparatus	1207
Experimental procedure	1210
Experimental results	1212
Copper sulfides	1212
Chalcocite	1212
Covellite	1214
Lead sulfide	1218
Galena	1218
Silver sulfide	1220
Argentite	1220
Iron sulfides	1222
Pyrite	1223
Pyrrhotite	1225
Ferrous sulfide	1225
Marcasite	1226
Zinc sulfide	1226
Sphalerite	1226
Summary and conclusions	1227
References	1229

ABSTRACT

Measurements of the single electrode potentials of sulfide minerals backed with basic understanding of their electrode behavior make it possible to clarify their oxidation or reduction mechanisms. The electrode potential of a sulfide mineral is controlled by the first-step reaction of the oxidation mechanism for the sulfide in an oxidizing solution, and by that of the reduction mechanism in a reducing solution. Sulfides of copper, lead, silver, iron, and zinc were studied. The results indicate that the direct oxidation of a simple sulfide mineral is a process in which the metal atoms move into the surrounding solution to become aqueous cations, accompanied by a step-wise decrease in the metal to sulfur ratio of the remaining solid phase. When solid sulfur is finally left over, it undergoes a series of reactions to be oxidized to sulfate ion. In case of reduction,

sulfur atoms move out into the solution to become aqueous sulfide ions with a step-wise increase in the metal to sulfur ratio of the solid phase. To illustrate, the oxidation of chalcocite proceeds as

$$(Cu_2S) \rightarrow \tfrac{1}{4}(Cu_9S_5 + Cu^{++})? \rightarrow (CuS + Cu^{++}) \rightarrow (2Cu^{++} + S).$$

The path of the step-wise oxidation is not necessarily the same as that of the step-wise reduction for a metal-sulfur system. In the case of disulfides of iron, namely pyrite and marcasite, ferrous ions and S_2 molecules appear to be released simultaneously upon oxidation.

INTRODUCTION

It is generally recognized that atmospheric oxygen is dissolved in meteoric water and oxidizes minerals, directly or indirectly, as the solution migrates downward. Sulfide minerals are oxidized ultimately to the corresponding metal ions plus sulfate ion. The metal ions may be precipiated as insoluble hydroxides, oxides, carbonates, sulfates, or silicates, or may be carried away in solution from the site of oxidation. In some cases, they migrate to the unoxidized depths and replace primary sulfide minerals as in the case of supergene enrichment of copper and silver. As to the chemical mechanism of oxidation of sulfide minerals, however, no agreement has been reached as yet. This is chiefly because of the complex chemical behavior of sulfur in aqueous solution. Not only can sulfur assume various oxidation states ranging from -2 to $+6$, but also it can link together into various polysulfur compounds. Compared to sulfur, the behavior of a metal is much less complex. There is a possibility, however, that the detected form of a metal does not necessarily represent the primary form that may exist at the moment of liberation from the reacting sulfide mineral. Of all the complexities of the oxidation reactions of a sulfide mineral, the most crucial and the least understood part is the first step of the heterogeneous reaction through which the solid sulfide is partially or totally dissolved into the surrounding solution upon breaking up its crystal bonds. Once this step is established, the rest of the consecutive reactions can be treated as a separate case for the oxidation reactions of sulfur and that of the corresponding metal. The understanding of this first-step reaction mechanism is essential in the discussion of the rate of reaction and the activation potential levels for the oxidation of sulfide minerals.

The present author studied the nature of sulfide electrodes in aqueous solution in connection with the oxidation mechanisms for sulfide minerals and the origin of self-potentials produced by sulfide ore bodies. As the result of his experimental work, a standard procedure for the identification of the first-step oxidation or reduction of a sulfide mineral through the use of electrode potential method has been established.

PREVIOUS WORK

Numerous papers discuss the oxidation of various sulfide minerals. The variety of the methods of investigation applied is equally extensive. They may be grouped, however, into four categories, namely, analytical, mineralogical, kinetic, and electrochemical approaches.

Analytical Approach.—Since the early works of Stokes (43, 44), numbers of investigators have attempted to establish the oxidation mechanisms of sulfide minerals through analytical studies on the oxidation and leaching products, using various solutions with or without the introduction of free oxygen. It seems, however, that nobody has come to a satisfactory conclusion. This is chiefly because of the complex chemical behavior of sulfur in aqueous solution. Not only can sulfur assume various oxidation states ranging from -2 to $+6$, but also it can link together by covalent bonds in various forms. In many cases, these various species of sulfur can easily change from one form to another, making both precise analyses of the species present and exact determinations of involved reactions extremely difficult. The sulfur species detected in the oxidation products included polysulfides, free sulfur, thiosulfate, polythionate, sulfite, and sulfate ions. Generally more than one of those species were present in solution. Consequently a difficulty was encountered in deciding whether they were all of simultaneous formation, or a specific one was the direct oxidation product and the rest were derived from the former by a sequence of reactions taking place in solution, or all of them were derived from some other undetected species. The presence of unstable, intermediate oxidation products of sulfur in many experiments indicated that the oxidation of a sulfide mineral is not a simple, straight-forward reaction from the sulfide to the corresponding metal sulfate, but is made up of a series of consecutive reactions. Compared to sulfur, the behavior of a metal is much less complex. There is a possibility, however, that the detected form of the metal species does not necessarily represent the primary form that may exist at the moment of the liberation from the reacting solid sulfide. For reasons mentioned above an approach through the study of the oxidation products of sulfides has included a large element of guesswork. Papers describing the results of studies on the oxidation of sulfide minerals along this line of approach include those by Stokes (43, 44), Buehler and Gottschalk (9), Gottschalk and Buehler (14), Ralston et al. (35), Sullivan (46, 47, 48, 49), Matsubara and Takubo (26), Bain (3), Eliseev and Negirnyak (12), and Plante and Sutherland (33).

Mineralogical Approach.—Various mineralogical studies on the course of the oxidation of sulfide minerals through macroscopic and microscopic observations of naturally oxidizing sulfide ores are included in this category. Attempts were made to infer the course of the oxidation of sulfide minerals from the observed textural relationships of minerals in oxidized ores with the aid of microscopes. Papers by Wang (57), Anderson (1, 2), Schwartz (38, 39), and Head (17) are cited. The study of leached outcrops, in an attempt to infer the type of ore deposit from the remaining oxidation products at the surface, developed rapidly during a short period between 1924 and 1928, when Morse and Locke (27), White (60), Locke (25), Blanchard and Boswell (5, 6, 8), and Blanchard (7) successively published their papers. Such mineralogical observation fails to provide direct information on the chemical mechanism and the rate of reactions involved, but it indicates the general directions of the chemical changes and, sometimes, the relative rates of the oxidation reactions of various sulfide minerals.

Kinetic Approach.—This group includes studies made through the measurements of rates of oxidation and dissolution of sulfide minerals using various agents of oxidation and solutions such as oxygenated water, ferric sulfate, and inorganic acids, along with combination of these agents. As information accumulated it soon became evident that there were considerable differences in the rate among sulfide minerals, despite the similarity of the attacking agents. The determination of the absolute rate of reaction appears to have little significance for the problem of oxidation of sulfide minerals, however, when we consider the apparent complexity of the reactions and the possible large number of rate-determining factors which are inherent to a heterogeneous reaction system. This is particularly true when an uncertainty is introduced in the time factor, as in the case of natural systems. A comparative study of reaction rates may yield useful information as to the relative persistence of sulfide minerals in the zone of weathering. A review of the literature reveals, however, that discrepancies exist among various authors as to the order of the relative rate of the oxidation of sulfides. The uncertainty of the order arises mostly from the diversity of the experimental conditions and failure in singling out the rate-determining variables. It is generally true, however, that polysulfides are more stable than simple sulfides, and that between two sulfides of a specific metal, the one with a higher formal oxidation state of the metal is more stable than the one with a lower oxidation state under oxidizing conditions. The earliest contributions along this line of approach were probably those by Vogt (53, 54), followed by Winchell (61), Grout (15, 16), Nishihara (30), Zies, Allen, and Merwin (63), and Carmichael (11). Probably the most comprehensible and successful application of the kinetic approach was made by Sullivan (46, 47, 48, 49), who treated various copper minerals with acidified ferric sulfate solution. He found that chalcocite dissolved in two steps, represented by the Cu_2S rapidly giving up one-half of its copper and changing to a form approximating CuS, which dissolved at a slower rate. When the leaching was continued, sulfur remained behind retaining nearly the original outline of the attacked mineral particles, which collapsed after being treated with carbon disulfide. From these observations, he established the mechanisms of oxidation for chalcocite as follows:

$$Cu_2S = CuS + Cu^{++} + 2e,$$
$$CuS = Cu^{++} + S + 2e.$$

More recently, Plante and Sutherland (33), Koch and Grasselly (21, 22), and Stenhouse and Armstrong (42) worked on the rates of oxidation of sulfide minerals.

Electrochemical Approach.—This approach has stemmed from a study of the electrode potentials of sulfide minerals in aqueous solutions. The earliest contributions include those by Fox (13), Skey (41), and Bernfield (4). Fox suggested that certain ores might act like metals in galvanic combinations. Skey first called attention to the accelerating or retarding effect of one sulfide mineral on another in chemical changes, when the two are in contact. Buehler

and Gottschalk (9), and Gottschalk and Buehler (14) experimentally demonstrated that the rate of oxidation of sulfides increased when dissimilar ones were mixed, showing similar cathodic-anodic relationships as in the corrosion of metals. Finding a close relationship between the electrode potentials and the relative rates of oxidation of sulfide materials, they arranged the minerals according to their measured electrode potentials in a series analogous to the electrochemical series of metals, thus providing a link between the electrode potentials and the oxidation reactions of sulfide minerals. Another important advance was made by Wells (58, 59) who carried out an extensive study of the electrochemical behavior of sulfides with better experimental controls than those of Gottschalk and Buehler. He observed that the electrode potentials of sulfide minerals, particularly those of polysulfides, were very similar to the oxidation potentials of the surrounding solutions. Since Well's work, a number of investigators made similar measurements but without any significant advance in the understanding of the nature of the sulfide electrodes. These include Tammann (51), Trümpler (52), Suzuki (50), Piontelli (34), Wada and Seki (55), Nakabayashi and Fujiwara (28, 29), Rechenberg (36), Kaku (18, 19), and Bulah and Khan (10). A few workers described the variation of the electrode potentials of sulfides with the varying pH of the solutions. A common characteristic of sulfide electrodes, almost invariably observed by these workers, is the poor reproducibility of their potentials. Measurements in solutions containing only foreign ions are out of question, since they represent irreversible potentials. Even the potentials measured in solutions containing corresponding product ions have exhibited considerable drift with time. Sometimes the measurements had to be continued for weeks before the potentials reached steady values. For this reason many authors were obliged to give the potentials of sulfide electrodes as functions of time. Unless the cause of the drifting is clearly understood, it is almost meaningless to assign a specific potential value to each sulfide electrode. It was probably this fact that discouraged a serious effort to correlate the measured single electrode potentials with specific half-cell reactions of sulfides, even though the procedure has long been established with metal electrodes. This procedure is simply to assume possible electrode reactions and calculate their oxidation potentials using independent thermodynamic data. The reaction whose calculated potential agrees best with the measured potential is regarded as the one actually taking place at the electrode. Recntly, Noddack and Wrabetz (31), Noddack, Wrabetz, and Herbst (32), and Wrabetz (62) ventured to correlate the measured potentials of several sulfides with the corresponding electrode reactions. They found that the reaction:

$$MeS = Me^{++} + S + 2e \qquad (Me = \text{metal}),$$

was operative in the case of PbS, MnS, and CoS, following the procedure described above. This achievement constitutes another advance in the electrochemical approach to the problem of the oxidation of sulfide minerals. A systematic understanding of the fundamental nature of sulfide electrodes with respect to their oxidation and reduction mechanisms, however, has remained to be solved.

METHOD OF INVESTIGATION

Single electrode potentials of several sulfide minerals were measured against a saturated calomel electrode in solutions of various chemical compositions. Oxidation potentials and pH values of the solutions were measured simultaneously, using a smooth platinum and a glass electrode, respectively. Temperature was read with a mercury thermometer. The electrodes and a testing solution were placed in an air-tight cell container, into which a desired gas was introduced. Air, hydrogen, and purified nitrogen were used in turn to control the oxidation potential of the solution. After being recorded with automatic recorders, the measured potentials were plotted graphically against pH values or activities of product ions in solution. Interpretation of the plotted data was made for each sulfide mineral through comparison with the calculated potentials for assumed electrode reactions.

Apparatus.—The major part of the experimental apparatus consisted of an air-tight cell with electrodes, magnetic stirrer, pH meter, amplifier-potentiometer, and automatic potential recorder. Frequently a relay-timer was used to record two potentials on a recording chart. One example of the potential measurement circuit is diagramatically shown in Figure 1.

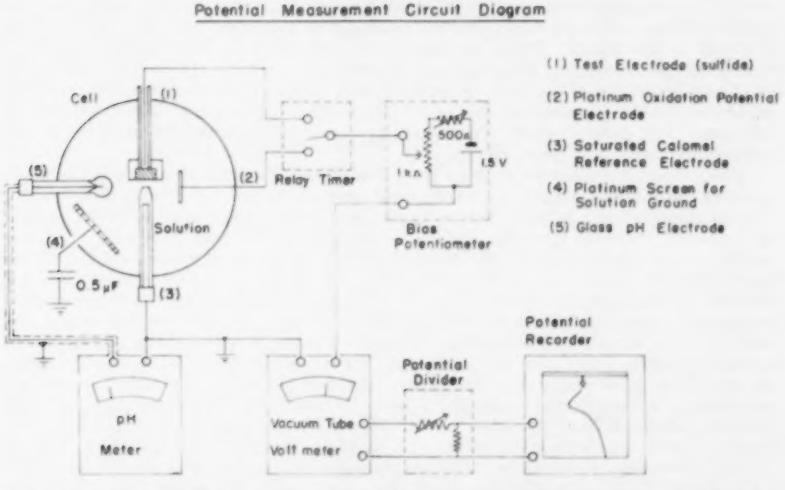

FIG. 1. A diagram showing one example of the potential measurement circuit used for the identification of electrode reactions of sulfide minerals.

The cell container is a plastic cylinder, 3″ long and 3″ wide, with a rectangular plastic plate cemented to the bottom. Its capacity is approximately 250 cc. A plastic plate with holes for electrodes, thermometer, burette, and glass tubes, is used as the cover. A circular rubber gasket is inserted between the container and the cover to seal off the gap. Four bolts fasten the cover tightly to the container to make the cell air-tight. The inlet tube has a pointed nozzle at one end to bubble a gas into solution, and a three-way valve at the other end to switch

between gases, or to close the tube. Stirring of the solution is accomplished by a glass-coated magnetic bar which is placed at the bottom of the container. A magnetic stirrer is placed beneath the cell container to rotate the bar. The rate of stirring can be adjusted by the rotational speed of the magnet.

Four different electrodes are used in the cell. They are: (1) a sulfide test electrode, (2) a thimble-style platinum electrode, (3) a fiber-type calomel reference electrode, and (4) a glass electrode. The structure of the sulfide test electrode is illustrated in Figure 2. It is prepared in the following way. A sulfide mineral to be tested is cut with a diamond saw to a cube approximately 1 cm in each dimension. It is placed in a steel cast, about 2 cm long, 1.5 cm wide and 1.5 cm deep. Cold-setting liquid plastic mixed with a polymerization catalyst is poured into the cast and allowed to stand for several hours until it solidifies. The exposed surface of the mineral is carefully polished and examined under a reflecting microscope to ensure the absence of inclusions of foreign minerals. If too many impurities are present, the mold has to be discarded. When only a few tiny inclusions are present, they can be eliminated with a needle point or a chemical agent. In the latter case, the surface has to be repolished. The small holes thus created are sealed with wax. When the purity of the mineral surface is confirmed, a hole with a diameter of 6 mm is drilled about half-way through from the top of the mold. A glass tube of the same diameter and 5 cm long is cemented into the upper half of the hole. Several drops of mercury are placed at the bottom of the hole to provide a good electrical contact between the mineral and a platinum lead wire. The sulfide electrode is suspended from the cover of the cell in such a way that the polished surface of the sulfide mineral diagonally intersects the rotating stream of the solution, so that a concentration gradient or a surface coating with insoluble products is minimized. Rapid stirring is also effective in this respect. All electrodes except the calomel electrode are set vertically through the cover. The latter is placed at an angle so that its pointed end comes close to the surface of the sulfide electrode, minimizing the effect of possible potential gradient within the solution. The calomel electrode serves as a reference electrode common to the sulfide, platinum, and glass electrodes.

The potential difference between the calomel and the glass electrode gives a pH value of the solution, which is directly read on a pH meter (Beckman N-2 model). The potentials of the sulfide electrode and the platinum electrode measured against the calomel electrode give the values of the single electrode potential of a test sulfide and of the oxidation potential of a testing solution, respectively, which are 0.242 volt less than those in the hydrogen scale at 25° C. The temperature coefficient of the calomel electrode may be neglected so long as the experimental temperature remains within a few degrees of 25° C. In the present study, the value of + 0.242 volt was inavariably added to measured potentials to convert them to the hydrogen scale (the electrode sign convention follows the one adopted by the American Electrochemical Society). The two potentials are either separately recorded on a dual-channel recorder (Sanborn model 152-100B) through two DC coupling preamplifiers (Sanborn model 150-1300), or alternately recorded on a single-channel recorder (Varian G-11A model) through a relay-timer with a suitable switching interval, followed by a microvolt-ammeter and amplifier (KAY LAB model 203). The latter method was used more frequently because of the ease of comparison of two recorded potentials. It is important that the potentiometer circuit connected to the sulfide electrode has a high input impedance, at least of the order of megohms. In order to increase accuracy, a bias potentiometer is inserted on the input side of the amplifier-potentiometer to give a bias potential, so that the range of the recorder can be expanded about the potential of interest. Usually the polarity and magnitude of the bias potential are so chosen that it counteracts the potential of a sulfide electrode to minimize electrode reactions caused by the flow of an electric current through the external circuit of the cell. The external electric current must be reduced nearly to zero to obtain a reproducible result with a sulfide electrode. Otherwise the potential of the sulfide electrode

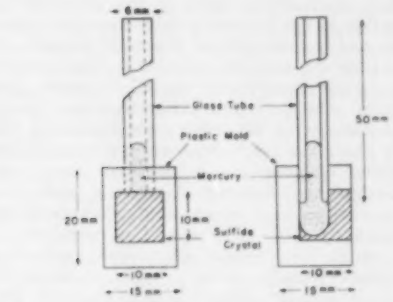

2

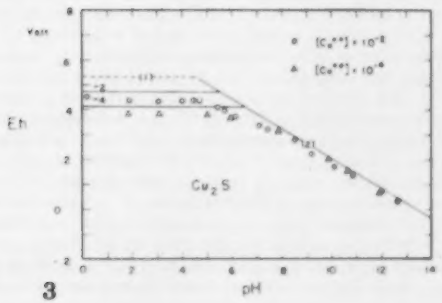

3

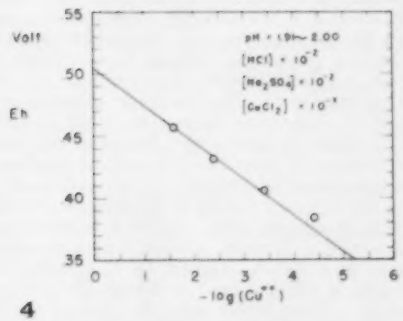

4

FIG. 2. The structure of the sulfide mineral electrode used in the single electrode potential measurements.

FIG. 3. Plots of the measured electrode potentials of chalcocite against the pH values of testing solutions. (1) $Cu_2S = CuS + Cu^{++} + 2e$, (2) $Cu_2S + 2H_2O = CuS + Cu(OH)_2 + 2H^+ + 2e$.

FIG. 4. Plots of the measured electrode potentials against the logarithms of cupric ion activities for chalcocite.

would vary with time approaching that of the reference electrode. This drift of the electrode potential occurs because a sulfide can be either oxidized or reduced, and its electrode potential is controlled by the activity ratio of the products of both reactions when in equilibrium with the solution. This point will be discussed in a separate paper covering the nature of the sulfide electrode potentials.

Gases are introduced into the cell in different ways. Compressed air is passed through a column of ascarite to eliminate carbon dioxide. Compressed hydrogen and hydrogen sulfide gases are fed from high-pressure cylinders through pressure regulators. Compressed nitrogen gas is supplied from a high-pressure cylinder through a pressure regulator, columns of ascarite and calcium chloride, and a heated column of copper powder in an electric furnace, whose temperature is controlled at approximately 400° C by a voltage regulator. The copper powder eliminates trace oxygen in the nitrogen gas. The outlet glass tube of the cell is connected to a gas-trap. Usually distilled water is placed in the trap to isolate the cell chamber from outside atmosphere and to maintain the gas pressure within the cell slightly higher than 1 atm. A solution of a desired acid, base, or salt is titrated into the cell from a burette which is set through a hole of the cover. The small gaps between the plastic cover plate and the burette as well as all the electrodes and a thermometer are sealed with a hard wax layer on top of the plate, which is remelted with a heated metal piece at the beginning of each experiment.

Experimental Procedure.—The amplifier-potentiometer, recorder, bias potentiometer, and pH meter are calibrated and adjusted prior to each experiment. A testing solution with the desired chemical composition is prepared according to the purpose of each experiment. 200 cc of the solution is placed in the cell container. All necessary electrical connections are made and the electrical instruments are set in order. The magnetic stirrer is adjusted to give a proper stirring rate. The temperature of the solution is frequently checked during an experiment and the temperature compensator of the pH meter is adjusted accordingly. A gas is bubbled through the solution at a suitable rate. The oxidation of the solution is accomplished by bubbling air, and the reduction by hydrogen gas. When neither oxidation nor reduction is desired, either the inlet valve is closed or nitrogen gas is bubbled through. Both the potential of a sulfide test electrode and the oxidation potential of the solution are recorded. The simultaneous observation of the two potentials is an important procedure for the following reason. The electrode potential of a sulfide mineral is presumably controlled by specific electrode reactions, through which the chemical bonds in the crystal structure are broken and the mineral components are partially or totally dissolved into the solution. Two different types of such potential-determining electrode reactions exist, namely, oxidation and reduction reactions. The electrode potential of a sulfide may be controlled by a reaction of either type; it may be either an oxidation potential or a reduction potential. Unless the nature of a measured potential is known, therefore, any attempt to correlate the potential to a specific electrode reaction becomes meaningless. The simultaneous observation of the electrode potential and the oxidation potential of the solution makes it possible to identify which electrode potential of the sulfide is being measured. When a solution can oxidize a sulfide mineral, its oxidation potential is more positive[1] than the electrode potential of the mineral. Oxidation of a sulfide mineral by a solution involves transfer of electrons from the mineral to the dissolved oxidizing ions which are colliding with the surface of the former. Many sulfide minerals conduct electricity. If a sulfide electrode is electrically connected to an inert metallic electrode, which is dipped in the same solution, the collision of the ions with the latter should also cause the oxidation of the former, since electrons can be transferred from the sulfide to the ions via the metallic electrode. Thus an electric current flows from the inert

[1] The convention of the electrode sign used throughout this paper follows the one adopted by the American Electrochemical Society. According to this convention, the potential of an inert metallic electrode measured against a standard hydrogen electrode is equal to the oxidation potential of the solution in electrode sign and magnitude.

electrode to the sulfide electrode so long as the solution is capable of oxidizing the sulfide. This implies that the potential of the sulfide electrode is more negative than that of the inert metallic electrode, the latter being equal to the oxidation potential of the solution. Through similar reasoning, it is easily seen that the oxidation potential of a solution is lower than the electrode potential of a sulfide mineral, if the solution can reduce the sulfide. When an equilibrium is reached between the sulfide and the solution with respect to oxidation-reduction reactions, the two potentials should be identical, since no electric current flows at equilibrium. If a convergence of the two potentials to such an identical value is obtained by gradually reducing an oxidizing solution, the potential value should correspond to the oxidation potential of the test sulfide in this particular solution. Similarly, the reduction potential of a sulfide is found by observing the approach of the two potentials upon the oxidation of a reducing solution.

The oxidation or reduction potential of a sulfide electrode is presumably dependent on the activities of the chemical species involved in a specific, potential-determining electrode reaction, as any other half-cell reactions. If hydrogen ion is involved, the potential should be a function of pH of the solution. The slope of the potential against pH of the solution is determined by the ratio of the number of hydrogen ions to that of electrons involved in the reaction. The potential value also varies in proportion to the logarithm of the activity of each product ion divided by the number of electrons involved. The activities of pure solids and of water are taken as unity; they do not affect the variation of the electrode potential. When the activities of dissolved product ions are all unity, the value of the measured electrode potential is equal to the standard oxidation potential of the potential-determining reaction. Instead of using such a solution, the value for the standard electrode potential may be obtained through extrapolation of measured potential values for different activities of the product ions to a value corresponding to unit activities. Knowing the type, dependency on pH, variation with the activities of specific ions, and extrapolated standard potential value of the measured electrode potentials, the electrode reaction operative at a sulfide electrode can be identified upon comparison with these factors predicted for assumed possible reactions, provided that necessary thermodynamic data are available.

The following is the standard experimental procedure applied in the present work to find the first-step oxidation or reduction reaction of a sulfide mineral through electrode potential measurements.

(1) Various solutions containing assumed oxidation or reduction products of a test sulfide are prepared. Since these products are not exactly known, possible combinations of various chemical species of the component metal and of sulfur must be tried. One restriction must be imposed, that is, the combination should be such that no formation of the same sulfide as the one being tested takes place in solution upon mixing. A mixture of the true oxidation products of a sulfide forms the sulfide only upon reduction.

(2) The activity of each component is varied independently, keeping the pH of the solution fixed. If a change in the activity of component causes a systematic change in the measured electrode potentials, this component must be participating in the potential-determining electrode reaction of the sulfide. A change in the concentration of a nonparticipating component may also affect the activity of a participating one (and consequently the electrode potential) by forming an insoluble or complex compound, or by changing the ionic strength of the solution. Such an indirect effect is, however, easily distinguishable from the former case which obeys the Nernst relationship.

(3) The pH value of the testing solution is varied by titrating an acid or base, while the concentration of other components is held fixed. The slope of measured potentials against pH values of a solution gives the ratio of the number of hydrogen ions to that of the electrons involved in the potential-determining electrode reaction. If the electrode potential is independent of pH, it implies that no hydrogen ion is involved in the reaction. A similar effect of pH on electrode potential

may be produced, however, when activities of other components vary with varying pH as the result of hydrolysis.

(4) The measured electrode potential values are plotted against the activities of each component found to be participating in the potential-determining electrode reaction, and also against pH values of solution. The potential value for unit activities of all participating chemical species and pH value of zero is extrapolated from these plotted data. This potential is a standard electrode potential of the sulfide, provided the temperature is 25° C and pressure 1 atm.

(5) Possible oxidation or reduction reactions are considered for the sulfide, and their standard oxidation potentials are calculated from thermodynamic data. Those reactions for which the calculated standard potentials are similar to the experimental standard electrode potentials are selected for further consideration.

(6) Final selection is made among these reactions with respect to the plausibility of the assumed mechanism, potential dependency on ionic activities and pH values, number of electrons involved, and other known chemical properties of the tested sulfide.

The above procedure has to be followed for both oxidation and reduction reactions with each sulfide, although the reduction may not necessarily take place in aqueous solution.

EXPERIMENTAL RESULTS

Copper Sulfides

The oxidation mechanism for copper sulfides indicated by the electrode potential method is in agreement with the conclusion reached by Sullivan (46, 47, 49), who in his rate study of leaching copper minerals with ferric sulfate solution stated that the oxidation of chalcocite Cu_2S proceeded in two steps:

$$Cu_2S = CuS + Cu^{++} + 2e,$$
$$CuS = Cu^{++} + S + 2e.$$

The second reaction was also found to be true with covellite. According to the above mechanism, the oxidation electrode potentials of copper sulfide are dependent only upon the activity of cupric ion, since the other oxidation products are solid. Their potentials are also independent of pH in acid solution. In basic solution, the potentials become dependent of pH, since the activity of cupric ion decreases exponentially with increasing pH due to hydrolysis.

Chalcocite.—The measured electrode potentials of chalcocite in 10^{-2} molal and 10^{-4} molal solutions of $CuSO_4$ are plotted against pH values of the solutions in Figure 3. The chalcocite crystals used for the electrode came from Superior, Arizona. The pH values of the solutions were adjusted by adding dilute HCl solution (pH smaller than 5) or KOH solution (pH greater than 5). The two horizontal solid lines on the diagram represent calculated potential values for the oxidation reaction of chalcocite in acid solution:

$$Cu_2S = CuS + Cu^{++} + 2e, \quad Eh = 0.530 + 0.0295 \log(Cu^{++}) \qquad (1)$$

corresponding to cupric ion activities of 10^{-2} and 10^{-4}, respectively. In this paper, rounded brackets denote activities of species, and square brackets

concentrations. Reference will be made to an earlier paper by Sato (*37*) as to the method of calculating oxidation potentials or equilibrium pH values from thermodynamic data. The values of free energy of formation used for the calculations are taken from Latimer (*24*), unless otherwise noted. In basic solution, cupric ion activity becomes a function of pH, due to the hydrolysis of Cu^{++} to $Cu(OH)_2$.[2] It is given by the following equation:

$$Cu^{++} + 2H_2O = Cu(OH)_2 + 2H^+, \quad \log(Cu^{++}) = 9.20 - 2\,pH. \quad (2)$$

Substituting the value for cupric ion activity in the first equation, we get

$$Eh = 0.802 - 0.0591\,pH. \quad (3)$$

The above procedure is essentially equal to adding the two chemical equations first and calculating the oxidation potential for the over-all reaction:

$$Cu_2S + 2H_2O = CuS + Cu(OH)_2 + 2H^+ + 2e,$$
$$Eh = 0.802 - 0.0591\,pH. \quad (4)$$

An inclined solid line on the diagram represents this potential. The observed potentials are generally lower than expected. Possible reasons for the discrepancies are: (1) the neglect of the activity coefficients for cupric ion, (2) the formation of digenite as an oxidation product instead of CuS, and (3) the effect of trace amount of sulfide ion in solution produced by dissociation. The first and second cases are discussed below. The third case, which may be appropriately called a "mixed electrode potential" effect in the sense that the electrode potential is affected by both oxidation and reduction electrode reactions, is characteristic to sulfide electrodes. A detailed discussion of this effect is, however, outside the scope of the present paper; it will be published in a separate paper elsewhere. It may be noted here that the order of magnitude of this effect is not so large as to affect the conclusions reached in this paper. The effect of the variation of the activities of cupric ion and sulfate ion in acid solution was studied separately. Figure 4 shows the variation of the electrode potential with varying cupric ion activity at a pH value of approximately 2, while the sulfate ion concentration was fixed at 10^{-2} molal. The activity coefficients for cupric ion at various concentrations are calculated through the use of the Debye-Hückel limiting law for a mean activity coefficient, $\gamma_\pm$, of a strong electrolyte in aqueous solution:

$$\log \gamma_\pm = -0.509\, z_+ z_- \sqrt{I}$$

where z_+ and z_- are the charges of positive and negative ionic species of the

[2] Cupric hydroxide gradually changes over to more stable CuO with time. Silman (*40*) reports that cupric sulfate solution precipitates antlerite $Cu_3(OH)_4SO_4$ and brochantite $Cu_4(OH)_6SO_4$, when an alkali hydroxide is added. In either case, however, the equilibrium cupric ion activity is in more or less similar order of magnitude for a given pH value, and the effect is essentially the same in that the precipitation of a solid phase controls the cupric ion activity as a function of pH. For the sake of simplicity, only the case of cupric hydroxide formation is discussed here.

electrolyte, and I the ionic strength of the solution. The ionic strength of a solution is defined by:

$$I = \tfrac{1}{2}\Sigma m_i z_i^2$$

The summation is carried out over all the ionic species in the solution, with molalities m_i, and charges z_i. Cupric ion activity is approximated from its molality times calculated mean activity coefficient for its salt. In case two different salts, e.g., cupric chloride and cupric sulfate, are present in about equal amount, a weighted average of the z_- values for the two anions is used for the calculation. When either one of the salts is predominant, the effect of the other is neglected. The slope of the plot of the electrode potential vs. logarithm of cupric ion activity agrees with the calculated value for the reaction (30 mv for $\log(Cu^{++}) = 1$), when the potential value for 10^{-4} molal cupric ion solution is excluded. The abnormally high potential value for this small concentration is probably due to higher cupric ion concentration at the electrode surface. The extrapolation of the potential values to unit activity of cupric ion gives a potential of approximately 0.505 volt as compared with the calculated standard potential of 0.530 volt. A 10^{-2} molal solution of cupric chloride gave essentially the same electrode potential as a 10^{-2} molal solution of cupric sulfate. This implies that sulfate ion does not participate in the potential-determining electrode reaction.

It is possible that chalcocite oxidizes first to digenite Cu_9S_5 instead of CuS, and the observed oxidation electrode potential of chalcocite corresponds not to reaction (1) but to the following reaction:

$$5Cu_2S = Cu_9S_5 + Cu^{++} + 2e.$$

The digenite thus formed is successively oxidized to CuS as:

$$Cu_9S_5 = 5CuS + 4Cu^{++} + 8e.$$

The difference of 0.02 volt between the observed value and the value calculated from equation (1) for the standard oxidation potential of chalcocite may be ascribed to the difference in the reaction mechanism. At present, however, no reliable value of free energy of formation is available for digenite, and the examination of this possibility is left for future work.

Covellite.—Large crystals of covellite CuS, probably of hypogene origin, were used for the testing electrodes. The locality of its occurrence is unknown. A small number of chalcocite inclusions in the crystals were carefully etched with an acidified 5% H_2O_2 solution. The electrode surface was then repolished. Complete elimination of chalcocite from the electrode surface is extremely important, since chalcocite in contact with covellite in a cupric solution establishes the potential corresponding to reaction (1). The measured electrode potentials of covellite in 10^{-2} molal and 10^{-4} molal solutions of $CuSO_4$ are plotted against pH values of solutions in Figure 5. A dilute solution of either HCl or KOH was added to adjust the pH values of the solutions as in the case of chalcocite. The two horizontal solid lines on the diagram represent calculated potentials for the reaction:

$$CuS = Cu^{++} + S + 2e, \quad Eh = 0.591 + 0.0295 \log(Cu^{++}) \qquad (5)$$

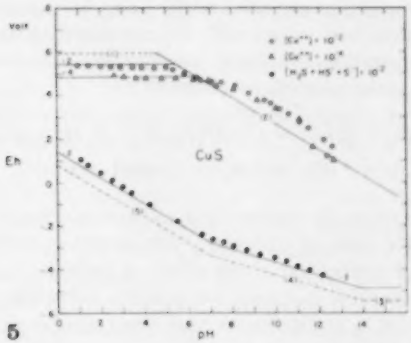

5

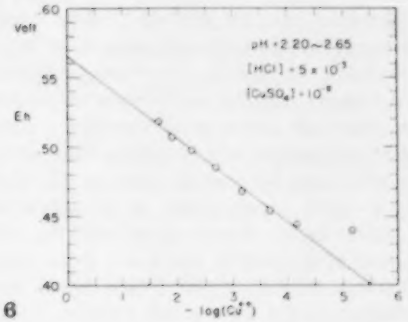

6

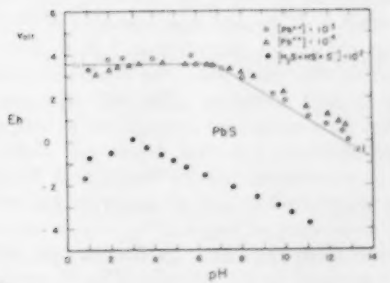

7

FIG. 5. Plots of the measured electrode potentials of covellite against the pH values of testing solutions. (1) $CuS = Cu^{++} + S + 2e$, (2) $CuS + 2H_2O = Cu(OH)_2 + S + 2H^+ + 2e$, (3) $Cu_2S + S^{--} = 2CuS + 2e$, (4) $Cu_2S + HS^- = 2CuS + H^+ + 2e$, (5) $Cu_2S + H_2S = 2CuS + 2H^+ + 2e$.

FIG. 6. Plots of the measured electrode potentials against the logarithm of cupric ion activity for covellite.

FIG. 7. Plots of the measured electrode potentials of galena against the pH values of testing solutions. (1) $PbS = Pb^{++} + S + 2e$, (2) $PbS + 2H_2O = Pb(OH)_2 + S + 2H^+ + 2e$.

corresponding to cupric ion activities of 10^{-2} and 10^{-4}, respectively. A good agreement of the measured values with the calculated values was observed in acid solutions. Assuming the same mechanism, the potential becomes a function of pH in basic solution, as given by:

$$CuS + 2H_2O = Cu(OH)_2 + S + 2H^+ + 2e,$$
$$Eh = 0.862 - 0.0591\ pH. \quad (6)$$

An inclined solid line at the upper right portion of Figure 5 represents this potential. As in the case of chalcocite, the second equation may be understood as an over-all expression of the effect of hydrolysis of cupric ion, and of the subsequent decrease in cupric ion activity, upon the electrode potential of covellite. $Cu(OH)_2$ is not one of the direct oxidation products, nor the only hydrolysis product of cupric ion. In basic solutions, rather large deviations of the observed values from the predicted values exist, the former being higher than the latter. This is probably because of a slow attainment of equilibrium between cupric ion and hydroxyl ion. Consequently, the cupric ion activity remains higher than the equilibrium value for a given pH, resulting in a higher electrode potential of covellite. The reason why this phenomenon is more conspicuous with covellite than with chalcocite is unknown. When the pH value becomes as high as 12, bluish white colloidal suspension changes to grey cupric oxide at an appreciable rate, and the observed potential values again closely agree with the calculated ones.

The electrode potential of covellite was found to be independent of sulfate ion activity, as in the case of chalcocite. It was found to satisfy the Nernst relationship with respect to the cupric ion activity in solution. Solutions with various concentrations of cupric sulfate were used for this study. They were all acidified with 5×10^{-3} molal concentration of HCl to avoid hydrolysis of cupric ion. Their pH values ranged from 2.20 to 2.65. A slight variation in pH is immaterial in this case, since the electrode potential of covellite is independent of pH in acid sodution. The activity values for cupric ion at various concentration were calculated through the procedure already described for chalcocite. The observed potential values are plotted against calculated cupric ion activity on a potential-activity diagram in Figure 6. The slope of the line connecting the plotted values agrees with the calculated slope, being 0.030 volt per unit increment of $\log(Cu^{++})$. As in the case of chalcocite, a considerable deviation from the linear relationship is observed when cupric ion concentration is as small as 10^{-5} molal. This is probably due to a higher concentration of cupric ion at the electrode surface. The extrapolation of the potential to unit activity of cupric ion yields a value of 0.567 volt as compared with the calculated standard potential of 0.591 volt. This amount of discrepancy is not so serious as to affect the over-all agreement between the experimental results and the theoretical predictions based on reaction (5). Sullivan (49) observed that covellite left a sulfur skeleton of original mineral grains when treated with ferric sulfate. It is concluded, therefore, that the first-step oxidation mechanism for covellite is the liberation of copper

as cupric ion into the surrounding solution, leaving elementary sulfur behind, as already suggested by Sullivan.

Another series of measurements was carried out to establish the reduction mechanism of covellite by the electrode potential method. Prior to the measurements, covellite electrodes were electrolytically reduced in a dilute solution of sodium sulfide for a few minutes, to remove the oxidation film from the surface. Solutions initially containing 10^{-2} molal concentration of Na_2S and 2×10^{-2} molal concentration of KOH were used as the testing solutions. Their pH values were adjusted by adding a small amount of 1 N HCl solution. In acid solution, sodium sulfide evolves hydrogen sulfide gas. In the present experiment, the cell container was kept closed during and after addition of HCl, so that the total amount of $(S^{--} + HS^- + H_2S)$ in solution remained unchanged for the series of measurements. The measured electrode potentials are plotted against the pH values of the solutions in Figure 5. The result indicates that the reduction of covellite involves the formation of a copper sulfide with a higher ratio of copper to sulfur and liberation of a part of the sulfur as S^{--} ion. Whether the product copper sulfide is Cu_2S or Cu_nS_5 is not distinguishable potential-wise. Since accurate thermodynamic data are not available for the latter, Cu_2S is taken as the reduction product of covellite until a definite proof is obtained for the formation of digenite. In strongly basic solution, S^{--} ion is stable and the reduction potential of covellite is independent of pH value of the solution, as given by:

$$Cu_2S + S^{--} = 2CuS + 2e, \quad Eh = -0.540 - 0.0295 \log(S^{--}). \quad (7)$$

In neutral to weekly basic solution, S^{--} ion is unstable and combines with hydrogen ion to form HS^- ion:

$$S^{--} + H^+ = HS^-, \quad \log(S^{--}) = \log(HS^-) + pH - 14.00. \quad (8)$$

The potential for covellite reduction is given by the following over-all equation:

$$Cu_2S + HS^- = 2CuS + H^+ + 2e,$$
$$Eh = -0.126 - 0.0295\,pH - 0.0295 \log(HS^-). \quad (9)$$

In acid solution, HS^- ion combines with another hydrogen ion to form hydrogen sulfide:

$$HS^- + H^+ = H_2S, \quad \log(HS^-) = \log(H_2S) + pH - 7.00. \quad (10)$$

The activity of hydrogen sulfide in solution is related to the partial pressure of hydrogen sulfide gas, P_{H_2S}, as

$$(H_2S)_{aq} = 0.102\,P_{H_2S}. \quad (11)$$

From the above relationships, the potential for covellite reduction in acid

solution is given by the following over-all equation:

$$Cu_2S + H_2S = 2CuS + 2H^+ + 2e,$$
$$Eh = 0.081 - 0.0591\ pH - 0.0295 \log(H_2S) \qquad (12)$$

or in terms of the partial pressure of hydrogen sulfide:

$$Eh = 0.111 - 0.0591\ pH - 0.0295 \log P_{H_2S}. \qquad (12')$$

The three solid lines at the lower portion of Figure 5 represent the calculated potential values against pH for the activity value of 10^{-2} of S^{--}, HS^-, or H_2S, depending on the range of pH. Although no measurement was made in strongly basic solution, the agreement between the measured potentials and the calculated ones is remarkably good. Slightly higher values for the measured potentials compared to those calculated are probably because of the neglect of the activity coefficients for the three sulfide ion species.

Lead Sulfide

A large crystal of galena from the Blackstone mine, near Shullsburg, Wisconsin, was used for the electrodes. Lead acetate solutions of 10^{-2} and 10^{-4} molal concentrations were used as the testing solutions. A dilute solution of either HNO_3 or KOH was added to adjust the pH values of the solutions. The measured electrode potentials of galena are plotted against the pH values of the solutions in Figure 7. The horizontal line in the figure represents the standard oxidation potential for the reaction:

$$PbS = Pb^{++} + S + 2e, \quad Eh = 0.354 + 0.0295 \log(Pb^{++}) \qquad (13)$$

in acid solution. The oxidation potential for the reaction in neutral to moderately basic solution can be calculated from the following over-all equation, as in the case of copper sulfides.

$$PbS + 2H_2O = Pb(OH)_2 + S + 2H^+ + 2e,$$
$$Eh = 0.765 - 0.0591\ pH. \qquad (14)$$

This potential is represented by the inclined solid line at the upper right portion of the diagram. Although the measured potential values are slightly higher than the calculated values, the over-all agreement between the two indicates that galena is oxidized to plumbous ion and elementary sulfur in the first step of its oxidation reactions. This conclusion agrees with the one reached by Noddack, Wrabetz, and Herbst (32) in their study of electrode potentials of sulfides. The fact that the observed potential values are higher than the calculated values could be due to a more negative value of the free energy of formation of galena than the one given by Latimer (24) for PbS. Alternatively, the sulfur produced may not be the stable rhombic form, accounting for the higher observed potential values. Further study on the points may be justified.

In acid and oxidizing environment, galena is often replaced by anglesite $PbSO_4$. It is of interest to find out the effect of the sulfate ion concentration upon the oxidation potential of galena. The data for the measurements of the electrode potential of galena in solutions containing various concentrations of sulfate ion are listed in Table 1. Measured amounts of Na_2SO_4 were

TABLE 1

POTENTIAL MEASUREMENT DATA FOR GALENA ELECTRODE
Solution: A mixed solution of 10^{-4} molal $Pb(CH_3COO)_2$, 10^{-3} molal CH_3COOH, and X molal Na_2SO_4. Temperature: 32° C

pH	Eh (mv)	$[Na_2SO_4]$ (molal)	$\log(SO_4^{--})$	$\log(Pb^{++})$
5.01	250	3×10^{-4}	−3.55	−4.34
5.00	241	1×10^{-3}	−3.05	−4.84
4.99	230	3×10^{-3}	−2.61	−5.28
4.99	216	1×10^{-2}	−2.15	−5.74
5.01	207	3×10^{-2}	−1.75	−6.14

added to 200 cc of 10^{-4} molal solution of lead acetate. The sulfate ion precipitates the plumbous ion in solution as white lead sulfate, when the activity product of the two ions exceeds the solubility product of lead sulfate. The reaction is not rapid. The solution was, therefore, kept stirred for at least 1 hour before each potential measurement. The effect of the sulfate ion upon the electrode potential of galena was found to be the lowering of the potential, by decreasing the plumbous ion activity with the formation of difficulty soluble lead sulfate. At the pH and the temperature ranges of the measurements (pH = 4.99 – 5.07, t = 32° C), the lead sulfate dissociates as follows:

$$PbSO_4 = Pb^{++} + SO_4^{--}, \quad K = (Pb^{++})(SO_4^{--}) = 1.3 \times 10^{-8}. \quad (15)$$

Using this value for the dissociation constant of lead sulfate, the activities of plumbous ion in the above solutions can be calculated. Division of the above dissociation constant by sulfate ion activity yields the equilibrium plumbous ion activity. The sulfate ion activities are estimated from the activity coefficients for various concentrations of Na_2SO_4 tabulated by Latimer (24). The measured electrode potential values of galena are plotted against $\log(Pb^{++})$ in Figure 8. The slope of the line connecting the plotted values is approximately 0.027 volt for unit increment of $\log(Pb^{++})$, as compared with the calculated value of 0.0295 volt assuming the Nernst relationship. It is inferred from this observation that the presence of a foreign ion generally lowers the oxidation potential of a sulfide, if the ion forms an insoluble solid or a complex compound with a soluble, direct oxidation product of the sulfide.

A series of potential measurements was made with galena in solutions containing 10^{-2} molal concentration of sodium sulfide. The measured electrode potential values are plotted against pH values in Figure 7. The ob-

served potential values do not agree with the calculated values, if the following reaction mechanism is assumed:

$$PbS + 2e = Pb + S^{--}.$$

They showed a consistent variation with varying pH, becoming increasingly more positive with decreasing pH, until a pH value of about 3 was reached, where the electrode potential started drifting rapidly to the negative direction with increasing acidity. The reason for this peculiar behavior of the galena is not fully understood.

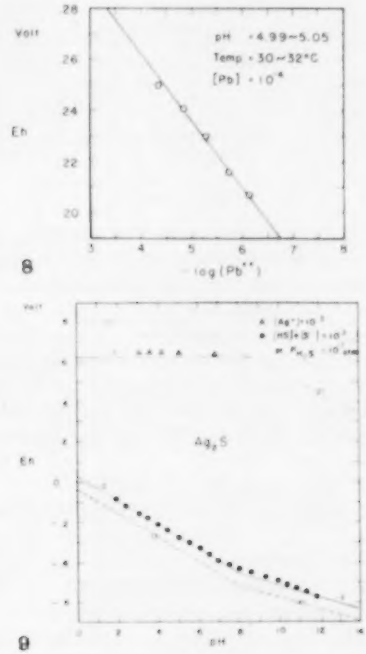

FIG. 8. Plots of the electrode potential values of galena measured in solutions with various activities of sulfate ion, which determine the equilibrium activity values of plumbous ion by forming lead sulfate precipitate.

FIG. 9. Plots of the measured electrode potentials of argentite against the pH values of testing solutions. (1) $Ag = Ag^+ + e$ (for comparison), (2) $2Ag + H_2O = Ag_2O + 2H^+ + 2e$ (for comparison), (3) $2Ag + H_2S = Ag_2S + H^+ + 2e$, (4) $2Ag + HS^- = Ag_2S + H^+ + 2e$.

Silver Sulfide

Large crystals of argentite Ag_2S from Cobalt, Ontario were used for the electrodes. The results of the electrode potential measurements with argentite in solutions containing sulfide ion species (S^{--}, HS^-, and H_2S) indicate that

the sulfide is reduced according to the following electrode reaction ($\triangle F^0$ value for Ag_2S is taken as –9.36 kcal/mole):

$$2Ag + S^{--} = Ag_2S + 2e, \quad Eh = -0.682 - 0.0295 \log(S^{--}). \quad (16)$$

In weakly basic solution, the potential for this electrode reaction mechanism is given by the following over-all equation:

$$2Ag + HS^- = Ag_2S + H^+ + 2e,$$
$$Eh = -0.268 - 0.0591\ pH - 0.0295 \log(HS^-). \quad (17)$$

In acid solution, it is given by:

$$2Ag + H_2S = Ag_2S + 2H^+ + 2e,$$
$$Eh = -0.061 - 0.0591\ pH - 0.0295 \log(H_2S) \quad (18)$$

or in terms of the partial pressure of hydrogen sulfide:

$$Eh = -0.032 - 0.0591\ pH - 0.0295 \log P_{H_2S}. \quad (18')$$

Solutions containing 10^{-2} molal Na_2S and 10^{-2} molal KOH were used as the testing solutions. 1 N solution of formic acid was added to adjust the pH values of the solutions. The data for the measurements are listed in Table 12. The measured potential values are plotted against pH in Figure 9. The two solid lines in the lower portion of the figure represent the potentials calculated from the equations (17) and (18′), for the 10^{-2} molal concentration of HS^-, and H_2S, respectively. Hydrogen gas was kept bubbling slowly at a pressure of 1 atm. during the measurements. In this condition, equation (18′) must be applied instead of equation (18) for acid solutions. Although no measurement was made in strongly basic solutions, the agreement between the observed values and the calculated values is satisfactory, hence it may be concluded that the reduction of argentite proceeds through the electrode reaction (16). The result indicates that argentite can be actively reduced to silver and sulfide ion species in basic solution. Incidentally, the above electrode potentials of argentite in sulfide ion solutions are essentially the same as those of the well-known Ag/Ag_2S electrode in similar solutions, although no silver metal was present as a distinct solid phase.

The measurements of the electrode potential values for argentite in Ag^+ ion solutions were made only in acid conditions. The measured electrode potentials of argentite in solutions containing 10^{-2} molal concentration of $AgNO_3$ are plotted against the pH values of the solutions in Figure 9. They are found to be independent of pH in acid solution. This fact leaves only the two following reactions to be considered for the electrode reaction.

$$Ag_2S = 2Ag^+ + S + 2e, \quad Eh = 1.002 + 0.0591 \log(Ag^+), \quad (19)$$

$$Ag_2S = AgS + Ag^+ + e. \quad (20)$$

The observed values do not agree with the calculated values for the first assumed reaction. The average of the five measured potentials is 0.643 volt

for 10^{-3} molal concentration of Ag^+ ion. When the activity coefficient is neglected, the standard electrode potential for the oxidation of Ag_2S is given approximately as 0.82 volt. This value is very close to the standard electrode potential of silver metal:

$$Ag = Ag^+ + e, \quad Eh = 0.799 + 0.0591 \log(Ag^+). \tag{21}$$

The horizontal solid line in Figure 9 represents the potential for reaction (21), corresponding to the activity value of 10^{-3} for the Ag^+ ion. The apparent similarity of the potential values may lead to an argument that reaction (21) is operative at the silver sulfide electrode without involving sulfur, owing to the free migration of silver atoms within the sulfide crystal. Rather prominent mobility of silver atoms in Ag_2S crystals has been reported by Wagner (56). The effect of sulfur on the electrode potential of Ag_2S, however, was observed by Noddack and Wrabetz (31) who reported that, when the sulfur content of the sulfide was increased above the stoichiometric value, the potential increased for as much as 50 millivolts from the value for Ag_2S of stoichiometric composition. Reaction (20) is, therefore, most likely to be operative at the argentite electrode. There is no direct way to examine the validity of this assumed reaction by the potential method, since the value of the free energy of formation for AgS is not available. The similarity of this mechanism to that of chalcocite may be noted. Although the occurrence of AgS in nature is unknown, Laist (23) reports that it has been artificially prepared by treating a benzonitrile solution of silver nitrate with sulfur dissolved in carbon disulfide. The similarity of the potential for the oxidation reaction of Ag_2S to that of silver is probably due to the similarity of the values of the free energy of formation between Ag_2S and AgS. If the standard oxidation potential for reaction (20) is taken as 0.82 volt, the free energy of formation of AgS can be calculated. It becomes –8.89 Kcal per mole, when those of Ag_2S and Ag^+ ion are taken as –9.36 Kcal and +18.43 Kcal per mole, respectively. If the mechanism of oxidation for AgS is assumed to be similar to that for CuS, the oxidation potential for AgS is given by the following equation:

$$AgS = Ag^+ + S + e, \quad Eh = 1.182 + 0.0591 \log(Ag^+). \tag{22}$$

It is possible that the well-known deficiency of silver in argentite from its stoichiometric composition is due to the partial oxidation of the sulfide, resulting in the so-called "defect structure." The similarity of the values of the free energy of formation for the two silver sulfides may allow the silver atoms to migrate freely through the interstices of the sulfur atoms, making the separation of the two sulfides impossible.

Iron Sulfides

The interpretation of the results of the potential measurements for sulfides of iron was found to be the most difficult to make among the various sulfide minerals studied. Considerable difficulty was encountered in controlling the oxidation potential and the pH values of iron solutions independently in

neutral to basic conditions, on account of the formation of hydroxides of iron. Also the formation of an adhesive coating of ferric hydroxide over the electrode surface sometimes gave considerable trouble in obtaining reproducible results.

Pyrite.—Large crystals of pyrite from Rico, Colorado, were used for the electrodes. The measured values of the oxidation electrode potential of pyrite in solutions containing 10^{-3} molal concentration of $FeSO_4$ and those in solutions containing 10^{-5} molal $FeSO_4$ plus 10^{-2} molal Na_2SO_4 are plotted against pH values of the solutions in Figure 10. The results seem to indicate that the oxidation potential of pyrite is independent of pH, when the pH values are smaller than 2. In more basic solutions, it becomes a linear function of pH, with a slope approximately corresponding to 0.059 volt per unit pH. This is probably because of the decrease in the ionic iron activities due to the formation of ferric hydroxide. The assumed oxidation reaction for pyrite which gives the closest fit to the observed potential values in dilute solutions of ionic iron species is the following one:

$$FeS_2 = Fe^{++} + S_2 + 2e, \quad Eh = 0.757 + 0.0295 \log(Fe^{++}). \qquad (23)$$

The value of the free energy of formation of pyrite, which is used in this paper, is –36.07 Kcal per mole as given by Kelley (20), instead of Latimer's value of –39.84 Kcal per mole. The sulfur in the above equation is not in crystalline state, but in diatomic molecular form. Its standard free energy of formation in gaseous state is given by Stull and Sinke (45) as 19.13 Kcal per mole. In the above equation the partial pressure of S_2 was taken as 1 atm., assuming that this much pressure must be exerted against the solution by the S_2 molecules before the latter are liberated from pyrite. The horizontal solid line in Figure 10 represents this potential for the ferrous ion activity of 10^{-3}. The potential for the above reaction mechanism in neutral to basic solution is given by the following over-all reaction, which takes both the oxidation of ferrous ion and the hydrolysis of ferric ion to ferric hydroxide into account:

$$FeS_2 + 3H_2O = Fe(OH)_3 + S_2 + 3H^+ + 3e,$$
$$Eh = 0.857 - 0.591\ pH. \qquad (24)$$

The inclined solid line at the upper right portion of Fig. 10 represents this potential. The agreement between the calculated and the observed potential values is fairly good, when we consider the uncertainty of the energy content of the diatomic sulfur molecules in aqueous solution. This mechanism is a plausible one from the standpoint of the crystal structure of pyrite. In the pyrite structure, two sulfur atoms exist close together, forming –Fe–S_2–Fe– type bonds. It is quite possible, therefore, that the bonds between sulfur and iron atoms are broken during oxidation, liberating S_2 molecules as one of the oxidation products. The slowness of the oxidation of pyrite under the action of many oxidizing agents may be explained by the high oxidation potential for this reaction. It should be noted, however, that the conclusion reached here as to the oxidation mechanism for pyrite is a tentative one and is open to further critical examinations.

An attempt to establish the reduction mechanism for pyrite has been unsuccessful. The reduction potential measurements were made in solutions of three types. The first type initially contained 10^{-2} molal concentration of Na_2S and no iron, the second and the third ones contained 10^{-3} molal and 10^{-4} molal concentrations of $FeCl_2$, respectively, in addition to 10^{-2} molal

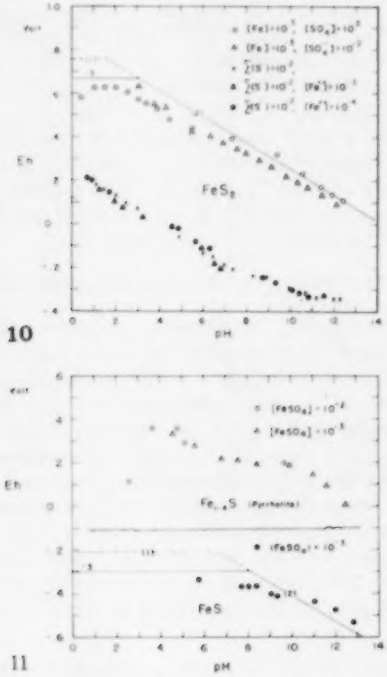

Fig. 10. Plots of the measured electrode potentials of pyrite against the pH values of testing solutions. (1) $FeS_2 = Fe^{++} + S_2$ (1 atm.) + $2e$, (2) $FeS_2 + 3H_2O = Fe(OH)_3 + S_2$ (1 atm.) + $3H^+ + 3e$.

FIG. 11. Plots of the measured electrode potentials of pyrrhotite and those of artificial ferrous sulfide against the pH values of testing solutions. (1) $3FeS = Fe^{++} + Fe_2S_3 + 2e$, (2) $3FeS + 2H_2O = Fe(OH)_2 + Fe_2S_3 + 2H^+ + 2e$.

Na_2S. A dilute HCl solution was used to acidify the solutions. The measured potential values are all similar for a given pH, regardless of the concentration of ferrous ion. They are plotted against pH values in Figure 10. The slope of the potential against pH appears to be approximately 0.06 volt per unit pH in acid solution, and 0.03 volt per unit pH in basic solution. Matsubara and Takubo (26) reported that pyrite evolved H_2S in dilute solution of H_2SO_4, when an external electromotive force was applied. These observed facts would fit to a reduction mechanism for pyrite involving the

liberation of sulfide ion and the formation of a solid iron sulfide. The observed potential values, however, do not agree with the calculated values for any of the three assumed reaction mechanisms, respectively involving Fe, FeS, and Fe_2S_3. It is likely that an iron sulfide with a higher S to Fe ratio is involved in the reaction. Further study is required to determine the reduction mechanism for pyrite.

Pyrrhotite.—The investigation of pyrrhotite was not completed. A massive aggregate of pyrrhotite crystals from Hybla, Ontario, was used for the electrodes. The potential measurements were made in 10^{-2} molal and 10^{-3} molal solutions of $FeSO_4$ with HCl or KOH being added as the pH adjustant. The measured potential values are plotted against pH values of the solutions in Figure 11. Reproducible results are difficult to obtain in acid solutions, since pyrrhotite readily produces both hydrogen sulfide and ferrous ion by the action of acids. In basic solution, the formation of iron hydroxides makes the control of the experimental conditions difficult. It is not possible to interpret the results of the measurements, as the value of the free energy of formation of pyrrhotite is not available. The low values of the electrode potential of pyrrhotite in ferrous ion solutions, however, confirm the known fact that pyrrhotite oxidizes much more readily than pyrite.

Ferrous Sulfide.—Artificially prepared ferrous sulfide crystals were used as electrodes. The measured electrode potentials in 10^{-2} molal solutions of $FeSO_4$ are plotted against pH values of the solutions in Figure 11. In acid solution, reliable potential values were not obtainable because of the active dissociation of ferrous sulfide with evolution of hydrogen sulfide. The observed potential values appear to be independent of pH in neutral to weakly acid solutions, and to be dependent on pH in basic solutions. This fact is indicative of an oxidation mechanism which involves the liberation of ferrous ion and the formation of either sulfur or an iron sulfide with a higher S to Fe ratio. The observed potential values do not agree with assumed reactions involving either sulfur or pyrite. A reaction mechanism involving Fe_2S_3:

$$3FeS = Fe^{++} + Fe_2S_3 + 2e, \quad Eh = -0.202 + 0.0295 \log(Fe^{++}) \qquad (25)$$

whose potential in basic solution is given by the following over-all equation:

$$3FeS + 2H_2O = Fe(OH)_2 + Fe_2S_3 + 2H^+ + 2e,$$
$$Eh = 0.190 - 0.0591\,pH \qquad (26)$$

appears to give a better fit, but the agreement between the calculated and the observed potentials is only fair. In Figure 11, the horizontal solid line represents the potential for reaction (25) calculated for ferrous ion activity of 10^{-3}, and the inclined solid line the potential for reaction (26). A reaction mechanism involving smythite Fe_3S_4 could give a satisfactory agreement between the observed and calculated potential values, if its free energy of formation becomes available.

It is improbable that ferrous sulfide is reduced to elementary iron and sulfide ion species in aqueous solution, since metallic iron is not stable in water.

Marcasite.—Several potential measurements were made for marcasite. The data for the measurements in acidified 10^{-3} molal solutions of $FeSO_4$ are listed in Table 2. No measurements were made in basic solutions. The results indicate that the oxidation potential for marcasite is independent of pH in acid solution. The measured potential values are slightly more negative than those for pyrite. This is expected from the higher energy content

TABLE 2

POTENTIAL MEASUREMENT DATA FOR MARCASITE ELECTRODE
Solution: 10^{-3} molal solution of $FeSO_4$. pH adjustant: 1 N HCl solution for pH values below 4

pH	Temp. (° C)	Eh (mv)	1 N HCl (cc)
3.90	26	547	0
3.83	27	572	0.05
2.98	26	560	0.15
2.50	26	572	0.5
1.98	26	573	1.7
1.50	26	570	5.0

of marcasite in comparison with pyrite. The comparison with calculated potential values has not been made, as no value of the free energy of formation of marcasite is available. The oxidation mechanism for marcasite is probably similar to that for pyrite, since the two sulfides have very similar crystal structures.

Zinc Sulfide

Sphalerite.—Repeated attempts to measure the electrode potential of amber-colored sphalerite from Santander, Spain, were unsuccessful, because of the very poor electric conductivity of the sulfide. The iron-rich variety, marmatite, from Wanlockhead, England, was also tried in vain. One electrode showed a definite potential value, but soon it was found that the potential was produced by the contact of the solution with the mercury drop placed within the plastic mold of the electrode through a minute fracture of the sphalerite crystal. The electrode potential values for sphalerite have been reported by other workers. The present author doubts the validity of their results. Sphalerite is, in fact, a good insulator of electricity. A different method to establish the oxidation mechanism for zinc sulfide was tried. The principle of the approach is as follows. If ZnS is to be oxidized according to the reaction:

$$ZnS\ (ppt.) = Zn^{++} + S + 2e, \quad Eh = 0.174 + 0.0295 \log (Zn^{++}) \qquad (27)$$

the oxidation potential of a solution containing both zinc ion and zinc sulfide should approach the potential calculated for the activity of the zinc ion in the solution from the above equation, as equilibrium condition is approached. This method is applicable to zinc sulfide, since the above assumed reaction has such a low potential as to allow elementary sulfur to exist in solution

without being actively oxidized. In basic solution, the oxidation potential for the above reaction mechanism is given by the following over-all equation:

$$ZnS\ (ppt.) + 2H_2O = Zn(OH)_2 + S + 2H^+ + 2e,$$
$$Eh = 0.520 - 0.0591\ pH. \qquad (28)$$

The following experiment was carried out. A 2×10^{-2} molal solution of $ZnSO_4$ was placed in the cell container. Nitrogen gas was constantly bubbled through the solution during the experiment. When the solution was deoxygenated, Na_2S solution was added in such an amount that one-half of the zinc ions was precipitated as zinc sulfide. After the addition of Na_2S, either KOH or HCl was added to the solution to adjust the pH value. Then the mixture was kept stirred until the system reached equilibrium. The measured oxidation potential values of the solution at equilibrium are listed in Table 3,

TABLE 3

OXIDATION POTENTIAL VALUES FOR ZnS-Zn^{++}-H_2O SYSTEM

pH	Temp. (° C)	Eh (obs.) (v)	Eh (calc.) (v)
2.67	28	0.166	0.115
5.20	29	0.153	0.115
6.80	29	0.076	0.118
7.59	29	0.042	0.072
9.78	28	−0.038	−0.058

together with the pH and the calculated oxidation potential values for the assumed reaction mechanisms. Although accumulation of more data is desirable, the agreement between the measured and the calculated potential values appears to be good. The oxidation mechanism for sphalerite is assumed to be similar to that for ZnS precipitate. It is tentatively concluded, therefore, that sphalerite oxidizes through the following reaction mechanism:

$$ZnS\ (sphalerite) = Zn^{++} + S + 2e, \quad Eh = 0.265 + 0.0295 \log (Zn^{++}). \quad (27')$$

SUMMARY AND CONCLUSIONS

An examination of the electrode potentials of chalcocite and covellite, whose oxidation mechanisms had been studied by Sullivan (49), indicated that the electrode potential of a sulfide mineral in an oxidizing solution is controlled by the first step of its consecutive oxidation reactions. In this step, the chemical bonds in the crystal structure are broken upon the loss of electrons, followed by rearrangement of the electron configuration of the constituent atoms. A similar relationship was also found to exist between the electrode potential of a sulfide mineral in a reducing solution and the reduction mechanism of the sulfide.

Based on the understanding of the above electrode behavior of sulfide minerals, an electrochemical method has been developed for the identification of their first-step oxidation or reduction reactions. Single electrode potential

of a sulfide mineral is measured in solutions containing its assumed oxidation or reduction product ions. Various combination of these product ions must be tried to find the ones which directly affect the electrode potential; the potential-controlling reactions involve these ions. Possible electrode reactions are assumed, and their potentials are calculated thermodynamically for comparison with the measured potential values. Unless an objectionable evidence exists, the first-step reaction for the mineral may be identified as the assumed reaction which fits best with the observational data with respect to the electrode sign, magnitude, pH dependency, and variation with varying activities of the chemical species involved.

Sulfides of copper, lead, silver, iron, and zinc were studied. The results indicate that the direct oxidation of a simple sulfide mineral at low temperatures is a process in which the metal atoms move into the surrounding solution to become aqueous cations, accompanied by a step-wise decrease in the metal to sulfur ratio of the remaining solid phase. When sulfur is finally left over, it undergoes a series of reactions to be oxidized to sulfate ion. In case of reduction, sulfur atoms move into the solution to become aqueous sulfide ion, with a step-wise increase in the metal to sulfur ratio of the remaining solid phase. The final reduction products of a sulfide mineral are presumably sulfide ion plus native metal. The reduction reactions usually do not proceed to this extent in aqueous solution, however, because water will be reduced to hydrogen gas before most of sulfide minerals are reduced to their respective metals. The formal charges for the metals in sulfides increase step-wise upon oxidation, and decrease similarly upon reduction. The path of the step-wise oxidation is not necessarily the same as that of reduction for a metal-sulfur system.

The probable oxidation steps for the metal-sulfur systems involving the sulfide minerals studied are as follows:

1. Cu-S System: $(2Cu + S^{--}) \rightarrow (Cu_2S) \rightarrow \frac{1}{8}(Cu_9S_5 + Cu^{++})? \rightarrow (CuS + Cu^{++}) \rightarrow (2Cu^{++} + S)$;
2. Pb-S System: $(Pb + S^{--}) \rightarrow (PbS) \rightarrow (Pb^{++} + S)$;
3. Ag-S System: $(Pb + S^{--}) \rightarrow (Ag_2S) \rightarrow (AgS + Ag^{+}) \rightarrow (2Ag^{+} + S)$;
4. Zn-S System: $(Zn + S^{--}) \rightarrow (ZnS) \rightarrow (Zn^{++} + S)$;
5. Fe-S System: $(Fe + S^{--}) \rightarrow (FeS) \rightarrow \frac{1}{n}(Fe_{n-x}S_n)? \rightarrow (Fe^{++} + S)$, $(0 < x < n)$.

In the presence of free oxygen, sulfur thus produced is not stable; it will be oxidized to sulfate ion through various stages of oxidation. Solid sulfur is not produced in the case of disulfides of iron, namely pyrite and marcasite, but instead S_2 molecules appear to be released into the solution simultaneously with ferrous ions. Such S_2 molecules are extremely unstable at room temperatures, and will instantly be oxidized to sulfur species of higher oxidation states.

ACKNOWLEDGMENTS

The experimental work presented in this paper was carried out at the University of Minnesota as an integral part of a research project on the origin of self-potentials under the supervision of Professor H. M. Mooney, Department of Geophysics, University of Minnesota. The project was sponsored by the Division of Raw Materials, U. S. Atomic Energy Commission, as contract AT (05-1)-719. The author is deeply indebted to Professor G. M. Schwartz for his advisorship throughout the author's study at the University. The author's gratitude for very helpful suggestions and critical comments is due to Professor R. M. Garrels, Department of Geology, Harvard University, and to Professor Z. Z. Hugus, Department of Inorganic Chemistry, University of Minnesota. The present manuscript has been prepared under the auspices of the Committee on Experimental Geology and Geophysics and the Division of Geological Sciences, Harvard University.

LABORATORY OF MINING GEOLOGY,
HARVARD UNIVERSITY,
CAMBRIDGE, MASS.
December 16, 1959

REFERENCES

1. Anderson, A. L., 1930, The incipient oxidation of galena: ECON. GEOL., v. 25, p. 528–542.
2. ——, 1932, Notes on the oxidation of jamesonite, sphalerite, and tetrahedrite: ECON. GEOL., v. 27, p. 687–703.
3. Bain, G. W., 1935, Pyrite oxidation: ECON. GEOL., v. 30, p. 166–169.
4. Bernfield, I. D., 1898, Studien über Schwefelmetallelektroden: Zeitschr. Physikal Chemie, v. 25, p. 46–78.
5. Blanchard, R., and Boswell, P. F., 1925, Notes on the oxidation products derived from chalcopyrite: ECON. GEOL., v. 20, p. 613–638.
6. ——, and Boswell, P. F., 1928, Status of leached outcrops investigation: Eng. and Min. Jour., v. 125, p. 280–285, p. 373–377.
7. ——, 1930, Limonite types derived from bornite and tetrahedrite: ECON. GEOL., v. 25, p. 557–580.
8. Boswell, P. F., and Blanchard, R., 1927, Oxidation products derived from sphalerite and galena: ECON. GEOL., v. 22, p. 419–453.
9. Buehler, H. A., and Gottschalk, V. H., 1910, Oxidation of sulfides: ECON. GEOL., v. 5, p. 28–35.
10. Bulah, A. S., and Khan, O. A., 1954, Potentials of copper and nickel sulfides: Zhur. Priklad, Khim., v. 27, p. 166–170.
11. Carmichael, F., 1926, Oxidation of sulphides: Toronto Univ. Geol. Studies, No. 22, p. 29.
12. Eliseev, L., and Nagirnyak, F., 1938, Oxidation of pyrite and interaction of reagents in flotation process: Tsvetnye Metally, v. 13, no. 10, p. 38–42.
13. Fox, R. W., 1830, On the electromagnetic properties of metalliferous veins in the mines of Cornwall: Philos. Trans., 1830, pt. 2, p. 399.
14. Gottschalk, V. H., and Buehler, H. A., 1912, Oxidation of sulfides: ECON. GEOL., v. 7, p. 15–34.
15. Grout, F. F., 1908, The oxidation of pyrite: ECON. GEOL., v. 3, p. 532–534.
16. ——, 1913, On the behavior of acid sulphate solution of copper, silver, and gold with alkaline extracts of metallic sulfides: ECON. GEOL., v. 8, p. 427.
17. Head, R. E., 1938, Mineralogical characteristics affecting the concentration of a semi-oxidized lead-silver ore: Am. Inst. Min. Met. Eng., Mining Tech., v. 2, no. 4, 9 p.
18. Kaku, I., 1952, On the electrical polarization of rocks by dipping in the solutions: Geophys. Exploration (Japan), v. 5, p. 201–205.
19. ——, 1954, On the electrical polarization of rocks by dipping in the solutions: Geophys. Exploration (Japan), v. 7, p. 25–29.
20. Kelley, K. K., 1937, Contributions to the data on theoretical metallurgy—VII. The thermodynamic properties of sulfur and its inorganic compounds: U. S. Bur. Mines Bull. 406.

21. Koch, S., and Grasselly, G., 1951, Processes occurring during the decomposition of sulfide ores: Acta Univ. Szegediensis, Acta Mineral. Petrolog., v. 5, p. 15–37.
22. ——, and Grasselly, G., 1952, Data on the oxidation of sulfide-ore deposits: Acta Univ. Szegediensis, Acta Mineral. Petrolog., v. 6, p. 23–30.
23. Leist, J. W., 1954, Comprehensive Inorganic Chemistry, v. II, Copper, Silver, and Gold: Book, Van Nostrand Co., New York, 248 p.
24. Latimer, W. M., 1952, The Oxidation States of the Elements and their Potentials in Aqueous Solution: Book, Prentice-Hall Inc., New York, 392 p.
25. Locke, A., 1926, Leached outcrops as guide to copper ores: Book, Williams and Wilkins Co., Baltimore, 175 p.
26. Matsubara, A., and Takubo, J., 1930, On the cathodic behavior of pyrite: Anniv. Vol. dedicated to Prof. M. Chikashige in celebration of his 60th birthday, p. 311–339, Kyoto, Japan; abs. Neues Jahrb., Ref. I (3), 1931.
27. Morse, H. W., and Locke, A., 1924, Recent progress with leached ore capping: Econ. Geol., v. 19, p. 249–258.
28. Nakabayashi, K., and Fujiwara, T., 1949, Generating mechanisms of spontaneous polarization—I. Classification of the generating mechanism: Tokyo Research Inst. Nat. Resources, Rept. 12, p. 16.
29. ——, 1950, Generating mechanisms of spontaneous polarization—II. Single electrode potential in ore: Tokyo Research Inst. Nat. Resources, Rept. 15, p. 6–16.
30. Nishihara, G. S., 1914, The rate of reduction of acidity of descending waters by certain ore and gangue minerals and its bearing upon secondary sulfide enrichment: Econ. Geol., v. 9, p. 749.
31. Noddack, W., and Wrabetz, K., 1955, On the electrochemical properties of some heavy-metal sulfides: Zeitschr. Elektrochemie, v. 59, p. 96–102.
32. ——, Wrabetz, K., and Herbst, W., 1955, The electrochemical potential series for sulfides: Zeitschr. Elektrochemie, v. 59, p. 752–755.
33. Plante, E. C., and Sutherland, K. C., 1948, Effects of oxidation of sulfide minerals on their flotation properties: Am. Inst. Min. Met. Eng., Tech Publ. 2297, Mining Tech., v. 12, no. 1.
34. Piontelli, R., 1949, Researches on the reactions between sulfides and electrolytic solutions—I. Galené: Bull. Soc. Chimique de France, Paris, Année 1949, Mises su Point, p. D197–203.
35. Ralston, O. C., et al., 1930, Reducing and oxidizing agents and lime consumption in flotation pulp: Am. Inst. Min. Met. Eng. Trans., v. 87, p. 369.
36. Rechenberg, H., 1951, Studies on the electrochemical potential-series of ore minerals: Neues Jahrbuch f. Mineralogie, p. 88–91.
37. Sato, M., 1960, Oxidation of sulfide ore bodies—I. Geochemical environments in terms of Eh and pH: Econ. Geol. (to be published).
38. Schwartz, G. M., 1934, Paragenesis of the oxidized ores of copper: Econ. Geol., v. 29, p. 55–75.
39. ——, 1938, Oxidized copper ores of the United Verde Extension Mine: Econ. Geol., v. 33, p. 21–33.
40. Silman, J. F. B., 1958, The stabilities of some oxidized copper minerals in aqueous solutions at 25° C and 1 atm total pressure: Ph.D. Thesis in geology, Harvard University, 98 p.
41. Skey, W., 1871, On the electromotive power of metallic sulfides: New Zealand Inst. Trans. and Proc., v. 3, p. 232–236.
42. Stenhouse, J. F., and Armstrong, W. M., 1952, The aqueous oxidation of pyrite: Canadian Min. Met. Bull., v. 45, no. 477, p. 49–53.
43. Stokes, H. N., 1901, On pyrite and marcasite: U. S. Geol. Survey Bull., 186, p. 44.
44. ——, 1907, Experiments on the action of various solutions on pyrite and marcasite: Econ. Geol., v. 2, p. 14–23.
45. Stull, D. R., and Sinke, G. C., 1956, Thermodynamic Properties of the Elements: Book, Advances in Chemistry Series, no. 18, Amer. Chem. Soc., Washington, D. C.
46. Sullivan, J. D., 1930, Chemistry of leaching chalcocite: U. S. Bur. Mines, Tech. Paper 473, 24 p.
47. ——, 1930, Chemistry of leaching covellite: U. S. Bur. Mines, Tech. Paper 487, 18 p.
48. ——, 1931, Chemistry of leaching bornite: U. S. Bur. Mines, Tech. Paper 486, 20 p.
49. ——, 1933, Chemical and physical features of copper leaching: Am. Inst. Min. Met. Eng. Trans., v. 106, Copper Metallurgy, p. 515–546.
50. Suzuki, Rensaku, 1941, The potential of some sulfide minerals in dilute solutions of strong electrolytes: Jour. Japan. Assoc. Mineral. Petrol. Econ. Geol., v. 26, p. 221–237.
51. Tammann, G., 1920, On the ion exchange at the surfaces of minerals: Zeitschr. anorg. allgem. Chemie, v. 113, p. 149–162.

52. Trümpler, G., 1921, Contribution on the electromotive relationships of metallic compounds with electronic conduction: Zeitschr. Phys. Chemie, v. 99, p. 9–56.
53. Vogt, J. H. L., 1901, Problems in the geology of ore deposits: Am. Inst. Min. Met. Eng. Trans., v. 31, p. 125–169.
54. ——, 1902, Problems in the geology of ore deposits: Am. Inst. Min. Met. Eng. Publ., "The Genesis of Ore Deposits" edited by F. Posepny, p. 636–680.
55. Wada, S., and Seki, Y., 1949, On the single electrode potentials of various sulfide minerals: Mitsubishi Mining Research Inst. (Japan), Bull. 1141.
56. Wagner, C., 1953, Investigations on silver sulfides: Jour. Chem. Phys., v. 21, p. 1819–1827.
57. Wang, Y. T., 1915, The formation of the oxidized ores of zinc from the sulfide: Am. Inst. Min. Met. Eng. Trans., p. 1001.
58. Wells, R. C., 1912, Mineral electrodes: Am. Electrochem. Soc. Trans., v. 22, p. 313–342.
59. ——, 1914, Electric activity in ore deposits: U. S. Geol. Survey Bull. 548, 78 p.
60. White, C. H., 1924, Prospecting for disseminated copper by a study of leached croppings: Eng. and Min. Jour., v. 117, p. 483–488.
61. Winchell, A. N., 1907, The oxidation of pyrite: Econ. Geol., v. 2, p. 290–294.
62. Wrabetz, K. E., 1956, On galvanic cells with sulfide electrodes: Zeitschr. Elektrochemie, v. 60, p. 722–731.
63. Zies, E. G., Allen, E. T., and Merwin, H. E., 1916, Some reactions involved in secondary copper sulfide enrichment: Econ. Geol., v. 11, p. 407–503.

Economic Geology
Vol. 55, 1960, pp. 1232–1243

A NEW GEOCHEMICAL METHOD FOR THE DETERMINATION OF MOLYBDENUM IN SOIL AND ROCK

J. KENT PERRY

ABSTRACT

A new geochemical method for the determination of molybdenum in soil and rock is given. Tungsten, chemically similar to molybdenum, does not react with the colorimetric reagent. The method can be used without modification for determining a much wider range of molybdenum than the commonly used thiocyanate method.

The method is based on carbonate-nitrate fusion of the sample and subsequent aqueous leaching, which remove elements that form insoluble hydroxides. A further separation of molybdenum from interfering elements is effected by solvent extraction with amyl acetate, followed by aqueous stripping. A colored complex molybdenum exanthate compound is formed by the addition of potassium ethyl xanthate, extracted into benzene, and compared with standards. Approximately 30 determinations can be made per man day. The test can be used in a field camp with the use of portable heat sources.

Radiochemical tracer techniques show that 45 percent of the molybdenum present in the sample aliquot is recovered as colored complex. This loss, however, is partially or wholly compensated for since standards are subjected to the same procedure. Standard deviation for the method was found to be ± 6.3 percent error.

The greatest error is caused by incomplete and inconsistent decomposition of silicate materials in the sample. This error appears to be of the same order of magniture for both the thiocyanate method and the new xanthate method presented in this paper.

INTRODUCTION

A NEW geochemical method for the determination of trace amounts of molybdenum in soil and rocks is given in the following procedure. It is suggested that the method be used in preference to the thiocyanate method (4, 9) under certain conditions. The colorimetric reagent used in the new method does not react with tungsten and so the method is ideal when the element is present. Furthermore, the method can be used without modification to determine as much as 800 parts per million of molybdenum, and larger amounts can easily be determined with slight modifications in the procedure.

The method is not as satisfactory as the thiocyanate method for amounts of molybdenum less than 5 parts per million. However, Rankama and Sahama (7) list the average molybdenum content of igneous rocks as 2.5 to 15 parts per million.[1] Molybdenum content of rocks in anomalous areas

[1] Later data give a maximum of 1 part for silic igneous rocks and 4.5 parts for shale—(Editor).

should be much higher, usually within the ideal range for this method. Samples from the Questa, New Mexico, property of the Molybdenum Corporation of America were obtained for comparison of the new method with the thiocyanate method. Many soil samples from this area actually contain in excess of 1,000 parts per million molybdenum.

The method involves carbonate-nitrate fusion of the sample followed by digestion and aqueous leaching. The fusion and leaching precipitate ferric iron which might interfere and other elements that form insoluble hydroxides. An aliquot of the aqueous leach solution is acidified and made 5 N with HCl. The molybdenum is extracted from the aqueous phase with amyl acetate and then stripped from the organic phase with demineralized water. A colored complex compound of molybdenum xanthate is then formed by the addition of potassium ethyl xanthate. The colored complex is extracted into benzene and the amount of molybdenum estimated by visual comparison with standards or by determining the percent transmittance of 510 millimicrons wavelength in a colorimeter.

The test can be used in the field by using a propane torch and gasoline stove as portable heat sources, and by visual comparison of the sample with standards. Of course, greater accuracy can be obtained in the laboratory by using a colorimeter-spectrophotometer for estimation of molybdenum content. Approximately 30 samples can be run per man day.

PROCEDURE

Reagents and Apparatus

Flux, a mixture of equal parts by weight of potassium carbonate and potassium nitrate, ground to pass an 80-mesh sieve of silk bolting cloth, mixed thoroughly, and passed through the sieve again.

Hydrochloric acid, concentrated. (CP grade) six pound bottle.

Hydrochloric acid, 1 : 20, allow 1 ml for each sample and standard.

Bromthymol blue, prepare enough saturated aqueous solution to fill a 30 to 60 ml dropper bottle.

Amyl acetate (Merck reagent 0968 satisfactory for this procedure), purchase in one or seven pound bottles, allowing 15 ml for each sample.

Standard molybdenum solution, 0.01 percent. Dissolve 75 milligrams of pure molybdic anhydride (MoO_3) in 1 N KOH, dilute with water, add 1 N hydrochloric acid until solution is just slightly acid, and dilute to 500 ml with water. This solution contains 100 micrograms of Mo per ml.

Standard molybdenum solution, 0.001 percent. Add 10 ml of the 0.01 percent solution to about 50 ml of water and dilute to 100 ml. Prepare daily at least one hour before use.

Mercaptoacetic acid (thioglycolic acid), Eastman Organic Chemical No. 2249, analytical grade. Prepare 40 percent aqueous solution and allow one drop per sample.

Potassium ethyl xanthate (Aero Xanthate 303, 4 ounce samples usually available from Mining Chemicals Dept., American Cyanamid Co., 30 Rockefeller Plaza, New York 20, N. Y. This grade, normally used as a flotation reagent, is entirely satisfactory for this procedure and shows no detectable molybdenum blank). Prepare a 2 percent aqueous solution daily by adding 2 grams to 98 ml of water.

Benzene, thiophene free, allow one to five ml for each sample and standard if color comparisons are to be made by eye, or 10 ml if a B & L Spectronic 20 colorimeter or comparable instrument is to be used.

Agate or mullite mortar and pestle, 75 mm outside diameter.
1 sieve, made of 80-mesh silk bolting cloth; *balance*, analytical.
1 camel's hair brush, 18 mm brush length; *1 small spatula*, stainless steel.
Pyrex culture tubes, 16 × 150 mm. One required for each determination.
20 Pyrex culture tubes, 18 × 150 ml, with polyethylene stoppers.
40 Pyrex culture tubes, 20 × 150 ml; *20 Pyrex culture tubes*, 13 × 100 ml.
40 Centrifuge tubes, to fit available centrifuge; *3 serological pipettes*, 1 ml, calibrated in tenths of a ml.
1 serological pipette, 5 ml, calibrated in tenths of a ml.
1 serological pipette, 10 ml, calibrated in tenths of a ml.
2 Wire test tube racks, capacity 40 test tubes each.
Sheet metal tray, 5″ × 8″ × 12″, for water-bath digestion of samples after fusion.
Cork stoppers, No. 5, for 16 × 150 mm culture tubes; *2 Pyrex volumetric flasks*, 100 ml, with stoppers.
2 Pyrex separatory funnels, 60 ml, Squibb, Pear shape, with T stopper and stopcock.
1 Graduated cylinder, 100 ml; *1 Graduated cylinder*, 25 ml.
Assorted Pyrex beakers, 50 ml (at least one dozen), 150 ml (1), 250 ml (1), and 600 ml (1).
1 Burette, 50 ml, calibrated in tenths of a ml, T stopcock, with burette stand.

Preparation of Standards

For Visual Estimation.—Pipette the appropriate amount of the molybdenum standard solution (Tables I and II) into 18 × 150 mm culture tubes, dilute to ten ml volume with demineralized water, add one ml 1:20 HCl, and one ml of 2 percent potassium ethyl xanthate solution. Add one ml of benzene to the low concentration standards and two ml benzene to the high concentra-

TABLE I

LOW CONCENTRATION STANDARDS

Ml of 0.001% Mo Solution	Micrograms Mo	Ml of 0.001% Mo Solution	Micrograms Mo
0.0	0	1.5	15
0.1	1	2.0	20
0.3	3	2.5	25
0.5	5	3.0	30
1.0	10		

TABLE II

HIGH CONCENTRATION STANDARDS

Ml of 0.01% Mo Solution	Micrograms Mo	Ml of 0.01% Mo Solution	Micrograms Mo
0.0	0	0.8	80
0.1	10	0.9	90
0.2	20	1.0	100
0.3	30	1.2	120
0.4	40	1.4	140
0.5	50	1.6	160
0.6	60	1.8	180
0.7	70	2.0	200

tion standards, stopper with polyethylene stoppers, shake vigorously for ten seconds, and let the phases separate. Check standards containing less than 30 micrograms molybdenum every few hours, since some fading may occur.

For Estimation with Spectrophotometer-Colorimeter.—Pipette the appropriate amount of the 0.01 percent molybdenum standard solution (Table II) into 18 × 150 mm culture tubes, dilute to 10 ml with demineralized water, and add one ml 1 : 20 HCl. Individually, add one ml of 2 percent potassium ethyl xanthate solution followed by 10 ml of benzene. Stopper with a polyethylene stopper, shake vigorously for 10 seconds, and allow the phases to separate. Transfer seven or eight ml of the benzene phase to a colorimeter cell and measure the percent transmittance at 510 millimicrons wavelength three minutes after addition of the potassium ethyl xanthate solution (enough time should be allowed for the escape of any air bubbles in the benzene, but the time should be kept constant to account for any fading of the low concentration standards).

If there is any doubt concerning the wavelength calibration of the instrument in use, a set of spectrophotometric curves should be made using standards containing zero, 20, 50, 100, and 200 micrograms of molybdenum (Fig. 1) by comparing the standard against pure benzene at each wavelength and plotting percent transmittance versus wavelength in millimicrons. Be certain to use a set of matched cells, or, if the more economical 13 × 100 mm Pyrex culture tubes are used, determine cell corrections for the tubes when filled with pure benzene. Maximum absorption for the molybdenum complex with potassium ethyl xanthate occurs in the range 505 to 515 millimicrons.

A standard calibration curve should be obtained by plotting percent transmittance at 510 millimicrons versus micrograms of molybdenum. A typical calibration curve is shown in Figure 2.

It will be helpful when determining the molybdenum content of samples to expand the scale of the calibration curve in two sections (as shown in Figure 3) to obtain a more useful slope.

Sample Solution Preparation.—Thoroughly mix 0.5 g of the finely ground sample with 3.0 g of the flux in the mortar. Transfer to a 16 × 150 mm culture tube and tap to dislodge any material adhering to the side of the tube. Heat the tube over a bunsen burner (propane torch or gasoline stove in the field) until fusion is complete and all of the sample has been attacked. About 4 or 5 minutes will be required and the tube will be filled with brown fumes formed by nitrate decomposition. Place the tubes in a test tube rack to cool after fusion is complete, or, if cracking of the tubes during cooling occurs due to contraction of cooled mass, a slower rate of cooling can be obtained by placing the tubes in a box filled with expanded perlite such as is used in plaster.

After cooling place any cracked tubes within a 20 × 150 mm culture tube. Pipette 10 ml demineralized water into each tube and place in a boiling water bath for one hour to digest the fused mass, or until the fused mass has been dissolved. Near the end of the digestion period place a corked Stevens Extraction Stick (4, p. 5) in the tube and continue boiling until air bubbles are escaping from the lower end of the stick. Remove from the water bath

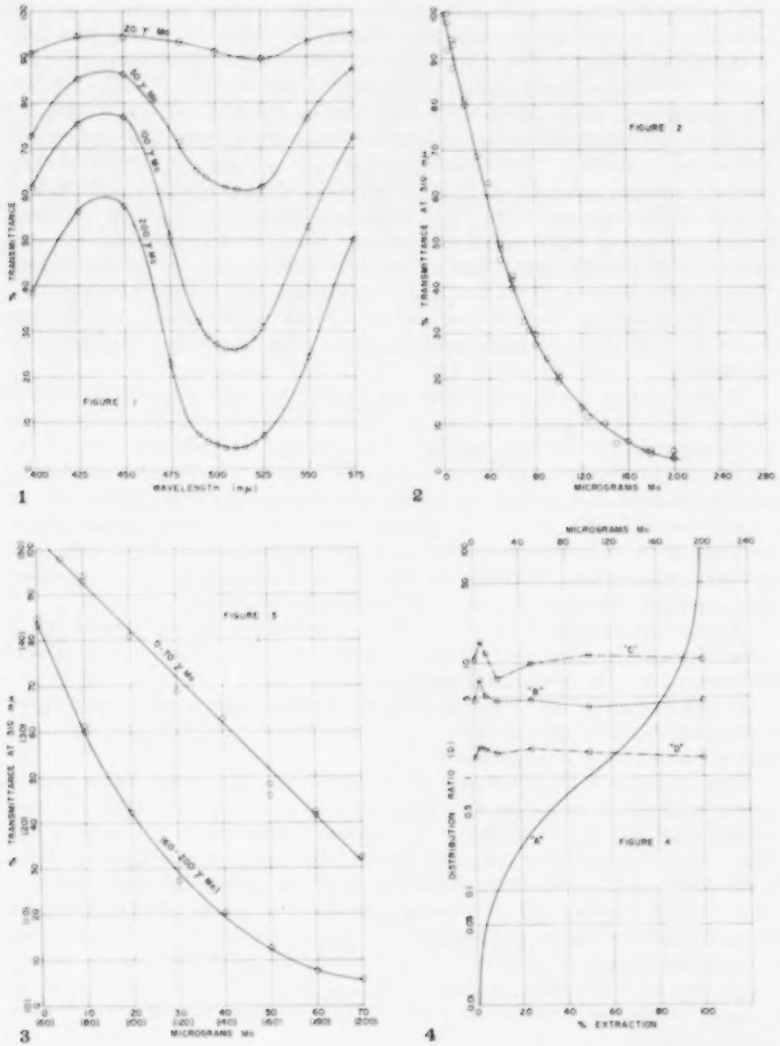

FIG. 1. Spectrophotometric curves showing percent transmittance of colored molybdenum xanthate complex compound in benzene, compared with pure benzene, at wavelengths from 400 to 575 millimicrons. Molybdenum concentrations of 20, 50, 100, and 200 microns. Determinations made with Bausch & Lomb "Spectronic 20" colorimeter-spectrophotometer.

and place in a test tube rack to cook, allowing a clear filtrate of the aqueous extraction to be drawn into the tube. Alternatively, if Stevens Extraction Sticks are not available, transfer the aqueous extraction to a centrifuge tube and centrifuge until a clear supernate is obtained. It is very important to obtain a clear filtrate or supernate by one of the above methods, since interfering elements such as iron and other elements which form insoluble hydroxides are removed by the carbonate fusion and subsequent aqueous leaching.

Transfer 5 ml of the clear filtrate or supernate to a 50 ml beaker, add one drop of bromthymol blue indicator solution, and add concentrated HCl, *dropwise*, until the solution is neutral or slightly acidic. Transfer to a centrifuge if any silica gel, which might later clog the separatory funnel stopcock, precipitates on the addition of HCl.

Solvent Extraction.—Transfer the slightly acidic sample aliquot to a 60 ml separatory funnel (either graduated or scribed at the 8.75, 10, 15, and 30 ml levels). Dilute with demineralized water to the 8.75 ml mark if necessary. Add concentrated HCl up to the 15 ml mark to make the solution 5 N with respect to HCl (Note: if the sample solution has a volume greater than 8.75 ml after neutralization a volume of concentrated HCl equal to 0.714 the volume of sample solution should be added to make the aqueous phase 5 N with HCl).

Add 15 ml amyl acetate to bring the volume to a total of 30 ml. Stopper and shake vigorously for 1 minute. The extracted species in a chloride system may be MoO_2Cl_2 according to Sandell (8, p. 641), or $MoO_3 \cdot 2HCl$ according to Nelidow and Diamond (6, p. 711). After the phases have separated, discard the lower (aqueous) phase and then add 10 ml demineralized water. Stopper and shake vigorously for 30 seconds to strip molybdenum from the organic phase. Allow the phases to separate.

Formation of Colored Xanthate Complex and Estimation of Mo Content

Transfer the final aqueous (lower) phase resulting from the above extraction to an 18 × 150 mm culture tube. Discard the organic (amyl acetate)

FIG. 2. Typical standard calibration curve showing percent transmittance at 510 millimicrons versus micrograms of molybdenum. Determinations made with Bausch & Lomb "Spectronic 20" colorimeter-spectrophotometer.

FIG. 3. Typical standard calibration curves similar to Figure 2, but expanded to facilitate determination of unknowns. Points plotted are thought to be the most reliable ones shown in Fig. 2. Numbers in parentheses correspond to the curve for range 60 to 200 micrograms molybdenum. Determinations made with Bausch & Lomb "Spectronic 20" colorimeter-spectrophotometer.

FIG. 4. Semi-logarithmic graph showing relationships of radiochemical data. Curve "A" shows mathematical relationship of distribution ratio to percent extraction. Curve "B" shows distribution ratios of various concentrations of molybdenum for extraction into amyl acetate from 5 N HCl. Similarly, curve "C" shows distribution ratios for stripping of molybdenum from amyl acetate with demineralized water, and curve "D" shows complexing of molybdenum with potassium ethyl xanthate and subsequent extraction into benzene.

phase and rinse the separatory funnel with a few milliliters of acetone. Add 1 ml of 1:20 HCl to the aqueous phase in the culture tube, followed by 1 ml of 2 percent potassium ethyl xanthate solution. According to Feigl (2, p. 116) the molybdenum and xanthate form a complex compound, $MoO_2 \cdot 2(SC(SH)(OC_2H_5))$, which is soluble in many organic liquids and may be to some extent the organic analog of $MoO_2 \cdot 2HCl$. In solution this complex ranges in color from faint pink at low concentrations to deep red-purple at high molybdenum concentrations.

Visual Estimation of Mo Content.—If the molybdenum content is to be determined by visual comparison with standards, note whether the amount of complex formed in aqueous solution is light pink or deep red-purple in color. If light pink, add 1 ml benzene from a burette, stopper with a polyethylene stopper, shake vigorously for 10 seconds, allow the phases to separate, and match the colored benzene (upper) phase of the unknown with one of the low concentration standards. If dark red-purple or some shade thereof, add 2 ml benzene from a burette, stopper, shake vigorously for 10 seconds, and match the unknown with one of the high concentration standards.

Estimation of Mo Content with Colorimeter-Spectrophotometer.—Add 10 ml benzene from a burette irregardless of the amount of complex formed, stopper with a polyethylene stopper, shake vigorously for 10 seconds, and allow the phases to separate. Pipette (use a Pumpett or similar instrument rather than mouth suction) 7 or 8 ml of the benzene (upper) phase into a matched colorimeter cell or Pyrex culture tube with previously determined cell correction. Determine the percent transmittance at 510 millimicrons wavelength in comparison with pure benzene and obtain the micrograms of molybdenum present in the aliquot from a calibration curve (such as Figure 2 or 3).

Both methods as here described are intended for sample aliquots containing up to 200 micrograms of molybdenum. Larger amounts can be determined by increasing the amount of benzene or decreasing the aliquot for visual estimation. For estimation of large amounts of Mo with the colorimeter-spectrophotometer, dilute the benzene phase with pure benzene until the percent transmittance falls on-scale and multiply the micrograms found by the dilution factor.

The parts per million of molybdenum in the original sample can be determined by use of Equation 1.

$$\frac{\text{Total volume of sample solution (aqueous leach)}}{\text{Weight of sample} \times \text{Volume of aliquot}} \times \text{micrograms of Mo found} = \text{ppm.}$$

DISCUSSION

Notes on Procedure.—A carbonate-nitrate sample fusion was found to be most effective in producing sample decomposition and formation of water soluble molybdenum compounds. A carbonate-peroxide fusion actually re-

covered slightly more of the molybdenum in the sample, but resulted in an intolerable amount of silica gel precipitation on acidification of the aqueous leach solution. Potassium salts are used rather than sodium since it was noted that excessive amounts of sodium appear to be carried through the solvent extraction and interfere to some extent with formation of the colored molybdenum xanthate complex (it is interesting to note that sodium ethyl xanthate is almost completely ineffective in producing a colored molybdenum complex as compared with the potassium salt used in this procedure). Amounts added by most granitic rock types do not appear to interfere. Various acids and acid mixtures were found to be ineffective in the decomposition of silicate samples and left extractable interfering elements in solution. Hydrofluoric acid decomposition of samples is unsatisfactory since fluoride complexes molybdenum.

It is very important that centrifuging of the aqueous leach solution or extraction with a Stevens Extractor remove all solid residues since the carbonate fusion is intended to remove iron and other hydroxide-forming elements by precipitation. Contamination by Iron III (which extracts into most organic liquids in chloride systems) results in a brown xanthate complex extractable into benzene, thus ruining the test. Mercaptoacetic acid (thioglycolic acid) will reduce ferric iron almost instantly to ferrous iron without reducing molybdenum (all other reducing agents tried also reduced molybdenum). If contamination of the sample aliquot by ferric hydroxide is suspected, add one drop of 40 percent mercaptoacetic acid to the acidified sample solution in the separatory funnel before making 5 N with HCl. If a blue color is formed, add another drop or two until it disappears. A red color may result from the reaction of mercaptoacetic acid with nitrate decomposition products formed during fusion. The ferrous iron produced either does not extract or does not form a colored complex with xanthates. Careful centrifuging is probably preferable to the use of mercaptoacetic acid, however.

Amyl acetate was selected as the organic liquid for the solvent extraction step in preference to ethyl ether because it has a higher boiling point (ether may actually boil when it comes in contact with the aqueous phase just previously made 5N with HCl and thus heated) and because it gives excellent extraction efficiency with one extraction. Although tributyl phosphate is an excellent extractant for molybdenum (8, p. 692) and is non-volatile, it was not chosen because both pure tributyl phosphate and tributyl phosphate-kerosene solutions formed emulsions with water. The separatory funnel at times had to be placed in a boiling water bath for 5 to 10 minutes to break these emulsions.

Benzene was selected for extraction of the final colored complex because it appears better than carbon tetrachloride, chloroform, and other solvents with respect to fading of the complex. Furthermore, since it floats on water it is in a more convenient position for comparison with standards or pipetting to colorimeter cells.

Interfering Elements.—One of the salient features of this method is that tungsten, chemically similar to molybdenum, either does not react with potassium ethyl xanthate under the conditions of the test (most probable),

or forms a colorless complex which does not interfere. This is true even of the addition of solutions containing high concentrations of tungsten to potassium ethyl xanthate and hydrochloric acid.

As noted before, ferric iron forms a benzene extractable brown xanthate complex that interferes. However, ferric iron (and other hydroxide-forming elements) is removed by the carbonate fusion and aqueous leaching followed by centrifuging or filtering with a Stevens Extractor. Alternatively, mercaptoacetic acid can be added to reduce ferric iron to non-interfering ferrous iron. Mercaptoacetic acid can also be used to reduce vanadium.

Other elements that form xanthate complexes and extract into benzene, thus interfering, are: copper (yellow), mercury (white), and tin (yellow). Zinc produces a white complex that is insoluble in the benzene layer and does not interfere; uranium produces a yellow complex (similar to copper) that becomes colorless when extracted into the benzene layer and thus does not interfere; and silver produces AgCl which becomes yellow on addition of the xanthate and collects at the interface between the aqueous and organic phases.

Nitrites, fluorides, $SnCl_2$ and EDTA interfere with the test because of complexing or reduction of molybdenum. As noted before, large excesses of sodium reduce the sensitivity of the test. The effects of other elements and compounds have not been investigated.

Comparison with Thiocyanate Method.—A number of soil samples from geochemical traverses were obtained for comparison purposes from the Questa, New Mexico, property of the Molybdenum Corporation of America. These samples had previously been tested for molybdenum using a modification of the commonly-used thiocyanate geochemical method for molybdenum. Results obtained by both visual comparison with standards and with the colorimeter using the new xanthate method are compared in the following table with results obtained using the thiocyanate method.

It will be noted that a number of samples show considerable variance between methods. Unfortunately, the standard error inherent in the modified thiocyanate method originally used on the samples is not known to the author. The standard error (68 percent confidence limits) was calculated for the standard samples used to plot Figure 2, on the basis of percentage error of each standard value in relation to the best-fitting curve. The standard deviation was found to be 6.3 (i.e., results would be within $\pm$ 6.3 percent, 68 percent of the time or within $\pm$ 12.6 percent, 95 percent of the time).

The greatest source of error in both methods is probably poor or inconsistent decomposition of samples, with failure to obtain all of the molybdenum in water-soluble form. This situation is particularly true of silicate samples, and probably accounts for variation between results by visual comparison with standards and colorimetric results using the xanthate method where both types of estimate were made on a single sample. Such results were obtained using separate fusions of the same sample material.

Radiochemistry.—Radiochemical tracer techniques were used to determine optimum test conditions and extraction efficiencies involved in each step of the procedure. The tests were carried out in the Isotope Laboratories of

TABLE III

COMPARISON OF XANTHATE AND THIOCYANATE METHODS

Sample no.	P.p.m. Mo by xanthate method (colorimeter)	P.p.m. Mo by xanthate method (visual comparison)	P.p.m. Mo by thiocyanate method
H10	—	0	0
H13	—	10	10
H14	—	520	500+
H15	—	8	20
H27	—	4	5
H29	—	480	500+
H30	264	280	300+
F7	—	20	5
F8	—	16	7
F10	—	4	5
F11	—	8	10
F12	—	8	10
F13	—	12	15
F14	—	32	40
A1	—	24	30
A2	—	20	20
A4	—	6	10
A5	—	8	8
A8	—	8	10
A10	—	16	15
DSu 1 P	—	26	30
DSu 2 P	—	10	20
DSu 2 S	—	16	20
DSu 10 S	56	—	35
DSu 19 P	44	40	40
DSu 37 P	28	—	50
DAp 1 P	56	—	30
DAp 2 P	60	—	10
DAp 6 P	48	—	20
DAp 7 P	32	—	40
DAp 8 P	48	—	30
DAp 20 P	68	80	90
DAp 20 S	40	—	60
DAp 36 P	1160	1100	1,000+
CiS 1	156	—	200
CiS 3	40	—	60
CiS 4	476	380	400
CiS 9	—	400	500
CiS 13	32	80	80
CiS 14	64	—	40
CiS 15	184	160	200

Note: (—) signifies no determination made).

the Colorado School of Mines Research Foundation by "tagging" molybdenum standard solution with 67-hour Mo^{99} purchased from Oak Ridge National Laboratory. Solutions were counted in a well-type integral scintillation counting system with a discriminator setting selected to eliminate gamma interference from the 6.04 hour Tc^{99m} daughter product and sensitive only to the higher energy gammas from the Mo^{99} (0.780 Mev maximum). Interference from the 2.12×10^5 year Tc^{99} (a pure beta emitter) was no problem since the system used was sensitive to gamma radiation only. All samples were counted to a statistical error of less than one percent and corrected for background.

Optimum extraction conditions and distribution ratios of the final procedure were determined by counting the phases obtained and using Equation 2.

$$D \text{ (distribution ratio)} = \frac{\text{Total concentration in extracting phase } (p_2)}{\text{Total concentration in extracted phase } (p_1)}$$

$$= \frac{\text{Counts per minute of extracting phase } (p_2)}{\text{Counts per minute of extracted phase } (p_1)}$$

It can be seen that the use of a radioisotope tracer technique provides an easy method of determining the distribution ratio between phases in a solvent extraction step, since the counts per minute due to radioactivity of the radioisotope of an element should be directly proportional to the total concentration of that element in a particular phase (the effects of isotopic fractionation are assumed to be negligible for the purposes of this work).

The percent extraction, of more practical interest, can be calculated from the distribution ratio by Equation 3.

$$\%E = \frac{100\,D}{D + (V_1/V_2)}$$

where V_1 and V_2 represent the volumes of the extracted and extracting phases, respectively. The optimum test conditions for the xanthate method were determined using tracer technique as a rapid check on whether or not a particular change in conditions was an improvement.

After optimum test conditions had been determined, distribution ratios for various concentrations of molybdenum were determined for each step of the procedure (Fig. 4). The average extraction percentage for extraction of molybdenum into the amyl acetate phase from the 5 N HCl aqueous phase was 82.79 percent, and for the stripping of molybdenum into a demineralized water phase from the amyl acetate phase 87.99 percent. The step involving complexing with potassium ethyl xanthate and extraction of the colored complex into benzene had an average extraction of 62.12 percent.

The combined percent extraction of the entire amyl acetate extraction is 72.85 percent. This value was checked using the colorimeter with a resultant average value of 73.0 percent, in excellent agreement. The extraction of the final complexing and extraction stage could not be checked with the colorimeter since it was calibrated with standard samples that involved the same error.

Thus, 45.25 percent of the molybdenum present in the aqueous aliquot prior to the amyl acetate extraction is recovered as the colored xanthate complex. The loss in the last stage is inherently eliminated because of comparison (either visual or with colorimeter) with standards involving the same loss. The loss in the amyl acetate extraction could be eliminated by running the standards through the extraction, or more easily by simply placing the factor 0.7285 in the denominator of Equation 1.

However, such corrections are not actually necessary since relative values are satisfactory for geochemical contour maps, and the more serious loss

involved in sample decomposition cannot be consistently evaluated. Actual assays for molybdenum show that the values obtained with the original thiocyanate geochemical method represent only about one-eighth of the total amount of molybdenum present in the samples (1).

SUMMARY

A new geochemical method for the determination of molybdenum is presented. This method can be used as an alternative to the commonly-used thiocyanate method. The method can be used for a wider range of molybdenum content without modification. The method is less suitable than the thiocyanate method for low concentrations of molybdenum, particularly less than five parts per million. The xanthate method should find its greatest application in delineating ore bodies and "target areas" responsible for distinctly anomalous molybdenum content in associated soils and rocks, rather than in broad regional exploration where the somewhat greater sensitivity of the thiocyanate method would be more desirable.

COLORADO SCHOOL OF MINES RESEARCH FOUNDATION, INC.
GOLDEN, COLORADO
February 25, 1960

REFERENCES

1. Carpenter, R. H., 1960, personal communication.
2. Feigl, F., 1958, Spot tests in inorganic analysis: Elsevier Publishing Co., N. Y., 600 p.
3. Friedlander, G., and Kennedy, J. W., 1955, Nuclear and radiochemistry: John Wiley and Sons, Inc., N. Y., 468 p.
4. Lakin, H. W., Almond, Hy, and Ward, F. N., 1952, Compilation of field methods used in geochemical prospecting by the U. S. Geological Survey: Geol. Survey Circ. 161.
5. Morrison, G. H., and Freiser, H., 1957, Solvent extraction in analytical chemistry: John Wiley and Sons, Inc., N. Y., 269 p.
6. Nelidow, I., and Diamond, R. M., 1955, Solvent extraction of molybdenum (VI): Jour. Phys. Chem., v. 59, p. 710–718.
7. Rankama and Sahama, 1950, Geochemistry: Univ. Chicago Press, Chicago, Ill.
8. Sandell, E. B., 1959, Colorimetric determination of traces of metals: Interscience Publishers, Inc., N. Y., 1032 p.
9. Ward, F. N., 1951, Determination of molybdenum in soils and rocks: Anal. Chemistry, v. 23, p. 788-791.

Economic Geology
Vol. 55, 1960, pp. 1244–1271

INTRUSION AND ORE DEPOSITION IN NEW MEXICO

CHARLES BANKS BELT, JR.

CONTENTS

	PAGE
Abstract	1244
Purpose of study	1245
Theoretical background	1245
Sampling and analytical procedure	1246
Collection and preparation of samples	1246
Experimental errors	1247
Modal analysis	1247
Chemical analysis	1247
Hanover, New Mexico	1247
Structure and petrology	1249
Alteration	1251
Geologic history of intrusion, alteration and ore deposition	1251
Results of chemical analysis	1252
Copper and zinc background	1252
Copper distribution	1252
Zinc Distribution	1254
Genetic concepts	1256
Magdalena, New Mexico	1258
Structure and petrology	1259
Alteration	1260
Chemical analyses	1260
Copper distribution	1260
Zinc distribution	1261
Conclusions from chemical analyses	1262
The Lordsburg, New Mexico mining district	1263
The Lordsburg intrusive and its outliers	1263
General description	1263
Location and petrology of outliers	1263
Alteration	1264
Chemical analyses	1265
Inter-district comparisons	1268
Conclusions	1269
Acknowledgments	1270
References cited	1270

ABSTRACT

In the early part of the twentieth century several investigators proposed that hydrothermal ore deposits are precipitated from solutions or fluids that had been separated from deep-seated magmas. The purpose of this paper is to test this concept, studying the primary petrology, hydrothermal alteration, and distribution of copper and zinc in silicic igneous plutons

genetically related (in the Niggli sense) to nearby hydrothermal ore deposits. Silicic Tertiary plutons were chosen in three New Mexico mining districts, the Hanover-Fierro intrusive at Hanover and Fierro, the Granite Mountain pluton at Magdalena, and four outliers of the Lordsburg intrusive at Lordsburg. The detailed petrographic and alteration study of each sample taken was accompanied by an analysis for copper and zinc through a newly developed, sensitive, and accurate dithizone technique.

The metal ion distribution of a given metal in an igneous country rock in an area of few veins bearing metals is apt to be related to primary igneous texture, composition and other features, but is not related to alteration. The average weight percent of alteration in this instance is low and the amount of metal introduced into the rock from the veins is small. Conversely, the metal ion distribution in an igenous country rock that is cut by numerous veins bearing metals is statistically far more clearly related to alteration than to primary igneous features. The average weight per cent of alteration and amount of metal introduced into this area is apt to be large. The same series of relations applies as well on a small scale, for as a single vein is approached from a distance in an igneous country rock, the content of alteration minerals and ore metals increases; both alteration and ore metals are more closely related to each other.

The results of the study raised the question whether the ore deposits of the three districts studied actually originated from the adjacent intrusives.

PURPOSE OF STUDY

Theoretical Background

In 1925 Niggli (13) formulated a physico-chemical explanation for the origin of hydrothermal ore deposits from a concept that had appeared earlier in the literature in the writings of Von Groddeck, Stelzner, Beck, de Launay, Kemp, and Lindgren. Niggli proposed that pressure at depth could force volatiles from deep-seated magmas. The volatiles would in turn form pegmatites and then ore deposits as the fluids cooled. This is one view of a general theory of ore genesis that gained ascendancy for years among such prominent geologists as Fenner (5) and Emmons (4). This general hydrothermal hypothesis suggests that ore deposits were precipitated from solutions or fluids that had escaped or been separated from a deep-seated magma by means of liquid immiscibility or crystallization or gas transfer. This idea is based on the presence of igneous rocks close in space and age to hydrothermal ore deposits in many mining districts of the world.

As is well known, there are many ore deposits apparently of hydrothermal origin that are neither spatially nor chronologically related to igneous rocks. In still other localities where there no hydrothermal ore deposits, igneous rocks occur that are similar in composition to those in mining districts. In view of these facts, the applicability of the Niggli theory to all hydrothermal ore deposits may well be questioned.

The chief purpose of this paper is to test the Niggli theory by studying the primary petrology, hydrothermal alteration, and distribution of copper and zinc in silicic igneous plutons supposedly related (in the Niggli sense) to nearby hydrothermal ore deposits. Silicic Tertiary plutons in three New

Mexico mining districts were chosen, the Hanover-Fierro intrusive at Hanover and Fierro, the Granite Mountain pluton at Magdalena, and the four outliers of the Lordsburg stock at Lordsburg.

First, it had to be established whether the observed plutons were or were not the source of the adjacent ore deposits. This was done by studying the relation between the copper or zinc distribution and the primary or secondary features in the plutons studied, and the time relations between intrusion and ore deposition. Primary igneous features are those formed prior to the complete solidification of the rocks—the minerals, texture, shape and character of the pluton. Secondary features include all changes that took place in a pluton after solidification. They are identified by their cross-cutting nature or as replacing primary minerals.

Secondly, if it is proved that the ore ions did not originate from the parts of the pluton now visible as immediately adjacent to the ore deposits, then in order to prove the Niggli hypothesis it must be established that the ore ions were separated from deeper parts of the intrusive. Some idea as to whether the copper or zinc ions originated from a related magma at depth may be gained from a comparison between the primary (that is, pre-alteration) zinc and copper abundances found in ore localizing intrusives studied and the average abundances for copper and zinc in silicic igneous rocks most recently given in the literature.

Finally, the relation between ore deposition and hydrothermal alteration was studied on a regional as well as on a local scale.

SAMPLING AND ANALYTICAL PROCEDURES

Collection and Preparation of Samples

The validity of conclusions drawn from this geochemical and petrologic study depends in part on the accuracy of sampling methods, the accuracy of petrographic study, and the analytical errors of copper and zinc. Thus the method of procedure and analytical errors will be briefly stated here. A detailed description of the analytical technique may be found in Barnes' Ph.D. Thesis (2).

Each pluton was sampled on a rough grid network. At Hanover, the samples were 1,000 feet apart, at Magdalena 500 feet apart, and at Lordsburg they average 100 feet apart. Samples from all plutons studied were of fresh rock least affected by alteration and oxidation. Close grid sampling with samples a few hundred feet apart could not be done at Hanover and Magdalena because exposures were poor, and large areas of intensely weathered and altered rock occurred in these two districts. The difficulty in obtaining unweathered samples in the districts studied was a major problem.

Large five pound blocks were taken from outcrops and broken with a sledge hammer. The core of each block was placed in an unwaxed Dixie cup and covered with a lid to exclude dust. Each sample weighed about a pound. The mineralogy, texture, and mode (in weight percent) of each sample were determined by thin section study. Modes were determined with a Chayes point counter. A minimum of 480 mm^2 was covered on a 40×24 mm thin

section and an average of 1,700 points was counted. Classification of the samples follows the system of Wahlstrom (20).

Experimental Errors

Modal Analysis.—The counting error of modal analysis for each mode was estimated by the calculation of σn, the error of the mean based on n observations (3, pp. 38–40; 15, pp. 373–374). This is an adaptation of the standard error of sampling distribution. Table 1 shows the estimated counting errors involved in the mode of a typical sample from the Hanover-Fierro intrusive, to give the reader an idea of the errors involved in modal analysis.

TABLE 1

A Mode of a Tonalite from the Hanover-Fierro Intrusive—with σ_n as an Estimate of the Counting Error

Mineral	Hornblende	Orthoclase	Plagioclase	Quartz	Magnetite	Sphene	Apatite
% by weight	13.1	13.3	59.4	11.5	2.5	0.1	0.1
σ_n	±0.8	±0.8	±1.2	±0.8	±0.4	±0.08	±0.08

Chemical Analysis.—Table 2 gives the analytical errors of copper and zinc. They were determined by multiple analysis of samples of many different copper and zinc concentrations.

TABLE 2

Errors of Copper and Zinc

Copper conc. range	V	s	Zinc conc. range	V	s
0– 4 ppm		±2 ppm	0– 40 ppm		±3 ppm
4– 35 ppm	±46%		40– 100 ppm	±8.0%	
35–100 ppm	±25%		100– 200 ppm	±9.0%	
> 100 ppm	±10%		200– 500 ppm	±10.0%	
			500–1,250 ppm	±25.0%*	

V is the relative error in percent. s is the standard deviation of the mean.
* Extrapolated from preceding data.

HANOVER, NEW MEXICO

The Hanover-Fierro intrusive is in the east-central part of Grant County, New Mexico, a few miles northwest of Santa Rita. The mining town of Hanover is at the southern end and the town of Fierro is at the northern end of the intrusive. The only folds in the region around the pluton are the result of forcible injection of igneous rocks. Faulting is mostly normal. The displacement in some faults is largely horizontal.

The ore deposits structurally associated with the Hanover-Fierro intrusive may be divided into two main types, magnetite replacement deposits, and replacement deposits of zinc with minor amounts of copper.

The magnetite deposits occur on the east and west margins of the northern end of the intrusive (Fig. 1). The magnetite is commonly mixed with

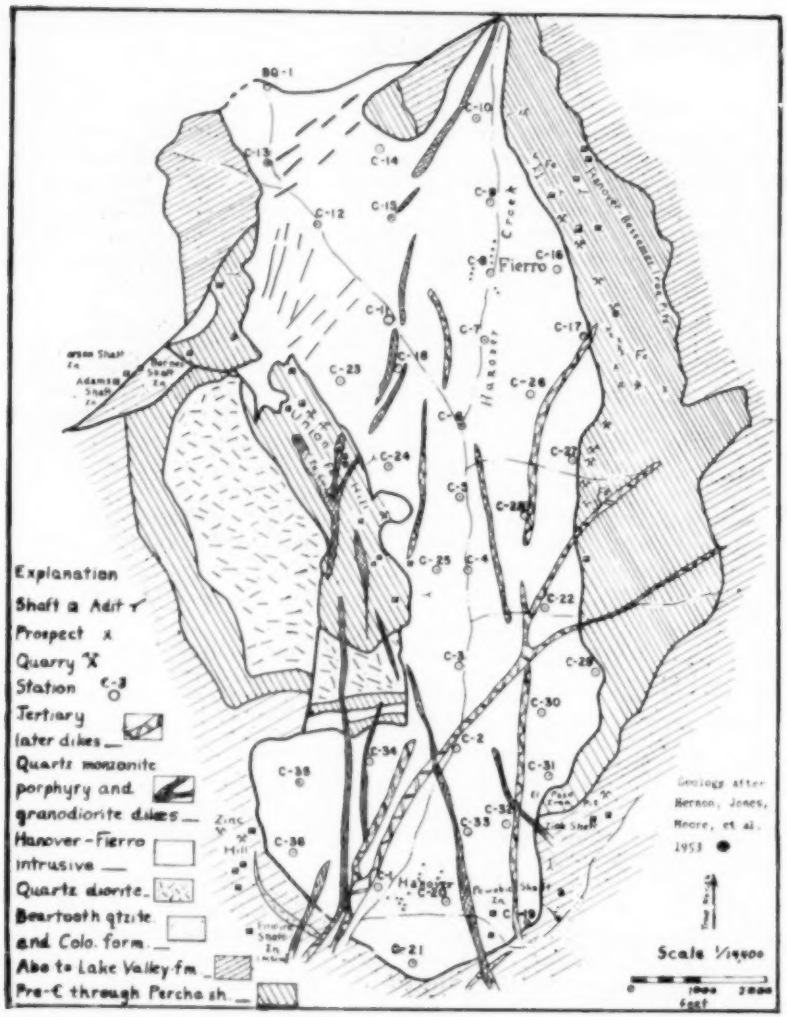

FIG. 1. Base map of the Hanover-Fierro intrusive.

serpentine, both minerals having replaced the Lower Paleozoic dolomites. Malachite staining in some areas and sphalerite in others suggests that copper and zinc minerals as well as magnetite have replaced the dolomite.

Deposits of nearly pure sphalerite replace the Hanover limestone around and underneath the southern lobe of the intrusive and on the northwestern

end of the intrusive where they are structurally associated with the Barringer Fault Zone.

The igneous history of the area around the Hanover-Fierro intrusive is very complicated, involving eight different types of intrusive rocks (6, p. 122; 10, pp. 26–38).

Structure and Petrology

The Hanover-Fierro intrusive is about 2¾ miles long and a mile wide at its widest part. Its long axis trends north. Forcible intrusion is shown by steeply upturned sedimentary rocks surround the pluton (Fig. 1).

The southern lobe of the intrusive is structurally the most complicated part of the pluton. Here tonalite pushed into the Paleozoic section, formed a laccolith, and, thrusting aside its borders, threw the surrounding sediments into a series of overturned folds (18, p. 786).

Generally speaking, the beds that lie near the contact of the northern part of the pluton are vertical or even overturned and suggest a stocklike structure.

On the northern end of the pluton the Barringer fault has caused the contact to be drawn out into an apophysis-like form, resulting in the isolation of a re-entrant of sediments in that area (Fig. 1). Movement on this fault postdating the intrusion allowed extensive silicification, the development of quartz veins and propylitic alteration in the vicinity.

Stratigraphic evidence indicates that intrusion of this pluton occurred at a depth that did not exceed 8,500 feet (18, p. 815).

The texture of the Hanover-Fierro intrusive varies from equigranular to porphyritic. Three different facies can be distinguished on the basis of textural evidence and field relations—an equigranular facies, a porphyry facies, and an aplitic facies. The percentage of groundmass in the intrusive obtained by modal analysis is shown by isopleths of groundmass percenta (Fig. 2). The area inside the zero isopleth, or zero contour, is the equigranular facies. The area outside the zero isopleth is the porphyry facies.

The equigranular facies is a medium-grained tonalite composed predominantly of prominently twinned and zoned hypidiomorphic andesine with green idiomorphic hornblende and pseudo-hexagonal books of biotite. Late crystallizing quartz and orthoclase have chinked in between the plagioclase and ferromagnesian minerals. Accessory minerals include magnetite, sphene, apatite and zircon. The equigranular facies occurs almost entirely in the southern lobe and spreads northward along the east and west intrusive contacts. A small patch is found near the contact on the east side (Fig. 2) of the northern end of the intrusive.

The porphyry facies ranges in composition from a fine-grained tonalite to a calci-alkalic granite. The minerals of this facies are similar to those of the equigranular facies in shape and optical properties. Phenocrysts of andesine and hornblende with less abundant phenocrysts of corroded quartz and books of biotite occur in a fine grained to dense groundmass of orthoclase and quartz with minor amounts of plagioclase. The accessory minerals of the porphyry facies are the same as those of the equigranular facies. The porphyry facies covers most of the intrusive.

The aplitic facies (not mapped) is composed predominantly of orthoclase and quartz and occurs as dikes cutting the other facies and forming chilled contacts.

Zircon studies and structural evidence indicate that the equigranular facies and the porphyry facies originated from the same magma, and that only a short space of time elapsed between their emplacement. But it is not known which facies was intruded first.

FIG. 2. Hanover groundmass contours.
FIG. 3. Hanover orthoclase/plagioclase map.

The Hanover-Fierro intrusive varies in composition from a tonalite to a calci-alkalic granite. Figure 3 is a map of the ratio of weight percent of orthoclase to the weight percent of plagioclase obtained from modal analysis. According to the Wahlstrom (20, pp. 268–350) classification the following rocks have the indicated range of orthoclase:plagioclase ratios and more than 5 percent quartz by weight: tonalite <0.6, granodiorite 0.6 to 1.0, quartz monzonite 1.0 to 1.67, and calci-alkalic granite 1.67 to 7. The greatest variation in composition occurs in the porphyry facies, as a result of the change in amount of orthoclase and quartz groundmass with respect to the plagioclase phenocrysts.

Alteration

Five types of alteration (in decreasing order of abundance) were observed in the Hanover-Fierro intrusive: chloritization, pyroxenization, epidotiziation, sericitization, and biotitization. The first three types are hydrothermal products. Because they were formed after the Hanover-Fierro intrusive solidified, sericite may be partly supergene and biotite is probably deuteric. Neither type is common enough to be dealt with here. Sericite commonly replaces plagioclase in the vicinity of veins and biotite replaces hornblende in scattered areas throughout the intrusive.

Chlorite, as observed in thin section, occurs as green pleochroic masses, fibers, or plates, and commonly replaces hornblende and biotite.

The pyroxene observed in the Hanover-Fierro intrusive occurs as light greenish gray masses replacing hornblende and forming pseudomorphs and veins. It has a $2V = 54 \pm 5°$, $Z \wedge C$ of 42°, a γ-α of 0.024, and a γ index of 1.693 ± 0.005. The pyroxene is a pseudomorph because it is rather irregular and granular; it does not show the uniform extinction of a single crystal; it has a diamond shaped outline customarily associated with hornblende; and the center of the crystal is hornblende, thus indicating replacement from the outside inward by pyroxene. The only pyroxene reported by Schmitt (18, pp. 795–807) and Allen and Fahey (1) to occur in the skarn zone of the Hanover-Fierro intrusive is a managanese-rich variety. All areas of pyroxenization within the intrusive occur near the contact. Therefore the pyroxene found in the Hanover-Fierro intrusive is probably rich in manganese and was formed as a result of pyrometasomatic alteration of the intrusive near its contact.

Epidote occurs only with pyroxene and replaces plagioclase or forms veins.

The distribution, amount, and principal types of alterations are shown in Figure 4, a map of the weight percent and types of alteration minerals observed in thin section, combined with a field map of hydrothermal alteration, oxidation and veins. The contours represent isopleths of the total weight percent of chlorite, pyroxene, and epidote as determined from the modal analysis of thin sections. All the areas that are high in weight percent of alteration minerals occur near the igneous contact where the ore deposits are localized. Areas of oxidation reflect local areas of mineralization within the intrusive itself. The large area of limonite stain and quartz veins in the northwest end of the intrusive is the result of mineralization along the Barringer fault zone.

Geologic History of Intrusion, Alteration, and Ore Deposition

After the presently exposed part of the Hanover-Fierro intrusive was emplaced, it cooled, was fractured, and intruded by aplites. Later, granodiorite dikes intruded the pluton and developed 3 to 5 feet of chilled contacts (8), indicating that the Hanover-Fierro intrusive as presently exposed had reached a temperature close to the geothermal temperature of the country rocks. The emplacement of the dikes was followed in general by the emplacement of (1) epidote and andradite (2) salite (3) chlorite, and either during or shortly after the emplacement of chlorite, the copper and zinc sulfide ores (8) and (18, pp. 791, 804, Fig. 4). Thus by the time the copper

and zinc ores were emplaced, the Hanover-Fierro intrusive as now exposed had completely solidified and cooled. By this time the entire pluton had cooled down considerably and had probably solidified completely.

Results of Chemical Analyses

Copper and Zinc Background.—After careful scrutiny of all the samples from the Hanover-Fierro intrusive, Samples C-1 and C-27, both tonalites, were observed to be the only entirely unaltered, unmineralized, and unoxidized samples taken. They were analyzed for copper and zinc. Since these samples were fresh, there has been no change in copper and zinc content resulting from the post-solidification processes; hydrothermal alteration, or ore deposition. Ore deposition occurring without alteration has not been observed or reported at Hanover or in any other mining district of unquestioned hydrothermal origin so far as the author knows. Hence, the average of copper and zinc from these samples is an approximation of the primary metal content of the intrusive and may be considered as "background." Thus the Hanover-Fierro intrusive has a primary copper concentration that is close to 51 ± 13 ppm and a primary zinc concentration that is close to 43 ± 5 ppm. This agrees very well with the average of 45 ppm zinc for all the samples from the pluton.

Samples having a content of copper or zinc higher than background would probably owe their high metal content to deposition by hydrothermal solutions. Lower than background values are considered to show a loss of metal as a result of weathering or hydrothermal leaching.

Copper Distribution.—All samples having copper concentrations that lie between 38 and 64 ppm are considered as primary background. Fig. 5 shows the copper distribution in the Hanover-Fierro intrusive. The location and copper concentration of each sample is indicated and contours are drawn through points of equal copper concentration.

It is important to determine whether the distribution of copper and zinc is related to primary igneous features or to secondary phenomena occurring after the solidification of the exposed part of the pluton. A primary copper and zinc distribution related to primary igneous features (such as the orthoclase:plagioclase ratio, the shape of the intrusive, or perhaps the weight percent of groundmass) may indicate that the zinc ore deposits of the Hanover district originated as emanations from the Hanover-Fierro intrusive. On the other hand, if the copper and zinc distributions are related mainly to post-solidification features such as the total weight percent of alteration minerals or to veins, or to known areas of secondary mineralization, this would indicate that the ore ions did not emanate from the adjacent intrusive to form ore deposits, but instead were introduced into the intrusive from elsewhere.

The correlation and degree of relationship between either the copper or the zinc distribution and primary or secondary features of the Hanover-Fierro intrusive and the other plutons studied is primarily determined by similarities in contour shape and in location of highs and lows observed by comparison of two respective maps. The correlation coefficient, r (19), which measures

the strength of linear correlation, was used as an aid in interpreting the relations tested by map comparison. Arithmetic plots show that as the relation between any two values becomes more linear the absolute value of r approaches 1. The significance of r is directly related to the number of degrees of freedom of r (d.f. = number of samples -2). As the degrees of freedom decrease, r has to have a higher absolute value in order to be significant. The significance of r was determined by Snedecor's table (19,

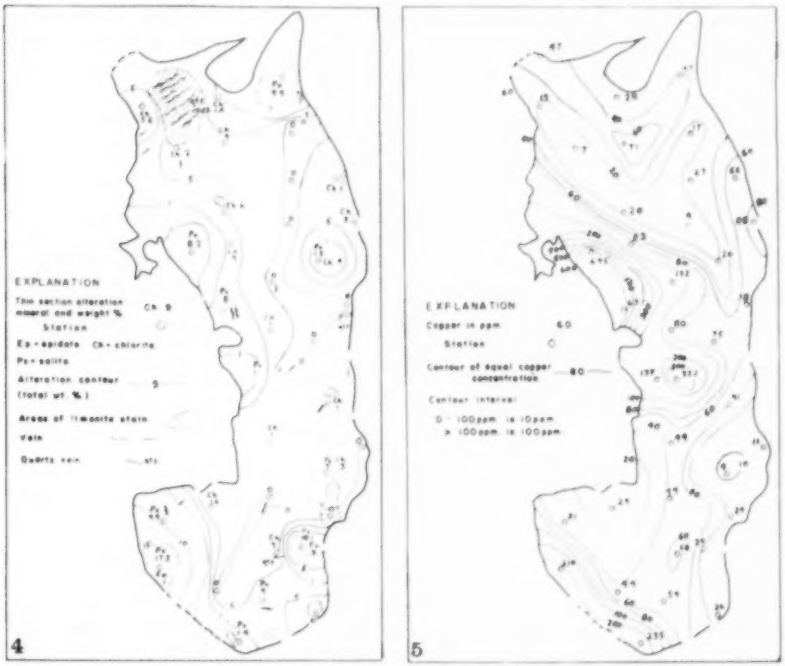

FIG. 4. Hanover alteration map.
FIG. 5. Hanover copper distribution.

p. 174, Table 7: 6.1). If the absolute value of r is less than the value of r given for the 5 percent level of significance in Snedecor's table, then r is not considered significant. A plus correlation coefficient indicates a direct correlation, a minus coefficient of correlation (Fig. 5) indicates an inverse relation.

The copper distribution in the Hanover-Fierro intrusive is not related significantly either to the weight percent groundmass minerals or to the orthoclase:plagioclase ratio. This is shown by map comparison and insignificant coefficients of correlation (Table 3) (Figs. 2, 3, and 5). The copper distribution is probably not related to alteration either. Though the distribu-

tion maps (Figs. 4, 5) are similar in shape, respective lows and highs do not coincide and the coefficient of correlation is not significant (Table 3).

Comparison of Figure 1 with Figure 5 reveals that four of the six copper anomalies occur close to copper mineralization of the intrusive contact. All anomalies are generally associated with intense alteration and limonite staining observed in the field. Since the copper distribution is not related to primary features within the intrusive and since copper was probably deposited after the complete cooling of the presently exposed part of the pluton, it is concluded that the observed copper anomalies probably are the result of the introduction of copper from the intrusive contact inward. Copper distribution is not related

TABLE 3

COEFFICIENTS OF CORRELATION FOR METAL CONTENT VERSUS PETROLOGY AND THEIR SIGNIFICANCE, THE HANOVER-FIERRO INTRUSIVE

x	y	r	n	Significnace
$[Cu^{++}]$	groundmass	+0.0528	36	Not significant
$[Cu^{++}]$	$\frac{\text{orthoclase}}{\text{plagioclase}}$	+0.040	36	Not significant
$[Cu^{++}]$	alteration	+0.0832	36	Not significant
$[Zn^{++}]$	groundmass	−0.109	36	Not significant
$[Zn^{++}]$	$\frac{\text{orthoclase}}{\text{plagioclase}}$	+0.00367	36	Not significant
$[Zn^{++}]$	alteration	−0.185	37	Not significant

in detail to alteration because: 1 Oxidation and movement of copper by ground and subsurface water probably changed the copper distribution and 2 alteration occurred at a different time than the copper mineralization. Most of the anomalies occur only at irregular intervals near the intrusive contact. This indicates that copper in excess of background was not a by-product of the local solidification of the intrusive but instead was introduced afterwards. Contact oriented anomalies may indicate the introduction of copper from the contact inwards. Though the Hanover-Fierro intrusive is not intensely fractured and anomalies far from the contact are few, the location of the two anomalies not on the contact can be explained as the result of the introduction of copper along fractures in the intrusive.

Zinc Distribution.—All samples having zinc concentration ranging from 38 to 48 ppm are considered as reflecting only background or primary concentration. The results of zinc analysis were plotted next to each station and isopleths of zinc concentrations were drawn to show the zinc distribution in the Hanover-Fierro intrusive (Fig. 6).

The zinc distribution is not related significantly either to the weight percent groundmass minerals or to the orthoclase:plagioclase ratio. The map of zinc distribution (Fig. 6) is unlike either the map of weight percent groundmass (Fig. 2) or the map of orthoclase:plagioclase ratio (Fig. 3). The coefficients of correlation for these relations are not significant (Table 3).

Zinc, like copper, is neither related in detail to primary nor to secondary features of the intrusive. However, the zinc anomalies, like most of the copper anomalies, are found in altered rock and areas near or adjacent to ore bodies or mineralized zones.

For the same reasons as previously stated for copper, zinc anomalies are considered to be the result of the introduction of ore ions from the contact inward. It is thought that originally both copper and zinc had distributions

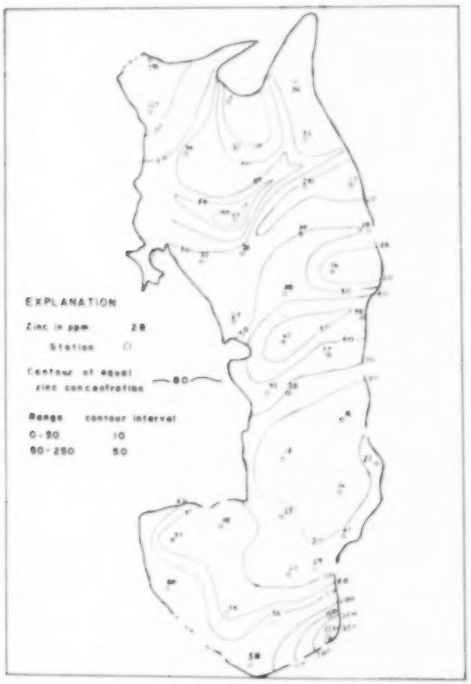

FIG. 6. Hanover zinc distribution.

that were related to primary features in the pluton. Later alteration and ore deposition so modified the copper and zinc distributions, perhaps by the mobilization of primary copper and zinc and by the introduction into the pluton of secondary copper and zinc. Now the distributions are not clearly related to either primary or to secondary features. There is also a possibility that the fluids that caused the alteration may have moved farther from the main channelways of fluid movement than the ore solutions. Most of the alteration probably occurred at another time than the ore deposition. Thus the hydrothermal process that took place in the country rock far from the veins so modified the original primary copper and zinc distribution that it

cannot be correlated with either primary or secondary features. This picture was undoubtedly complicated by later weathering and groundwater action. Zinc may be more closely related to alteration than copper because r for Zn versus alteration is greater than the r for Cu versus alteration (though not significant).

Genetic Concepts

The ore deposits of Hanover and Fierro came from depth instead of the adjacent exposed pluton, because the ore deposition occurred after the solidification and complete cooling of the exposed part of the Hanover-Fierro intrusive. It is also improbable that the ore deposits originated as a result of the contact metamorphism of the presently exposed country rock because the ore deposition took place after the complete cooling of the exposed pluton. Schmitt's geochemical calculations (18, pp. 797–804) confirm this view and he concludes that most of the oxides (FeO, Fe_2O_3, SO_2, Al_2O_3, MgO, MnO) added to the zone of mineralization around the southern lobe of the intrusive "came from a source below the Hanover intrusive" (18, p. 804). Calculations indicate that the zinc also originated from depth. Schmitt (18, p. 803) calculated that the southern lobe of the intrusive contains 2.4×10^8 tons of rock and the zinc added to the exomorphic zone is 6×10^5 tons. If all the zinc added to the exomorphic zone came from the southern lobe of the intrusive, the magma would have contained about 25% Zn. No igneous rock has yet been reported that has a primary zinc content that even approaches 25 percent. Wedepohl (21, pp. 119–124) reports a maximum value of 210 ppm zinc in silicic igneous rocks.

The Niggli concept supposes that as a magma crystallizes, the residual fluids are enriched in volatiles and these volatiles carry the ore ions. The volatiles are forced out of the magma by crystallization and as they cool, form in turn pegmatites; then hydrothermal ore deposits. A depth of only 2 km is sufficient to cause this process to take place (14, 1929, p. 8). Stratigraphic evidence shows that part of the Hanover-Fierro intrusive that is now exposed was buried under at least 2 km of sedimentary rocks and volcanics when it was intruded, yet the veins and ore deposits in and around the intrusive originated from depth.

Since the ores originated from depth, they came from a deeper portion of the Hanover-Fierro intrusive. The mechanism of emanation of the ore fluids from the deep portion of the intrusive instead of the exposed portion might be explained in three ways: 1, The exposed portion of the intrusive cooled too rapidly to allow the contained volatiles and ore ions to escape. 2, The deeper part of the intrusive has a much higher content of ore ions than the exposed part and hence is the source of ore deposits. 3, The volatiles that carried the ore ions are only expelled at depth where the pressure is great enough for the pneumatolytic stage to be reached.

The first possibility seems to be excluded as a valid explanation, for if the exposed portion of the Hanover-Fierro intrusive cooled in such a manner as to trap the enclosed volatiles then it is difficult to explain why the resulting

igneous rock has a relatively coarse texture that seems to indicate fairly slow cooling. If, however, the copper- and zinc-bearing volatiles were trapped in the cooling magma in that manner, the resulting rock might be expected to be abnormally high in these ions, yet the primary copper and zinc abundances are not abnormally high. The average primary copper content is 51 ± 13 ppm. This is twice as high as the average copper content of 29 silicic igneous rocks of 21 ppm reported by Sandell and Goldich (17, p. 174). The average of Sandell and Goldich was obtained from only 29 samples and may be too low; besides, the primary abundance of copper from the Hanover-Fierro intrusive lies well within the range of their extreme values (3 to 140 ppm Cu). The primary zinc content of the Hanover-Fierro intrusive is 43 ± 5 ppm. This agrees excellently with Wedepohl's (21, pp. 119–124) average for 70 acidic igneous rocks of 45 ppm Zn, with a range from 7 to 210 ppm. So the primary copper and zinc content of the Hanover-Fierro intrusive is believed to be neither abnormally high or abnormally low.

If the lower part of the intrusive were to be richer in both volatiles and accompanying ore ions than the exposed part, then it is difficult to explain how the top and bottom portions could be isolated in such a manner as to prevent mixing by convection or upswelling of the magma. It would also seem possible that the volatiles would tend to rise to the top of the intrusive in such a manner as proposed by Kennedy (9). Not much is known about the trace element distribution in deeply buried plutonic rocks or about the vertical variation of trace metals in plutons associated with the roots of ore deposits. Intensive work along these lines may provide a clue as to the origin or ore deposits.

The ore-carrying volatiles in the magma that became the Hanover-Fierro intrusive were expelled at a greater depth than the exposed portion of the intrusive, as a result of critical phenomena (a process proposed by Niggli). This would adequately explain the emplacement of the ore deposits in the vicinity of the pluton after it had solidified. The time it took the ore fluids to emanate from the deeper part of the intrusive might well be sufficient to allow for the solidification of the exposed portion of the intrusive. Sales holds similar views (16). Perhaps a greater depth than the 2 km suggested by Niggli is required that this process take place. However, the contention that volatiles could stay at depth and would not move upward in the intrusive or out into the contacts into regions of lower pressure is hard to visualize. Kennedy (9) holds this view.

The results of this study raise the question as to whether the ore deposits at Hanover are actually genetically related (in the Niggli sense) to the Hanover-Fierro intrusive. The evidence presented here indicates that a genetic relation does not exist. A firmer clue to the relations could be obtained if it were known exactly how much zinc and copper was added to the zone of alteration around the pluton and this data were used in geochemical calculations. Information of the amount of ore mined from, and the reserves of the mines along the Barringer fault zone and in the rest of the northern part of the intrusive is not available. Further parallel studies elsewhere in similar districts may afford a more fruitful approach to the problem.

MAGDALENA, NEW MEXICO

The Magdalena mining district lies in Socorro County, Central New Mexico, 28 miles west of Socorro. The pluton studied, the Granite Mountain pluton, is situated in the northwest corner of the area mapped by the U. S.

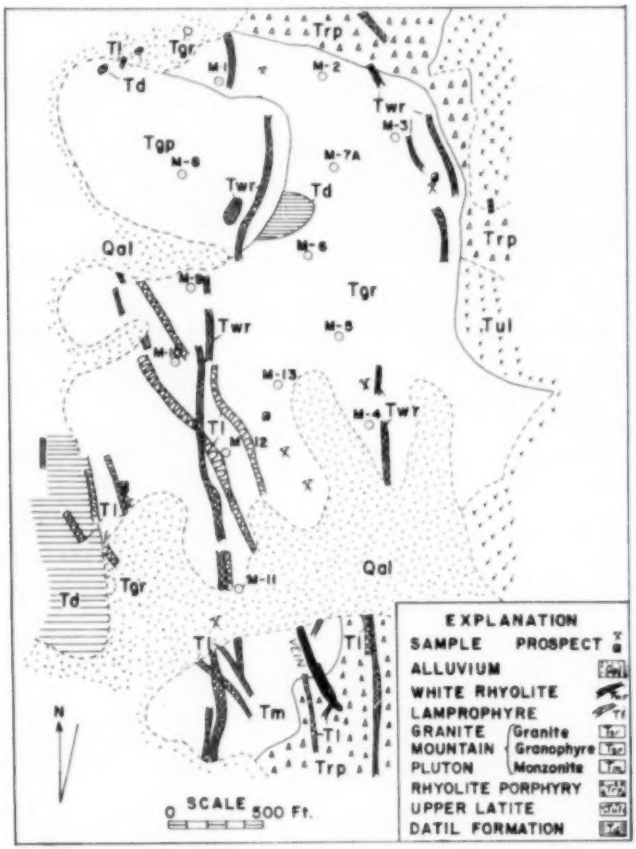

FIG. 7. Base map of the Granite Mountain pluton (geology by Loughlin and Koschmann, 1942).

Geological Survey in the Magdalena mining district (12, Fig. 2), a quarter of a mile north of the right of way of the Santa Fe Railroad and some two miles west of Magdalena.

This district is characterized by Tertiary block or normal faulting with a few minor folds.

The ore deposits of the district are mesothermal mixed sphalerite-chalcopyrite types that replace limestone beds where fissures intersect them. Deposits of high-temperature silicates, wollastonite, diopside, andradite, and hedenbergite replace limestone but, unlike similar deposits at Hanover, are not related to the sulfide ores.

The intrusion of the Granite Mountain pluton was contemporaneous with the emplacement of the other granite plutons of the district. It was both preceded and followed by the emplacement of sills and dikes of andesite and rhyolite and some silicic extrusives.

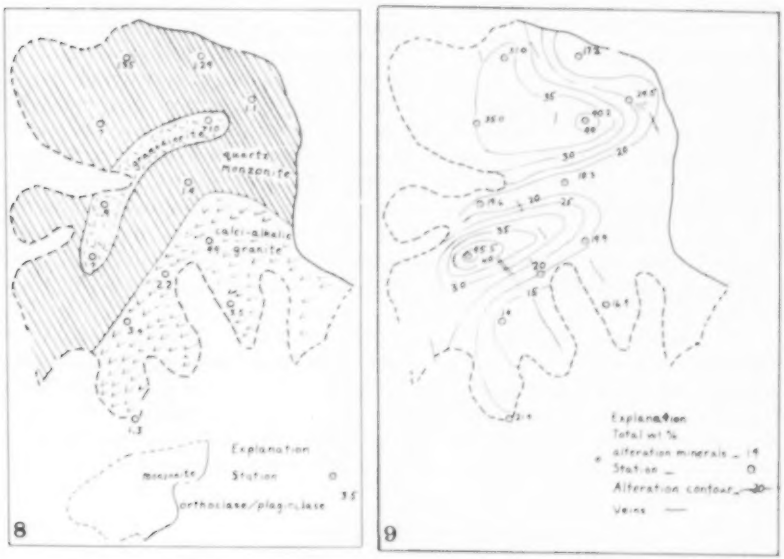

FIG. 8. Facies of the Granite mountain pluton.
FIG. 9. Alteration map of the Granite Mountain pluton.

Structure and Petrology

The Granite Mountain pluton is a complex intrusive body 3,000 feet long and 2,000 feet wide. The pluton is definitely intrusive in character, for it cuts across the structure of the country rocks (Fig. 7). The pluton is in turn intruded by a set of prominent north-trending white rhyolite dikes that are cut by a series of northwest-trending veins bearing lead and zinc of no commercial importance.

The Granite Mountain pluton varies in composition from a granodiorite to a calci-alkalic granite and has a small patch of monzonite in the south (not sampled) (Fig. 8). The northern part is a fine-grained quartz monzonite with a granophyric intergrowth of orthoclase and quartz. The rest of the

pluton is mostly granitic. The southern part of the pluton is an igneous complex, the core of which is a fine-grained calci-alkalic granite containing large laths of oligoclase and hornblende sparsely scattered in a groundmass of xenomorphic potassium feldspar and quartz. Surrounding the granite core is an area of quartz monzonite that contains smaller amounts of orthoclase than the more silicic facies; otherwise their mineralogy is the same.

Alteration

Five types of alteration were observed in thin sections of the Granite Mountain pluton: sericitization, argillitization, chloritization, epidotization, and carbonatization. All forms of alterations are considered as hydrothermal except sericitization and argillitization which may be partly the result of weathering. Sericite is an alteration product of feldspar, particularly of plagioclase. Orthoclase, and to a lesser extent, plagioclase, is clouded by submicroscopic flakes of brownish hue and low birefringence that are probably clay minerals. Chlorite was observed in all except one locality; it replaces biotite, hornblende, pyroxene and perhaps feldspar, and forms veinlets. Epidote is universally present throughout the pluton and replaces pyroxene, orthoclase, hornblende, and plagioclase. It also forms veins and porphyroblastic patches. Carbonate minerals, probably calcite, commonly occur with sericite as alteration products or plagioclase or with chlorite as an alteration product of hornblende.

Two northeast trending areas of intense alteration occur in the Granite Mountain pluton (Fig. 9). The trend of the alteration is approximately perpendicular to the northwest trending veins. The whole pluton may have been altered on a grand scale through a set of east to northeast fractures. The ore deposition and attendant alteration probably took place locally along the northwest set of fractures at a different time from the large scale alteration of the pluton.

Chemical Analyses

Copper Distribution.—The average copper content of all samples from the Granite Mountain pluton is 71 ± 20 ppm. No primary copper content or background could be determined because of the altered and oxidized condition of the rocks. A high in the center of the pluton has a value of 109 ppm and trends northwest (Fig. 10).

The copper distribution in the Granite Mountain pluton is neither related to rock types (the orthoclase:plagioclase ratio) nor to alteration. The map of copper distribution (Fig. 10) is unlike either the facies map (Fig. 8) or the alteration map (Fig. 9). The coefficients of correlation for these relations are not significant (Table 4).

The copper distribution is apparently not related to veins as the axis of the copper anomaly and the veins have different trends. However, if the contouring of the copper map were changed only slightly, there would be a good relation between copper and veins. It is believed that the primary affinities of copper have been strongly modified by the introduction of copper

TABLE 4

COEFFICIENTS OF CORRELATION FOR METAL CONTENT VERSUS PETROLOGY AND THEIR SIGNIFICANCE, THE GRANITE MOUNTAIN PLUTON

x	y	r	n	Significance
$[Cu^{++}]$	Orthoclase:plagioclase	+0.233	13	Not significant
$[Cu^{++}]$	Alteration	−0.0157	15	Not significant
$[Zn^{++}]$	Orthoclase:plagioclase	+0.495	13	Not significant
$[Zn^{++}]$	Alteration	+0.116	15	Not significant

into the area around the center of the copper anomaly, but not enough to make the copper distribution related to alteration.

Zinc Distribution.—The average zinc concentration of the samples examined from the Granite Mountain pluton is 122 ppm with a range from 62 to 284 ppm. No background or primary zinc content could be arrived at

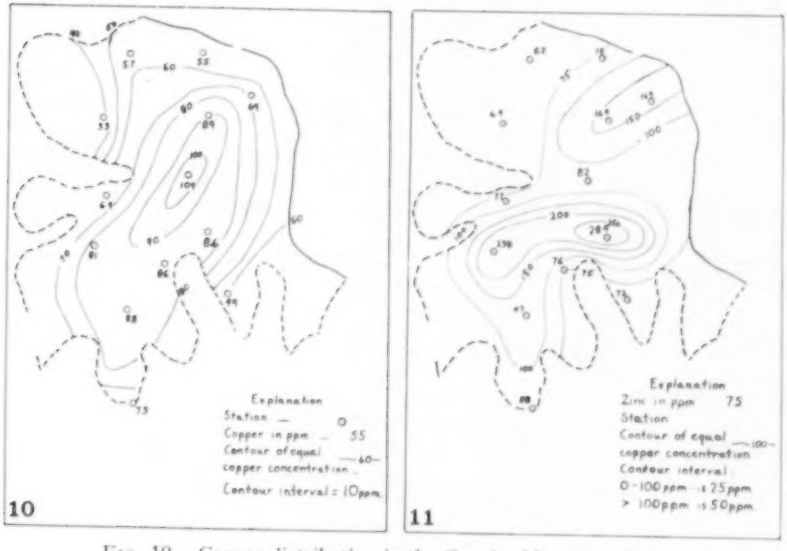

FIG. 10. Copper distribution in the Granite Mountain pluton.
FIG. 11. Zinc distribution in the Granite Mountain pluton.

as all the samples are highly altered and oxidized. Two zinc anomalies occur in the Granite Mountain pluton. The first has two maximum values of 164 ppm each, trends northeast and is in the northeastern corner of the intrusive (Fig. 11). The southern anomaly has an eastward elongation and a maximum value of 284 ppm.

The zinc distribution is not apparently related to rock types within the pluton as Figures 11 and 8 are dissimilar and the coefficient of correlation

between zinc and the orthoclase:plagioclase ratio is not significant (Table 4). There is a fairly good relation between zinc distribution and alteration. Figure 11 is very similar to Figure 9 (the alteration map), however, the coefficient of correlation between zinc and the weight percent of alteration minerals is not significant (Table 4). There is, however, a slight downslope shift of the zinc anomalies with respect to the highs of alteration that can be easily accounted for by the transporting action of groundwater and oxidation

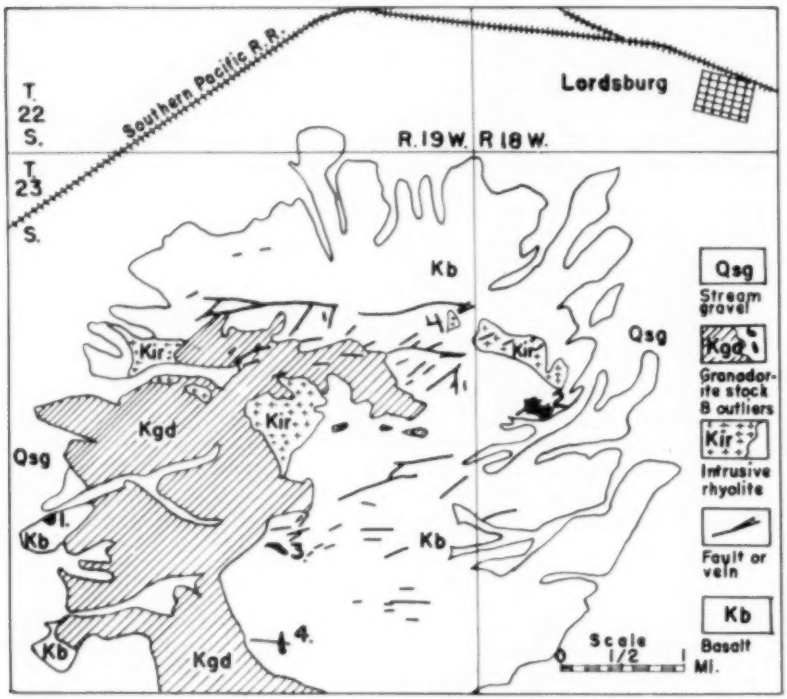

FIG. 12. Index map of Lordsburg outliers (after Lasky, 1938).

of the zinc anomalies. This probably explains the low coefficient of correlation. It is believed that the primary zinc distribution has been modified by the introduction of hydrothermally transported zinc related to alteration and subsequently modified by supergene processes.

Conclusions from Chemical Analyses.—Zinc is more strongly related to secondary features than is copper. The differences in the affinities are more marked in the Granite Mountain pluton than in the Hanover-Fierro intrusive.

The ore deposits of Magdalena probably originated from depth rather than from the exposed portion of the Granite Mountain pluton or the other plutons

of the district because: 1, The deposition of the ore was preceded by the intrusion of lamprophyre and white rhyolite dikes that cut the pluton of the district (12, p. 111). The presently exposed part of the pluton had solidified and cooled completely by the time the dikes were intruded otherwise they would be coarse-grained instead of aphanitic. 2, The zinc distribution is related to alteration and other secondary features rather than to primary features. 3, Veins of copper and zinc cut the pluton. 4, The ore deposits and plutons are not structurally related. The ore deposits are controlled by fissures and faults.

The Niggli theory could not be tested adequately in this district because no fresh rocks could be found from which to obtain an estimate of primary copper and zinc abundances within the pluton.

THE LORDSBURG, NEW MEXICO, MINING DISTRICT

The Lordsburg copper mining district is southwest of the town of Lordsburg in the northern part of Hidalgo County, New Mexico, about 17 miles east of the Arizona State line. The rocks of the district, with the exception of the Lordsburg intrusive, are extrusive volcanics. Numerous volcanic vents and necks occur. The district is cut by three zones of normal faulting (11, pp. 20–21). The ore deposits are fillings of faults and fractures of the region. The veins show evidence of repeated opening, brecciation, leaching and replacement (11, p. 33, Plate 8). The ore mineral is chalcopyrite with minor sphalerite and galena. Gangue minerals in the veins include quartz, calcite, specularite, manganosiderite, barite and fluorite. Alteration minerals include chlorite, sericite, specularite, calcite and tourmaline.

General Description of the Lordsburg Intrusive and Its Outliers

The main pluton in the Lordsburg mining district is the Lordsburg intrusive, a discordant pluton 6½ miles long by 1½ miles wide. It has definitely intruded into basalts as it has an irregular contact with them and cuts across their structure (Fig. 12). In addition to the main intrusion, many small outliers are present, particularly on the northeastern side of the intrusive. They indicate the extension of the intrusive at depth and that the Lordsburg intrusive is a stock.

The Lordsburg intrusive itself was not sampled because it is cut by many veins, is too altered, is not entirely exposed, and would require a prohibitive number of samples to cover it adequately. As a result, four outliers of the main intrusive, two of which were cut by veins (Outliers 2 and 4), and two which were not transected (Outliers 1 and 3) were chosen for study.

Location and Petrology of the Outliers

The location of the outliers studied is shown in Fig. 12. With the exception of Outlier 1, which is all fine grained tonalite, the outliers range in composition from tonalite or granodiorite to calci-alkalic granite (Fig. 13).

This is the result of variations in the orthoclase:plagioclase ratio. The variation in texture is more extreme than the variation in composition. The grain size averages 0.3 mm. The large outliers (Outliers 2 and 4) have more variations in texture and composition than the smaller ones.

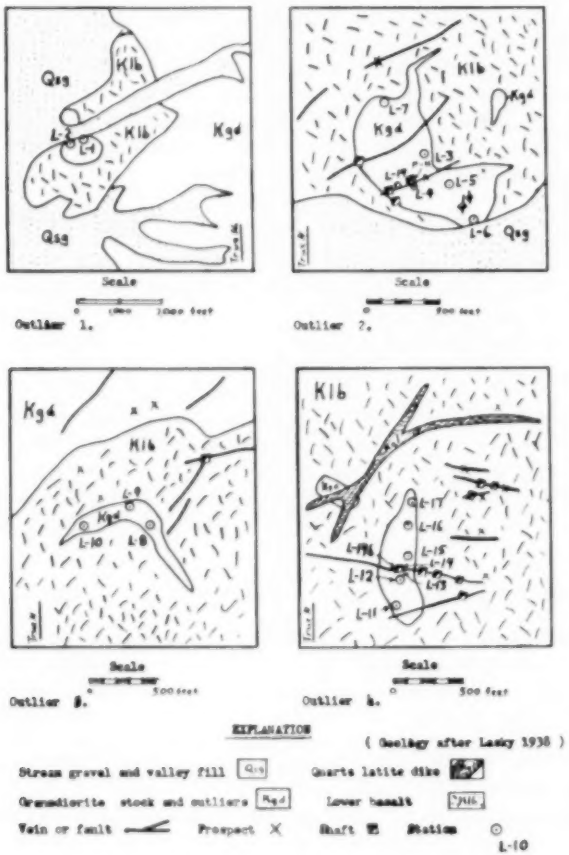

FIG. 13. Base map of the Lordsburg outliers.

Alteration

Sericitization, argillic alteration, chloritization, carbonatization, and epidotization were observed in thin sections of the Lordsburg outliers. With the exception of the alteration of pyroxene to hornblende and biotitie, which are probably deuteric phenomena, and sericitization and argillic alteration which may in part be due to weathering, all the types of alteration observed

are considered hydrothermal. Only the hydrothermal alteration will be dealt with here.

Figure 14 is an alteration map of the outliers. The total weight percent of alterations is plotted against the corresponding sample locations. Contours were not drawn as there were too few sample locations. Each outlier except Outlier 1 is moderately altered throughout. The areas near or in veins are

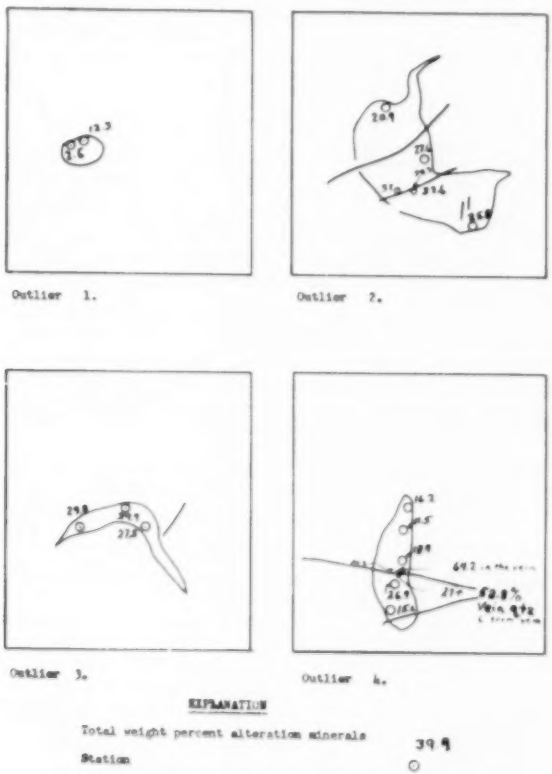

FIG. 14. Alteration map of the Lordsburg outliers.

the most intensely altered. Alteration not associated with veins is mainly sericitization and kaolinization of the feldspars with chloritization of the ferromanganesian minerals; vein alteration is mainly complete and intense sericitization of the feldspars together with the introduction of silca and a little fluorite.

Chemical Analyses

The copper and zinc content are higher in outliers transected by veins (Outliers 2 and 4) than in those not transected (Outliers 1 and 3). Figure 16 is a map of copper and zinc distribution in the outliers.

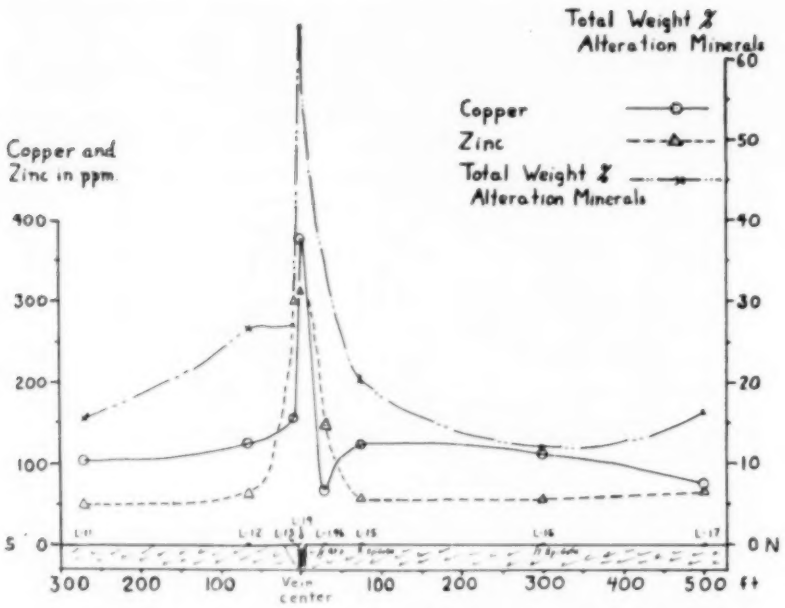

FIG. 15. Heavy metal and alteration distribution about a vein in outlier 4 of the Lordsburg, New Mexico, intrusive.

TABLE 5

COEFFICIENTS OF CORRELATION FOR METAL CONTENT VERSUS PETROLOGY AND THEIR SIGNIFICANCE, OUTLIERS OF THE LORDSBURG STOCK

x	y	r	n	Significance
		Outlier 2		
$[Cu^{++}]$	Groundmass	−0.778	6	Not significant
$[Cu^{++}]$	Alteration	+0.280	6	Not significant
$[Zn^{++}]$	Groundmass	−0.732	6	Not significant
$[Zn^{++}]$	Alteration	−0.353	6	Not significant
		Outlier 4		
$[Cu^{++}]$	Alteration	+0.742	8	Significant below the 5% level
$[Zn^{++}]$	Alteration	+0.956	8	Significant below the 1% level
		Outliers 1 and 3		
$[Cu^{++}]$	Alteration	−0.632	5	Not significant
$[Zn^{++}]$	Alteration	−0.934	5	Significant below the 5% level

The copper and zinc distributions in outliers that are cut by veins are definitely related to the veins and there is a significant relation between copper and zinc on the one hand, and alteration on the other, especially in Outlier 4 (Table 5).

Copper, zinc, and the total weight percent of alteration minerals have "diffusion gradients" from the veins to the country rock (Fig. 15), indicating that the fluids that produced both alteration and copper and zinc concentrations

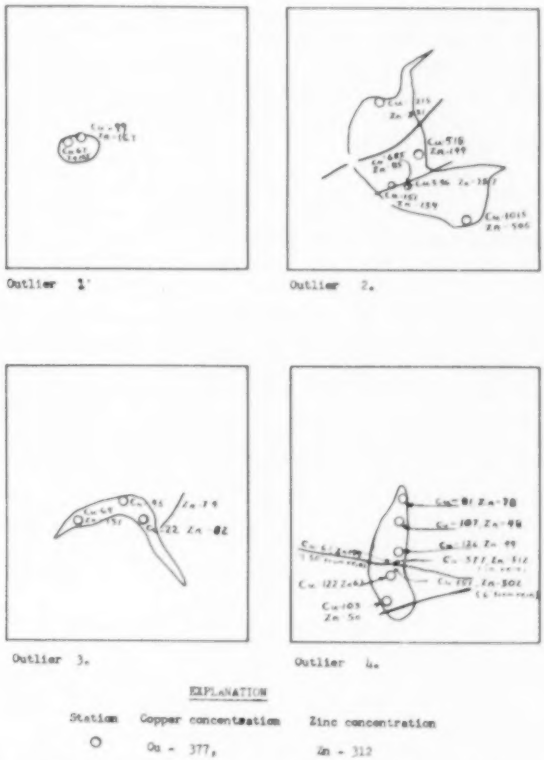

FIG. 16. The copper and zinc distribution in the Lordsburg outliers.

above background in the country rock emanated from the adjacent vein. Thus the primary copper and zinc distribution has been strongly modified by hydrothermally introduced copper and zinc. There is a significant negative correlation between zinc concentration and hydrothermal alteration in the outliers not cut by veins. This is believed to indicate hydrothermal leaching; the greater the weight percent of alteration minerals, the greater the leaching.

At Lordsburg, as at Hanover and Magdalena, zinc has much stronger

secondary affinities than does copper. Zinc is more closely related to alteration and less closely related to primary features than copper.

The ore deposits of the Lordsburg mining district originated from depth instead of the exposed intrusive because: 1, The copper ores are younger than the intrusive. The ores were emplaced after a period of district-wide faulting and complicated hydrothermal history that followed the solidification of the exposed pluton. 2, There is evidence that copper and zinc were introduced into the pluton from the vein, not vice versa (Fig. 15). 3, The distributions of copper and zinc are related to alteration and veins, not to primary features in parts of the intrusive that are cut by veins.

No idea of the primary copper and zinc content of the pluton could be obtained because no really fresh unaltered rock could be found. Therefore, it was impossible to test the Niggli theory in this case for the data tends neither to prove nor disprove it.

INTER-DISTRICT COMPARISONS

The primary copper and zinc concentrations of the Granite Mountain pluton and the outliers of the Lordsburg intrusive could not be estimated as they are altered, oxidized, and cut by too many large veins.

Zinc is more closely related to alteration and has more marked secondary affinities in the Granite Mountain pluton than in the Hanover-Fierro intrusive. The zinc distribution in the Granite Mountain pluton is related to alteration whereas the zinc distribution in the Hanover-Fierro intrusive is neither related to primary nor secondary features of the pluton. This is certainly the result of greater hydrothermal zinc introduction within the Granite Mountain pluton than in the Hanover-Fierro intrusive. Field evidence supports this theory. The Granite Mountain pluton is more extensively and intensively altered, and it has an average of 24.6 percent by weight of alteration minerals as compared to 2.9 percent in the Hanover-Fierro intrusive. It is also cut by a greater number of larger zinc veins per unit area than the Hanover-Fierro intrusive.

Therefore, in these two igneous intrusives, the degree to which the ore ion distribution is related to alteration instead of primary igneous features and the average weight percent of alteration minerals in the pluton is a function of 1, the size of the metal bearing veins and 2, their density or number per unit area.

The copper and zinc distributions are related in a positive way to alteration in the outliers of the Lordsburg intrusive cut by veins (Outliers 2 and 4) but the relation is negative, suggesting hydrothermal leaching, in those not cut by veins (Outliers 1 and 3). The outliers not cut by veins are less intensely altered (21 percent by weight alteration) and have a smaller average copper and zinc content (Cu = 60.4 ppm, Zn = 124 ppm), as compared to the outliers cut by veins which contain an average of 31 percent alteration minerals, 348 ppm Cu and 180 ppm Zn. The relations previously stated, between the intensity and amount of heavy metal introduced into igneous country rock and secondary phenomena on a district-wise scale as at Hanover

and Magdalena, is borne out on a local scale in Lordsburg. On an even smaller scale both copper and zinc are more closely related to the weight percent of alteration minerals in and close to the vein studied at Lordsburg (Fig. 15) than in the country rock farther away.

It was previously noted that in the Hanover-Fierro intrusive and in the Granite Mountain pluton zinc had a closer relation to alteration and areas of ore deposition than had copper. The same is true of Lordsburg, even though copper is more abundant in the veins than zinc. Zinc apparently has a closer statistical relation to alteration in the districts studied than has copper. The most abundant metal in the vein, copper, it is noted (Fig. 15) moves farther out into the country rock than the less abundant metal. Therefore the predominant metal in the ores of a district is apt to have a distribution in the country rock that is more closely related to mineralized areas, and a broader dispersion from the veins and ore bodies than the less abundant metal. The dispersion of a metal from a vein into the country rock can serve as an indicator of the relative abundance of the metal in hidden veins. This criterion may be best applied to rocks that are coarse-grained and sensitive to hydrothermal alteration.

CONCLUSIONS

1. The plutons studied are complex intrusives, ranging in composition from tonalite or monzonite to calci-alkalic granite, and in texture from equigranular to porphyritic.

2. The Hanover-Fierro intrusive has a primary copper abundance of 51 ± 13 ppm and a primary zinc abundance of 43 ± 5 ppm. The primary copper is twice as high as the average for acidic igneous rocks reported by Sandell and Goldich (17, p. 108), but the copper in the pluton is not believed to be abnormally high as it lies in the range of the average of Sandell and Goldich, though indeed they report only 29 analyses. The primary zinc abundance in the Hanover-Fierro intrusive agrees with Wedepohl's average of zinc in 70 acidic igneous rocks.

3. The metal ion distribution in an igneous country rock in an area of few veins bearing metals is apt to be related to primary igneous texture, composition and other features, but is not related to alteration. The average weight percent of alteration is low and the amount of metal introduced into the rock from the veins is small. Conversely, the metal ion distribution in an igneous country rock that is cut by numerous veins bearing metals is statistically far more clearly related to alteration than to primary igneous features. The average weight percent of alteration and the amount of metal introduced into the area are apt to be large. This same series of relations applies as well on a small scale, for as a single vein is approached from a distance in an igneous country rock, the content of alteration minerals and ore metals increases. Both alteration and ore metals are more closely related to each other.

4. Of two metals in a mining district, the more abundant metal in the vein moves farther out into the country rock than the less abundant metal.

5. The results of the study raised the question whether the ore deposits of the three districts studied actually originated from the adjacent intrusives. It is suggested that further parallel studies elsewhere may afford a more fruitful approach to the problem of the genesis of such ores.

ACKNOWLEDGMENTS

The author is greatly indebted to Professor Chas. H. Behre, Jr. of the Department of Geology at Columbia University, his thesis advisor, for numerous suggestions and field review. Sincere thanks are also extended to Professors Paul F. Kerr and Arie Poldervaart, also of the Department of Geology, for their help; to Dr. Hubert L. Barnes for his untiring work on the method of zinc and copper analysis which he and the author developed in 1956. Thanks are due to William R. Jones and Samuel Moore of the U. S. Geological Survey for assistance at Hanover, New Mexico. The U. S. Smelting, Refining and Mining Company, the Peru Mining Company and the New Jersey Zinc Company kindly gave permission to study their respective properties at Fierro and Hanover, New Mexico. To his brother, John H. K. Belt, the author owes much for assistance in the field; also to Mrs. Robert Tack and Louise McKeon Belt.

The laboratory investigations connected with this research were carried out in the Ore Genesis Laboratory of Columbia University and were aided by the Kemp Fund of the Department of Geology and allotments from the Ore Genesis Laboratory and Gift Funds.

ORE GENESIS LABORATORY,
DEPARTMENT OF GEOLOGY,
COLUMBIA UNIVERSITY, NEW YORK CITY,
AND
DEPARTMENT OF MINING AND GEOLOGICAL ENGINEERING,
SCHOOL OF MINES, UNIVERSITY OF UTAH,
SALT LAKE CITY, UTAH,
February 25, 1960

REFERENCES CITED

1. Allen, V. T., and Fahey, J. J., 1957, Some pyroxenes associated with zinc deposits in Mexico and New Mexico: Geol. Soc. America Bull., v. 68, p. 881–896.
2. Barnes, H. L., 1958, The source of base metals: Ph.D. Thesis, Columbia University, New York.
3. Chayes, Felix, 1956, Petrographic modal analysis: John Wiley and Sons, New York, p. 1–113.
4. Emmons, W. H., 1926, Relations of metalliferous lode systems to igneous intrusions: A.I.M.E. Trans., v. 74, p. 29–76.
5. Fenner, C. N., 1926, The Katmai magmatic provinces: Jour. Geol., v. 34, p. 697.
6. Hernon, R. M., Jones, W. R., and Moore, S. L., 1953, Some geological features of the Santa Rita Quadrangle, New Mexico: New Mexico Geol. Soc. Fourth Field Conference Guidebook, p. 117–130.
7. Imbrie, John, 1956, Biometric methods in the study of invertebrate fossils: Amer. Mus. Nat. Hist. Bull., v. 108, Art. 2, p. 217–252.
8. Jones, W. R., Personal Communication 1957.
9. Kennedy, G. C., 1955, Some aspects of the role of water in rock melts: Geol. Soc. America Special Paper 62, The Crust of the earth, p. 489–504.

10. Lasky, S. G., 1936, Geology and ore deposits of the Bayard area, Central Mining District, New Mexico: U. S. Geol. Survey Bull. 885, p. 1–63, Plate 8.
11. ——, 1938, Geology and ore deposits of the Lordsburd Mining District, Hidalgo County, New Mexico: U. S. Geol. Survey Bull. 885, pp. 1–63.
12. Loughlin, G. F., and Koschmann, A. H., 1942, Geology and ore deposits of the Magdalena Mining District, New Mexico: U. S. Geol. Survey Prof. Paper 200, p. 1–182.
13. Niggli, Paul, 1925, Versuch einer naturlichen Klassification, etc.: Abhandl. prakt. Geol., Bnd. 1, Halle, p. 1–69.
14. ——, 1929, Ore deposits of magmatic origin: Trans. by H. C. Boydell, Thomas Murby and Co., London, p. 93.
15. Peatman, J. G., 1947, Descriptive and sampling statistics: Harper Bros., New York, p. 1–577.
16. Sales, R., 1954, Genetic Relations between granites, porphyries, and associated copper deposits: Mining Eng., v. 6, p. 499–505.
17. Sandell, E. B., and Goldich, S. S., 1943, The rarer metallic constituents of some American igneous rocks: Jour. Geol., v. 51, Part II, p. 167–189.
18. Schmitt, Harrison, 1939, The Pewabic mine: Geol. Soc. America Bull., v. 50, p. 777–818.
19. Snedecor, G. W., 1956, Statistical methods, fifth edition: Iowa State College Press, Ames, Iowa, p. 160–163, 174.
20. Wahlstrom, E. E., 1947, Igneous minerals and rocks: John Wiley and Sons, New York, p. 268-350.
21. Wedepohl, K. H., 1953, Untersuchingen zur Geochemie des Zinks: Geochim. et Cosmochim. Acta, v. 3, p. 93–142.

Economic Geology
Vol. 55, 1960, pp. 1272–1284

RESIDUAL CHARACTERISTICS OF CRYSTALLATES GENETICALLY ASSOCIATED WITH ORE DEPOSITS

J. H. RATTIGAN

ABSTRACT

Ore deposits are specialized products of geochemical differentiation and a basic assumption in many theories of genesis, whether magmatic, metamorphic or metasomatic is that ores are related to crystallization in a source system. The crystallates from which particular ore metals have been fractionated are considered to have a specific geochemical character expressed in features of petrology, mineralogy, and chemistry of the crystallates in mass or in some components. These characteristics may be of value in restricting areas for exploration. The occurrence of some base metals such as tin, copper, lead, zinc, and chromium is discussed in terms of the geochemical character of associated crystallates.

INTRODUCTION

DESPITE the many theories of ore genesis that have been proposed, most economic mineral deposits have one fundamental characteristic in common in that they are products of geochemical differentiation. In considering the natural processes responsible for this geochemical differentiation we must take account of four aspects of metalliferous ore occurrence. These are:

1. Parent material; in which we may reasonably assume most economic metals are present as minor constituents associated with an overwhelming abundance of major constituents,
2. Fractionation; for which we must consider processes whereby minor constituents are not fixed with major constituents and are thus available for concentration,
3. Collection; for which we must consider mechanisms that allow migration and concentration of the fractionated minor elements into a differentiated system segregated from a residual differentiate consisting of major constituents of the original system,
4. Deposition; for which we must consider principles governing deposition of metals as ore.

For epigenetic deposits the nature of the source material must always be the most speculative aspect in any consideration of metalliferous ore genesis. The parent material has been variously inferred as being primary magmatic material, magma produced by fusion or selective fusion of crystallized or clastic rocks, or solid crystallized or clastic rocks on which metamorphic or metasomatic processes have acted to achieve fractionation.

The processes involved in fractionation, collection, and deposition of ore metals are to some extent less speculative, as we can observe the products

resulting from the action of these in the natural laboratory, which is the earth, and in some cases, simulate similar products under artificially controlled conditions. By these means explanations can be reasonably proposed from our present knowledge of physical and chemical principles.

From the point of view of exploration for economic mineral occurrences the processes of fractionation, collection, and deposition are more important than the nature of the original parent material as, in operating, the processes may imprint on the natural products associated with ores characteristics that may be used as guides in prospecting. In mineral exploration most guides to ore are concerned with depositional and post-depositional effects such as the physical and chemical characteristics observed in known ore deposits and their environs. These guides include the commonly used structural and stratigraphic guides, wall rock alteration, geophysical anomalies and such post-depositional effects as leached outcrops or geochemical dispersion patterns surrounding orebodies.

To date the geochemical characteristics of associated residual differentiates from the fractionation and collection stages of genesis have been used only as very broad indicators of ore. These residual differentiates are the rocks associated with ores that have often been termed "parent rocks" but they are perhaps better described as genetically associated differentiates, which with the ore minerals are products of the processes of fractionation and collection in an original source system.

The purpose of this paper is to discuss the fractionation aspect of some economic metals and the use of residual criteria in associated geochemical differentiates as guides to ore. The discussion relates chiefly to orebodies for which a magmatic, metamorphic, or metasomatic ("granitization") origin is supposed.

MINOR ELEMENT DISTRIBUTION AND ORE CONCENTRATION PROCESSES

There can be little doubt as to the chemical heterogeneity of the earth particularly in the crustal layers where it is most obviously expressed in the distribution of major constituent elements as minerals. It can be reasonably assumed that there is also wide variation in minor element content in different parts of the crust. Turneaure (16) has suggested that the recurrence of the same ore types points to a certain uniformity in metal distribution in the crust and in the processes of ore concentration. The writer's view is that the similarity of ore type in different geographic regions is argument in favor of similarity in ore concentration processes that have operated, but does not necessarily imply any uniformity in minor element distribution.

An ore type is qualitative in nature and we have little factual data apart from economic deposits, concerning quantities of metals in different mineralized districts. Ore concentration processes are specialized geochemical processes and, although much remains to be known concerning the principles governing these, it is reasonable to expect that in operating they could lead to a similar qualitative end product (ore type) from source materials with quite different absolute contents of minor elements.

In any consideration of natural processes we are at some disadvantage in applying physical and chemical principles in that reactions have generally taken place in multicomponent systems that may be open or partly open, and under physical conditions of which we have little direct knowledge. However in explaining the geochemical differentiation of any parent material leading to ore occurrence we may consider in the interest of working theories the processes active in three broad classes of system that may be described as:

1. Source systems; in which fractionation of ore metals from major constituents proceeds leaving these available for collection and transportation,
2. Differentiated ore metal systems; into which minor elements are concentrated by some form of collector mechanism (7) and these are complementary to residual differentiates from which the ore metals have been extracted,
3. Depositional systems; which may be merely the ore metal differentiate under different physical conditions or modified after transportation by incorporation of components from host rocks in which ore deposits form.

It should be realized that, for any initial parent material, preliminary differentiation might produce progressively several independent source systems. Thus a primary magma may give rise to several partial magmas each in itself acting as a source system for particular metals. Likewise if an essentially solid pile of clastic or crystalline rocks is considered to be the parent material several independent source systems may arise by migration through the pile of different qualities or quantities of transforming fluids.

CRYSTALLIZATION AND ORE OCCURRENCE

Most metallic ores, with the exception of some secondary types such as the placers, may in their present state be described as crystallates, having resulted through crystallization from systems in response to particular physical and chemical controls. It is natural therefore that ore deposition should be explained in terms of principles governing crystallization. The physical and chemical character of the media into which minor elements are collected by any collector mechanism and of the host environment are fundamental to any argument concerning the final deposition of ore as a crystallate. These questions are however, beyond the scope of this paper.

It has become apparent in recent years that the principles governing crystallization in natural systems are also extremely important at an earlier genetic stage than deposition, in the fractionation of minor elements before a collector mechanism has operated. The origins of many types of ore deposits are ascribed to magmatic, metamorphic, or metasomatic processes operating within the source material. These processes involve crystallization whether it is crystal formation from a melt or recrystallization of clastic or previously crystalline rocks of any type. The nature of the crystalline state and the principles governing the development of normal or imperfect mineral structures and trace and other deviations from ideal storchiometric mineral compositions are fundamental to considerations of ore genesis.

FRACTIONATION IN SOURCE SYSTEMS

The principles applying in the fractionation stage in source systems are important not only for an understanding of ore genesis, but also from the viewpoint of exploration for mineral deposits by reason of the fact that if metals are fractionated and are available for collection by any process, a residual crystallized product may remain, which in its detailed geochemical characteristics may be an indicator that metal concentration has occurred.

Recently sedimentary sygenetic theories have been proposed for some of the less obviously stratified base metal ore bodies (12), but there is still fairly general acceptance that many ore deposits are genetically associated with magmas. The rise of the transformist school has led to controversy over the origin of some crystalline rocks, particularly the acid types, and attempts have been made to explain ore occurrence in terms of granitization processes. More recently metamorphic transformations, less obviously metasomatic, have been proposed to account for the source of ore metals (5, 6).

The principles applying to the behavior of minor elements during crystallization provide in some cases a common ground of argument in magmatic, metamorphic and metasomatic theories of ore genesis. The schism in the several working theories is mainly in regard to inferences concerning the nature of the initial parent material and in the collector mechanisms. Thus, if we assume a collector mechanism has operated in concentrating fractionated metals, some distinctive characteristics may be present in the residual crystallized differentiate and this may apply whether magmatic, metamorphic or metasomatic processes have operated.

A starting point for understanding the fractionation of ore metals in source systems lies in the close associations of specific ore types and metals with particular crystalline rock types. General relationships of this type have been adequately reviewed from the genetic aspect. Qualitatively we have such examples as the district groupings of ore types in the base metal fields of Canada, which Wilson (20) has referred to not as examples of zoning, but as distinct localized ore groups associated areally with distinct groupings of igneous rocks. This is empirical argument in favor of specific ore concentration processes operating in localized districts and reflected in both ore type and residual crystallized differentiates. Quantitatively there are some empirical grounds for presuming the scale of ore concentration is reflected in the size of ore deposits and the size of genetically associated residual crystallates. Vogt (19) has pointed out that there seems to be a relation between the size of Norwegian copper sulfide deposits and associated basic intrusives.

It is not proposed to discuss all aspects of ore occurrence but brief mention is made of principles that have been enunciated and used to explain the geochemical behavior, in particular the distribution and fractionation, of ore metals. Goldschmidt's Rules, which are sufficiently well known not to bear repetition, have formed the basis of much argument in explaining the fractionation of ore metals. Ringwood (14) has modified and extended these rules following consideration of the influence of electronegativity of ions and complex ion formation in magmas. Ringwood's papers describe the general

trend of fractionation and distribution of minor elements in magmatic crystallization but some of his principles would apply to crystallization in general. Most emphasis in geochemical reasoning applied to minor element distribution has been placed on ions occupying regular lattice positions in mineral structures. DeVore (5, 6) in a series of stimulating papers has produced arguments concerning the possible influence of adsorption and crystal growth in fractionation or fixation of minor elements. One argument is that important quantities of trace elements do not occur at regular lattice positions but on growth surfaces and other interfaces within a crystal, being fixed by adsorption during crystal growth. DeVore's data relate chiefly to metamorphic rocks in which the order of association of minor elements with major elements can perhaps be best determined because of the greater range of coexisting mineral structures and compositions than in common igneous rocks. DeVore also illustrates the possiblity of this adsorption mechanism fractionating ore metals during metamorphic transformations. He gives some quantitative estimates of amounts of fractionated elements available for concentration as ore from specific crystallates formed during such transformations. There are no particular reasons why the adsorption mechanism should not be applied to magmatic crystallization.

It seems probable, in view of the geological associations of ore and the geochemical principles that have been invoked in explaining these, that detailed geochemical studies embracing mineralogy, petrology and macro and trace chemistry of crystalline rocks may reveal peculiarities which indicate that fractionation of particular elements has occurred and that concentration processes that may have led to ore deposition have been active. Moreover, quantitative studies might give some lead not only to ore metal type but to the scale on which fractionation has been carried out. From the viewpoint of economic geology detailed studies of this type have lagged in that critical laboratory data have not been obtained in support of general relationships observed in the field and examined in terms of crystal chemistry. However the paper by Wilson (5) was a stimulating preliminary study on some base metals.

CHARACTERISTICS OF RESIDUAL DIFFERENTIATES GENETICALLY ASSOCIATED WITH ORES

In this section of the paper it is proposed to illustrate by reference to some ore metals with particular associations how the characteristics of crystalline rocks may be used as guides in exploration. Undoubtedly ore deposits of some metals may arise through several genetic concentration processes as we have the example of copper occurring in magmatic sulfide segregations, hydrothermal deposits and probably in sedimentary sulfide occurrences. However, in these cases the geological environment is generally quite different for each type of ore occurrence and in applying exploration principles on the lines set out in this paper the general geological character of the terrain should always be considered.

Acid Igneous Crystallates

It has long been accepted that many ore deposits are associated genetically with acid igneous rocks. Emmons (9) for example estimates that 90 percent of hydrothermal deposits are genetically related to granite batholiths. The origin of granite is controversial and for the purpose of this paper the writer follows the views of Turner and Verhoogen (17) and adopts their definition of igneous.

The genetic associations of a particular ore type with a particular acid crystallate is harder to establish than for such ores as the magmatic oxide and sulfide segregations so closely associated with basic and ultra-basic crystallates, by reason of the fact that hydrothermal deposits may be localized far from any igneous contact. Because of this, many references to the associations of ores with granitic rocks are very broad and often refer merely to the general petrological character of an intrusive body. Batholiths or smaller plutons within which granitic rocks are contained are generally composite and there is commonly a considerable range in the chemical and mineralogical composition of individual crystallates, whether these are hybrids or differentiates. Few detailed studies have been made concerning the question of which particular acid differentiates might be associated with particular ore types. Some studies, such as that by Lovering and Goddard (13), have indicated how stages of petrological differentiation show a relation to ore types in a mineral belt. The writer considers that it would be unreasonable to expect that differentiation in acid magmas does not have a similar influence in controlling ore type as in basic rocks where it is more obviously displayed. The chemical and mineralogical character of each differentiate as it crystallizes is considered to have a significant influence on the type of metals that may be fractionated and collected to form ore fluids.

Tin and Granites.—The association of tin with granite provides one of the most consistent examples of the association of ore bodies of a particular element with a particular type of igneous rock. Ferguson and Bateman (10) in an early review showed that in 40 out of 41 tin bearing regions, ore deposits were associated with acid intrusives. Westerveld (21), in reviewing this single exception in the light of later work, showed that there were grounds for presuming that in this also acid rocks may be genetically related. Thus the relation is universal and when the many individual deposits in each province are also considered the relationship of tin to acid crystallates is seen to be extremely close.

Tin is presumed to accumulate in residual acid magmas and a geochemical explanation is advanced by Ringwood (14) in terms of the relative electronegativity of the Sn^{2+} ion and of complex ion formation for the Sn^{4+} ion in magmas. While these arguments apply to some degree there seems to be other factors that control the fractionation of tin within acid magmas themselves. In this discussion the writer is not considering the collector mechanisms such as pneumatolytic or hydrothermal fluids that may collect tin but why tin is fractionated and available for collection.

One feature of tin occurrence is that though tin deposits are invariably associated with granitic rocks the converse is by no means true. Thus many granites including acid types superficially similar to stanniferous granites and occurring in the same general regions, have no associated tin occurrences. Some writers have considered this to be due to the degree of erosion relative to the roof of intrusive bodies, because of the observed localization of tin deposits near roof contacts. Although this erosion hypothesis no doubt applies in certain districts there are many instances where acid intrusives are unroofed or only partially unroofed and yet carry no tin. Sullivan (15) has used the distribution of stanniferous granites as argument in support of his views on ore and granitization. His view is that tin deposits occur in later periods of geological time by reason of granitization in areas where tin has been progressively added to the crust by vulcanism. Sullivan's arguments are not all critically based as has been shown in the discussion by Edwards and Gaskin (7).

The writer has been studying the characteristics of acid igneous rocks associated with tin within Australia, which was once an important producer and has many provinces particularly over a belt 3,000 miles in length, stretching from North Queensland to Tasmania. In this region deposits are associated with batholiths that are generally of huge dimensions, composite in nature and would be classed as subsequent intrusions. In these batholiths the rocks described as tin granites, that is, those having the closest presumed genetic relationship to the tin deposits on field associations, are late differentiates in the composite intrusive bodies and are typically much subordinate in volume to more basic granitic types. A highly acid nature shown by the SiO_2 content expresses the stage of differentiation but from the point of view of the genesis of the tin deposits the SiO_2 content may not be as significant as the relatively high alkali content relative to cafemic constituents which also characterizes the tin granites. In this respect the sequence of association of major elements with minor elements in mineral structures which DeVore (5) has recorded may be significant. The closest agreement between Sn and the major elements shows the following order of decreasing affinity Mg-Ca-Na-K. Whether the affinity of tin for these elements in mineral structures is to be explained in terms of an adsorption mechanism or by other principles, if this relationship holds it could be of significance in understanding the genesis of tin deposits. If differentiation of an acid magma trended in such a way that a highly alkaline late magmatic source system was generated, any Sn remaining in this system would only be taken up to a limited degree by the alkali-bearing felspars and micas and the residue would be available for collection by the generally accepted collector mechanisms of pegmatitic, pneumatolytic, and hydrothermal fluids. If however, the trend of differentiation was such that crystallization was effectively completed without any significant volume of highly alkaline late magmatic fraction developing, tin could be accepted into some silicate mineral components to a greater degree because of the higher Ca and Mg content. The absolute fixation of tin in any of the minerals of granites need not of course be great, as we are dealing with huge volumes of

source material, and in such case, small differences in the relative affinities between Ca-Mg and K-Na bearing minerals is important.

The above argument was tested from both qualitative and quantitative aspects with Australian granite masses. The batholiths with which tin is associated such as the New England and Blue Tier masses show a trend of differentiation through granodiorite, hornblende and biotite granites to alkaline acid types which have been termed the tin granites.

Batholiths with which no tin ores are known to be associated such as the Kanimbla Batholith of New South Wales are differentiated but differentiation has not resulted in the production of significant volumes of late crystallates with a high K + Na to Ca + Mg ratio. In so far as areal expression allows the comparison, the size of individual masses of tin granite in the tin-bearing batholiths show a relationship to the amount of free tin associated as gauged from the number and size of primary and placer deposits of consequence. Thus the tin granite of Stanthorpe Queensland, covers tens of square miles and has associated many deposits. This district was an important producer, whereas small bodies at Gundle, N.S.W. connected with the same batholithic intrusion have small occurrences from which little tin has been won. Likewise the Kanimbla Batholith considered to be non-stanniferous has no economic deposits associated, but small aplitic veins that most closely approach the composition of the tin granites of stanniferous batholiths carry some free cassiterite.

Throughout the granite masses the higher the ratio of K + Na to Ca + Mg in acid differentiates the greater is the frequency that cassiterite occurs as a free accessory constituent in orthomagmatic rocks and the less the trace tin content in the total silicate mineral components. This confirms the greater degree of fixation of Sn with Ca and Mg in accord with DeVore's major element sequence. It is stressed that this data relates to crystallates that have not been autometasomatized by hydrothermal or pneumatolytic alteration.

In attempting to make conclusions, based on a number of provinces in one region, more universal by applying to world wide occurrences the difficulty faced is that in many regions the petrological, mineralogical and chemical data is not critical enough to afford firm support. In many regions geological study has not been detailed enough to make an inference that a particular differentiate is genetically associated with tin deposits and critical analytical data is lacking. Thus the data presented in the papers by Ferguson and Bateman (10) and Westerveld (21) to illustrate the characteristics of granites associated with tin ores is not critical enough in that it includes single analyses from large composite masses and allows no comparisons of the several differentiates in these masses. However, some broad features noted by these writers may be significant as Ferguson and Bateman refer to the tendency for granites in tin provinces to be somewhat low in Ca and Mg content; and Westervelt concludes that tin granites appear to be more or less end stages of differentiation of acid magmas and mentions the tendency for Malayan tin granites to split off differentiates rich in potash felspar. The important Bolivian deposits have a somewhat different environment to other major tin provinces in that they are associated with less acid crystallates. It is not

certain that the exposed rocks are necessarily the direct genetic associates or ore bringers. Chace (3) concludes that the ore-bearing solutions responsible for the tin veins of Central and Southern Bolivia were derived from a common magmatic source as the associated quartz-latite porphyries but mentions that the nature of this source is speculative. It should be noted that conclusions drawn from Australian provinces point to alkali content rather than SiO_2 as the dominant factor controlling fractionation of tin and in this respect the rather low Ca and high alkali content of the quartz-latite porphyries of Oruro with respect to the granodiorite and latite, as mentioned by Chace, and an analysis of granodiorite from the Sorata Batholith (1) showing a higher potash content than Daly's average for granite (4) may be significant.

It appears that certain principles could be enunciated to assist in preliminary exploration for many tin ores, both primary and placer. Tin appears to be fractionated in magmas having a higher proportion of alkalis, particularly potash, relative to calcium and magnesium and tin deposits should be sought in areas where such crystallates occur. In composite batholiths the chance of tin deposits occurring would appear to depend on whether differentiation proceeds in such a way that a significant volume of alkalic magma is produced, which would allow fractionation of tin and collection in sufficient quantities in ore solutions. Such a magma would normally be highly acid but it is stressed that the high SiO_2 content is not necessarily a critical feature.

Copper and Acid Crystallates.—Copper deposits occur in several geological environments but for those hydrothermal deposits associated with acid igneous rocks there are some empirical grounds for assuming that the less acid crystallates such as granodiorites are genetically related to copper. Thus Buddington (2) draws a relationship between the more basic character of intrusions on the western margins of the Coast Range Batholith and the copper occurrences localized in that district. Within Australia one of the few major producing copper mines closely adjacent to an intrusive body is Mt. Morgan where the orebodies adjoin a granodiorite, the "Mount Morgan Granite." Many small intrusive bodies similar in mineralogy and chemistry to the "Mount Morgan Granite" in eastern Australia are also characterized by a copper association that is distinct but generally uneconomic.

The observed geological association is strengthened from the genetic aspect by the trend of affinity of copper with the major elements in mineral structures which DeVore (5) records in decreasing degree of association as Mg-K-Na-Ca. Thus we may expect a magmatic differentiate rich in Ca and Na, such as one that crystallizes with an abundance of plagioclase, would in crystallizing not accept copper in mineral structures to as great a degree as one characterized by potash felspars, and thus release this metal for collection and ore deposition.

The Cu-Pb-Zn Association and Acid Crystallates.—Wilson (20) has referred to the common association of copper, zinc, and lead in ores and suggests that the similarity of occurrence of these metals in ores and igneous rocks is suggestive of a genetic relationship. This is confirmed by the fact that the three elements have a common sequence of order of affinity with

major elements that DeVore has given as Mg-K-Na-Ca in decreasing order of association. Thus fractionation of all three elements might be expected in acid crystallates with an abundance of Ca and Na. The fact that a similar order of association exists for the three elements does not however imply that each major element in the sequence has the same absolute affinity for each of the three ore metals and the reasons for distinct Cu, Cu-Zn, Zn-Pb-Cu, and Zn-Pb associations in ore types in different districts might be due to differences in absolute affinities of the major elements with the ore metals when considered in terms of the general chemistry of particular magmatic fractions.

Zoned Deposits, Complex Ores and Paragenetic Sequences in Ores.—The theme of the discussion has been that separate magmatic fractions may be considered to constitute during crystallization systems that are sufficiently closed to allow fractionation and indirectly collection of a particular metal or metals. This concept does not necessarily conflict with zonal theories where zoned deposits are displayed, or the occurrence of composite ores and paragenetic sequences in ores, as these features are essentially depositional. Thus it is possible that the chemical composition and physical environment of some acid magmas during crystallization is such that the interplay of affinities between major and minor elements leads to several ore metals being fractionated and ore fluids may carry several metals from which deposition could occur in terms of the zonal theory. Alternatively different crystallates could give rise to different ore solutions and a zonal attitude could result from independent deposition from the several ore fluids being controlled by the thermal gradient about the composite intrusive mass. Crystallization of quite different chemical fractions might also be taking place contemporaneously in a composite body through such factors as heterogeneity in the melt or hybridization, and ore solutions from these fractions might mingle to give on deposition zoned deposits. Complex ore types and paragenesis in ores could be explained by similar arguments.

Basic Crystallates

The association of base metals with basic magmas has been discussed by Wilson (20) and while his geological associations of specific elements with specific stages of differentiation is not questioned his geochemical explanations are not necessarily accepted by the writer. It is not proposed to retrace all of the ground covered by Wilson, but reference is made to one example to illustrate differences in principles used to explain empirical geological associations.

Chromite Ores.—Chromite may be taken as representative of early magmatic oxide crystallates that are generally accepted as segregating from basic magmas. Wilson uses the lithophile nature and ionic radius of Cr^{3+} to explain why chromium fractionates as the oxide in the silicate phase at an early stage in the crystallization of ultrabasic rocks. The enrichment of Cr^{3+} in early formed oxides at the expense of ions of similar character V^{3+}, Fe^{3+} and Ti^{3+} is attributed purely to the smaller ionic radius of Cr^{3+}. Ringwood suggests that this behavior cannot be so explained and proposes that preferential

concentration of Cr^{3+} with respect to Fe^{3+} is due to the small electronegativity of Cr^{3+}.

Chromium also enters into magnesium rich silicate minerals but reasons for this are also conflicting. Goldschmidt (11) and several later workers explained this in terms of camouflage at regular lattice sites in lieu of Mg^{2+} whereas Ringwood (4) suggests that Fe^{2+} is the element replaced. DeVore (5) argues that an adsorption mechanism best explains the concentration of Cr^{3+} in magnesium-rich minerals.

Despite the divergences in explaining the geochemical behavior of chromium the empirical data is sufficiently well known to enunciate exploration principles for chromite deposits. Because of the strong tendency for chromium to enter early formed oxide and silicate minerals of basic magmas the metal is rapidly extracted from melts and economic deposits must therefore be sought in association with ultrabasic magmas.

Both oxide and silicate differentiates may have significant characteristics that point to whether chromite deposits may or may not occur.

The highest chromium content and Cr:Fe ratio in oxide minerals is to be expected in the earliest magmatic oxide differentiate and if this does not indicate an economic quality for the chrome-bearing oxides no better can be expected in the same body or later formed oxide segregations. In silicate differentiates a high trace Cr content in the magnesium bearing minerals is to be expected whether associated with ore or not. However a high dispersed chromite content in the silicate differentiate may indicate that concentration of oxide has not occurred.

METAMORPHIC AND METASOMATIC CRYSTALLATES

The preceding discussion has related to igneous rocks but the writer considers that it would be unreal, in the light of field and laboratory evidence concerning metamorphic and metasomatic transformations that are most obviously displayed in the redistribution of major component elements, not to expect significant changes in the distribution of minor elements during recrystallization. There has been much controversy over possible collector mechanisms that could transport metals, fractionated during metamorphic processes, to form ore deposits but there is increasing acceptance by geologists of "wet" mechanisms that have been proposed.

The writer considers that, in general, similar principles could be applied to fractionation of metals during crystallization whether igneous, metamorphic, or metasomatic. Thus, though van Bemmelen (21) inclines to transformist views in explaining the origins and variation of certain Indonesian granites, in view of the data recorded by DeVore there seems no reason why tin should not be fractionated during metasomatic transformations leading to the production of an high alkali acid crystallate or fixed in a less alkaline crystallate.

The metal groupings of DeVore (6) and conclusions he has drawn from these may provide a basis for determining the characteristics of metamorphic rocks associated with ore deposits in some metamorphic terrains. DeVore

(5) has indicated how titaniferous deposits may be derived from granulation and recrystallization of plagioclases of anorthosite.

CONCLUSIONS

In known mineralized fields the basic guides of the exploration geologist such as structural and stratigraphic control of ore deposition have long been used with success. In virgin or poorly explored areas however, these controls are lacking and it is considered that the characteristics of crystallates in igneous or metamorphic terrains may provide an indicator that particular metals may have fractionated during crystallization and provided a source for economic metals in ore deposits. Such characteristics would rarely provide guides to the specific localization of mineral deposits except in special cases such as magmatic oxide and sulfide segregations associated with basic magmas or tin-bearing autometasomatized rocks near the roofs of acid intrusives. However, residual characteristics of crystallates could be useful in restricting areas for employing detailed exploration techniques applicable to depositional characteristics of ore deposits.

Detailed qualitative and quantitative studies on the geochemistry of crystallates associated with specific ore types are few, but present data indicates that when these are more advanced reliable genetic ore guides may result.

NEWCASTLE UNIVERSITY COLLEGE,
UNIVERSITY OF NEW SOUTH WALES, AUSTRALIA,
April 19, 1960

REFERENCES

1. Ahfeld, F., 1932, Die Erzlagerstatten in der tertiaren magmaprovinz der bolivia-nischen Zentralanden: Neues-Jahrb. Für Min., Geol. und Paläont, v. 65, Beil-Bd. 4, p. 208–319.
2. Buddington, A. F., 1927, Coincident variations of types of mineralization and of Coast Range intrusives: ECON. GEOL., v. 22, p. 158–179.
3. Chace, F. M., 1948, Tin-silver veins of Oruro, Bolivia: ECON. GEOL., v. 42, p. 333–383, 435–470.
4. Daly, R. A., 1933, Igneous Rocks and the Depths of the Earth: McGraw-Hill Book Co., New York.
5. DeVore, G. W., 1955a, The role of adsorption in the fractionation and distribution of elements: Jour. Geology, v. 63, p. 159–190.
6. ——, 1955b, Crystal growth and the distribution of elements: Jour. Geology, v. 63, p. 471–494.
7. Edwards, A. B., 1956, The present state of knowledge and theories of ore genesis: Aust. Inst. Min. Met. Proc., No. 143, p. 69–116.
8. Edwards, A. B., and Gaskin, A. J., 1949, Discussion of paper by Sullivan: ECON. GEOL., v. 44, p. 234–241.
9. Emmons, W. H., 1933, On the mechanism of the deposition of certain metalliferous lode systems associated with granitic batholiths: A.I.M.M.: Ore deposits of the Western States, p. 327–349.
10. Ferguson, H. G., and Bateman, A. M., 1912, Geologic features of tin deposits: ECON. GEOL., v. 7, p. 209–262.
11. Goldschmidt, V. M., 1937, The principles of distribution of chemical elements in minerals and rocks: Jour. Chem Soc., p. 655–673.
12. King, H. F., 1958, Notes on ore occurrence in highly metamorphosed Precambrian rocks: Austr. Inst. Min. Met., Stillwell Memorial Volume, p. 69–116.
13. Lovering, T. S., and Goddard, E. N., 1938, Laramide igneous sequence and differentiation in the Front Range, Colorado: Geol. Soc. America Bull., v. 49, p. 35–68.

14. Ringwood, A. E., 1955, The principles governing trace element distribution during magmatic crystallization: Geochim. et. Cosmochim. Acta, v. 7: Pt. I, p. 169–209; Pt. II, p. 242–254.
15. Sullivan, C. J., 1948, Ore and granitization: Econ. Geol., v. 43, p. 471–498.
16. Turneaure, F. S., 1955, Metallogenetic provinces and epochs: Econ. Geol., Fiftieth Anniversary Volume, Pt. I, p. 38–39.
17. Turner, F. J., and Verhoogen, J., 1951, Igneous and Metamorphic Petrology: McGraw-Hill Book Co., N. Y., p. 602.
18. Van Bemmelen, R. W., 1949, The Geology of Indonesia, The Hague.
19. Vogt, J. H. L., 1923, Nickel in igneous rocks: Econ. Geol., v. 18, p. 307–353.
20. Wilson, H. D. B., 1953, Geology and geochemistry of base metal deposits: Econ. Geol., v. 48, p. 370.
21. Westerveld, J., 1936, The granites of the Malayan tin-belt compared with tin-granites from other regions: Royal Acad. Amsterdam Proc., Vol. XXXIX, p. 1199–1209.

Economic Geology
Vol. 55, 1960, pp. 1285–1290

A BAUXITE DEPOSIT IN THE PALEOZOIC OF LEON, SPAIN

M. FONT-ALTABA AND J. CLOSAS M.

ABSTRACT

The recent discovery of a bauxite deposit in Portilla de Luna, province of Léon, Spain, in the Paleozoic, differs from other Spanish deposits. Its mineralogy, geology, and origin is therefore of interest.

A chemical analysis of an average sample gives the following composition: Al_2O_3 47.9%, SiO_2 15.4%, Fe_2O_3 0.3%, CaO 1.3%, MgO 0.4%, weight loss at 800° C 36.5%.

The minerals present, identified by X-rays and differential thermal analysis, are gibbsite (54–58%) and halloysite (38–32%).

The deposit lies in middle Devonian, Eifelian sup., and is considered to have been formed by laterization of clays through the combined action of microorganisms and a humid climate. Later metamorphic action produced partial crystallization of the material. Similar deposits occur in Iss and Serov in the middle Urals (URSS).

In 1957 a bauxite deposit was found near Portilla de Luna, province of León, Spain. This deposit is unusual since it is in Paleozoic strata, in contrast to all other Spanish and European deposits, which are always found in Eocene and Oligocene. Bateman in his "Economic Mineral Deposits" states the deposits of Tikhvin, Russia, are the only known Paleozoic bauxite deposits (5). For this reason a study of its mineralogy, geology, and origin is presented.

MINERALOGY

The material is composed of a white mass dotted with black spots, which in places are irregularly concentrated. It reduces to a fine powder with a slight pressure of the fingers. Chemical analyses of two white samples (2 and 3) with few black plots, and another one of slightly yellowish color, are given in Table 1.

A detailed study shows that the analyzed samples are composed chiefly of hydrated aluminum oxide and hydrated aluminum silicate, with coaly material, and small quantities of calcium and magnesium carbonates and ferric hydroxide.

X-rays Study.—The hydrated aluminum oxides found in the deposit are: gibbsite, $Al_2O_3 \cdot 3H_2O$, considered as $\gamma - Al(OH)_3$ (monoclinic), and boehmite or diaspore, $Al_2O_3 \cdot H_2O$ (rhombic), (22). The X-ray identification is as follows: gibbsite has two strong diffraction lines at 4.83 and 4.34 *kX*, which do not exist in the monohydrates; boehmite has a characteristic diffraction line at 6.14 *kX*, and diaspore at 3.98 *kX* (4).

The hydrated aluminum silicate is evidently a kaolin mineral. The series kaolinite-nacrite-dickite are distinguished by the basal reflections 001 and

TABLE 1

	Sample 1 %	Sample 2 %	Sample 3 %
Al_2O_3	49.70	44.61	47.92
SiO_2	13.20	14.26	15.43
Fe_2O_3	1.10	0.35	0.28
CaO	1.39	1.37	1.29
MgO	2.44	3.08	0.42
TiO_2	Traces	Traces	Traces
Weight loss at 800° C	32.95	36.87	36.55
	100.78	100.54	101.89

002 at 7.14 *kX* and 3.57 *kX*, respectively. These basal reflections in metahalloysite are generally very wide, and the intensity of the 020 band reflections is stronger than the other diffraction lines. The hydrated halloysite is recognized by its strong 001 basal reflection at 10.1 *kX*, which becomes 7.4 *kX* when the mineral is heated to 100° C, or it is placed in a dry atmosphere or in the vacuum (4, 8).

In the study of the X-ray diagrams of different samples of the minerals of the deposit, the following is observed:

1. Two strong reflections at 4.82 and 4.37 *kX*, and two others of half intensity at 2.455 and 2.385 *kX*, typical of gibbsite;

2. The diffraction lines at 10.2, 2.564 and 1.480 *kX*, typical of halloysite; and

3. That the reflection at 10.2 *kX* disappears when the material is heated at 110°C.

TABLE 2

No.	a) Unknown		b) Gibbsite (3)		c) Halloysite (3)	
	d kX	I/I_1	*d kX*	I/I_1	*d kX*	I/I_1
1	10.4	10			10.1	10
2	4.82	9	4.83	10		
3	4.37	10	4.337	6	4.422	10
4	3.32	6	3.303	3	3.366	6
5	3.16	1	3.165	2		
6	2.564	3			2.559	7
7	2.445	4	2.451	5		
8	2.385	4	2.374	5		
9	2.232	2	2.236	2	2.218	1
10	2.166	2	2.157	3		
11	2.032	4	2.039	4		
12	1.981	4	1.986	3		
13	1.918	2	1.909	3		
14	1.788	3	1.797	4		
15	1.747	3	1.743	4		
16	1.683	5	1.677	4	1.678	5
17	1.480	5			1.481	8
18	1.455	2	1.452	4		
19	1.408	2	1.405	3		

The coincidence of the X-ray diagrams of the material under study with gibbsite and halloysite diagrams can be seen in Table 2.

Differential Thermal Analysis.—The d.t.a. has been carried out on an average sample of the mineral. The curve obtained is shown in Figure 1. Three endothermic peaks at 168°, 330°, and 562° C, and one exothermic at 971° C are observed.

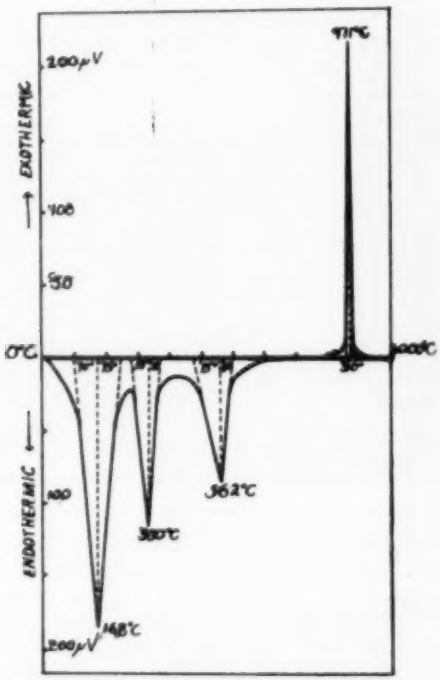

FIG. 1. A. t. d. curve of a sample of bauxite.

The first of the endothermic peaks has a symmetrical form and a higher intensity than the rest; it begins between 100°–105° C and finishes between 240°–245° C, yielding its highest value at 168° C. The peak width is 145° C and the amplitude 185.3 μV; the slope ratio is 1.

The second one, of regular almost symmetrical form, slope ratio 1.5, begins at 275° C and finishes between 360°–365° C, with its highest value at 330° C. The peak width is 90° C and the amplitude 117.7 μV.

The third endothermic one is disymmetrical, with the slope ratio of 2.5. It begins between 485°–490° and finishes at 590° C, with its highest value at 562° C. The peak width is 105° and the amplitude 86.1 μV.

The exothermic peak of strong intensity, is symmetrical, slope ratio 1,

beginning at 955° C and finishing at 985° C, with the highest value at 971° C. The peak width is 30° C and the amplitude 218 μV.

In the interpretation of the curve the following points have been considered (18, 21):

1. The exothermic peak at 971° C is characteristic of the minerals of the kaolin group (18);

2. The endothermic peak at 562° C is the one produced by the elimination of the combined water in the kaolinitic minerals, and permits identification of the minerals of the group among themselves; allophane has no peak, and kaolinite has one at 600° C, nacrite at nearly 700° C, and halloysite at 570° C; as for the form, the slope ratio for kaolinite is 1.55 (average value) and for halloysite it is between 2.40 and 3.20 (18);

3. The endothermic peak at 168° C, corresponds to the one of the hydrated halloysite (18);

4. The endothermic peak at 330° C, corresponds to the most characteristic one of the gibbsite d.t.a. curve (21).

From these points it is concluded that the sample is composed of gibbsite and halloysite, which is in accordance with the results of the X-ray analysis.

Quantitative Mineralogical Composition.—The semiquantitative valuation carried out by X-rays and d.t.a. gives the result, 54–58 percent of gibbsite and 32–38 percent of halloysite.

The estimated molecular composition from the chemical analysis is gibbsite 56.10 percent, halloysite 35.15 percent, coaly material 5.10 percent, impurities ($CaCO_3$, $MgCO_3$, Fe_2O_3) 3.55 percent, which agrees with the above mentioned.

GEOLOGY

The deposit is lenticular shaped interstratified and is about 250 m long and 0.80–1.00 m. thick. It is underlain by very fragile clay slates and overlain by fossiliferous limestone. The ensemble has a rather pronounced dip, and trends at NNE. The outcrop is in the surroundings of Portilla de Luna, towards the hill of Cullacorros, and below Peña de los Machaos (Fig. 2).

The footwall slates contain abundant but poorly preserved fossils, which Dr. J. F. Villalta has identified as *Uncinulus Orhignyanus Vern., Uncinulus Princeps Barr., Cyathocrinites Pinnatus Gold.*, and plenty of indeterminable corals, with forms that resemble *Zaphrentis*. These fossils place the slates in the Eifelian inf., with facies of shallow waters in a cold climate.

The limestones of the roof contain *Hexacrinus* sp., *Atrypa Reticularis* Lin., *Fenestrella* sp., and *Fenestrellina* sp., forming the Givetian limestone of Portilla, as indicated by Compte (11, 12, 13, 14, 15, 23, 1). Although dips are difficult to recognize, there appears to be a disconformity between the two strata. Thus, in the middle Devonian, Eifelian sup., there is a short stratigraphic break where laterization of the subjacent clays took place.

This laterization was at the expense of a clay of the following composition: Al_2O_3 27.43%, SiO_2 44.10%, Fe_2O_3 11.63%, TiO_2 0.90%, weight loss at 800° C 11.97% which was probably laid down in a shallow basin, perhaps

on the coast. There it would have undergone the almost total loss of iron by the action of microorganisms (25, 9, 10), and also a greater hydration of the clay by the climatological and humic action, resulting in a white coalish bauxite.

This material has undergone later some metamorphism during orogeny, which produced a partial crystallization of its constituents.

FIG. 2. The Portilla de Luna valley from the hill of Cullacorros; Portilla in center. Right side is north. E, Eifelian slates; H, bauxite deposit; G, Givetian limestone; V, Vizean slates.

We have looked for other occurrences of similar deposits, but the only ones we found are the Russian bauxite in the Urals (19, 7), which we do not know about in detail. It is interesting to mention the deposits in Iss and Serov of the middle Urals (17), which occur in the Eifelian-Givetian, as in our case, and in the Septentrional Urals in the basement of the Urasnaya-Shapocka Givetian.

ACKNOWLEDGMENTS

The authors thank Dr. Coronas, Professor of Inorganic Chemistry at the University of Barcelona, for kind permission to use the d.t.a. instrument, and Dr. Pujol for his co-operation in obtaining the d.t.a. curve.

DEPARTAMENTO DE BARCELONA
INSTITUTO DE EDAFOLOGÍA Y FISIOLOGÍA VEGETAL
UNIVERSIDAD DE BARCELONA (NÚCLEO DE PEDRALBES)
BARCELONA, SPAIN.
February 26, 1960

REFERENCES

1. Almela, A., 1951, Delimitación del carbonifero de la zona La Robla-Vegarienza (León): Bol. Inst. Geol. Min. Esp., v. 63, p. 219–256.
2. Ansheles, I. M., 1927, Mikroskopicheskoye issledovaniye glin. peskov i boksitov, Cherepovetskoy gubernii: SSSR Geol. Kom. Izv., v. 46, p. 113–140.
3. Arkhangel'sky, A. D., 1933, Kvoprosu ob usloviyakh obrazovaniya boksitov v SSSR, Moskow Obshch. ispytateley Prirody, v. 41, Geol. Ser. 11, p. 405–436.
4. A. S. T. M. X-ray powder data filled card, no. 5-0190, 7-324, 2-0043, 5-0143, 5-0144, 6-0221, 7-350, 3-0041, 2-0088.
5. Bateman, Alan M., 1951, Economic Mineral Deposits, 2nd edition: John Wiley and Sons, New York, p. 219; Spanish edition, 1957, p. 243.
6. Bemmelen, J. M. van, 1904, Beitrage zur Kenntnis der Verwitterungs produkte der Silikate in Ton-Vulkanischen und Laretit-Boden: Anorg. Ch., v. 42, 3, 265–314.
7. Berg, L., 1948, Oproiskhozhdenii Ural'skikhpaleozoyskikh boksitov: Akad. nauk. SSSR, Izv. Ser. Geol., Moskow, v. 37, p. 127–140.
8. Brindley, G. W., 1951, The kaolin minerals: X-ray identification and crystals structures of clay minerals: The Mineral. Soc., London, p. 32–75.
9. Choubert, B., Stephane, H., and Betremieux, R., 1952, Essais de purification de bauxites riches en constituants férrugineux: C. R. A. S., Paris.
10. Closas M., J., 1957, El concepto de bolsada en los yacimientos de bauxita: Publ. Universidad de Barcelona, v. Homenaje póstumo F. Pardillo, Barcelona.
11. Compte, P., 1936, La serie Dévonienne du Léon: C. R. A. S. Paris, v. 202, p. 397.
12. Compte, P., 1936, Le Dévonien moyen et supérieur du Léon: C. R. A. S. Paris, v. 202, p. 1198.
13. Compte, P., 1938, Les facies du Dévonien supérieur dans la Cordillère cantabrique: C. R. A. S., v. 206, p. 1496.
14. Compte, P., 1938, La transgression du Famennien sup. dans la Cordillère cantabrique: C. R. A. S. Paris, v. 206, p. 1741.
15. Compte, P., 1939, La structure du bord sud de la Cordillère cantabrique en Léon et les mouvements orogéniques qu'elle revèle: C. R. A. S. Paris, v. 208, p. 2008.
16. Delepine, G., 1932, Sur l'extension des mers paléozoiques en Asturies (Espagne): C. R. A. S. Paris, v. 195, p. 1401.
17. Gladkovsky, A. K., 1942, Eifelian and Givetian bauxite deposits of Iss and South parts of Serov districts and lower: Akad. nauk. SSSR, Izv. Ser. Geol., Moskow, v. 37, p. 35–46.
18. Holdridge, D. A., and Vaughan, F., 1957, The kaolin minerals: The differential thermal investigations of clays: The Mineral. Soc., London, p. 98–139.
19. Krotov, B. P., 1941, Rôle and significance of epirogenetic movements in the formation of deposits of iron and manganese ore and bauxites: Akad. nauk. SSSR Doklady, Moscow, v. 33, p. 54–56.
20. Lotze, F., 1945–1950, Algunos problemas de la meseta Ibérica: Publ. Extr. Geol. Esp., Madrid.
21. Mackenzie, R. C., 1957, The oxides of iron, aluminum, and manganese: the differential thermal investigation of clays: The Mineral. Soc., London, p. 299–328.
22. Rooksby, H. P., 1951, Oxides and hydroxides of aluminum and iron: X-ray identification and crystal structure of clay minerals: The Mineral. Soc., London, p. 244–265.
23. Sitter, L. U., 1945–1950, El dessarrollo del Paleozoico en el Noroeste de España: Publ. Extr. Geol. Esp., Madrid.
24. Stolyar, M. Ya, 1945, On further search after Paleozoic bauxites in the mountain ranges of the Kuznetsk basin: Akad. nauk, SSSR, Izv. Ser. Geol., Moskow, v. 37, p. 149–162.
25. Vinogradov, A. P., 1942, Descomposition of kaolin by diatoms: Akad. nauk. SSSR, Izv. Ser. Geol., Moskow, v. 37, p. 135–138.

Economic Geology
Vol. 55, 1960, pp. 1291–1302

RELATIONSHIP BETWEEN THE STRATIGRAPHY AND PETROGRAPHY OF POTTSVILLE SANDSTONES AND THE OCCURRENCE OF HIGH-ALUMINA MERCER CLAY[1]

E. G. WILLIAMS

ABSTRACT

Stratigraphic and petrographic study of 32 sections of the Mercer and Connoquenessing formations in western Pennsylvania has shown that certain consistent relationships exist between the presence or absence of high-alumina Mercer clay and the stratigraphy and petrography of underlying outcropping sandstones. In sections where flint or diaspore clays are present, the clay is underlain by 0–150 feet of fine-to-medium-grained, very light-gray Lower Connoquenessing sandstone. In sections where plastic clay or silty claystone occur below the Mercer coal, the clay is underlain by 20–150 feet of fine-grained to conglomeratic, medium-light-gray Upper Connoquenessing sandstone. The distribution of the high-alumina clay is believed to be related to ancient topographic highs where flint clay was deposited directly on the Lower Connoquenessing sandstone. The Upper Connoquenessing sandstone was deposited in adjacent topographic lows, while the flint clay still present on the topographic highs was leached to form diaspore. Areas where the Upper Connoquenessing sandstone is thin or absent would be the most favorable regions for further prospecting for high-alumina Mercer clay in western Pennsylvania.

INTRODUCTION

High-alumina flint and diaspore clay found below the Mercer coal is one of the valuable mineral resources of western Pennsylvania. The purpose of the present investigation was to determine whether the rocks associated with the Mercer clay have any distinctive properties that might be useful in clay prospecting. Most of the effort was concentrated on the Pottsville sandstones below the Mercer coal, because these rocks outcrop most commonly and would therefore be most useful in reconnaissance exploration.

Thirty-two complete or partial sections of Pottsville rocks were studied by field and laboratory methods. In eighteen of the sections the Mercer coal was underlain by either diaspore or flint clay or both, whereas in fourteen sections, the Mercer coal was underlain by plastic clay, shale or siltstone. The locations of the sections and major structures are shown in Figure 1.

The validity of some of the conclusions reached in this study depend upon accurate and independent field correlations of the Mercer coal and the several underlying Pottsville sandstones. Correlation of the Mercer coal was based on the work of Williams (7), Williams and Nickelsen (8) and Weitz (6). Correlations of the Pottsville sandstones were made on the basis of field

[1] Contribution No. 59-58 from the College of Mineral Industries, Pennsylvania State University.

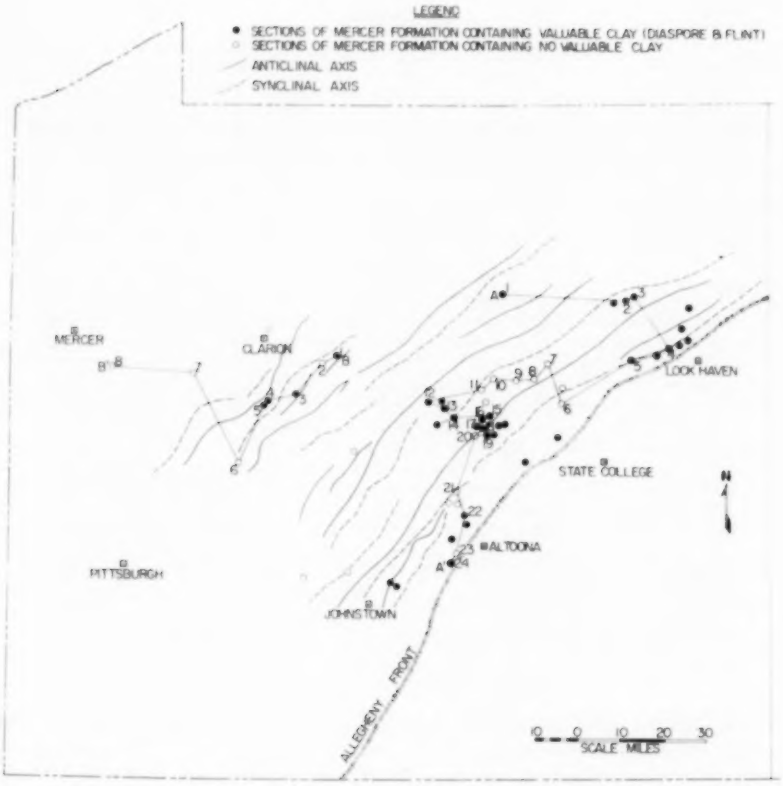

FIG. 1. Index map of section localities. (Structural axes after Fettke, 1954). (Note: The black circle above 14 should be open.)

descriptions, which included color, grain size, and mineralogy. The Pottsville sandstones below the Mercer coal were sampled and analyzed by thin-section heavy mineral and X-ray diffraction techniques. A total of 121 samples were studied.

STRATIGRAPHY

A generalized section of outcropping rock in the area of study is shown in Figure 2. The Pottsville Group, which contains the Mercer coal and high-alumina clay, consists of two formations: the Mercer above and the Connquenessing below. The Mercer formation consists of a complex, variable sequence of coals, clay, dark shales, and sandstone. The principal coals are the Lower and Upper Mercer, which are identified by characteristic fossils and concretions that occur in shales above them (Williams and

Nickelsen, 1958). The flint and diaspore clay occurs below the Lower Mercer coal.

The Connoquenessing formation consists of two sandstone members, the Upper and Lower Connoquenessing, which are separated by a thin coal or coaly shale, the Quakertown. The stratigraphic position of these beds is shown in Figure 2. In the sections studied, the Lower Connoquenessing is

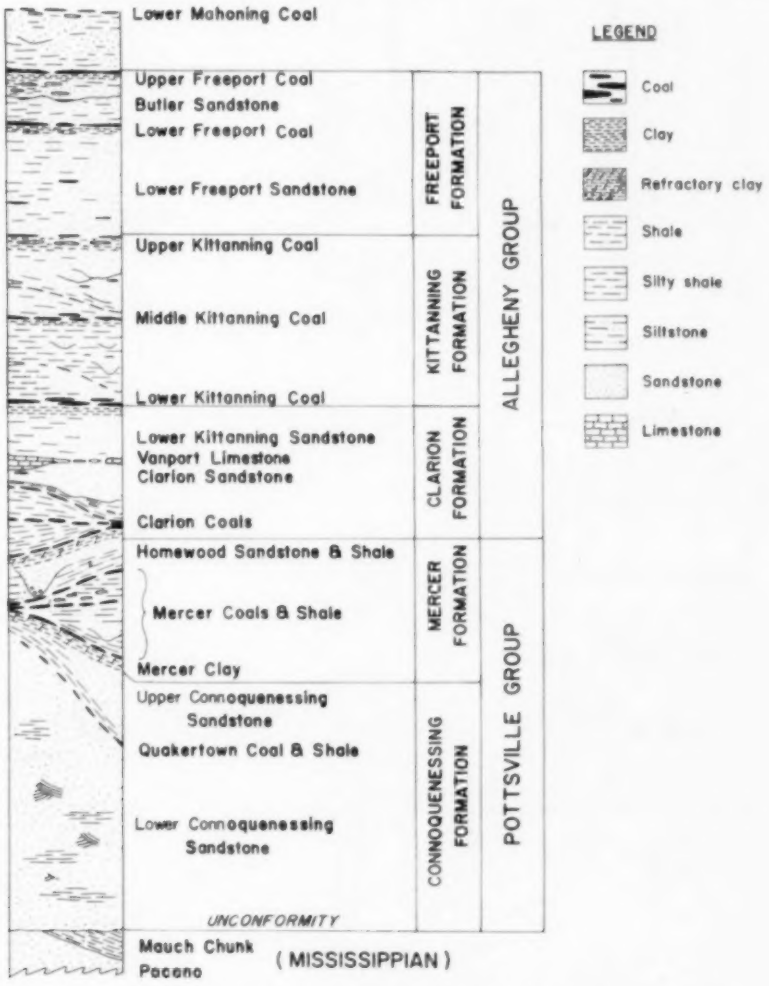

FIG. 2. Generalized diagram of the Pottsville and Allegheny groups in western Pennsylvania.

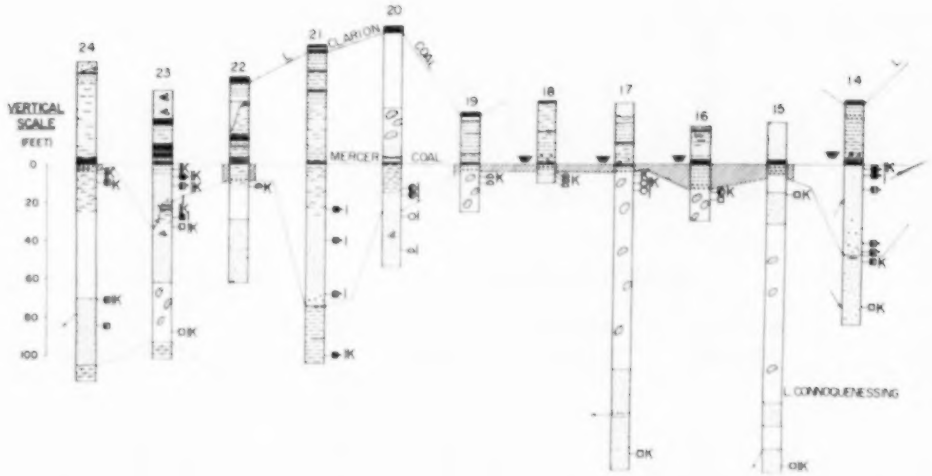

LEGEND

- FINE TO VERY FINE GRAINED SANDSTONE
- MEDIUM GRAINED SANDSTONE
- PEBBLY TO CONGLOMERATIC SANDSTONE
- CONGLOMERATE
- PLASTIC CLAY
- FLINT CLAY
- DIASPORE CLAY
- NON-BEDDED CLAYSTONE
- NON-BEDDED SILTY CLAYSTONE
- SHALE
- SILTY SHALE
- NON-BEDDED SILTSTONE
- BEDDED SILTSTONE
- RED SHALE
- SIDERITE CONCRETIONS
- COAL

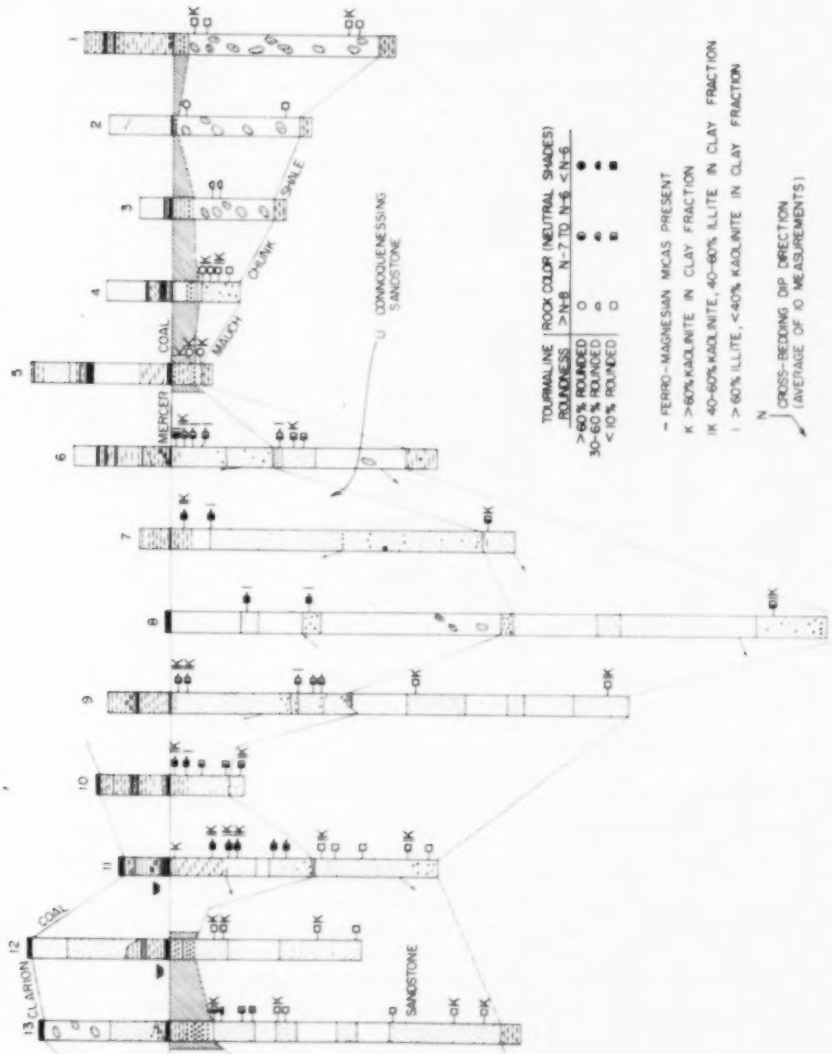

FIG. 3. Correlation diagram of the Pottsville group in the eastern plateau region.

a medium-grained, very-light-gray (N8 to N9), lenticular and cross-bedded sandstone, varying in thickness from a few feet to 150 feet. In the thickest sections, the lower 10 to 15 feet are, in places, coarse grained to conglomeratic. The relationships between the Lower Connoquenessing and the underlying Mississippian Mauch Chunk formation are not well known, but both gradational and disconformable contacts have been observed. The cross-bedding dip direction is generally south.

The Upper Connoquenessing is a fine- to medium-grained, medium- to medium-light-gray (N5 to N7), cross-bedded sandstone, varying in thickness from 0–150 feet. In thicker sections the lower 10 to 15 feet are, in places, conglomeratic. The cross-bedding dip direction is mainly north.

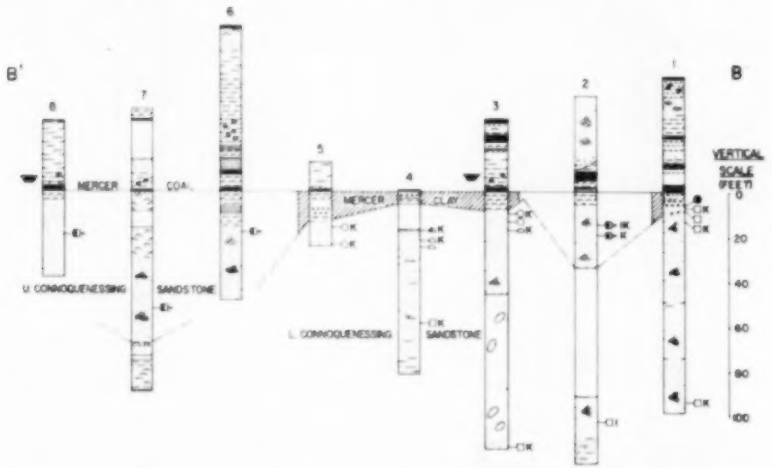

FIG. 4. Correlation diagram of the Pottsville group in the central plateau region.

Correlation diagrams for the Mercer and Connoquenessing formations are shown in Figures 3 and 4. The most important features are the rapid variations in thicknesses of the Upper and Lower Connoquenessing sandstones, and the stratigraphic position of the high-alumina clay relative to these sandstones. In sections where the Upper Connoquenessing sandstone is present, it grades upward into siltstone, claystone or shale. No flint and diaspore clay has been observed in these sections. However, in areas where the Upper Connoquenessing sandstone is absent, the Lower Connoquenessing is abruptly overlain by the high-alumina clay. In some places, fragments of flint clay are found in the upper few feet of the Lower Connoquenessing but there appears to be no intergradation between the clay and sandstone. The lateral relationships of the Mercer flint and diaspore clay have not been observed. However, based on stratigraphic position and the absence of observable disconformities within the clay, it is inferred that at least part

of the high-alumina clay is equivalent in age to the Upper Connoquenessing sandstone.

PETROGRAPHY OF THE CONNOQUENESSING SANDSTONES

Sampling.—The petrography of the Upper and Lower Connoquenessing sandstones was studied in order to obtain quantitative estimates of certain parameters that might be useful in substantiating the field correlations and might be useful as prospecting tools. A total of 121 samples were obtained for petrographic analysis; 39 from the Upper Connoquenessing and 82 from the Lower Connoquenessing. The sampling program was designed to accomplish two main objectives; (1) to obtain estimates of the maximum variation in composition and texture of the respective sandstone members, and (2) to obtain precise information about the upper 20 feet of sandstone below the Mercer coal. Therefore, where possible, samples were obtained from the lower, middle and upper parts of each member with the upper parts sampled in greatest detail.

Methods of Analysis.—All samples were analyzed for the presence or absence of chlorite, biotite and apatite as well as for tourmaline roundness. Selected samples were analyzed for total quartz content, quartz grain size and clay mineral content.

The heavy minerals were obtained by separating the minus 0.50 mm fraction in bromoform. Tourmaline roundness was determined by counting the number of rounded grains (all edges round) in 50 grains of sample.

Total quartz and quartz grain size were estimated in thin section. The quartz content was obtained by the point-count method, counting 300 points per thin section. Quartz grain size was estimated by measuring the long axis of 25 randomly selected grains per thin section.

The clay mineral composition of the sandstones was estimated by X-ray diffraction. Samples were disaggregated by gentle crushing in a mortar and then dispersed in water and allowed to settle for 30 minutes. The less than 7 micron fraction was decanted, poured over a glass slide and evaporated in an oven at 40° C. The oriented clay slides so obtained were X-rayed and the (001) peak areas of illite and kaolinite computed by planimeter. The weight percent of each mineral was assumed to be proportional to the (001) peak areas (5).

Discussion of Results.—As shown in Figure 5, the amount of total quartz in both Upper and Lower Connoquenessing sandstones is negatively correlated with the median grain size in phi units, (positively correlated with median size in millimeters). For a given grain size, the Lower Connoquenessing contains somewhat more quartz than does the Upper Connoquenessing, a feature sometimes useful in differentiating the two sandstones. The grain size of the Upper Connoquenessing decreases upward (Figs. 3, 4) and so does the quartz content. However, in some sections, especially where high-alumina clay is present, the quartz content of the Lower Connoquenessing is higher in the upper few feet. Table 1 shows that in five of six sections studied, the upper sample contained more

quartz than the lower. In two of the five sections showing differences in quartz content the grain size decreases upward whereas in the remaining three sections it increases. The relative concentration of quartz in the upper few feet of the Lower Connoquenessing in these areas might be related to selective sorting on topographic highs and would seem to deserve further study as a possible criteria for predicting the occurrence of high-alumina clay.

The heavy mineral suite of the Lower Connoquenessing is remarkably simple, consisting of tourmaline, zircon, rutile, and opaques, with tourmaline most abundant. Brown and green are the most common tourmaline color types, although blue, pink, black and colorless types have also been observed

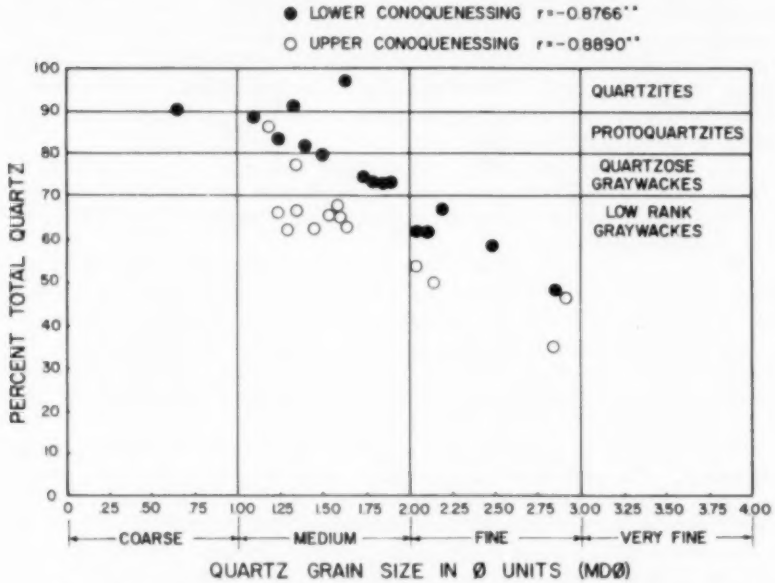

FIG. 5. Graph of the relationship between quartz and grain size in the Lower and Upper Connoquenessing sandstones.

in most samples. The tourmaline grains are angular throughout most of the member. However, in fourteen of the eighteen sections studied in which high-alumina clay is present, the upper 1 to 5 feet of the Lower Connoquenessing contain a relatively high proportion of rounded tourmaline grains. ($> 30\%$ of grains rounded). These relationships are shown in Figures 3 and 4, and for selected samples in Table 1 and and Figures 6A and 6B.

The mechanism for concentrating rounded tourmalines in the described areas is not known. Roundness of the quartz grains in clay areas and non-clay areas is currently under investigation.

The heavy mineral suite of the Upper Connoquenessing member is more complex than that of the Lower Connoquenessing. In addition to tourmaline,

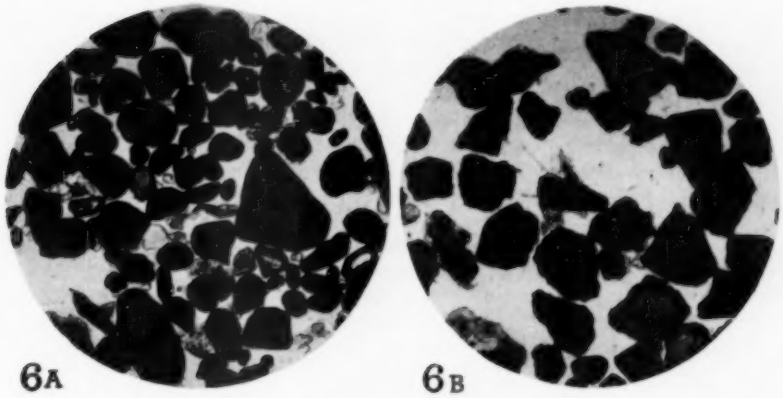

FIG. 6-A. Photomicrograph of rounded tourmaline (dark grains) from Lower Connoquenessing sandstone, 1 ft. below Mercer flint clay. Sample 60-457, 1 mile southeast of Brookville, Pa.; 50×.

FIG. 6-B. Photomicrograph of angular tourmaline (dark grains) from Lower Connoquenessing sandstone, 3 ft. below Mercer flint clay. Sample 60-455, 1 mile southeast of Brookville, Pa.; 50×.

zircon, rutile and opaques, the Upper Connoquenessing contains chlorite, biotite and apatite. Chlorite occurs in 87% of the samples analyzed, biotite and apatite in about 20%. The tourmaline grains are angular except in one section (section 20, Figure 3). Brown and green are the only color types observed.

Kaolinite is the principal clay mineral in the majority of Lower Connoquenessing samples whereas illite is the principal clay mineral in most of the

TABLE I

Sample no.	Locality	Dist. below clay in feet	% Total quartz	$\bar{X}$ size mm	% Round tourmaline
60-459	Climax (4)	1	93	0.21	44
60-460	Climax (4)	43	75	0.26	0
60-472	Mayport (3)	1	76	0.29	76
60-458	Mayport (3)	105	63	0.22	0
60-369	Faunce (17)	3	88	0.29	82
60-422	Faunce (17)	145	77	0.36	4
60-445	Curwensville (13)	2	73	0.45	76
59-780	Curwensville (13)	20	40	0.15	8
60-173	Farrandsville (4)	5	89	0.34	60
60-323	Farrandsville (4)	15	79	0.29	0
60-447	Renovo (2)	4	86	0.43	76
60-448	Renovo (2)	52	85	0.41	16

Upper Connoquenessing samples. In the Lower Connoquenessing the clay occurs mainly as matrix intimately mixed with silica. In the Upper Connoquenessing the clay occurs both in micaceous rock fragments and matrix.

Summary of Petrographic Data.—Table 2 summarizes the frequency of occurrence of the most important petrographic properties of the Lower and Upper Connoquenessing sandstones. Color and presence or absence of chlorite and biotite are the most useful criteria in identifying the respective

TABLE II

SUMMARY OF PETROGRAPHIC DATA

Sandstone member	Chlorite or biotite present	<7 Micron fraction			Color: >N-8*	>30% Rounded tourmaline	>70% Quartz in med. grain size
		>60% Kaolinite	Kaolinite =illite	>60% Illite			
U. Connoquenessing	39 87%	30 6%	30 47%	30 47%	39 0%	39 5%	10 20%
L. Connoquenessing	82 0%	58 64%	52 27%	52 13%	82 76%	82 34%	22 96%

Upper figure, number of samples analyzed.
Lower figure, per cent of samples possessing sedimentary property.
* N-8 (neutral color shade).

sandstones. Clay mineral composition, tourmaline roundness, and quartz content are additional criteria. If all of these criteria are used in conjunction, the probability is high that the two sandstones can be consistently differentiated.

SEDIMENTARY HISTORY

A generalized diagram, Figure 7, shows the stratigraphic relationships of the Connoquenessing sandstones and the Mercer high-alumina clay in a selected area. In areas where high-alumina clay is now present, the absence of the Upper Connoquenessing sandstone and the presence of well rounded tourmalines and the higher quartz content in the upper few feet of the underlying Lower Connoquenessing sandstone, suggest that such areas were once topographic highs. Topographic highs would be favorable areas for prolonged current activity and the subsequent concentration of quartz and rounded tourmaline by selective sorting. As pointed out by Keller, et al. (4), they would be areas of good drainage, a factor considered essential by Keller for the formation of high-alumina clays of Missouri.

Factors responsible for the topographic highs are not known. Erosion, compaction, or tectonism are possible alternatives. Apparently highs in different areas developed at different times. The marked thinning of both Upper and Lower Connoquenessing sandstones in areas 4 and 5 (Fig. 7) suggests that these areas were topographic highs prior to the deposition of the Lower Connoquenessing. However, the fact that in areas 12 and 13,

(Fig. 7) the Upper Connoquenessing is thin or absent whereas the Lower Connoquenessing does not change in thickness would indicate that a topographic high developed in this area during the later stages of Lower Connoquenessing deposition.

The lateral relationships of the high-alumina clay have not been observed and must be inferred. In many places the high-alumina clay grades upward into plastic clay. It seems logical to infer that an equivalent lateral variation exists. The facies relationships between the Mercer clay and the Upper Connoquenessing sandstone is inferred on the basis of similarity in stratigraphic position. This would suggest that high-alumina clay was forming on the topographic highs while sand and gravel were being deposited in adjacent lows.

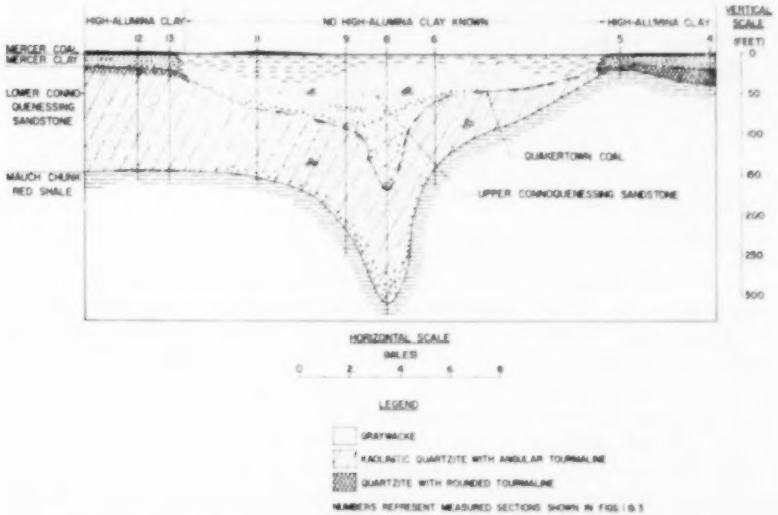

FIG. 7. Generalized cross-section of the Pottsville group in Clearfield and Clinton counties.

The differences in composition and cross-bedding dip direction between the Lower and Upper Connoquenessing sandstones suggest that these rocks were derived from different sources undergoing different degrees of chemical weathering. The Lower Connoquenessing is believed to have been derived from the north or northeast where intense chemical weathering had reduced the source rocks to quartz, kaolinite, lesser amounts of illite, and stable heavy minerals such as tourmaline, zircon, and rutile. The Upper Connoquenessing was probably derived from the southeast where chemical weathering was less intense so that chlorite and biotite and greater amounts of illite were preserved. Based on type of cross-bedding, the absence of marine fossils

and the environmental studies of Degens, et al. (1) it is concluded that both of these sandstones are of fluvial origin.

PROSPECTING FOR HIGH-ALUMINA CLAY

Evidence has been presented that suggests that the known high-alumina clay deposits of Mercer age in western Pennsylvania occur on topographic highs developed on the top of the Lower Connoquenessing sandstone. The clay deposits are lenticular and do not occur everywhere on the highs. If these conclusions are valid, elevated topography was a necessary but not sufficient condition for the formation of the high-alumina clay.

Initial stages of prospecting should therefore be directed toward locating structural highs on the Lower Connoquenessing sandstone and outlining favorable areas in which the Upper Connoquenessing sandstone is absent. This will involve careful mapping of the Mercer coal horizon and the Upper and Lower Connoquenessing sandstones, using the petrographic criteria outlined in Table 2. Detailed exploration methods, including closely spaced drilling, perhaps supplemented by geophysical methods (3), will be required to determine the location of individual clay deposits within the favorable areas.

The principal potential value of the proposed criteria for distinguishing the two sandstone types is that they provide methods of eliminating large areas as unfavorable for clay prospecting.

ACKNOWLEDGMENTS

The investigation was part of a research program of the Mineral Conservation Section of the Pennsylvania State University. The writer thanks Dr. M. L. Keith, Director of the Mineral Conservation Section, for useful discussions of the problem and critical reading of the manuscript.

PENNSYLVANIA STATE UNIVERSITY,
UNIVERSITY PARK, PENNSYLVANIA,
Feb. 9, 1960

REFERENCES

1. Degens, E. T., Williams, E. G., and Keith, M. L., 1958, Environmental studies of Carboniferous sediments. Part II: Application of geochemical criteria: Am. Assoc. Petroleum Geologists Bull., v. 42, p. 981–997.
2. Fettke, C. R., 1954, Structure-contour maps of the plateau region of north-central and western Pennsylvania: Pennsylvania Topog. and Geol. Survey Bull. G. 27.
3. Gross, G. W., and Moore, J. E., 1959, Spontaneous polarization potentials in clay and limonite deposits in the Gatesburg formation of central Pennsylvania: ECON. GEOL., v. 54, p. 1056–1067.
4. Keller, W. D., Westcott, J. F., and Bledsoe, A. O., 1954, The origin of the Missouri fire clays: Proceedings of the Second National Conference on Clays and Clay minerals, p. 7–44.
5. Schultz, L. G., 1955, Quantitative evaluation of the kaolinite and illite in underclays: Proceedings of the Third National Conference on Clays and Clay Minerals, p. 421–429.
6. Weitz, J. H., 1954, The Mercer fire clay in Clinton and Centre counties, Pennsylvania: Unpublished Ph.D. Thesis, The Pennsylvania State University.
7. Williams, E. G., 1957, Stratigraphy of the Allegheny series in the Clearfield basin: Unpublished Ph.D. thesis, The Pennsylvania State University.
8. Williams, E. G., and Nickelsen, R. P., 1958, Correlation of the Pottsville and Lower Allegheny series in parts of Clearfield and Centre counties: Min. Ind. Expt. Sta. Bull. 71, Pennsylvania State University, p. 37–49.

Economic Geology
Vol. 55, 1960, pp. 1303-1312

SCIENTIFIC COMMUNICATIONS

CONTACT PRINTING OF DRILL CORES

WILLIAM C. KELLY

The technique of chemical contact printing as described by Hiller (1937), Gutzeit (1942) and others holds promise as a practical aid in the routine examination of drill cores. The method is currently used in many laboratories for the identification and localization of elements in mineral fragments, flat rock surfaces and polished ore sections, but its use in the study of core samples has not been exploited. It offers a rapid and simple means of spotting the presence and distribution of minerals that might otherwise be missed in core because of their inconspicious appearance or occurrence in small quantities.

The method proposed here is a simple modification of the original technique and differs only in that the chemical print is made on the curved surface of a core rather than on the more convenient flat surface of a polished section. Prints of excellent quality may be obtained from core of any size provided the surface is not unusually rough or pitted.

Any glossy photographic paper, preferably single weight, may be used in this process. The silver salts are first removed from the paper by fixing in a standard hypo bath such as Kodak F-6. The paper is then washed in running water for about 30 minutes and dried.

The paper is next impregnated with a solvent such as nitric acid or aqua regia which is known to dissolve the mineral being sought in the core. The solvent may either be applied to the paper with a glass dropper, or the paper may be immersed in a beaker containing the solvent. The latter procedure is recommended because it assures a more uniform saturation of the gelatin layer left on the photographic sheet. In either case, the distribution of solvent may be checked by holding the paper up to a light. It is necessary to wear rubber gloves while handling the paper.

Excess solvent is sponged from both sides of the saturated paper, which is then laid emulsion-side up on a pad of soft foam rubber about $\frac{3}{4}$" thick. A final check is made to see that all droplets of excess solvent have been removed from the glossy surface of the paper. The drill core to be tested is next pressed down onto this moist surface and the loose ends of the foam-rubber pad are wrapped around the core bringing the paper into tight contact with the entire surface of the specimen. Wrapped in this manner, the core is gripped firmly by hand for a period of time depending upon the strength of the solvent used and the susceptibility of the minerals to attack. Usually a contact of 15 to 30 seconds will suffice for minerals of moderate solubility.

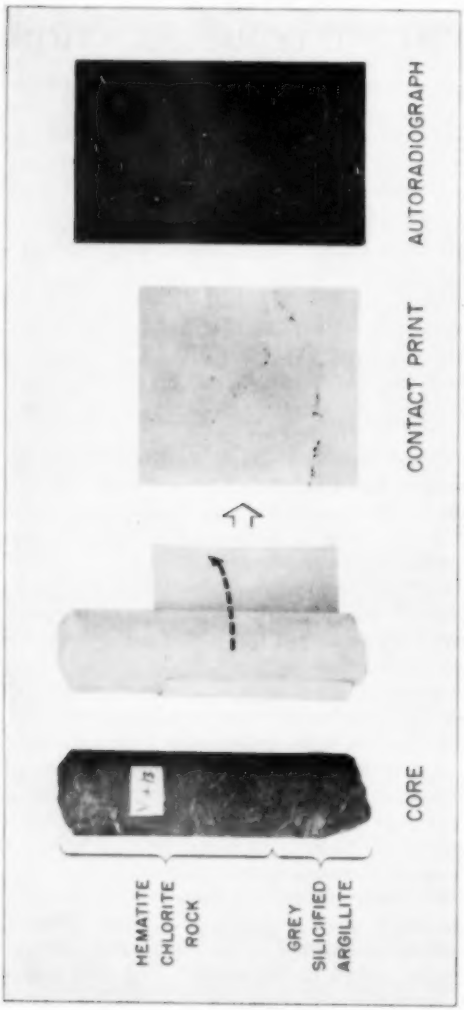
HEMATITE CHLORITE ROCK
GREY SILICIFIED ARGILLITE
CORE
CONTACT PRINT
AUTORADIOGRAPH

FIG. 1.

After this contact, the paper is dipped into a beaker containing a reagent that will form a colored precipitate with the element in question. If the procedure is carefully carried out, a mirror image of the element sought will appear on the paper.

If the contact print is to be preserved, the developed paper should be washed in running water for about 20 minutes and then dried. Many separate prints may be made of a single specimen with relatively little damage to the surface of the core.

As an example of this process, a contact print of a low-grade pitchblende-bearing core is shown in Figure 1. This specimen is from the Verna Mine, Beaverlodge district, Saskatchewan, and was loaned to me by Dr. John S. Dudar. It consists of metamorphosed and hydrothermally altered argillite. The lower portion of the core is dull-gray, highly silicified argillite, and the upper is reddish, iron-stained chloritized argillite locally referred to as chlorite rock. Late veinlets of chlorite, hematite, calcite, and sericite cut across both portions of the core. The chlorite rock serves as a host for uranium mineralization in the district and reddish hematite alteration of this unit is a guide to ore. The core gives a scintillometer count slightly above background but no pitchblende is evident to the naked eye.

An autoradiograph of this specimen (Fig. 1) revealed the location of radioactive material at several isolated points within the chlorite rock but mainly along the undulating contact between the chlorite rock and the silicified argillite in the lower part of the core. The autoradiograph required a continuous exposure of 72 hours.

Contact prints of this same core were made using 40% HCl as a solvent and potassium ferrocyanide as the developing reagent. In these prints (Fig. 1) uranium appeared as a dark brown stain against a light blue background for iron. The photograph shown in Figure 1 was taken in blue light to emphasize the uranium stain. The distribution of the uranium coloration corresponds to the distribution of radioactive material indicated by the autoradiograph. The contact print, however, required only several minutes to prepare in contrast to the long exposure required by the autoradiograph.

This contact print test for uranium is used by the U. S. Geological Survey and is described here as only one of many tests that have potential usefulness in the application to drill core. Many of the metallic and some of the nonmetallic elements common in ore deposits can be identified by this method. Gutzeit (1942) has outlined the procedure for numerous tests specific for other elements and all seem adaptable to the use proposed here.

UNIV. OF MICHIGAN,
ANN ARBOR, MICH.,
May 15, 1960

REFERENCES

Gutzeit, G., 1942, Determination and localization of metallic minerals by the contact print method: A.I.M.M.E. Trans., v. 153, p. 286–298.

Hiller, Th., 1937, Sur l'application de la methode des empreintes a la determination des mineraux opaques en section polie: Schweitz. Min. und Petr. Mitt. 17, p. 88–145.

REFLECTIVITY MEASUREMENTS WITH A HALLIMOND VISUAL MICROPHOTOMETER[1]

B. F. LEONARD

Reflectivity, a fundamental, quantitative, and diagnostic optical property of ore minerals, is seldom measured by American geologists, or if it is, the results are seldom published. Yet it is reflectivity, together with qualitative optical properties, habit, and relative hardness, that we observe when we first examine a polished section. Devices for measuring reflectivity have been available for many years, and promising new ones have been developed in the last decade. Their impact on American ore microscopy seems to have been slight.

The main devices for measuring the reflectivity of opaque minerals are visual photometers, photoelectric cells, and photomultiplier tubes. Each device has certain advantages. Visual photometers include the Berek slit photometer (1, p. 313–317; 11, p. 121–125; 12, p. 78–83), and the Hallimond visual microphotometer (5, p. 131–136). Descriptions of photocells adapted to ore microscopy are given by Bowie and Taylor (2, p. 265–271), Capdecomme and Orcel (3, p. 81–84, 86–105), Folinsbee (4, p. 425–431), Pudovkina (9, p. 146–170), Schneiderhöhn (11, p. 126–128), Short (12, p. 83–92), and others. Photomultiplier tubes have been used by Lévy and Prouvost (7, p. 65) for mineralogic studies, and by many workers, including Newton and Vacher (8, p. 3), for metallographic studies.

The purpose of this note is to report on one visual microphotometer that has yielded satisfactory results in conjunction with equipment found in many small laboratories. The microphotometer has been described by Hallimond (5, p. 131–136) in a publication that seems not to be widely known among economic geologists. The instrument is compact, simple, inexpensive, and adaptable to several models of ore microscope. A quartz standard, light-absorbing container, conversion tables, and complete instructions are supplied with the microphotometer. It requires no accessory equipment except a source of stable current, such as a storage battery, "constant-voltage" transformer, or electronic regulator. The microphotometer comes equipped with a green filter only. Additional color filters are available from the manufacturer. Since the color filters must be used inside the microphotometer, ordinary filters of 2-inch size cannot be substituted for those of special diameter and thickness. One can, of course, remove the color filter from the microphotometer and measure reflectivity in white light. With the lighting arrangements described below, this does not require the addition of a neutral density filter. However, the use of white light for visual photometry is seldom endorsed, owing to the difficulty of estimating light intensity on differently colored objects.

Essential elements of the microphotometer are an ocular; an inclined, internally illuminated, metallized glass plate (the comparison area); two fixed

[1] Publication authorized by the Director, U. S. Geological Survey.

polaroid filters; and a third polaroid filter that is rotated by a knurled dial. The microphotometer is set on the draw tube of an ore microscope in place of the usual ocular. Light from the bulb in the microphotometer passes horizontally through the polaroid filters, strikes the inclined comparison area, and is reflected upward through the ocular. The intensity of light on the comparison area is matched to that of the object in the microscope field by rotating the movable filter. The intensity of light so determined is closely proportional to $\sin^4\theta$, θ being the angle of rotation (5; 6, p. 487). Separate measurements of light intensity are made on polished mineral sample, standard, and light-absorbing container; the angular values so determined are converted to values of $\sin^4\theta$ by means of tables; and the value of stray light in the optical system is deducted from that of test mineral and standard. These corrected values are proportional to the reflectivities of test mineral and standard.

The curve of the function $\sin^4\theta$ is nearly linear in the interval $\theta = 40° - 70°$. Therefore, comparisons of light intensity made in this interval will, for angular readings of comparable precision, be almost linearly proportional. Unless the range of reflectivities is extreme, all comparisons of light intensity except that of the stray light can usually be confined to this favorable interval. In matching the light intensities of comparison area and object, an initial scale setting of 60° to 70° is selected for the brightest object in the series to be measured, and the external illumination is adjusted accordingly. (For details, see below.) The scale setting is carefully read, and other objects in the series are then placed on the microscope stage, focused, and measured in like manner. Once the reading has been taken for the brightest object, external illumination is kept constant; only the internal illumination is varied, by rotating the movable polaroid in the microphotometer. The precision of measurement can be increased somewhat by repetition, but one must avoid tiring the eyes and thereby drastically reducing the accuracy of one's comparisons.

Depending on the microscope, lamp, and transformer available, lighting may be arranged in several ways (cf. 5). The following notes describe an arrangement used with a conventional ore microscope, Monla lamp, and variable transformer.

The line current is stabilized by an electronic regulator. An ordinary "constant-voltage" transformer, used at the start of the investigation, did not prevent excessive fluctuations in current during periods of heavy load. In some laboratories, a separate current stabilizer might not be required.

Stabilized current passes through a conventional variable transformer that controls the intensity of illumination in both Monla lamp and microphotometer. The lighting elements are connected in parallel, so that both receive the same current. With the above arrangement, the small 6 volt, 6 watt bulb originally supplied in the microphotometer gave too bright and off-color a light on the comparison plate of the microphotometer for settings at which the instrument itself has maximum reliability. It was replaced by a No. 46 panel-lamp bulb, rated at 0.25 amp at 6.3 volts. This gave a more agreeable light for my eye and has operated without replacement for more

than 80 hours. Panel-lamp bulbs of this type have the additional virtue of being readily available in this country.

The attachment and very simple adjustment of the microphotometer are fully described by Hallimond (5). Getting even illumination over the microscope field, viewed through the microphotometer, is easy; whatever the operator finds good for ordinary microscope work generally is suitable for photometry. If color filters are to be used, the frosted "daylight" (blue) glass plate commonly supplied with the microscope lamp should be replaced by one of frosted white glass. On microscopes whose vertical illuminators have a compensating prism as well as a plane glass plate, one should remember to use the plate, not the prism, in making reflectivity measurements. One should also be sure to remove the analyzer (upper nicol) from the optical system. After the diaphragm behind the polarizer has been stopped down, focused, and centered, and the dial of the microphotometer has been set near 60°, one can approximately match the intensities of light on microscope field and comparison area of microphotometer by (1) adjusting the voltage by means of the variable transformer, and by (2) opening or closing the iris diaphragm on the housing of the supplementary collecting lens that is commonly set in front of the vertical illuminator on an MOP ore microscope. The use of the latter diaphragm makes it unnecessary to modify light intensity by means of opposed polaroid filters. These lighting arrangements must be supplemented by polaroids or by a neutral density filter of moderate absorption if one chooses to use the highly-reflecting compensating prism, instead of the glass plate, in the vertical illuminator.

The technique of making the reflectivity measurements and calculating the result is very clearly stated by Hallimond (5). The precautions noted by him should be followed. Three other points deserve comment.

The quartz standard that accompanies the microphotometer is mounted in a metal housing coated with dull black paint. Unless one prudently experiments to find out which organic solvents will clean the quartz plate without dissolving and redistributing the paint, one may spoil the standard. I found it convenient to have the metal housing cut open and the quartz plate remounted, flush, in bakelite. The quartz plate is then easily cleaned with benzene or alcohol. Also, the contact between bakelite and quartz offers a convenient object to focus on, if one is using a high-power objective. After focusing, it is best to move the mount a short distance, so that only the quartz standard, free of internal reflections, is in the field when a measurement of its brightness is made.

One should be careful to use the same objective for a given set of measurements involving the test mineral, standard, and black box. If one regularly uses the high-power objective for reflectivity measurements, but temporarily uses the medium-power objective to find another suitable grain in the polished section, it is all too easy to resume measuring without returning the original objective to its clutch. Frequent changing of objectives does not seem to affect the precision of reflectivity measurements, provided the appropriate objective is in place throughout a given set of measurements.

If one has truly stable electrical current and undisturbed apparatus, it is possible to measure the standard and black box once and then make comparisons with a number of minerals of similar reflectivity or with specimens of the same mineral, carrying out the work intermittently over three or four days and checking the standard only at rare intervals. This greatly reduces both eyestrain and the total number of observations required. However, one should not indulge in this practice without making sure that working conditions are indeed constant.

TABLE 1

COMPARISON OF REFLECTIVITY VALUES FOR SOME OPAQUE MINERALS

	R (percent)[1]					
	Green light				White light	
	Leonard Hallimond visual photometer			Ramdohr (10) Berek slit photometer	Bowie and Taylor (2) Photocell	Pudovkina (9) Photocell
	Number of localities	Range	Average[2]		Mean[2]	
Ilvaite	2	8.5–9.0	8.8	[8.2]	—	8.2
Sphalerite	1	—	18.0	18.5	17.5	17.0; 18.0
Ilmenite	2	18.0–18.6	18.3	18	19.4	18.6
Magnetite	4	20.6–21.4	21.1	21	21.1	19.1
Hematite	3	26.8–28.2	27.3	26	27.5	25.9
Tetrahedrite	1	—	31.5	27	30.7	30.9
Pyrrhotite	2	35.7–38.5	37.1	37	41.6	39.8
Chalcopyrite	2	37.8–46.7	42.2	42	44.0	43.4
Galena	2	43.1–43.6	43.4	43.5	43.2	43.0
Pyrite	2	54.0–54.4	54.2	54	54.5	57.0
Arsenopyrite	1	—	54.8	49	53.7	54.6
Cobaltite	1	—	53.2	52	52.7	54.7
Copper	2	60.2–62.9	61.6[3, 4]	61[4]	81.2[4]	71.2[4]
Silver	2	92.8–97.4	95.5[3]	95.5	95.0	84.4

[1] For the anisotropic minerals, $R = \frac{Rg + Rp}{2}$, or $\frac{Rg' + Rp'}{2}$, or R measured in 45°-position.

[2] "Average" indicates arithmetic mean. The "mean" values reported by Bowie and Taylor (2) seem to be values of the mid-range (mid-point). For Leonard's observations, mid-range and average have separate values for magnetite and hematite, but the difference (0.2 percent) is negligible.

[3] Reported values of R were measured relative to pyrite, whose R for green light was accepted as 54 percent, the value reported by Ramdohr (10, p. 614). Relative to the quartz standard used for Leonard's other determinations, R for copper = 63.4 percent, R for silver = 98.0 percent. The latter values are too high, owing to the extreme range in R between quartz standard and mineral, and the eye's inability to adjust readily to this extreme difference in brightness.

[4] The extreme dispersion of R for copper presumably accounts for the discrepancy between the green-light and white-light values reported here.

Table 1 shows the results of my reflectivity measurements, made in the spring of 1959, compared with the data of several other workers. The values I obtained were not intended to be definitive, and my trial of the Hallimond microphotometer was not exhaustive. I merely wanted to see if, with existing equipment and a minimum of practice, I would get values comparable to

those generally accepted, as reported by Ramdohr (10). The agreement was rather close, as the unrounded numbers show. For most of the values I reported, rounding to the nearest 0.5 percent would be appropriate; that convention is adhered to by Ramdohr (10). Quartz was apparently a suitable standard for all minerals except those having very high values of R. The reproducibility of my earlier measurements is shown in Table 2. R for all minerals except cobaltite was determined while I was still learning to use the instrument. The figures are offered for the encouragement of other be-

TABLE 2

REPRODUCIBILITY OF REFLECTIVITY MEASUREMENTS MADE BY A BEGINNER
(B. F. LEONARD, SPRING 1959)

	R (percent), green light; Hallimond visual microphotometer		
	Individual determinations	Average	Maximum difference
Ilvaite			
Idaho	8.4, 8.4, 8.7	8.5	0.3
Arizona	8.9, 9.0	9.0	0.1
Magnetite			
New York—1	20.5, 20.5, 20.6, 20.7	20.6	0.2
New York—2	21.0, 21.1, 21.2, 21.2	21.1	0.2
New York—3	21.2, 21.7	21.4	0.5
California	21.4	—	—
Tetrahedrite			
Nevada	31.4, 31.6	31.5	0.2
Chalcopyrite			
Idaho	45.8, 46.5, 47.8	46.7	2.0
Nevada	37.8	—	—
Pyrite			
Idaho	53.5, 53.9, 55.9[1]	54.4	2.4
New York	54.0	—	—
Cobaltite			
Idaho	52.5, 53.8	53.2[2]	1.3

[1] Eyes tired. Value would ordinarily be rejected.

[2] Redetermination, February 1960. Original values were high and disparate for reasons unknown.

ginners. The increase in maximum difference with increasing value of R is, I believe, due to the difficulty of matching the light intensities of mineral and comparison area of microphotometer in green light, rather than to the increasing disparity between R's of mineral and standard. Work done in the winter of 1959–1960, with an orange filter (Ilford spectrum No. 607), stable current, stable regulating transformer, more attention to uniform lighting, and a resolve not to accept results obtained with tired eyes, suggests that a precision of about 0.1 percent is attainable for measurements in the 5–25 percent reflectivity range. The precision of measurements above R = 25 percent has not been adequately investigated.

The reflectivity of grains about 0.03 mm in diameter can be measured without change in the set-up. The precision of measurement on grains of this size is virtually the same as it is for grains large enough to fill the field of the microscope. However, on magnetite grains 0.01 mm in diameter, the measured value of R was 95 to 105 percent of the accepted value for specimen New York-1, Table 2. Pits and scratches on a polished surface are a nuisance, but their effect on the reflectivity measurements seems negligible, provided a well-polished area about 0.01 mm across is available for measurement. (0.01 mm corresponds roughly to the apparent width of the microphotometer's comparison plate when the field of view is determined by the 10 × ocular of the photometer and the 6FL objective of the microscope.) When R must be measured on such very small areas, the eye is less distracted by pits and scratches in an otherwise homogeneous grain than by contrasts in reflectivity between adjacent grains of different minerals. An auxiliary diaphragm placed in the microscope tube, near the base of the ocular, was used by Bowie and Taylor (*2*) to isolate small and imperfectly polished grains for measurement of reflectivity by photocell. Such a diaphragm is not generally needed for use with the Hallimond microphotometer, though I suspect that the precision of readings taken on large as well as small grains could be improved by using such an auxiliary diaphragm.

An approximate determination of the reflectivity of an isotropic mineral can be made without haste in about 10 minutes. This includes positioning a grain previously selected; adjusting the lighting; comparing the light intensities of mineral, standard, and black box; and calculating the result. A careful determination takes me about half an hour. However, if the line current is stable and the unknown minerals have similar reflectivity, so that the standard and black box need be carefully measured only once for the set, precise determinations on three or four minerals can be completed in about an hour.

The disheartening effects of fatigue on the accuracy and precision of reflectivity measurements must be faced. For example, separate, subjectively "good" determinations of R for a magnetite specimen gave, at various times, 21.2, 21.0, 21.2, 21.1 percent in green light. A subjectively "poor" determination gave 20.7 percent. Three determinations on this same specimen, made on different days when my eye felt tired and a match of light intensity was difficult, gave 17.5, 19.2, 18.1 percent. Such readings are worthless. A man has to know when to quit; a photocell does not.

The principal disadvantage of the Hallimond visual microphotometer is that it tires the eye. This disadvantage, by no means peculiar to the Hallimond instrument, is an important consideration if many observations are to be made. Moreover, a photocell of the sort devised by Bowie and Taylor (*2*) is better suited for use with the compact microhardness testers used by them and by Pudovkina (*9*). This, too, is an important consideration, for Bowie and Taylor's identification scheme (combining microhardness and reflectivity) seems elegant, precise, and rapid.

I am especially indebted to my associates Messrs. K. K. Ketner, T. G. Lovering, G. J. Neuerburg, and R. E. Wilcox for thoughtful criticism of

this note. Mr. I. J. Mittin kindly translated the paper by Pudovkina (9). Messrs. E. E. Parshall and H. M. Weeden adapted certain electrical equipment for special use.

U. S. Geological Survey, Denver, Colo.,
June 20, 1960

REFERENCES

1. Berek, Max, 1953, Rinne-Bereks Anleitung zu optischen Untersuchungen mit dem Polarisationsmikroskop, 2d ed. [Edited by C. H. Claussen, A. Driesen, and S. Rösch]: Stuttgart, E. Schweizerbart'sche Verlagsbuchhandlung, 366 p.
2. Bowie, S. H. U., and Taylor, K., 1958, A system of ore mineral identification: Mining Mag. [London], v. 99, p. 265–277, 337–345.

or

——, 1958, A system of ore mineral identification: U. N. Internat. Conf. (2d) Peaceful Uses Atomic Energy Proc., v. 3, p. 527–540.
3. Capdecomme, Laurent, and Orcel, Jean, 1941, Détermination des propriétés optiques des cristaux opaques à l'aide du microscope métallographique polarisant: Revue d'Optique théorique et instrumentale, v. 20, p. 47–114.
4. Folinsbee, R. E., 1949, Determination of reflectivity of the ore minerals: Econ. Geol., v. 44, p. 425–436.
5. Hallimond, A. F., 1953, Manual of the polarizing microscope, 2d. ed.: York, England: Cooke, Troughton & Simms, 219 p. [Reprinted 1956, with Appendices 5 and 6.]
6. ——, 1957, Direct measurement of standard reflectances with the microphotometer: Mineralog. Mag., v. 31, p. 487–494.
7. Lévy, C., and Prouvost, J., 1957, Rapport entre la chalcopyrite, la stannite et la reniérite: Bull. Soc. franç Minér. Crist., v. 80, p. 59–66.
8. Newton, C. J., and Vacher, H. C., 1954, Correlation of polarized light phenomena with the orientation of some metal crystals: Jour. Research [U. S.] Nat. Bur. Standards, v. 53, p. 1–12.
9. Pudovkina, I. A., 1957, Tochnye metody opredeleniya otrazhatel'noi sposobnosti i tvyordosti rudnykh mineralov [Precise methods of measurement of the reflectivity and hardness of ore minerals], p. 139–183 *in* Rozhkova, E. V., ed., Sovremennye metody mineralogicheskovo issledovaniya gornykh porod, rud i mineralov [Modern methods of mineralogic investigation of rocks, ores, and minerals]: Moskva, Vses. Nauch.-Issled. Inst. Mineral'nova Syr'ya, 264 p.
10. Ramdohr, Paul, 1955, Die Erzmineralien und ihre Verwachsungen [2d ed.]: Berlin, Akademie-Verlag, 875 p.
11. Schneiderhöhn, Hans, 1952, Erzmikroskopisches Praktikum: Stuttgart, E. Schweizerbart'sche Verlagsbuchhandlung, 274 p. [Anhang. Erzmikroskopische Bestimmungstafeln, 10 p. + 24 tables.]
12. Short, M. N., 1940, Microscopic determination of the ore minerals, 2d ed.: U. S. Geol. Survey Bull. 914, 314 p.

Economic Geology
Vol. 55, 1960, pp. 1313–1314

DISCUSSIONS

TITANIUM MINERALOGY OF CERTAIN BAUXITES AND THEIR PARENT MATERIALS

Sir: I have received a personal communication from Dr. M. Fleischer regarding the above paper (3). On page 1396 of this paper (3) I referred to papers by Fleischer et al. (1) and by Gordon and Murata (2) concerning the distribution of columbium in Arkansas bauxite. As Fleischer points out in his letter, Gordon and Murata only present the following statement as to the distribution of columbium in Arkansas bauxite: "Niobium is probably largely in combination with several titanium-bearing minerals that are found in the heavy mineral fraction of the bauxite, such as anatase, ilmenite and rutile." Thus the reference to Gordon and Murata should not have been made.

Dr. Fleischer also takes issue with the conclusion attributed to him in the subject paper (3, p. 1396) concerning the distribution of columbium in the Arkansas bauxite deposits. The following sentence which served as the basis of my conclusion is taken from the abstract in USGS Circular 225 (1): "Fractionation of black sand from Arkansas bauxite shows the niobium to be concentrated chiefly in an ilmenite fraction containing more than 40 percent TiO_2 and as much as 0.86 percent Nb." Dr. Fleischer informs me he means only to convey in this statement that ilmenite contains the highest concentration of columbium of any mineral in the black sands obtained from bauxite tailings but that this does not apply to the bauxites as he did not analyze any fractions that had high concentrations of rutile or anatase. He further states that a literature survey leads him to the conclusion "that when rutile and ilmenite occur together, rutile generally has the higher niobium content." This may apply to the polymorphs of TiO_2 and ilmenite when they crystallize in the same environment; it does not follow a priori that the conclusion is valid when the polymorphs of TiO_2 have formed by surface or near-surface alteration of ilmenite which, like ilmenite of the Arkansas bauxite deposits, was formed in a magmatic environment.

JAMES A. HARTMAN

2410 KENTUCKY AVENUE,
KENNER, LOUISIANA,
May 5, 1960

REFERENCES

1. Fleischer, Michael, Murata, K. J., Fletcher, Janet D., and Narton, Perry F., 1952, Geochemical association of niobium (columbium) and titanium and its geological and economic significance: U. S. Geol. Survey Circ. 225, 13 p.

2. Gordon, M., Jr., and Murata, K. J., 1952, Minor elements in Arkansas bauxite: Econ. Geol., v. 47, p. 169–179.
3. Hartman, James A., 1959, Titanium mineralogy of certain bauxites and their parent materials: Econ. Geol., p. 1380–1405.

THE SYSTEM Cu-Fe-S-O

Sir: Before anyone else proceeds to do so, may I correct an error in my discussion of the ternary system Cu-S-O? (1, p. 990–991) I said that the associations chalcocite-tenorite and covellite-tenorite are not common, as indeed they are not, but nevertheless I showed these tie-lines in the diagram, Figure 5. Actually both joins would be precluded by joins between chalcocite and copper sulfate, which I erroneously omitted from the diagram for the reason that anhydrous copper sulfates do not occur as natural species. Thus the only stable three-phase assemblage of "insoluble" minerals in the three-component system would be native copper-chalcocite-cuprite. Even the assemblage chalcocite-cuprite would be unstable in a hydrous system with enough water to form brochantite, antlerite, or chalcanthite, as can be shown by calculation of free energies from Garrels' data (2).

Correction in Figure 5 leads to a corresponding correction in Figure 7 (p. 995) by eliminating the joins cv-to-hem and cc-cup-hem.

While in the business of correcting, "pyrite" in the first line on p. 985 should read "chalcopyrite"; the diagrams in Figure 4 should be lettered a, b, and c, respectively and on page 998 the composition of cuprite should, of course, be Cu_2O. If readers find other errors, as they doubtless will, I shall welcome corrections.

Hugh McKinstry

REFERENCES

1. McKinstry, H. E., 1959, Mineral assemblages in sulfide ores: the system Cu-Fe-S-O: Econ. Geol., v. 54, p. 975–1001.
2. Garrels, R. M., 1960, Mineral Equilibria. Harper & Brothers, N. Y., p. 228.

Economic Geology
Vol. 55, 1960, pp. 1315–1318

REVIEWS

SHORT REVIEWS OF NEW RUSSIAN BOOKS

Izbrannye Sochineniya. [Selected works] of V. I. VERNADSKII. Vol. I, 1954, pp. 696. Price, 40r.; vol. II, 1955, pp. 614. Price, 40r.; vol. III, 1959, pp. 508. Price 37r. 60k.; vol. IV, part i, 1959, pp. 624. Price 38r. 40k. Academy of Sciences, Moscow.

The standard edition of the works of the great Russian geochemist Vladimir Ivanovich Vernadsky (1863–1945) will consist of six large "volumes" (at least one being in two 'books'), edited by Academician Vinogradov. Volume one forms the sixth (third Russian) edition of "Essays on Geochemistry" (first published in French as *La Géochemie* in 1924), to which various other papers on geochemistry are added. Volumes two, three and four reprint his "Experimental and Descriptive Mineralogy," "History of the Minerals in the Earth's Crust," and a series of shorter works on mineralogy. Volume five will include his writings on biogeochemistry, and volume six works on the history of science. The whole compilation forms a reference series of outstanding importance, too little known to Western scientists; and it is to be regretted that it is already difficult to acquire the earlier volumes in the collection.

Geokhimicheskie Metody Poiskov Neftyanykh i Gazovykh Mestorozhdenii. [Geochemical methods of prospecting for oil and gas deposits.] Pp. 462. Academy of Sciences, Moscow, 1959. Price 27r. 35k.

In April 1959 the Academy of Sciences sponsored a symposium on geochemical prospecting for oil and gas deposits, attended by 237 representatives from 68 organizations in the Communist countries. The report of this meeting comprises 77 short contributions, subdivided into the sections: (1) Basic theoretical questions (5 papers); (2) Gas surveys at the surface and in bore holes (24 papers); (3) Analytical techniques (7 papers); (4) Microbiological methods (9 papers); (5) Radiometric methods (6 papers); (6) 'Bituminological' methods (7 papers); (7) Organic geochemical investigations on soils (6 papers); (8) Hydrogeochemical investigations (13 papers). A literature list of 123 references includes only 15 papers in Western languages.

Kristallicheskii Fundament Finlyandii. [The crystalline basement of Finland.] By KH. VYAYURYUNEN. Pp. 295, figs. 69. Gosinostranizdat, Moscow, 1959. Price 16r. 90k.

This work is a Russian translation of a text-book in Finnish on the solid geology of Finland, by Heikki Väyrynen, published in Helsinki in 1954. It gives a good readable review of the Precambrian history of the country, but little is said about ore deposits. Much could now be added by extrapolation from recent geochronological studies in the Karelian ASSR.

Mestorozhdeniya Urana i Zarubezhnykh Stran. [Uranium deposits of foreign countries.] By V. I. Gerasimovskii. Pp. 143, Academy of Sciences, Moscow, 1959. Price, 4r. 20k. (Paper covers).

It is perhaps a sign of the times that the title of this little book has been changed from "The Uranium Deposits of the Capitalist Lands," as originally advertised. Following some 60 pages on the geochemistry and mineralogy of uranium, most of the work is taken up by a well-balanced account of the world's principal ore deposits (excluding those in the U.S.S.R.). The bibliography makes reference to another eight Russian publications on precisely the same theme, and at least two more are in the press. One cannot but wonder a little about the reactions of the average Russian student, who must gain all his precise knowledge of uranium deposits from descriptions initially published outside the Soviet Union.

Zapiski Vostochno-Sibirskogo Otdeleniya Vsesoyuznogo Mineralogicheskogo Obshchestva. [Memoirs of the East Siberian Division of the All-Union Mineralogical Society.] No. 1. Pp. 131. Academy of Sciences, Moscow, 1959. Price, 7r. 30k.

The first number of yet another new serial publication contains nine papers and eight short communications on various aspects of the topographical mineralogy of the country east of the Urals.

Mineralogiya, Tipy Mestorozhdenii i Osnovnye Cherty Geokhimii Selena i Tellura. [Mineralogy, types of deposit, and principle features of the geochemistry of selenium and tellurium.] By N. D. Sindeeva. Pp. 257, figs. 89. Academy of Sciences, Moscow, 1959. Price 16r. 40k.

The title of this important and well-produced work explains its compass, which the book admirably fulfils. Like most of the studies emanating from the Institute for the Mineralogy, Geochemistry and Crystallography of the Rare Elements it is a scholarly composition. After an introduction of 25 pages there follows a detailed account of the mineralogy of selenium and tellurium (80 pages), descriptions of different ore deposits in the U.S.S.R. and elsewhere (66 pages), a geochemical review (30 pages), and tables of X-ray and other diagnostic data (22 pages). Half of a bibliography of more than 250 items relates to Russian literature. Following Vinogradov, the author recalls that as long ago as the year 1275 Marco Polo described a region in eastern Turkestan where the vegetation was poisonous to beasts of burden, causing the hoofs of the animals to drop off, and she attributes this to selenium enrichment. [Similar difficulties were encountered in the same region by Sir Aurel Stein, over 600 years later. As in the Colorado Plateau, this selenium-rich vegetation could well be an indication of uranium deposits.]

C. F. Davidson

University of St. Andrews,
Scotland.
June 1, 1960

Geotektonische Forschungen, Heft 13. Die Kleintektonische Arbeitsweise unter besonderer Berücksichtigung ihrer Anwendung im deutschen Paläozoikum. By Bruno Engels. Pp. 129; figs. 146; pl. 6. E. Schweizerbart'sche Verlagsbuchhandlung, Stuttgart, 1959. Price, DM 37.60.

This volume on microtectonic methods is concerned chiefly with the German paleozoic. The author shows how macrotectonic methods can be supplemented

by microtectonic methods of investigation based upon structures and deformations, which supply further information regarding the make-up of the earth's crust. Although little utilized, microtectonics open up new opportunities, independent of other geologic methods in deciphering structures, deformation, and even stratigraphic events. Two general chapters are followed by Chapter 3, which is the main body of the book, and deals with the various methods and interpretations of microtectonics. These are amply illustrated by drawings and photographs. Six plates at the back contain sixteen beautiful photographs of microtectonic structures.

The Sea Off Southern California. By K. O. Emery. Pp. 366; figs. 248. John Wiley & Sons, New York, 1960. Price, $12.50.

A subtitle to this book states "A Modern Habitat of Petroleum," and much of the discussion has a bearing on the origin, migration, and accumulation of petroleum. This book is the first and only full scale treatment of the underwater area off Southern California.

All aspects of geology are treated. Interrelation is pointed out between geomorphology, structure, water, life, and sedimentation. Oil geologists will be interested in the distribution and ages of off-shore rocks, location of oil seeps, and new data on the origin of oil, production of phytoplankton, oxidation, and dilution by detrital sediment. Other parts cover descriptions of the coasts, shelves, basins, and troughs, and their slopes, and submarine canyons. Lithology, paleogeography, and structure receive attention. Currents, waves, tides, and paleoceanography are covered. The littoral, sublittoral, pelagic, and shelf environments are treated in connection with organic matter. As would be expected sediments, along with organic constituents, receive extensive and thorough consideration. Under the discussion of the origin of petroleum the role of physoplankton is emphasized. The last chapter deals with the economic aspects of water, shorelines, sea flow, and ownership. A 21-page list of references along with indices conclude the book.

The format is double-column and the large page size, 7 by 10 inches, permits large illustrations, of which there are many excellent ones.

The book brings together a great mass of marine and submarine data that have been accumulating in many widespread publications. It is of interest not only to petroleum geologists and their companies but can be considered as an excellent text and reference on coastal oceanography.

Subsurface Mapping. By Margaret S. Bishop. Pp. 198. John Wiley & Sons, New York, 1960. Price, $5.75.

A book for student and practicing geologist that brings up-to-date the new techniques of geological subsurface mapping. The principles underlying the interpretation of stratigraphic and structural maps based on subsurface data are emphasized. This book is the only recent one dealing entirely with the problems of constructing and interpreting geologic maps based upon isopach, facies, paleogeographic, paleogeologic, paleotechtonic, and palinspastic maps.

The author also takes up the preparation of contour maps, cross-sections, and topographic maps, and dips into the geological implication of geophysical and geochemical maps. This part includes also brief descriptions of the various methods of geophysical prospecting. A list of selected references follows each chapter, and an extended bibliography concludes the book. Many well chosen illustrations add to the text.

The author was formerly a geologist for the Pure Oil Co. and now is an Associate Professor of Geology at the University of Houston.

The book is a good job well done.

Application de la Géologie aux Travaux de l'Ingénieur. By JEAN GOGUEL. Pp. 358; figs. 118. Masson & Cie., Paris, 1959. Price, 4,300 F.

The author of this engineering geology is Chief Engineer of Mines, Professor at l'Ecole de Mines, and Director of Service de la Carte Géologique, and has had wide experience in France and abroad.

The book presents those parts of general geology pertaining to engineering design and construction with numerous examples of practice. The 18 chapters take up geologic observations and documentation, geophysical prospecting, drilling, exploration excavations, hydrology, thermal phenomena, rock alteration, mechanical properties of rocks, deformation, vulcanism, erosion sedimentation, glaciation, sea and wind action. These various processes are treated with respect to engineering as practiced in relation to them, and engineering projects to overcome or to circumvent these processes. Many examples are drawn upon for illustrative material.

New Observations on the Ores of the Witwatersrand and Their Genetic Significance. By PAUL RAMDOHR. Pp. 50; pls. 61. Geol. Soc. South Africa, Vol. 61. Academie Verlag, Berlin. 1959.

This paper is a translation of most of Professor Ramdohr's former paper in German, arranged by the Geological Society of South Africa. This one relates on the Witwatersrand. Because it is meant largely for South Africans the familiar geology of the Rand is condensed. Some new microphotographs are added.

The main body of the paper is a detailed discussion of the components of the Rand ores as revealed by the ore microscope. Each mineral is described in detail, but most space is devoted to pyrite and "uranpecherz." The author recognizes several kinds of pyrite: (1) pebble pyrite, which he considers to be abraded pyrite pebbles brought in along with quartz pebbles; (2) pebbles of other minerals that have been pyritized; (3) compact and skeleted crystals of pyrite that have grown *in situ;* (4) concretions that have developed as pyrite during the formation of the conglomerate; (5) "hydrothermal" pyrite formed as compact or loose fracture fillings or as thin coatings on joint planes. In some cases allogenic pebbles have authigenic overgrowths. Arsenopyrite is also considered to be detrital. Other "redeposited" minerals are linneaite, skutterudite, pyrrhotite, and others.

The "uranopecherz" is considered to be detrital, some "pebbles" of which are said to be shattered and cemented by redeposited gold, skutterudite, etc. Gold, which is considered to be recrystallized, is younger than the carbonaceous matter and pyrite. Other authogenic minerals described are galena, sphalerite, pentlandite, tetrahedite, millerite and rutile.

Considerable references are made to the opposing ideas of Davidson.

The author believes the gold, pyrite, and uranium to have been of placer origin, reworked and redeposited during metamorphism of the enclosing rocks. Other authors believe the pyrite pebbles to be replacements of chert pebbles by introduced pyrite.

The descriptions of the minerals are detailed and the plates are made up of beautiful microphotographs. Not everyone will be convinced, however, that the gold, uraninite, and pyrite are detrital.

BOOKS RECEIVED

General Climatology. H. J. CRITCHFIELD. Pp. 465. Prentice-Hall, Inc., Englewood Cliffs, N. J., 1960. Price, $7.95. *Up-to-date volume of world climates. Part I—Physical Elements of Weather and Climate; Part II, Classification of Climate Types and Distribution; Part III, Relation of Climate Elements to Biotic Environment and Human Activities. A thoughtful modern text and good reference on climatology.*

Crystals and the Polarising Microscope—A Handbook for Chemists and Others—3rd Edit. N. H. HARTSHORNE and A. STUART. Pp. 557; figs. 339. St. Martin's Press, Inc., London and New York, 1960. Price, $17.50. *Considerably revised to bring in newer developments and accessories of the polarizing microscope and their utilizing for the examination of crystals, particularly for the chemist. Theoretical treatment of crystals, their optical properties, and methods of determination. A handy reference—hardly justified by its fantastic cost.*

Vistas in Astronomy, Vol. 3. Edited by A. A. BEER. Pp. 346. Pergamon Press, Inc., New York, 1960. Price, $18.00. *Prepared by 21 authors from many countries. Part I—Dynamics, Instruments, Geophysics, Solar System; Part II—Stellar Astronomy and Evolution, Photometry, Spectroscopy, Galaxies, and Cosmology. An authorative, up-to-date discussion of the above features.*

Physical Science. D. S. ALLEN and R. J. ORDWAY. Pp. 825. D. Van Nostrand Co., New York, 1960. Price, $8.25. *A general science course for students without science background. Part I, Physics and Chemistry; Part II, Geology, Astronomy, and Meterology. The geology part covers materials, crustal movements and geologic time, minerals and rocks, weathering and erosion, subsurface water, glaciation, volcanoes, structure, Appalachian history, and the fossil record. A good elementary review.*

Optical Crystallography, with Partial Reference to the Polarizing Microscope, 3rd Edit. E. E. WAHLSTROM. Pp. 356. John Wiley and Sons, New York, 1960. Price, $8.50. *An elementary text completely rewritten with a new chapter on crystal rotation methods and 100 new illustrations to convey a pictorial rather than a mathematical understanding. Review of optical crystallographic theory. Treats of the theory and identification of minerals by the various optical methods. Of value to geologists, mineralogists, chemists and ceramists.*

Crystal and Mineral Collecting. W. A. SANBORN. Pp. 145; figs. 89. Lane Book Co., Menlo Park, Calif., 1960. Price, $3.50. *For the amateur. General features, physical properties, crystals, where and how to collect, type collections, Dana collections, housing and cataloging, valueing.*

Molybdän. H. P. RECHENBERG. Pp. 128; figs. 11. Ferdinand Enke Verlag, Stuttgart, 1960. Price, DM 24.60. *Twelfth volume of the series Die Metallischen Rohstoffe. Minerals, occurrence and origin, geochemistry, prospecting, mining, beneficiation, marketing statistics; occurrences in various countries of world.*

Search for the Past—An Introduction to Paleontology. J. R. BEERBOWER. Pp. 562; figs. 225, with 1000 line drawings. Prentice-Hall, Inc., New York, 1960. Price, $7.50. *An elementary text that emphasizes methods and principles and presents a synthesis of geologic and biologic aspects of paleontology. Discusses fossils, species, evolution, genetics, classification, and systematic treatment of species and genera. A thorough treatment.*

Seaman's Mineral Tables. KIRIL SPIROFF. Pp. 84; figs. 5. Michigan College of Mining and Technology Press, Houghton, 1959 (1960). Price, $2.00. *Complete revision of 1934 edition. Sections on cleavage, crystallography and physical properties, followed by mineral tables based upon 1 to 6 cleavages, and upon crystal systems, luster, streak, taste, fibrosity, nodular and earthy. Designed as a supplement to Dana's Textbook of Mineralogy.*

Overvoltage Research and Geophysical Applications. Edited by J. R. WAIT. Pp. 158. Pergamon Press, New York, 1960. Price, $9.00. *Twelve articles by geophysicists on overvoltage types of geophysical methods and some applications to ore finding.*

Information Circulars 37–40, Geologic Interpretation of Aeromagnetic Maps. A. A. SOCOLOW. Pennsylvania Geological Survey, Harrisburg, Pa., 1960. *Pottstown, Wagontown, Downingtown, Coatesville, Unionville, Honeybrook, Parkesburg; Temple, Fleetwood, Manatawny, Reading, Birdsboro, Boyertown; Easton, Riegesville; Hatboro, and Langhorne quadrangles.*

Serviços Geologicos de Portugal, Vol. 42, Lisbon, 1958 (1960) (Centenary number). *Contains ten articles on general geology, petrography, paleontology, and economic geology of various areas. One paper by T. S. Webb (in English) describes the massive replacement pyritic deposit of San Domingos.*

South Africa Geological Survey, Pretoria, 1960. Geologic maps, colored, scale *1/250,000: 2328—Pretersburg; 2326—Elliswas.*

Geological Interpretation of Airborne Magnetometer and Scintillometer Survey. Mt. Bonaparte, Bodie Mt., Curlew, Aeneas, and Republic Quadrangles, and Okanogan and Ferry counties. Pp. 34; plates 1–5, 1A–5A, 1B–5B, 1C–5C, 1D–5D; scale 1/62,500. Price, $1.50. State of Washington, Division of Mines and Geology, Olympia, 1960. *Maps give magnetic contours, fiducial points, flight lines, and scintillation anomalies.*

Geological Survey of Canada—Ottawa, 1960.

Geology maps (uncolored): Wakwekobi Lake, Ont., scale 1/63,660; **Tulsequah, B. C.,** and **Michikamau Lake, Quebec-Nfld.,** scale 1/253,440; **Sakami Lake, New Quebec,** scale 1/506,880.

Aeromagnetic Maps of Amherst, New Germany, Gaspereau Lake, Berwick, Cape Chignecto, and Alma, Nova Scotia; Hillsborough, Kouchibouguac, Chatham, Tabusintac River, Burnsville, and Grand-Anse, New Brunswick, Nos. 797g–808g, scale 1/63,360; **Geologic maps 1094A, St. George, New Brunswick,** scale 1/63,360 (colored); Nos. 7 and 8, **Quiet and Finlayson Lakes, Yukon,** scale 1/253,440 (uncolored); geology (black and white) **Cassiar Distr., British Columbia,** scale 1/253,440, map 5701929; **Flin Flom—Mandy District, Manitoba and Saskatchewan** (in colors), scale 1/12,000, map 1078A.

Illinois Geological Survey—Urbana, 1960.

Rept. of Investigations 213. Ground-Water Geology of Winnebago County, Illinois. J. E. HACKETT. Pp. 63; pls. 2; figs. 11. *Cambrian aquifers and thick glacial outwash in bedrock valleys are the main sources of ground water.*

Educational Series 6. Field Book—Pennsylvanian Plant Fossils of Illinois. CHARLES COLLINSON and ROMAYNE SKARTVEDT. Pp. 35; figs. 5. Map. *A field book for beginners.*

Ontario Department of Mines—Toronto, 1960.

Geology of the Dyment Area. J. SATTERLY. Vol. 64, Pt. 6. Pp. 32; photos 11, figs. 2. Colored map, scale 1 inch/¼ mile. *Small gold, copper and molybdenum deposits have been found in the metamorphic and intrusive rocks.*

Geology of the Manitouwadge Area. E. G. PYE. Vol. 66, Pt. 8, 1957. Pp. 114, photos 23, figs. 12. Colored map, scale 1 inch/¼ mile. *The Precambrian metamorphic rocks have been mapped and the economic geology reviewed with the intent of aiding future mineral exploration.*

Industrial Mineral Circ. 5. The Limestone Industries of Ontario. D. F. HEWITT. Pp. 177; tbls. and figs. 149; 3 geologic sections; 2 maps, scale 1 inch/20 miles and 1 inch/1 mile. *Report includes specifications and uses of limestone and dolomite, the distribution and characteristics of major limestone formations and quarry operations, and the utilization of Ontario limestone resources.*

Geological Sketch Map Blind River Area. (Black and white.) Scale 2 miles/1 inch. *Details of Blind River uranium formations.*

Quebec Department of Mines—Quebec, 1960.

Geological Rept. 91. New Glasgow-St. Lin Area, Electoral Districts of Montcalm, Terrebonne and L'Assomption. F. F. OSBORNE and T. H. CLARK. Pp. 41, pl. 7; fig. 1. Colored map, scale 1 inch/1 mile. *The area lies across the boundary of the Precambrian Shield and the St. Lawrence Lowland. Economic mineral deposits of garnet, titaniferous iron ores, and gold have been found on the Shield, and limestone is abundant in the lowland.*

Geological Rept. 92. Rawdon Area, Montcalm and Joliette Electoral Districts. RENÉ BÉLAND. Pp. 35; pl. 8. Colored map, scale 1 inch/1 mile. *The general geology and petrology of the Grenville rocks is described.*

Geological Rept. 93. Chertsey Area, Joliette, Montcalm and Terrebonne Electoral Districts. P.-E. CÔTÉ. Pp. 30; pl. 8. Colored map, scale 1 inch/1 mile. *The area is underlain by anorthosite, Grenville rocks, and grey granite in that probable order of age. Traces of lead and silver have been discovered.*

Geological Rept. 93. Doncaster Area, Electoral Districts of Terrebonne and Montcalm. M. A. KLUGMAN. Pp. 25; fig. 1. Colored map, scale 1 inch/1 mile. *Two massive sulfide deposits, now being tested, lie within the Grenville rocks of the area.*

United Nations—New York, 1959.

Mineral Resources Development Series No. 10. Proceedings of the Symposium on the Development of Petroleum Resources of Asia and the Far East. Pp. 251, tbls. 72. Price, $2.50 (U. S.) or equivalent in other currencies. *A collection of reports and abstracts covering the current petroleum industry in Asia and the Far East.*

Mineral Resources Development Series No. 10 (Annex). Annex to the Proceedings of the Symposium on the Development of Petroleum Resources of Asia and the Far East. Pp. 73; figs. 72. Price, $1.00 (U. S.) or equivalent. *Consists of 72 figures for the documents included in the number 10 publication.*

Mineral Resources Development Series No. 11. Mining Developments in Asia and the Far East 1957. Pp. 50; tbls. 68. Price $.75 (U. S.) or equivalent. *Review of mining activity by element and country.*

U. S. Geological Survey—Washington, D. C., 1960.

Bull. 1061-F. Glacial Geology of the Mystic Lakes-Fresh Pond Area, Massachusetts. NEWTON E. CHUTE. Pp. 187–216; pls. 4; fig. 1. *Ground water flow is affected by a deep sediment-filled bedrock valley that is about 80 feet below sea level; an inner gorge is cut 60 to 90 feet below the flow of this old valley.*

Bull. 1072-O. Geology and Oil-Shale Resources of Naval Oil-Shale Reserve No. 2, Uintah and Carbon Counties, Utah. W. B. CASHION. Pp. 753–793; pls. 4; figs. 9; tbls. 4. Price, $1.00. *Two oil-shale zones may become of economic importance. Oil and gas production from Mesozoic strata may be possible.*

Bull. 1074-F. Geology and Uranium Occurrences in the Miller Hill Area, Carbon County, Wyoming. J. D. VINE and G. E. PRICHARD. Pp. 201–239; pls. 7; figs. 5; tbls. 5. *Uranophane, the principal uranium mineral, occurs predominantly in beds of brecciated limestone. Deposits are thought to be secondary concentrations deposited from ground-water solutions. The suggested mechanism for deposition is the reaction of silica- and uranium-rich ground water upon contact with limestone.*

Prof. Paper 294-M. Foraminifera of the Monterey Shale and Puente Formation, Santa Ana Mountains and San Juan Capistrano Area, California. PATSY BECKSTEAD SMITH. Pp. 463–495; pls. 8; figs. 3; tbls. 10. Price, 40 cents. *The sharp faunal break at the end of the Luisian state found during this study may be due to a change from a tropical middle Miocene Sea to a temperate late Miocene Sea.*

Prof. Paper 332. Cretaceous and Tertiary Formations of the Book Cliffs, Carbon, Emery, and Grand Counties, Utah, and Garfield and Mesa Counties, Colorado. D. J. FISHER, C. E. ERDMANN, and J. B. REESIDE, JR. Pp. 80; pls. 12; fig. 1; tbls. 20. *Description of 7,000 feet of strata ranging in age from Early Cretaceous to Eocene.*

Prof. Paper 334-D. Late Paleozoic Gastropoda from Northern Alaska. E. L. YOCHELSON and J. T. DUTRO, JR. Pp. 111–147; pls. 3; figs. 7; tbl. 1. Price, 50 cents. *Descriptions, illustrations, and stratigraphic significance of 34 species and 1 new genus.*

Prof. Paper 356-A. Oil Yield and Uranium Content of Black Shales. V. E. SWANSON. Pp. 1–44; figs. 21; tbl. 1. Price, 30 cents. *A fair positive relation between oil yield and uranium content exists for some shales, i.e., parts of the Chattanooga and Antrim shale, but in other shales no relation is apparent.*

Water-Supply Paper 1459-B. Restraints on Dissolved Ferrous Iron Imposed by Bicarbonate Reedox Potential, and pH. J. D. HEM. Pp. 33–55; figs. 3; tbls. 2. Price, 15 cents. *At equilibrium, pH and ferrous iron content of ground water provide a basis for estimating the Eh. Estimates of Eh from artesian wells were good; those from a water-table well ran much too high.*

Water-Supply Paper 1479. Geohydrologic Evaluation of Streamflow Records in the Big Wood River Basin, Idaho. R. O. SMITH. Pp. 70; pls. 2; figs. 24; tbls. 2. *An assessment of the geohydrologic conditions that affect the adequacy of streamflow records in measuring the water yield of a basin.*

Water-Supply Paper 1481. Geology and Ground-Water Resources of the Winter Garden District, Texas, 1948. S. F. TURNER, T. W. ROBINSON, and W. N. WHITE; revised by D. E. OUTLAW, W. O. GEORGE, and others. Pp. 248; pls. 4; figs. 22; tbls. 12. *The principal aquifers and the Carrizo sand (Tertiary) and Leona formation (Quaternary). Present rate of withdrawals exceeds the average rate of natural recharge.*

Economic Geology
Vol. 55, 1960, pp. 1323–1342

SOCIETY OF ECONOMIC GEOLOGISTS

DENVER MEETING—OCT. 31 TO NOV. 1, 1960

PROGRAM

Monday Morning, Grand Ball Room

Economic Geology I

Charles F. Park, Jr., and James M. Harrison, *Co-chairmen*
(After each paper 5 minutes is allowed for discussion)

1. 8:30 Rolland R. Reid: Geology and heavy-mineral content of placer deposits in the Elk City region, Idaho.
2. 8:45 Gerald P. Brophy: Copper mineralization in the Catoctin formation, Virginia.
3. 9:00 C. P. Jenney: Geology and ore deposits of the Mattagami area, Quebec.
4. 9:15 Arnold L. Brokaw: Geologic structure in the Mascot-Jefferson City, Tennessee, district.
5. 9:30 H. D. B. Wilson * and W. C. Brisbin: Thompson-Moak Lake nickel belt.
6. 9:45 Leo J. Miller: Massive sulfide deposits in eugeosynclinal belts.
7. 10:00 C. J. Sullivan: Magmatic and nonmagmatic ores.
8. 10:15 P. K. Sims: Hypogene mineral zoning, Central City district, Colorado.
9. 10:30 Presidential Address, Society of Economic Geologists: Duncan R. Derry, *Economic Aspects of Archean-Proterozoic Boundaries*

Monday Noon, Empire Room

12:00 SEG Cocktail Party. 12:30 SEG Luncheon and Annual Meeting.

Monday Afternoon, Empire Room

Economic Geology II

Robert W. Boyle and A. E. J. Engel, *Co-chairmen*
(After each paper 5 minutes is allowed for discussion)

1. 2:30 L. C. Huff, T. G. Lovering,* H. W. Lakin, and A. T. Myers: Comparison of analytical methods used in geochemical prospecting for copper.
2. 2:45 C. W. Field * and M. L. Jensen: Sulfur-isotope geology of vein-type and sandstone-type uranium deposits.
3. 3:00 John D. Ridge: Behavior of sulfur under magmatic and hydrothermal conditions and its effect on S^{32}/S^{34} ratios.
4. 3:15 John S. Brown: Geological interpretation of lead-ore isotopes.
5. 3:30 Motoaki Sato: Application of reaction Eh-pH diagrams to the problems of supergene oxidation and enrichment of sulfide ore bodies.

* Indicates speaker.

6. 3:45 Charles S. Robinson * and John N. Rosholt, Jr.: Apparent age and migration of uranium in deposits in sandstone, based on radiochemical analyses.

7. 4:00 E. Wm. Heinrich * and P. C. Masterman: Nonconglomeratic ores of the Pronto uranium deposit, Blind River area, Ontario, Canada.

8. 4:15 R. A. Gulbrandsen: Minor elements in phosphorites of the Phosphoria formation.

9. 4:30 Leonid Bryner: Breccia and pebble columns associated with hydrothermal ore deposits.

10. David M. Lapham: Photomicrography of the Cornwall magnetite ore body, Cornwall, Pennsylvania.

Tuesday Afternoon, Junior Ball Room

Economic Geology III

Gunnar Kullerud and Frank G. Snyder, *Co-chairmen*
(After each paper 5 minutes is allowed for discussion)

1. 2:45 Donald E. Pruss and Gerald W. Freeman:* Quantitative geophysics applied to metallic mineral property (e.g., iron-ore) evaluation.

2. 3:00 E. N. Cameron,* J. H. Davis, J. M. Guilbert, L. T. Larson, J. J. Mancuso, and R. K. Soren: Rotation properties of certain anisotropic ore minerals.

3. 3:15 Paul B. Barton, Jr.,* Priestley Toulmin, 3d, and Paul K. Sims: Role of chemical potential of sulfur in controlling mineral assemblages in sulfide deposits.

4. 3:30 Philip M. Bethke,* Paul B. Barton, Jr., and Marc W. Bodine, Jr.: Time-space relationships of the ores at Creede, Colorado.

5. 3:45 Edwin Roedder: Studies of primary fluid inclusions in sphalerite crystals from the OH vein, Creede, Colorado.

6. 4:00 Roy A. MacDiarmid: Controls on ore deposition at the Bristol silver mine, Pioche, Nevada.

7. 4:45 Conrad Martin: Origin of crystalline magnesite deposits.

Economic Geology
By Title

Victor T. Allen: Clay minerals in bauxite deposits of Europe.

Charles C. Hawley: Origin of asphaltite-rich ore bodies at Temple Mountain, Emery County, Utah.

Vance C. Kennedy: Origin of uranium-vanadium deposits in the Lisbon Valley area, San Juan County, Utah.

D. S. Krishnaswamy and G. C. Amstutz: Geology of the Decaturville disturbance in Missouri.

Roy Angus MacDiarmid: Application of thermoluminesce to prospecting for hydrothermal ores.

A. T. Myers and J. C. Hamilton: Rhenium in plant samples from the Colorado Plateau.

Council Meeting: Sunday, Oct. 30, 8:00 P.M., Colorado Room; Tuesday, 10:00 A.M., Biltmore Room.

* Indicates speaker.

Paul Dean Proctor: Fringe-zone alteration in carbonate rocks, North Tintic mining district, Utah.

David S. Robertson: Diamond-drill hole deviation in the Blind River area, Ontario, Canada.

John N. Rosholt, Jr.: Radiochemical determination of apparent age of uranium migration in sandstone-type ore deposits.

GEOLOGY AND HEAVY MINERAL CONTENT OF PLACER DEPOSITS IN THE ELK CITY REGION, IDAHO

ROLLAND R. REID

Department of Geology and Geography, University of Idaho, Moscow, Idaho

Stream placer gravel in the Elk City region, studied by the Idaho Bureau of Mines and Geology to determine presence or absence of commercial concentrations of detrital heavies, totals 55 million cubic yards, of which 25 million cubic yards has been mined for its gold content. Minable gravels occur in local wide-valley areas of low gradient, connected by narrow-valley areas of high gradient. Average values of 15 samples, in pounds per cubic yard, are Allanite 0.2, monazite 0.15, rutile 0.07, brookite 0.1, sphene 0.1, zircon 0.25, ilmenite 6.9, magnetite 16.8. Brannerite, euxenite, and columbite are present in trace amounts.

Quartzose Tertiary basin deposits cap certain ridges and benches, streams having cut below the bottom(s) of the former basin(s). The outcrop area of these deposits is about 18 square miles, and their average thickness is probably more than 20 yards (volume more than 1×10^8 cubic yards). Average values of four small grab samples, in pounds per cubic yard, are: monazite 1.6, rutile 0.3, brookite 0.3, zircon 1.5. Such concentrations of heavy minerals in the Tertiary deposits, when considered in conjunction with the high quartz content of the deposits, seem to imply rather intense weathering of the erosion surface from which the deposits were derived.

Most of the Elk City region is underlain by biotite gneiss. Data in hand indicate that the major part of the heavy minerals in the placer deposits was derived from the biotite gneiss.

COPPER MINERALIZATION IN THE CATOCTIN FORMATION, VIRGINIA

GERALD P. BROPHY

Department of Geology, Amherst College, Amherst, Massachusetts

Precambrian basalt flows, pyroclastics and interbedded sediments constitute the Catoctin formation cropping out along the crest of the Blue Ridge Mountains in Virginia and east in the Piedmont of Virginia. Copper mineralization occurs in the western belt of volcanics (1) in abnormal amount in magnetite and pyroxene in some relatively fresh flows and dikes, (2) as chalcopyrite in some dikes believed to be Catoctin feeders, (3) as disseminated native copper in some flows, and (4) as disseminated native copper and in association with quartz-serpentine veins in certain epidotized basalts.

Copper concentrations are localized in flows that were initially rich in copper, where these are in contact with pre-Catoctin topographic highs. The topographic highs have impeded the lateral slippage of individual flows at their boundaries during regional deformation and metamorphism in the late Paleozoic. Intense

epidotization facilitated redistribution of copper into fractured basalt. Epidotized basalts are bordered by albitized basalts. Alkali expelled during epidotization could account for the alkali increase in some portions of the formation.

GEOLOGY AND ORE DEPOSITS OF THE MATTAGAMI AREA, QUEBEC

C. P. JENNEY

372 Lakeshore Hy. West, Oakville, Ontario

The Mattagami area comprises some 750 square miles approximately 120 miles northeast of Noranda, Quebec. Less than 5% of the surface area is outcrop and glacial overburden averages about 75 feet width depths of 200 feet in places.

Although the area has been prospected by conventional methods since 1928, the original ore deposit was located by an airborne magnetic and electromagnetic survey followed by similar work on the ground.

The zinc-copper ores of the area are irregular replacement deposits in a series of typical Keewatin lavas, tuffs and fragmentals. In general, the mineralized zone appears to extend around the west, northwest and north sides of an area of basic intrusives known as the Bell River Complex. Lineal extent of this mineralized horizon is about 25 miles.

The lava-tuff series dips moderately to steeply away from the central basic complex and ore deposits have been found on minor anticlinal flexures adjacent to a key tuff horizon in the series.

At the end of 1959, published ore reserves for the area were 30 million tons averaging 12% zinc, 0.75% copper, 0.02 oz. gold and 1.25 oz. silver. Additional ore is being added to this total by extensive diamond drilling. Ultimate potential of Mattagami is still unknown.

GEOLOGIC STRUCTURE IN THE MASCOT–JEFFERSON CITY, TENNESSEE, ZINC DISTRICT

ARNOLD L. BROKAW

U. S. Geological Survey, Denver, Colorado

The zinc deposits of the Mascot-Jefferson City area, Tennessee, are confined to the Longview dolomite and overlying Kingsport limestone of Early Ordovician age. The district is near the southwest end of a lens-shaped structural block that extends about 45 miles in a N 35° E direction from Mascot to Mooresburg. The northwest boundary of the block is the Saltville fault. Folds and faults of the Rocky Valley fault slice form the southeast boundary. Southwest of Mascot the block is a simple southeast-dipping homocline about 3 miles wide. Northeast of Mascot, where it passes between Jefferson City and Joppa the block widens to a maximum of 15 miles and then tapers to about 4 miles near Mooresburg. In its wide part, the block is characterized structurally by the deep Strawberry Plains basin, by several broad open folds, and by minor thrust faults.

The known ore bodies occur in a belt 1 to 3 miles wide and about 20 miles long between Mascot and Jefferson City. The belt trends N 75–80° E across the regional structural features that trend N 35° E. The belt is defined structurally by a line of elongate domes and sharp northwest bends in the axes of folds that otherwise trend northeast. Minor faults are numerous. These structures apparently resulted from horizontal compression in a northeast-southwest

direction within a structural block produced by regional northwest-directed compressive forces. Shortening caused by this folding and faulting exceeds a mile. Comparable structure is unknown in other parts of the Tennessee Valley.

THOMPSON-NOAK LAKE NICKEL BELT

H. D. B. WILSON AND W. C. BRISBIN

The Thompson-Noak lake nickel belt lies along the root of a Precambrian mountain chain of the Island Arc or Alpine type. The nickeliferous peridotites and nickel ores occur along a negative gravity strip which also coincides with strong thrust faulting and the axis of greatest deformation of the mountain range. Similar structures and highly nickeliferous peridotites occur in present day island arcs.

Much of the belt is covered by Paleozoic rocks but a length of 270 miles may be explored by present day methods. Nickel deposits have been located along sixty miles of the belt. The length of the favorable structure and the size of the known deposits suggest that this will be one of the world's major nickel regions.

The regional gravity anomalies which consist of the negative strip bordered by two positive strips are best explained by major warps of the boundary between granitic and basaltic layers of the crust.

The ore deposits occur in serpentinized peridotite or in gneiss near peridotite. The sulfide mineralogy is similar to that of the Sudbury ores but the structure of the ore in gneiss is different and the Manitoba ores are almost entirely nickel. The mineralogy of the silicate gangue in the gneissic ore is typical of the almandine amphibolite facies, sillimanite-almandine subfacies. Possible igneous and metamorphic origins are considered as a guide to further research on the problem of genesis.

MASSIVE SULFIDE DEPOSITS IN EUGEOSYNCLINAL BELTS

LEO J. MILLER

519 Pineland Ave., Oakville, Ontario, Canada

Massive pyrite deposits occur exclusively within eugeosynclines and are associated with volcanic and sedimentary rocks of the spillitic sequence. These deposits are in marked contrast to the massive lead-zinc-copper deposits of miogeosynclinal shelf zones.

Pyritic deposits were formed during most geologic periods from the Precambrian to Recent and may be separated into three varieties based on the primary lithologic environment: (1) the volcanic type, wholly within volcanic pyroclastic rocks or at the facies change of sediments and pyroclastics (Noranda, Que. and Bathurst, New Brunswick); (2) the sedimentary type, occurring within sediments stratigraphically far removed from volcanism (Sullivan, British Columbia and Ducktown, Tenn.); (3) the ultramafic-mafic type, intimately associated with gabbros, norites or peridotites, within crystalline rocks or adjacent volcanics and sediments (Frood-Stobie, Sudbury, Ont., and Opemiska, Que.).

This classification of sulfide deposits based on the lithology of the host rock suggests that they formed during volcanism and sedimentation and before folding, intrusion and metamorphism. The massive sulfide deposits in Japan which are of late Tertiary and Recent age have formed before orogenesis. These recent deposits are genetically related to concentrations of H_2S gas. Massive sulfide deposits are currently forming on Hokkaido by the action of ferrous sulfate on

banded elemental sulfur beds. Pliocene deposits on Honshu appear to have formed by the localization of H_2S in stratigraphic traps and diagenetic folds.

All late Cenozoic massive sulfide deposits are of the volcanic type but lack the superimposed orogenic and metamorphic features of their more ancient counterparts.

MAGMATIC AND NON-MAGMATIC ORES

C. J. SULLIVAN

Kennco Expl. (Canada) Ltd., 25 King St. West, Toronto 1, Canada

In prospecting, it is of importance to distinguish ores of magmatic origin, from those derived by metamorphism and granitization of source rocks, and from those accumulated in certain sedimentary facies. The magmatic ores are characterized by their occurrence along fault structures, and may be associated with volcanic (including explosive) phenomena. Heat effects are local.

The magmatic sequence is well defined:

Kimberlite, with diamond pipes; ijolite, with carbonatites; peridotite, with nickel deposits; norite, with nickel-copper deposits; diabase-gabbro, with copper-zinc deposits. These deposits are characteristic of Precambrian Shields, where a thick sialic crust may rest on basic to ultrabasic magma.

In the Paleozoic terrains (in a broad sense) the sequence is resumed with monzonite porphyries and associated copper, copper-gold, and copper-lead-zinc deposits.

The monzonite and andesite intrusives, with associated copper and copper-lead-zinc deposits extend into the Mesozoic and Tertiary belts, where they have their greatest development. In some cases, as at Braden, Chile, the ores are found in actual explosive volcanic centres.

In Tertiary to Recent rocks, there has been the development of the gold-silver telluride ores, mercury ores, and hot springs with sulfur deposition—generally along lines of crustal weakness.

The above sequence represents decreasing depth, decreasing time, and decreasing temperature, and conforms to Lindgren's temperature-depth classification.

The numerous non-magmatic metalliferous provinces, in most cases, have little to do with crustal weakness, "main breaks," etc., and prospecting thinking applicable to magmatic ores may be quite misleading in these cases. There has been much confusion in this matter.

HYPOGENE MINERAL ZONING, CENTRAL CITY DISTRICT, COLORADO

P. K. SIMS

U. S. Geological Survey, Denver Federal Center, Denver, Colorado

The gold- and silver-rich base-metal sulfide ore deposits of the Central City district, Colorado, are arranged in well-defined concentric zones manifested by systematic changes in mineralogy, metal content, metal ratios, and mineral textures. The zones extend southwestward into four adjacent mining districts.

The principal mineralogic zones in the Central City district consist of a central core of pyrite-quartz veins and an outer zone, not present to the south, of veins containing dominant galena and sphalerite in a quartz or less commonly a carbonate, barite, or fluorite gangue. Transitional veins in an intermediate area are pyritic veins that contain copper minerals, galena, and sphalerite. Chal-

copyrite and tennantite are the dominant copper minerals; locally this assemblage is replaced by enargite and tennantite.

Gold and copper decrease and concomitantly silver, zinc, and lead increase outward; also, silver-gold, lead-copper, and zinc-copper ratios increase outward. In the same way, the quartz gangue becomes noticeably finer-grained outward.

A COMPARISON OF ANALYTICAL METHODS USED IN GEOCHEMICAL PROSPECTING FOR COPPER

L. C. HUFF, T. G. LOVERING, H. W. LAKIN, AND A. T. MYERS

U. S. Geological Survey, Denver, Colorado

Residual soil near a copper-bearing vein at the Malachite mine, Jefferson County, Colo., was analyzed repeatedly to obtain comparisons of different analytical methods used in geochemical prospecting for copper. In this area "barren" samples (of only background copper content) have a mean copper content of 58 ppm (parts per million) and samples anomalously high in copper have a mean copper content of 216 ppm. Most anomalous samples are above 100 ppm and most barren samples are below.

Rapid or semiquantitative methods, such as the spectrographic, biquinoline, dithizone and chromograph tests for copper and the citrate soluble and acid-soluble tests for total heavy metal, are almost as sensitive but are less precise and less accurate than standard quantitative trace analysis methods. Statistical techniques based chiefly upon the coefficient of variation show that the field methods differ considerably among themselves in sensitivity, precision, and accuracy. This study indicates that the dithizone and the biquinoline tests for copper are the best for geochemical prospecting in this area.

SULFUR ISOTOPE GEOLOGY OF VEIN-TYPE AND SANDSTONE-TYPE URANIUM DEPOSITS

C. W. FIELD AND M. L. JENSEN

Department of Geology, Yale University, New Haven, Connecticut

Sulfur isotopic abundance data from over 500 sulfur-bearing samples of vein-type and sandstone-type uranium deposits have been obtained to determine the importance of bacterial processes in the localization of ore deposits and to provide additional knowledge concerning the distribution of sulfur isotopes in several geologic environments. The isotopic data for sulfides are as follows:

	Vein-type deposits	Sandstone-type deposits
Range of S^{32}/S^{34} ratios	22.10–22.35	21.18–23.40
Percentage variation	1.2	10.0
Range of percentage variation/deposit	0.1–1.0	0.1–6.1
Mean percentage variation/deposit	0.5	2.5
Mean S^{32}/S^{34} ratio/deposit	22.22	22.66

The relatively narrow range of S^{32}/S^{34} ratios, near the meteoritic value (22.21),

for primary sulfides of vein-type deposits is indicative of magmatic hydrothermal mineralization.

Sulfides associated with sandstone-type deposits characteristically exhibit broad S^{32}/S^{34} ratio variations and are commonly enriched in S^{32} relative to meteoritic sulfur. The evidence would suggest that the mineral constituents were deposited from ground water solutions in local reducing environments. The precipitating agent is considered to be hydrogen sulfide, variably enriched in S^{32}, generated by sulfate reducing bacteria.

A mechanism involving the bacterial reduction of a finite quantity of sulfate is proposed to account for the anomalously low S^{32}/S^{34} ratios for sulfides of the Woodrow mine.

A cursory study of the C^{12}/C^{13} ratios of carbonates associated with sandstone-type deposits indicates that, in general, the quantity of calcite-carbon derived from organic material is small as compared with that derived from sedimentary carbonates in the enclosing sediments.

BEHAVIOR OF SULFUR UNDER MAGMATIC AND HYDROTHERMAL CONDITIONS AND ITS EFFECT ON S^{32}/S^{34} RATIOS

JOHN DREW RIDGE

College of Mineral Industries, The Pennsylvania State University, University Park, Pennsylvania

It is suggested the appreciable variation of S^{32}/S^{34} ratios in the minerals of sulfide ore deposits of magmatic and hydrothermal origin may be due to processes operating within the ore fluids. Such processes include: (1) polymerizations of metal-sulfur complexes with the screening sulfur ions removed from any complex being of higher S^{32}/S^{34} ratios than the ratio of the complex prior to the polymerization stage in question, (2) oxidation of sulfur concomitant with the reduction of certain metal ions (such as Cu^{+2}, As^{+5}, Sb^{+5}, and Sn^{+4}) to a lower valence state with the sulfur ions oxidized being of a lower S^{32}/S^{34} ratio than the ratio of the complex prior to the oxidation in question, (3) probable preferential precipitation at higher temperatures of sulfides with higher S^{32}/S^{34} ratios than the original averages for the ore solutions involved and at lower temperatures of sulfides with lower S^{32}/S^{34} ratios than the original averages of the ore solutions concerned (this is analogous to the hydrothermal Leadville dolomite in which the O^{18}/O^{16} ratios are lower, the higher the temperature of carbonate emplacement), and (4) the taking over of sulfur deposited at higher temperatures by sulfides deposited by replacement at lower temperatures (or occasionally the reverse) so that the S^{32}/S^{34} ratios resulting in the guest minerals will be anomously high (or low). Examples are given to show how possible combinations of these factors can explain many of the wide variations from the norm of 22.13 known in natural ores, particularly in low-temperature deposits. The correspondence in the isotopic behavior of oxygen in silicon-oxygen complexes in silicate magmas and of sulfur in metal-sulfur complexes in hydrothermal solutions is discussed.

A GEOLOGICAL INTERPRETATION OF LEAD ORE ISOTOPES

JOHN S. BROWN

942 Dulaney Valley Road, Towson 4, Maryland, Apt. 1

It is a well-known fact that all lead ores consist of four isotopic forms (Pb 204, 206, 207, 208) in varying proportions and that the last three are end products

of the disintegration of uranium 238, U-235, and thorium 232. Since these are disintegrating constantly, the relative amount of the non-radiogenic form (Pb 204), always small, is constantly diminishing.

From a study of the data from some 500 isotopic analyses of lead ores widely distributed through the world and the geologic column, and in the light of their geological relationships, it is the author's conclusion that the amount of Pb 204 in an ordinary lead ore is an excellent index of its true age of generation. Acceptance of this thesis leads inevitably to the conclusion that the ores of lead and its associated metals (zinc, copper, etc.) are not related genetically to the igneous rocks with which they are often associated but have merely been redeposited and modified by the intrusives. They stem from original deposits formed by deep-seated emanations which ascended into the lower part of thick sedimentary sequences at a time when these were still flat-lying and generally undergoing diagenesis.

The Mississippi Valley deposits, hitherto generally considered anomalous, are interpreted as normal unmodified representatives of the prototypes from which ores associated with igneous rocks were derived. In some cases (Broken Hill, Balmat, N. Y.) dynamic metamorphism occurred without igneous action. Either igneous or regional metamorphism results in homogenization of the originally variable isotopes.

APPLICATION OF REACTION Eh-pH DIAGRAMS TO THE PROBLEMS OF SUPERGENE OXIDATION AND ENRICHMENT OF SULFIDE ORE BODIES

MOTOAKI SATO

Dept. of Geology, Harvard University, Cambridge 38, Mass.

Reaction Eh-pH diagrams, based on the potentials of observed oxidation and reduction reactions, show the limits of metastability of minerals in aqueous environments; they supplement *equilibrium* (stability) diagrams in kinetic aspects of geochemical processes. Comparison of reaction diagrams for several sulfide minerals indicates two separate electrochemical series for sulfides, namely oxidation and reduction series.

In the oxidation series, the order and magnitude of reaction potentials depend directly on the activities of metal ions, and indirectly on the activities of hydroxyl, carbonate or other ions that form solids or complexes with the metal ions. For unit activities of metal ions, argentite .82 (volts) is followed by pyrite .76, covellite .59, chalcocite .53, galena .35, and sphalerite .27; whereas for 10^{-6} activities pyrite .58 is followed by argentite .47, covellite .41, chalcocite .35, galena .18, and sphalerite .09. These sequences would correspond to increasing ease of oxidation in the zone of active oxidation and leaching where acidity is high.

Precipitation of solids by hydroxyl ion and/or carbonate ion causes lowering of metal ion activities as functions of pH in neutral to basic solution. At pH 7 and under P_{CO_2} equal to that of the atmosphere, the sequence is: argentite .72, covellite .41, chalcocite .35, pyrite .33, sphalerite .20, and galena .20. This order would apply to the zone of secondary enrichment where neutralization by rock-forming minerals is effective. Excepting pyrite, an earlier mineral in the sequence will replace a later one.

APPARENT AGE AND MIGRATION OF URANIUM IN DEPOSITS IN SANDSTONE BASED ON RADIOCHEMICAL ANALYSES

CHARLES S. ROBINSON AND JOHN N. ROSHOLT, JR.

U. S. Geological Survey, Denver, Colorado, and U. S. Geological Survey Marine Laboratory, Miami University, Miami, Florida

The results of radiochemical analyses and apparent age calculations for a series of samples from the Hulett Creek area, Wyoming, were selected to evaluate the use of apparent age determinations in understanding the migration of uranium in deposits in sandstone. The samples represent oxidized deposits above the water table, oxidized and unoxidized deposits just above and below perched water tables, and unoxidized deposits at least 250 feet below the water table.

The geology, geochemistry, and age results indicate that the original uranium in those deposits now at or above the water table was introduced more than 250,000 years ago. The deposits now above the water table started oxidizing with the lowering of the water table about 80,000 years ago. As the water table moved downward, uranium was leached from the zone of oxidation and reprecipitated below the water level. The oxidation, leaching, and reprecipitation stopped about 10,000 years ago when the water table was lowered below the deposits. The deposits now at the water table started oxidizing about 60,000 years ago. Oxidation, leaching, and reprecipitation of the uranium has continued to the present. The first uranium was introduced into those deposits 250 feet below the water table about 180,000 years ago, and uranium has been accumulating since then.

From radiochemical analyses the probable original grade of leached deposits can be calculated. Knowing the probable grade, and the stratigraphy, structure, and geomorphic history of an area, the present location of the leached uranium and its possible grade can be estimated.

NON-CONGLOMERATIC ORES OF THE PRONTO URANIUM DEPOSIT, BLIND RIVER AREA, ONTARIO, CANADA

E. WM. HEINRICH AND P. C. MASTERMAN

University of Michigan, Ann Arbor, Michigan, and Pronto Uranium Mines, Ltd., Algoma Mills, Ontario, Canada

The uranium deposits of the Blind River Area, Ontario, are widely cited as classic examples of the disseminated U-Th-pyrite mineralization in meta-conglomerates. The beds are described as being uniform both in structure and petrology and similar to those of the Witwatersrand. Although this characterizes most of these deposits, it inadequately describes several. Widespread non-conglomeratic ("altered") ores were encountered at the Pronto deposit on the third level in 1956, and have continued through the sixth (bottom) level, at times constituting 40% of the rock mined.

The "altered" rocks include: (1) albitized conglomerates, (2) albitites (some pyritic), (3) chloritic albitites, (4) chloritites, and (5) carbonate rocks (calcitic and dolomitic). Some dolomitic rocks contain pseudomorphs of dolomite after quartz pebbles, together with barite. Locally, vugs contain calcite crystals enclosing sulfides. Sulfides are: pyrite, pyrrhotite, chalcopyrite, galena and sphalerite. The radioactive minerals include: uraninite and metamict brannerite, both of which may be euhedral, anatase, sphene, globules of hydrocarbon and several uranyl species.

The non-conglomeratic ores show four types of contacts with conglomerate:

(1) faulted, (2) brecciated, (3) gradational, and (4) selective replacement. They flank both sides of a major, west-northwest diabase (No. 3), are confined to areas of faulting, and are themselves faulted and sheared. Within altered ores, uranium values, which are concentrated near footwall contacts, are generally two to four times mine grade. However, ore thicknesses are greatly reduced compared to adjacent conglomerate.

The altered rocks have been formed by replacement of conglomerate and locally of quartzite. The effect of these transformations upon uranium distribution has been profound.

MINOR ELEMENTS IN PHOSPHORITES OF THE PHOSPHORIA FORMATION

R. A. CULBRANDSON

U. S. Geological Survey, Menlo Park, California

Analysis of 60 samples representative of phosphorites of the Phosphoria formation in Idaho, Wyoming, Montana, and Utah gives the following modal and maximum contents of minor elements:

SPECTROGRAPHIC ANALYSES

[Charles Annell and Joseph Haffty, U. S. Geological Survey, analysts]

Element	Mode	Maximum	Element	Mode	Maximum
	Weight (percent)			Weight (percent)	
Ag	0.0003	0.003	Nd	0.03	0.03
As[1]	.004	.02	Ni	.01	.1
B	<.005	.01	Pb	<.001	.003
Ba	.01	.03	Sb[1]	.0007	.004
Be	<.00005	.0003	Sc	.001	.003
Cd	<.005	.03	Se[1]	.001	.007
Co	<.001	.003	Sr	.1	.1
Cr	.1	.3	U[2]	.009	.021
Cu	.01	.03	V	.03	.1
Ga	<.001	.001	Y	.03	.1
La	.03	.1	Yb	.001	.003
Mn	.003	.03	Zn	.03	.03
Mo	.003	.03	Zr	.003	.01

[1] Arithmetic average of colorometric analyses by H. E. Crowe, J. E. Swick, and R. R. Beins.
[2] Arithmetic average of chemical analyses by G. Edgington, A. Schrenk, W. Tucker, G. Daniels, and R. Moore.

Chromium is the most abundant of all the minor elements. It is greater than or equal to the vanadium content in all the samples. Eight samples contain 0.3 percent chromium and high amounts of most of the other elements. One of these contains 0.8 percent total minor elements, the greatest amount of all the samples, of which Cr, V, Mo, Ni, Cu, and Zn make up 0.5 percent and As, Sb, Se, U, Cd, Ba, and Zr are present in their respective highest or higher than average amounts. The high chromium samples, which are also the highest in total minor elements, contain 3.6 percent organic matter compared to an average of 2.1 percent in all the phosphorites.

BRECCIA AND PEBBLE COLUMNS ASSOCIATED WITH HYDROTHERMAL ORE DEPOSITS

LEONID BRYNER

Geology Department, Colorado School of Mines, Golden, Colorado

Columns of rock fragments show a wide variety of form and structure and are associated with many different kinds of ore deposits. The fragments range from angular to rounded and from blocks weighing many tons to the particles that constitute a matrix of rock paste in many columns. The columns usually develop on planar structures or at structural intersections mostly in competent rocks.

Two broad divisions of mineralized rock fragment columns are proposed, namely pre-hydrothermal and co-hydrothermal. In the pre-hydrothermal type the spatial coincidence between the column and the ore shoots in most cases is poor because the column developed prior to and independently of mineralization, and other controls besides the configuration of the column were operative in localizing the ore. In the co-hydrothermal type there is closer coincidence in time and usually in space between ore and the column because the column results from the corrosive action of the hydrothermal fluids.

Tectonic breccias, volcanic vent fillings, intrusive igneous breccias, and filled sink and circle deposits formed by ground water leaching of carbonate rocks, generally come under the heading of pre-hydrothermal structures. Breccia and shatter pipes, hydrothermal pebble dikes, and probably most porphyry copper deposits come under the heading of co-hydrothermal structures.

The incidence of ore most likely is higher in co-hydrothermal than in pre-hydrothermal structures though important ore deposits occur in both types.

PHOTOMICROGRAPHY OF THE CORNWALL MAGNETITE ORE BODY, CORNWALL, PENNSYLVANIA

DAVIS M. LAPHAM

Pennsylvania Geological Survey, Dept. Internal Affairs, Harrisburg, Pennsylvania

The Cornwall magnetite deposits are considered to be a type deposit for metasomatic limestone replacement ore spatially and genetically associated with a diabase intrusive. Recent studies show that the genesis of these ores is more complex than previously believed. Most important has been a systematic petrographic examination of ore and gangue interrelations vertically and laterally throughout the more recent eastern ore body. Thin section color photomicrographs reveal that 1) the diabase is not noticeably depleted in iron content, 2) fissure veins cut and disseminated magnetite replaces the diabase chill zone from the top downward, 3) amphibolitization, chloritization, and sericitization of the upper part of the diabase increase toward the ore contact, 4) crystallization of the diabase was followed first by thermal and metasomatic silication, later by metal sulfides and oxides, and finally by late, low temperature hydrous silicates, and 5) ore localization controls include the composition of the host metasediments, primary compositional bands within these metasediments, grain size textures both of the metasediments and of the metasilicates, and the quantity distribution of the metasilicates, especially pyroxene and amphibole. Lateral and vertical mineral variation is present with respect to the ore footwall at the diabase contact. From the petrographic evidence it may be concluded that the ore was emplaced later than the diabase crystallization, that it is associated with hydrothermal mineralization, and that replacement locally is compositionally and texturally controlled.

QUANTITATIVE GEOPHYSICS APPLIED TO METALLIC MINERAL-PROPERTY (E.G., IRON-ORE) EVALUATION

DONALD E. PRUSS AND GERALD W. FREEMAN

Geodynamics, Inc., 10809½ Strathmore Drive, Los Angeles 24, Calif.

A survey of contemporary Russian and American literature concerning exploration geophysics indicates conductive mineral deposits may be interpreted quantitatively from co-ordinated magnetic, electromagnetic, and/or gravimetric surveys. The use of electromagnetic devices demonstrates the feasibility of estimating ore grade for certain buried conductive mineral assemblages, e.g., copper and nickel sulfides, iron ore. Such analyses may be helpful in determining the economic potential of mineral properties, at the outset of an exploration-development program or in establishing present value.

Electromagnetic and magnetic field studies were conducted over tabular deposits of copper sulfides, nickel sulfides, magnetite, and magnetite-hematite. A primary field was created by use of a long grounded wire, up to 5,000 feet long. Variances in amplitude and phase of vertical component of the electromagnetic field were determined by a Wien type bridge connected to two horizontal three-foot coils. Magnetic data were obtained through use of an Askania Schmidt type magnetometer, readable to three gammas.

The electromagnetic technique allowed interpretation of the spatial distribution of conductivity, the magnetic technique that of permeability, from which grade (e.g., % Fe) and tonnage estimates were thereby inferred.

ROTATION PROPERTIES OF CERTAIN ANISOTROPIC ORE MINERALS

E. N. CAMERON, J. H. DAVIS, J. M. GUILBERT, L. T. LARSON, J. J. MANCUSO, AND R. K. SOREM

Dept. of Geology, Univ. of Wisconsin, Madison, Wisconsin

Over a period of five years, the authors have measured the rotation properties of 82 anisotropic ore minerals at 470, 520, 546, 589, 620, and 650 $m\mu$ in air, and at 589 $m\mu$ in oil. Values of the rotation angles for the various minerals range from sensibly 0° to 23.2°. Phase differences of most of the minerals are positive. The minerals studied show four patterns of dispersion of the rotation angle (A_r) with wavelength and several patterns of dispersion of the phase difference 2θ.

The data obtained lead to the following conclusions:

(1) The range of rotation angles of anisotropic ore minerals in air is very broad relative to the accuracy of measurement, which is commonly ± 0.1 to $\pm 0.2°$. Measurement of rotation angles therefore can assist substantially in mineral identification.

(2) Dispersion phenomena are a second aid to identification.

(3) The sign of the phase difference for a mineral is easily determined and is a supplemental aid to identification.

(4) The color phenomena of polarization figures are in some cases distinctive, hence useful in identification of certain minerals.

(5) For most of the minerals studied, surface films produced by polishing do not affect the reliability of rotation angles for identification of minerals in polished surfaces.

In sum, the use of rotation properties greatly extends the range of minerals that can be identified rapidly under the microscope without recourse to special supplementary techniques.

THE ROLE OF CHEMICAL POTENTIAL OF SULFUR IN CONTROLLING MINERAL ASSEMBLAGES IN SULFIDE DEPOSITS

PAUL B. BARTON, JR., PRIESTLEY TOULMIN, 3D, AND PAUL K. SIMS
U. S. Geological Survey, Washington, D. C., and Denver, Colorado

For a given bulk composition of metals the sulfide assemblages in most mineral deposits are determined by two primary variables, temperature and chemical potential of sulfur. Total pressure can almost be neglected. A diagram in which chemical potential of sulfur is plotted against temperature thus provides a generally applicable frame of reference for most hydrothermal deposits. This grid is useful in interpreting the paragenetic and zoning relations in ore deposits and is particularly helpful in the application of the sphalerite geothermometer to pyrite-sphalerite assemblages.

The hypogene zoning in the Central City district, Colorado (see abstract by Sims), is reflected by a change in composition of sphalerite as well as by changes in gross mineralogy. The overall pattern is interpreted as having formed from solutions which initially were at a temperature of the order of 600° C and cooled to 300°–400° C as they moved upward and outward. As cooling progressed the chemical potential of sulfur dropped so slowly that more sulfur-rich assemblages were deposited peripherally. Presumably the chemical potential of sulfur changed through homogeneous reactions in the ore fluid, for there is no indication of extensive reaction with wall rock at this stage. The rate of change of chemical potential of sulfur with temperature followed two trends, and led to the formation of two assemblages: 1) pyrite-galena-tennantite-chalcopyrite-sphalerite and 2) pyrite-galena-tennantite-enargite-sphalerite. Sphalerite (1) contains much more FeS than (2).

TIME-SPACE RELATIONSHIPS OF THE ORES AT CREEDE, COLORADO

PHILIP M. BETHKE, PAUL B. BARTON, JR., AND MARC W. BODINE, JR.
U. S. Geological Survey, Washington, D. C., and Bowdoin College, Brunswick, Maine

A knowledge of the details of the time-space relationships among ore and gangue minerals is prerequisite to the understanding of the processes of ore genesis. To this end we have begun a detailed mineralogic study in what appears to be an ideally suited deposit: the OH vein at Creede, Colorado. (See also: Roedder, these abstracts.)

The ores are coarse, unsheared open space fillings in a tabular, nearly vertical vein filling a minor antithetic fault within a major graben extending northward from the Creede Caldera. The wall rock is uniform welded tuff of rhyolitic composition. Hydrothermal alteration is minor. The vein has been developed for about 1,000 feet vertically, and laterally for a distance of more than a mile.

The mineral assemblage includes galena, sphalerite, chalcopyrite, pyrite, quartz, hematite, and chlorite, with minor fluorite, barite, and ankerite.

Compositional zoning and several stages of alternate precipitation and leaching are recognizable in individual sphalerite crystals, and can be correlated throughout most of the mine, thereby providing "marker horizons." Galena and chalcopyrite are similarly zoned and leached, and various "generations" of these minerals can be established in the time sequence by their relationships to the various "horizons" in sphalerite.

Time-space relationships in ore deposits of this type may be much more com-

plex than is generally appreciated. Conclusions based on the assumption that equilibrium was established between phases require thorough knowledge of the detailed paragenetic relations and may be applicable only over small increments of the time sequence and short distances.

STUDIES OF PRIMARY FLUID INCLUSIONS IN SPHALERITE CRYSTALS FROM THE OH VEIN, CREEDE, COLORADO

EDWIN ROEDDER

U. S. Geological Survey, Washington, D. C.

Fluid inclusions in successive zones of large multiply-zoned sphalerite crystals were examined in detail as a part of a larger study of a single ore-body (Bethke et al., these abstracts).

Total salt concentrations in the included fluids were estimated from the depression of the freezing points of approximately 400 inclusions. A special circulating-fluid microscope cell (temperature range $-35°$ to $+250°$ C) was used, and the fluids were assumed to be water solutions of alkali and alkaline earth chlorides, as indicated by chemical analyses. Check measurements made by crushing selected single inclusions *in vacuo* for water analysis, followed by leaching and microanalysis for soluble salts, were in good agreement with the freezing point data.

Systematic variations from 6 to 15 weight percent total salts were found, earlier zones having the higher concentrations. Filling temperatures also showed a systematic change from $\sim 250°$ C for earlier zones to $\sim 200°$ C for later ones, regardless of crystal size. Significant variations in salt compositions and deuterium-hydrogen ratios were also found.

Conclusions: 1) The inclusions are primary and have not lost or gained significant amounts of material since trapping; 2) concentration, composition, and temperature of the fluids changed during the depositional history; 3) inclusions provide a possible tool for recognition of epochs of deposition of sphalerite, and for recognition of co-deposited minerals; and 4) we cannot yet discriminate between possible explanations of the variations found: a) changes, with time, of the fluid at its source, and b) mixing of two sources.

CONTROLS ON ORE DEPOSITION AT THE BRISTOL SILVER MINE—PIOCHE, NEVADA

ROY A. MACDIARMID

Department of Geology, Tulane University, New Orleans 18, Louisiana

The Bristol Silver Mine, located 14 miles northwest of Pioche, in Lincoln County, Nevada, produces silver, copper, lead, and zinc from limestones and dolostones of the Cambrian Highland Peak formation. The area has been extensively faulted, and metallization was controlled both by structural and by combined structural-stratigraphic factors.

The ore at Bristol occurs in oxidized replacement bodies as carbonates and silicates, with rare kernels of primary sulfides. The ore bodies have many shapes, from nearly vertical pipes and flat-lying "mantos" to irregular fissures surrounding large breccia fragments. Concentrations of ore are found where faults intersect favorable host rocks, beneath impermeable lithologic horizons, in breccia zones, at the intersections of faults, and along single structures where there may have been open or brecciated zones. The principal pipes apparently formed in minor

faults where movements of small magnitude developed pinches and swells along the fault surface; the cavities thus opened, which probably contained collapse breccias, permitted the influx of ore-bearing solutions.

THE ORIGIN OF CRYSTALLINE MAGNESITE DEPOSITS

CONRAD MARTIN

9426 University Station, Reno, Nevada

The magnesite at Gabbs, Nevada, occurs within dolomite—part of the 10,000 feet of conglomerate, limestone, argillite, and dolomite which was deposited in a local embayment of the Late Triassic sea. These were folded, repeatedly faulted, and intruded by several generations of dikes and a granodiorite stock. The magnesite is involved in all, but its emplacement appears controlled by none, of the intrusive and orogenic history.

Stress-zones within the magnesite are generally dolomitized. Pendants of magnesite within the stock are largely converted to brucite in which apophyses of granodiorite are partly changed to serpentine. Large masses of dolomite, remote from intrusives, have been transformed to diopside rock.

The deposits at Chewelah, Washington, are similar to those at Gabbs. At Cranbrook, British Columbia, the magnesite occurs within quartzite. Except for the extensive metamorphism of the Grenville rocks, the geologic setting of the magnesite at Kilmar, Quebec, is similar to the Gabbs and Cranbrook deposits. All are interpreted as being sedimentary in origin, having been deposited, with the enclosing dolomite, in shallow, restricted, unstable, marine embayments similar to some of the Caspian Sea in which magnesite and dolomite are presently being precipitated.

The diopside masses at Gabbs, and the roughly concordant serpentine and diopside bands traversing the magnesite at Kilmar, are interpreted as having been formed by metamorphism of contemporaneously deposited silica and carbonates, possibly in the form of a hydrous silica-carbonate gel. Many serpentine and related sills, usually interpreted as being intrusive, may have a similar origin.

CLAY MINERALS IN BAUXITE DEPOSITS OF EUROPE

VICTOR T. ALLEN

Department of Geology and Geological Engineering, Saint Louis University, St. Louis, Mo.

Bauxite and aluminous laterite deposits of France, Yugoslavia, Greece, Italy, Spain, Germany and Northern Ireland were studied under a grant of the National Science Foundation in 1957. In all the deposits examined clays composed of kaolinite and locally some montmorillonite minerals occur in association with bauxite minerals and suggest that clays were the source materials of the bauxite. Refractory ceramic kaolinite clay and boehmite from Missouri are similar megascopically and mineralogically to specimens collected in France and Yugoslavia; also, diaspore specimens from Missouri can be duplicated in the diaspore deposits of Greece. The aluminous laterites of Germany and Northern Ireland derived from basaltic rocks are similar to those of Oregon.

The commercial bauxite of France, Yugoslavia, Italy, Greece, and Spain fills solution pockets in dolomitic limestones. Kaolinite-boehmite diaspore deposits of Missouri and bauxite in Georgia fill pockets in dolomite limestones formed by groundwater solutions. Clays and alumina hydrates were transported from suitable source areas in Europe and the United States, and were deposited in cavities prepared by solution. Magnesium bicarbonate carried by groundwater

removed silica from clay to form alumina hydrate minerals. Observations in Georgia, Alabama, Arkansas, Oregon, and Washington suggest desilication of clays can form bauxite.

ORIGIN OF ASPHALTITE-RICH ORE BODIES AT TEMPLE MOUNTAIN, EMERY COUNTY, UTAH

CHARLES C. HAWLEY

U. S. Geological Survey, Building 25, Denver Federal Center, Denver, Colorado

Uranium ore bodies at Temple Mountain are composed principally of sandstone impregnated with solid uraniferous carbonaceous substances termed "asphaltite." Most are in petroliferous, sparsely coal-bearing sandstones of the Moss Back member of the Chinle formation, but, near a large pipe-like collapse, small bodies are found in petroliferous rocks of other units. The deposits in the Moss Back member are in a belt about 2 miles long and 2,000 feet wide, a few thousand feet downdip from the collapse. Within the belt ore bodies are dominantly elongated rolls oriented across the belt; regardless of location most ore bodies have one sharp contact with altered rock nearly devoid of petroleum and one gradational contact with nearly unaltered petroliferous rock. The sharp ore contacts are inferred to mark interfaces formed between carbonated aqueous solutions, introduced through the collapse, and petroleum-rich fluids saturating the sandstones. The introduced solutions displaced oil components from the altered sandstone, and asphaltite, derived from the displaced oil, formed along with uraninite and other metallic minerals near stabilized interfaces. Coal extracts may locally have been incorporated in the asphaltite, but judging from the field occurrence the presence of coaly materials was not essential. The cause of precipitation at the interface was probably an increase in pH due to depletion of carbon dioxide in the introduced solution. This mechanism is suggested principally by epigenetic concentrations of elements which form soluble bicarbonates near the sharp ore contacts.

ORIGIN OF URANIUM-VANADIUM DEPOSITS IN THE LISBON VALLEY AREA, SAN JUAN COUNTY, UTAH

VANCE C. KENNEDY

U. S. Geological Survey, Denver, Colorado

Uranium-vanadium deposits occur in and near sandstones in the upper part of the Permian Cutler formation and near the base of the Triassic Chinle formation along the southwest flank of the longitudinally faulted, northwest trending Lisbon Valley anticline. Sandstones of the Salt Wash member of the Jurassic Morrison formation contain similar deposits.

Interbedded red sands, gravels, and muds were deposited near the Lisbon Valley area during Cutler time. Later, the Triassic Moenkopi formation was deposited and Cutler beds, uplifted along the Lisbon Valley anticline, were truncated by erosion.

Northwestward flowing Chinle streams deposited interbedded carbonaceous mud, sand, and gravel on Moenkopi and truncated Cutler beds. Carbonaceous material produced a reducing environment in basal sediments of the Chinle and, locally, in Cutler beds. During compaction in Late Triassic and Jurassic time, connate water from Cutler and Moenkopi red beds possibly carrying dissolved U^{+6}, V^{+4}, and V^{+5}—migrated horizontally through interbedded sandstones and

then upward into basal Chinle sandstones where U^{+4}, V^{+3}, and possibly V^{+4} minerals may have been precipitated.

Connate water, mainly from basal red beds of the Brushy Basin member of the Morrison formation, probably moved toward the Lisbon Valley fault through sandstones of the upper Salt Wash during compaction after deposition of thick Late Cretaceous sediments. Ore bodies may have formed in carbonaceous zones within those permeable sandstones which transmitted large volumes of connate water.

If connate water was the ore fluid, much Cutler and Chinle ore is of Late Triassic and Jurassic age and Morrison ores are of Late Cretaceous and early Tertiary age.

GEOLOGY OF THE DECATURVILLE DISTURBANCE IN MISSOURI

D. S. KRISHNASWAMY AND G. C. AMSTUTZ

University of Missouri, School of Mines and Metallurgy, Rolla, Mo.

The area of the Decaturville uplift comprises 20 km² in Camden and Laclede Counties in west-central Missouri. The present study is based on detailed surface mapping, four open pits, and 85 diamond and 5 churn drill holes with an aggregate footage of approximately 22,000 feet.

The sedimentary rocks consist of sandstones, dolomites, and shales of Cambrian and Early Ordovician age. In the center a granite pegmatite body is exposed and isolated pegmatite apophyses or wedges have been met at a few places in different drill holes. A mylonitic sericite schist zone surrounds the outcropping pegmatite.

The lead, zinc, and iron sulfide mineralization within the structure is restricted almost exclusively to some portions of a strongly brecciated zone, which may correspond to a fault zone in the sedimentary rocks.

All rock units are disturbed by multiple rejuvenated faulting. Some portions of the drill cores show overturned and overthrusted, repeated sequences. The beds immediately surrounding the pegmatite, to a distance of 2 km away from it, exhibit variable dip and strike, even within short distances. The overall structural pattern is that of a complex zoned polygonal uplift, similar to the Crooked Creek structure in Central Missouri and to the other polygonal structures of the Middle West.

The tectonic history, together with the presence of the pegmatite(s), supports the conclusion that the Decaturville disturbance is caused by polygonal or ring tectonic movements in the basement, connected with, or caused by igneous activity.

AN APPLICATION OF THERMOLUMINESCE TO PROSPECTING FOR HYDROTHERMAL ORES

ROY ANGUS MACDIARMID

Geology Department, Tulane University, New Orleans, La.

A given mineral will produce luminescence only on the first application of heat. The light is a result of electrons escaping from traps within the crystal lattice, and once a trap is drained, there is no new supply of electrons.

Most minerals that exhibit thermoluminescence have glow peaks at specific temperatures. The absence of these sharp peaks should signify that the rock has been heated above the corresponding temperature sometime in the past; the presence of peaks implies either a cold history or else heating with subsequent

refilling of the electron traps. Accordingly, it is proposed to prospect for the "fossil" heat aureole around hydrothermal deposits, using underground drill-hole samples. Young, high-temperature ore bodies should be most amenable to this prospecting technique.

The possibility of prospecting with thermoluminescence was investigated by McDougall in 1954 (ECONOMIC GEOLOGY, v. 49), but his study was based on the supposition that radioactive materials are added to the contact aureole, increasing the thermoluminescence within this zone. Even without refined techniques McDougall obtained some positive results.

The present idea was tested on limestones and dolostones at the Bristol Silver Mine, Pioche, Nevada, with some favorable and some conflicting results, which in general were in disagreement with those of McDougall. Further studies are in preparation to determine whether or not thermoluminescence can be used for prospecting, and if so, which effect (traps drained by heat or traps filled by activators) describes the contact aureole.

FRINGE ZONE ALTERATION IN CARBONATE ROCKS—NORTH TINTIC MINING DISTRICT, UTAH

PAUL DEAN PROCTOR

Department of Geology, Missouri School of Mines, Rolla, Missouri

Roughly zoned hydrothermal alteration occurs in the folded and faulted Paleozoic carbonate rocks, near the north fringe of the Tintic mining district. At least five types of alteration are recognized: dolomitic, argillic, jasperoid, calcitic, and productive. This resembles the alteration described by Lovering *et al.* for the East Tintic area.

Hydrothermal dolomite is the earliest and most widespread stage and decreases with increasing distance northward. Argillic alteration is least abundant and of local occurrence. A jasperoid stage of alteration occurs as replacements of carbonate rock, is less abundant than the hydrothermal dolomite and becomes sporadic northeastward. Calcitic alteration includes the replacement and/or open space filling in carbonate rock by red hematite-impregnated calcite. Northward, orifices resembling former hot spring pipes are partially to completely filled by this and other calcite types and aragonite. The calcitic stage mainly post-dates the jasperoid stage. It lies north of the jasperoid masses and is more abundant. Iron, lead, zinc and probable silver sulfides, minor manganese and reported bismuth and gold characterize the last or productive stage. This is closely associated with the calcitic stage, although the gold and bismuth occur near jasperoid rock. Except for the argillic stage the productive alteration has the least known quantity of introduced materials. While exact time dating of the hydrothermal alteration stages is not possible in this area, the sequence appears to be dolomitic, argillic, jasperoid, calcitic and productive in a crudely zoned distribution pattern north of the main Tintic district.

DIAMOND DRILL HOLE DEVIATION IN THE BLIND RIVER AREA

DAVID S. ROBERTSON

804–80 Richmond St., W., Toronto 1, Ontario

Over 700,000 feet of diamond drilling in the Blind River area provide data bearing on many facets of drilling of interest to those involved in an appraisal of ore deposits. One of these facets is diamond drill hole deviation.

The data show that most deviation in deep holes (holes below 2,000') takes place in the upper part of the hole. However, there is some relation between amount of deviation and stratigraphy.

Deviation is caused by the planar elements in rocks, but is enhanced or reduced by various drilling techniques. A drill hole in rocks with planar elements should be engineered from the target upward to the collar so as to take advantage of any natural tendency to deviate.

The location of some deep holes underground permits a qualitative examination of the accuracy of hole surveying using acid tests and tropari bore hole compass. Use of numerous tropari tests gives a survey sufficiently accurate for mine planning purposes.

RADIOCHEMICAL DETERMINATION OF APPARENT AGE OF URANIUM MIGRATION IN SANDSTONE-TYPE ORE DEPOSITS

JOHN N. ROSHOLT, JR.

U. S. Geological Survey, Marine Laboratory, Univ. of Miami, Miami, Fla.

The migration of uranium may be studied by the distribution of the radioactive daughter products, which serve as natural tracers in the migration of uranium. The distribution of the daughter products is determined by radiochemical analyses of samples from sandstone-type ore deposits. From the radiochemical analyses, the apparent minimum and maximum dates of uranium introduction or redistribution may be calculated from the Pa^{231}/Th^{230} ratio. The primary assumption required is that the protactinium and thorium do not migrate in measurable quantities from the place where they were produced by the radioactive decay of the parent uranium isotopes. This assumption in most cases is justified on the basis of the chemical properties of these two elements in natural geochemical environments. The practical limit of age determination is about 250,000 years, based on the 34,300 year half life of Pa^{231} and 80,000 year half life of Th^{230}. The difference in the half lives of these isotopes is reflected in their differential rates of growth and decay corresponding to migrations of the parent uranium during the time range considered. The growth and decay patterns, analyzed mathematically, are used to determine the apparent date of uranium migration.

The sandstone-type uranium deposits, for the purpose of calculation, are classified into those at or above the water table and those at considerable depth below the water table. Different methods are used to calculate the maximum and minimum dates of introduction and migration of uranium for the two classes of deposits.

Economic Geology
Vol. 55, 1960, pp. 1343–1344

SCIENTIFIC NOTES AND NEWS

EMMONS MEMORIAL FELLOWSHIP

The S. F. Emmons Memorial Fellowship in economic geology will be available for the academic year 1961–62. The Fellow may use the stipend ($2,000) to support study and research in any university or institute approved by the Committee. He should be qualified by training and experience to investigate some problem in economic geology, and will be expected to devote full time to the investigation. Its results may, if desired, be used as a doctoral dissertation. Forms may be obtained from any member of the Committee: Alan M. Bateman, Yale University; Charles H. Behre, Jr., Columbia University; H. E. McKinstry, Harvard University. Applications and supporting letters should be submitted to the Committee not later than February 15, 1961, and should include a detailed statement of the problem to be investigated.

H. I. ALTSHULER, Mining Engineer, Vice President of New York and Honduras Rosario Mining Company, has become an associate member of Behre Dolbear & Company, New York, mining, geological and metallurgical consultants.

FRED H. HOWELL has left the Kennecott Copper Corporation, Braden Mine, Chile, to accept a position with Duval Sulfur and Potash Company as their Chief Geologist with headquarters at Tucson, Arizona.

W. B. RICHARDSON and H. R. COOKE, JR., of Cooke, Everett & Assoc., Inc., are on a trip through Costa Rica and Mexico, examining gold, manganese, and mercury properties.

W. JAMES BICHAN, Vice-President, Mining and Geological Divisions of Beaco Limited, has been in the West Indies for Canadian Engineering (International) Limited as technical adviser to the Government of Trinidad and Tobago. Mr. Bichan served on the government negotiating team that recently concluded an agreement with substantial United States interests for the airborne geophysical survey of the Northern Range of Trinided.

MURL H. GIDEL, formerly Assistant Chief Geologist of the Anaconda Co., died in his sleep at Butte on March 18, 1960.

EDWARD C. T. CHAO, U. S. Geological Survey geologist-mineralogist, was examining specimens of strongly sheared Coconino sandstone collected by Survey Geologist, Dr. Eugene M. Shoemaker, at Meteor Crater, Arizona, and discovered that the sample contained coesite, a dense and highly stable form of silica not previously known to occur naturally on earth. Like diamond, it had been predicted that extremely high temperatures and pressures are required for coesite, and that it could only be formed in the earth naturally at great depth. When repeated searching failed to uncover it among samples taken from the diamond "pipes" of South Africa and from quartz samples subjected to schocks of several hundred thousand atmospheres, investigators predicted it might never be found as a natural mineral. Even a kilo-ton nuclear device proved incapable of causing the transition. The occurrence of coesite at Meteor Crater is not rare but rather extensive and abundant.

RICHARD V. GAINES, who was manager of exploration in Mexico for Dresser Industries, Inc., has become affiliated with Perforadora Latina S. A. as director of mineral investigations.

PHILIP L. PLATT has taken a position as geologist with Mine Management Associates Ltd. in Monrovia, Liberia. He has been geologist with the National Iron Ore Co.

JACK F. B. SILMAN has joined the mining and exploration department of International Minerals & Chemic.l Corp. as an exploration geologist.

The Michigan College of Mining and Technology recently announced the appointment of JAMES M. NEILSON, professor of geology, as assistant dean of faculty of the college.

GLEN A. BOYD, mining geologist for the Northern Pacific Railway, has been appointed district mining geologist in charge of Northern Pacific's geology division activities in Washington, Oregon, and Idaho.

OSCAR W. BILHARZ has been appointed director of the Office of Minerals Mobilization. He has been acting director of the Department of Interior organization since the retirement of Spencer S. Shannon last December.

PAUL S. PATCHICK has been appointed staff geologist in the Research and Development Department of Collier Carbon and Chemical Corporation.

C. HARRY BURGESS has been elected vice president, exploration of Kennecott Copper Corporation. He has been president of Bear Creek Mining Company for the past four years.

INCREASE IN SUBSCRIPTION RATE—ECONOMIC GEOLOGY

Effective immediately on all orders for Vol. 56 and subsequent volumes until further notice:

	Per Vol.
Domestic Rate	$8.50
North, South and Central America	8.80
All others	9.25

Single issues $1.50 per copy

ROCK ANALYSIS FOR GEOLOGICAL RESEARCH

Rapid accurate results from an authoritative laboratory—carefully directed by graduate chemists and physicists—using modern techniques—spectrographic—spectrophotometric—chemical—reporting results six weeks after receipt of samples or sooner.

Request Details or Submit Samples to:

TECHNICAL SERVICE LABORATORIES

355 KING STREET WEST TELEPHONE EMpire 2-4248
TORONTO 2B CANADA

Specialists in rock and mining analysis

Research facilities available for:

Ore Dressing—process development—extractive metallurgy investigations—mill and plant analytical control methods

FIFTIETH ANNIVERSARY VOLUME

ECONOMIC GEOLOGY

1905–1955

CONTENTS

Part I

FOREWORD ii
ECONOMIC GEOLOGY ..... *Alan M. Bateman* 1
METALLOGENETIC PROVINCES AND EPOCHS ..... *F. S. Turneaure* 38
THERMAL SPRINGS AND EPITHERMAL ORE DEPOSITS ..... *Donald E. White* 99
THE CLASSIFICATION OF ORE DEPOSITS ..... *James A. Noble* 155
STRUCTURE OF HYDROTHERMAL ORE DEPOSITS ..... *H. E. McKinstry* 170
THE ZONAL THEORY OF ORE DEPOSITS ..... *Charles F. Park, Jr.* 226
TEMPERATURES IN AND NEAR INTRUSIONS ..... *T. S. Lovering* 249
SYNTHETIC MINERALS ..... *W. A. Weyl* 282
HYDROTHERMAL ALTERATION AS A GUIDE TO ORE ..... *George M. Schwartz* 300
OXIDATION OF COPPER SULFIDES AND SECONDARY SULFIDE ENRICHMENT *Charles A. Anderson* 324
METHODS AND PROBLEMS OF GEOLOGIC THERMOMETRY ..... *Earl Ingerson* 341
SEDIMENTARY DEPOSITS OF RARE METALS ..... *Konrad B. Krauskopf* 411
ORIGIN OF URANIUM DEPOSITS ..... *V. E. McKelvey, D. L. Everhart and R. M. Garrels* 464

Part II

ENGINEERING GEOLOGY—A FIFTY YEAR REVIEW ..... *Robert F. Legget* 534
INFLUENCE OF GEOLOGICAL FACTORS ON THE ENGINEERING PROPERTIES OF SEDIMENTS ..... *Karl Terzaghi* 557
RECENT DEVELOPMENTS IN CLAY MINERALOGY AND TECHNOLOGY *Ralph E. Grim* 619
PROPERTIES OF CALCIUM AND MAGNESIUM CARBONATES AND THEIR BEARING ON SOME USES OF CARBONATE ROCKS ..... *D. L. Graf and J. E. Lamar* 639
THE QUANTITATIVE APPROACH TO GROUND-WATER INVESTIGATIONS *John G. Ferris and A. Nelson Sayre* 714
TIME OF PETROLEUM ACCUMULATION ..... *A. I. Levorsen* 748
COAL PETROLOGY ..... *C. E. Marshall* 757
THE USE OF GAMMA RAY MEASUREMENTS IN PROSPECTING *William L. Russell* 835
ECONOMIC APPLICATIONS OF PALEOCOLOGY ..... *Samuel P. Ellison* 867
GEOPHYSICS APPLIED TO PROSPECTING FOR ORES ..... *Louis B. Slichter* 885
MINOR ELEMENTS IN SOME SULFIDE MINERALS ..... *Michael Fleischer* 970
THE STUDY OF PEGMATITE DEPOSITS ..... *Richard H. Jahns* 1025–1130

order from

ECONOMIC GEOLOGY PUBLISHING COMPANY

105 Natural Resources Building, Urbana, Illinois

Price to Subscribers (including members, non-member Journal subscribers, and students whether subscribers or not) $6.00

Price to Non-Subscribers to Journal 8.00

"There are many separations which would prove impossible without this apparatus . . ."

FRANTZ ISODYNAMIC Magnetic SEPARATOR

The selectivity of the Isodynamic Separator is due to the shape of the pole pieces. This produces a magnetic field of such configuration that a uniform force is produced on a particle of given susceptibility anywhere in the working space.

Feeding at slow rates, using the vibrator and inclined feed chute shown at the right, the most delicate separations of fine powders, down to 200 mesh are made even on feebly magnetic materials. The intensity of vibration may be adjusted to suit various materials.

Inclined Feed

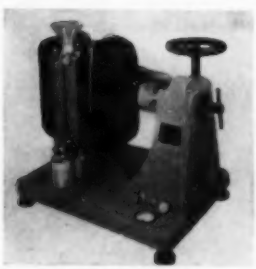

Vertical Feed

Vertical Feed Attachments also available

For separating heavy sands between 40 and 100 mesh, vertical feed is highly satisfactory. Rapid separations are sometimes made at rates up to 20 lb. per hour.

Write for Bulletin

S. G. FRANTZ Co., Inc.

E N G I N E E R S

329 Kline Ave. at Brunswick Pike . . . P. O. Box 1138 . . . Trenton 6, N. J., U.S.A.

Cable Address: MAGSEP, Trentonnewjersey

A COMPLETE PRINTING SERVICE

GOOD PRINTING does not just happen; it is the result of careful planning. The knowledge of our craftsmen, who for many years have been handling details of composition, proofreading, presswork and binding, is at your disposal. For seventy-five years we have been printers of scientific and technical journals, books, theses, dissertations and works in foreign languages. Consult us about your next printing job.

• PRINTERS OF • ECONOMIC GEOLOGY

LANCASTER PRESS, Inc.

PRINTERS • BINDERS • ELECTROTYPERS

ESTABLISHED 1877 LANCASTER, PA.

ANNOTATED BIBLIOGRAPHIES OF ECONOMIC GEOLOGY

Available—Vols. **I–XXXI** (**1928–1958**).

Vol. **XXXII** (**1959**) current volume for 1960.

Price **$5.00** per volume anywhere in the world thru Volume 27.

Effective Volume 28—price change to **$6** per volume.

General Index, Vols. **I–XXV**, in preparation.

Order now from

ECONOMIC GEOLOGY PUBLISHING COMPANY

105 Natural Resources Building **Urbana, Illinois**

ECONOMIC GEOLOGY JOURNAL INDEX to Vols. **XXXI–XL** (**1936–1945**)—published September, 1947

Price **$2.00**

Also available Index to Vols. **I–XX** (1906–1926) —**$3.00**
Index to Vols. **XXI–XXX** (1927–1935)— **2.00**
Index to Vols. **XXXI–XL** (1936–1945)— **2.00**
Index to Vols. **XLI–L** (1946–1955) — **3.00**

ECONOMIC GEOLOGY PUBLISHING COMPANY

105 Natural Resources Building **Urbana, Illinois**

Leitz **first in precision optics**

NEW POLARIZING MICROSCOPE SM-pol

Leitz sets a new standard with this student polarizing and chemical microscope of modern design, with dual, low-position focusing controls and large field of view. A reasonably priced polarizing microscope, the model SM-pol, has rugged, one-piece construction with Bertrand lens and pinhole diaphragm built into the tube. Inclined monocular tube will accommodate wide-field eyepieces and the microscope can be used faced away from the observer, permitting easy accessibility to the stage.

A reputation for integrity and a tradition of service have led thousands of scientific workers to bring their optical problems to Leitz. If you have problems in this field, why not let us help you with them?

See your Leitz dealer and examine these Leitz instruments soon. Write for information.

E. LEITZ, INC., Dept. G-9
468 Fourth Avenue, New York 16, N. Y.

Please send me the Leitz _____ brochure.

NAME _____

STREET _____

CITY _____ ZONE _____ STATE _____

E. LEITZ, INC., 468 FOURTH AVENUE, NEW YORK 16, N.Y.
Distributors of the world-famous products of
Ernst Leitz G.m.b.H., Wetzlar, Germany—Ernst Leitz Canada Ltd.
LEICA CAMERAS · LENSES · MICROSCOPES · BINOCULARS

Special Price—

A.A.P.G. COMPREHENSIVE INDEXES, 1917—1955

Encompass all A.A.P.G.'s Bulletins and special publications for a 38-year period.
A valuable addition to the geologist's library. Cloth bound.

BOTH INDEXES	member price, $5.00; others, $7.00		
SINGLY	1917–45, one volume	3.00	4.00
	1946–55, one volume	3.00	4.00

ORDER FROM

THE AMERICAN ASSOCIATION OF PETROLEUM GEOLOGISTS
Box 979, Tulsa 1, Oklahoma, U. S. A.

THIN SECTIONS
Processed to your specifications from Rocks, Minerals Well Cuttings

Mounted Polished Ore Sections

Charge Schedule sent upon request.

Established 1949

Fred Roberts » » »

PETROGRAPHIC SECTION SERVICE

1300 S. MONTEREY PASS RD., MONTEREY PARK, CALIF.

SWAN ENGRAVING COMPANY

PHOTO ENGRAVERS COMMERCIAL ARTISTS

BRIDGEPORT, CONN. NEW HAVEN, CONN

POUGHKEEPSIE, N.Y.

---

d. m. organist
PETROGRAPHIC LABORATORY
BOX 176 • NEWARK, DELAWARE

THIN SECTIONS OF
ROCKS, MINERALS, ORES, CERAMICS
PREPARED ROCK SECTIONS FOR STUDENT USE
GRAIN COUNTS • PETROGRAPHIC ANALYSIS

Geophysics for Economic Geologists

GEOPHYSICAL CASE HISTORIES, VOLUME I (1948) $10.00
GEOPHYSICAL CASE HISTORIES, VOLUME II (1956) $10.00
CUMULATIVE INDEX, 1931–1953 (All publications) $5.00
GEOPHYSICS Per year $10.00

Detailed list of publications on request

Send Order with Remittance to

SOCIETY OF EXPLORATION GEOPHYSICISTS
Box 1536 Tulsa 1, Oklahoma

PROBLEMS OF PETROLEUM GEOLOGY

Sidney Powers Memorial Volume

A Sequel to *Structure of Typical American Oil Fields*

A compilation of 43 papers prepared for this volume by 47 authors

1,073 pp., 200 illus. Cloth. Price, postpaid: to members, $4.00; to non-members, $5.00. Usual discounts to educational institutions.

The American Association of Petroleum Geologists
Box 979 . . . Tulsa 1, Oklahoma

BOOKS IN GEOLOGICAL SCIENCE

Address ECONOMIC GEOLOGY, Urbana, Ill. Books not in this list (except the publications of official Surveys and those of the Geological Society of America) will be furnished at Publishers' prices.

AREAL GEOLOGY AND REGIONAL

Guidebook to the Geology of North and Middle Parks Basin, Colorado. By ROCKY MOUNTAIN ASSOCIATION OF GEOLOGISTS. WILLIAM C. FINCH, Editor. 1957. Pp. 152 ..... 8.50

Geology of the Golden-Green Mountain Area, Jefferson County, Colorado. By STANLEY O. REICHERT. 1953. Pp. 96. 19 halftone photographs and a folder of detailed maps and tables 1.50

Geological Survey of Great Britain. By EDWARD B. BAILEY. 1952. Pp. 278. Pls. 4. Figs. 39 ... 4.00

The Geology of the Commonwealth of Australia. By T. W. E. David. 1950. Volumes 1 & 2 ..... 30.00

I. Historical Geology. Pp. 720. Pl. 57. Figs. 208.

II. Physiography. Pp. 645. Pl. 28. Figs. 164.

III. Maps: Geological Map of the Commonwealth of Australia (11 sections on 4 sheets), and **Geological Sketch-Map of Australian New Guinea** (1 section).

The Geology of South Australia. Prepared by members of the South Australian Division of the Geological Society of Australia. 1958. Pp. 163. Illus. Plates 8.50

The Stratigraphy of Western Australia. By J. R. H. MCWHAE, P. E. PLAYFORD, A. W. LINDNER, B. F. GLENISTER and B. E. BALME. 1958. Pp. 161. Illus. 8.50

Geology of India and Burma. By DR. M. S. KRISHNAN. 1956. Pp. 554. 22 plates, tables, and figures 5.43

The Geology of South Africa. By A. L. DU TOIT. 1954. Pp. 611. Illus. 12.00

The Geology of Ireland. By J. K. CHARLESWORTH. 1953. Pp. 292. Illus. 3.50

Late Cenozoic Erosional History of the Raton Mesa Region. By WILLIAM S. LEVINGS. 1951. Pp. 111. Illus. 31. 16 large contour and cross-section maps 2.50

Historical Geology of the Antillean-Caribbean Region. By CHARLES SCHUCHERT. 1935. Pp. 811. Illus. 6 x 9½ 16.00

Structural History of the East Indies. By J. H. F. UMBGROVE. 1949. Pp. 63. Figs. 68. 10 plates 10.00

The Geology of Indonesia. By R. W. VAN BEMMELEN. 1949.

Vol. I: General Geology of Indonesia and Adjacent Archipelagos. Pp. 732. Tables 124.

Vol. II: Economic Geology of Indonesia. Pp. 265. With 52 figures and 56 tables.

Price of the two volumes and portfolio. Cloth ..... 75 Guilders

Geology of India. 3rd Ed. By D. N. WADIA. 1957. Pp. 552. Pl. 18. 6 maps, 25 x 30 full color geological map of India 11.50

Geology of the Manganese Deposits of Cuba. By FRANK S. SIMONDS and JOHN A. STRAZEK. 1958. Pp. 283. Figs. 50 ..... 6.00

COSMOGONY

Astrophysics. By LAWRENCE H. ALLER. 1953.

Vol. 1. The Atmospheres of the Sun and Stars. Pp. 412. Figs. 118 ..... 12.00

Vol. 2. Nuclear Transformations, Stellar Interiors, and Nebulae. Pp. 291. Figs. 51 ..... 12.00

The Changing Universe. By JOHN PFEIFFER. 1956. Pp. 243. Illus. 4.75

Expanding Universes. By E. SCHRODINGER. 1956. Pp. 94. Illus. 10 ..... 4.00

The Physical World. By PAUL MCCORKLE. 1956. Pp. 465 ..... 5.95

The World We Live In. By LINCOLN BARNETT and editorial staff of Life. 1955. Pp. 304. Illus. ... 13.50
deluxe 15.50

The Radiant Universe. By GEORGE W. HILL. 1953. Pp. 489 ..... 4.75

The Earth as a Planet. GERARD P. KUIPER, Editor. 1954.
Vol. II of the Solar System. Pp. 751 ..... 12.50

The Planet Jupiter. By BERTRAND PEEK. 1958. Pp. 283. Illus. 8.50

Astronomy of Stellar Energy and Decay. By MARTIN JOHNSON. 1951. Pp. 216. Figs. 22 ..... 3.50

CRYSTALLOGRAPHY AND MINERALOGY

Elementary Crystallography. By M. J. BUERGER. 1956. Pp. 528 ..... 8.75

General Crystallography: A Brief Compendium. By W. F. DEJONG. 1959. Pp. 281. Figs. 231; Tables 41. Illus. 6.00

Elements of Crystallography and Mineralogy. By F. ALTON WADE and RICHARD B. MATTOX. 1960. Illus. 7.50

Crystal-Structure Analysis. By MARTIN J. BUERGER. 1960. Pp. 664 ..... 16.00

Concepts of Classical Optics. By JOHN STRONG. 1958. Pp. 692. Illus. Drawings by Roger Hayward 9.50

Vector Space and its Application in Cryst-Structure Investigation. By MARTIN J. BUERGER. 1959. Pp. 347 ..... 12.00

An Introduction to Crystallography. By F. C. PHILIPS. 1956. 2nd Edition. P. viii + 324; Figs. 515 6.00

Laboratory Manual of Crystallography for Students of Mineralogy and Geology. By GEORGE TUNELL and JOSEPH MURDOCK. 1957. Pp. 55. + v. ° Figs. 20 ..... 2.75

Crystal Data, a classification of substances by space groups and their identification from cell dimensions. 1954. Memoir 60. Pp. 719. Figs. 4 ..... 5.00

Crystal Growth. By H. E. BUCKLEY. 1951. Pp. 571 ..... 11.00

(Continued on Page ix)

(*Continued from Page viii*)

BOOKS IN GEOLOGICAL SCIENCE

CRYSTALLOGRAPHY AND MINERALOGY (Continued)

Crystals and the Polarizing Microscope. 3rd Ed. By N. H. HARTSHORNE and A. STUART. 1960. Pp. 557. Diags. 313 ..... 17.50

Optical Crystallography. 3rd Ed. By E. E. WAHLSTROM. 1960. Pp. 352. Figs. 209 ..... 7.00

X-Rays in Practice. By W. T. SPROULL. 1946. Pp. 603. Illus. 12.50

Crystal Structures. Volume I. By RALPH W. G. WYCKOFF. 1948. Pp. 256. Illus. 66. 256 pages of tables. Loose-leaf with binder 9.00

Supplement Volume I: 1951. 72 text pages. 64 pages of tables 5.00

Crystal Structures. Volume II. 1951. By RALPH W. G. WYCKOFF. 253 text pages, 74 illus. 122 pages of tables. With binder 11.00

Supplement II: 1953. 30 Pp. 64 tables 5.00

Crystal Structures. Volume III. 1953. By RALPH W. G. WYCKOFF. 244 Pp., 176 Illus. 220 tables 15.50

Supplement III: 1958. Tables 182. Illus. 372 ..... 20.00

Crystal Structures: Vol. IV. 1957. Pp. 270. Tbls. 55 ..... 8.00

Supplement IV: 1958. Pp. 699. Illus. 160 ..... 22.00

The Crystalline State. Edited by SIR LAWRENCE BRAGG

Vol. 1: A General Survey. New Ed. By L. BRAGG. 1949. Pp. 352. Illus. 5.50

Vol. 2: Optical Principles of the Diffraction of X-Rays. By R. W. JAMES. 1949. Pp. 623 ..... 13.00

Vol. 3: Determination of Crystal Structures. By LIPSON and COCHRAN. 1954. 345 Pp. 8.00

The Barker Index of Crystals.—A Method for the Identification of Crystalline Substances. By M. W. PORTER and R. C. SPILLER. 1951. Pp. 1500.

Vol. I, Part 1 ..... 6.00

Part 2 ..... 18.00

Cours de Cristallographie, Vol. I, Cristallographie Geometrique. By R. GAY. 1959. Pp. 253. Figs. 108 ..... 6.17

Imperfections in Nearly Perfect Crystals. By W. SHOCKLEY. 1952. Pp. 490; figs. 175 ..... 10.00

Phase Microscopy. By A. BENNETT and others. 1951. Pp. 320 ..... 11.00

X-Ray Analysis of Crystals. By J. M. BIJVOET and others. Translated by H. LITTMAN FURTH. 2nd Ed. 1951. Pp. 310. Illus. 8.00

X-ray Crystallography. 4th Ed. By R. W. JAMES. 1950. Pp. 88 ..... 1.75

X-ray Crystallography. By MARTIN J. BUERGER. 1942. Pp. 531. Illus. 252 ..... 9.95

The Powder Method in X-Ray Crystallography. By LEONID V. AZAROFF and MARTIN J. BUERGER. 1958. Pp. 342 ..... 8.75

Nuclear Structure. By LEONARD EISENBUD and EUGENE WIGNER. 1958. Pp. 128 ..... 4.00

Elements of Optical Mineralogy. By ALEXANDER N. WINCHELL.

Pt. I. Principles and Methods. 5th Ed. 1937, Pp. 263. Illus. 305 ..... 6.75

Pt. II. Description of Minerals. 4th Ed. 1951. Pp. 551 ..... 13.50

Pt. III. Determinative Tables. 2nd Ed. 1929. Pp. 231 ..... 7.50

Optical Mineralogy. 3rd Ed. By PAUL F. KERR. 1960. Pp. 442. Figs. 369. Cloth 8.50

Tables for Microscopic and X-ray Identification of Ore Minerals. By ALEXANDER NOVITZKY. In Spanish. 1957. Pp. 270 ..... 12.00

Stereograms for the Determination of Plagioclase Feldspars in Random Sections. 5th Ed. By W. NIEUWENKAMP. 1948. Pp. 29 ..... 6.40

Principles of Mineralogy. By WILLIAM H. DENNEN. 1959. Pp. 429 ..... 7.50

Mineralogy: Concepts, Descriptions, Determinations. By L. G. BERRY and BRIAN H. MASON. 1959. Pp. 623. Illus. Drawings by Roger Hayward 8.75

Mineralogy: An Introduction to the Study of Minerals and Crystals. 5th Ed. By E. H. KRAUS, W. F. HUNT and L. S. RAMSDELL. 1960. Pp. 686 ..... 9.00

Identification and Qualitative Chemical Analysis of Minerals. By ORSINO C. SMITH. 1953. Pp. 420. Col. Pl. 27. Figs. 22 ..... 8.50

Mineral Equilibria at Low Temperature and Pressure. By ROBERT M. GARRELS. 1960. Pp. 245. Figs. 88. Illus. 6.00

Clay Mineralogy. By RALPH E. GRIM. 1953. Pp. 384. Fig. 121. Tables 46 ..... 10.00

Clay and Clay Minerals. (Proceedings of the Sixth National Conference on Clays and Clay Minerals). Edited by ADA SWINEFORD. 1959. Pp. 411 ..... 8.50

Mineralogical Study on Clays of Japan. By TOSHIO SUDO. 1959. Pp. 328 ..... 10.00

Analysis of Minerals and Ores of the Rarer Elements. By W. R. SCHOELLER and A. R. POWELL. 3rd Ed. Rev. 1956. Pp. 408 ..... 9.75

Dana's System of Mineralogy. By CHARLES PALACHE, HARRY BERMAN and CLIFFORD FRONDEL.

Vol. I. Elements, Sulfides, Sulfosalts, Oxides. 7th Ed. 1944. Pp. 834. Illus. 14.00

Vol. II. Halides, Carbonates, etc. 7th Ed. 1951. Pp. 1124. Illus. 16.00

Manual of Mineralogy. By J. S. DANA—17th Ed. Revised by C. S. HURLBUT. 1959. Pp. 609 ..... 11.50
Textbook Edition 9.50

Minerals and How to Study Them. 3rd Ed. By EDWARD S. DANA. Revised by CORNELIUS S. HURLBUT, JR. 1949. Pp. 323. Illus. 384 ..... 6.50

Elements of Mineralogy. 24th Ed. By FRANK RUTLEY (Revised by H. H. READ). 1953. Pp. 535. Illus. 138 ..... 2.50

(*Continued on Page x*)

(*Continued from Page ix*)

BOOKS IN GEOLOGICAL SCIENCE

CRYSTALLOGRAPHY AND MINERALOGY (Continued)

Textbook of Mineralogy. 14th Rev. Ed. By KLOCKMANN (Revised by RAMDOHR). 1954. Pp. 669. Illus. 687 ..... Stitched 15.94 Bound 16.46

Dana's Textbook of Mineralogy. 4th Ed. Revised by WM. E. FORD. 1932. Pp. 851. Illus., Diagrams 8.00

A Field Guide to Rocks and Minerals. By FREDERICK H. POUGH. 1953. Pp. 331. 12 Color Pls., 32 black and white numerous crystal drawings 3.95

Mineralogische Tabbellen. By HUGO STRUNZ. 1957. Pp. 448 ..... 7.82

Rutley's Elements of Mineralogy. 25th Ed. By H. H. READ. 1953. Pp. 525, figs. 137 ..... 2.50

Introduction to Study of Minerals. 3rd Ed. By AUSTIN L. ROGERS. 1937. Pp. 626. Illus. 8.50

Handbook of Mineralogy, Blowpipe Analysis and Geometrical Crystallography. Combined Ed. By G. MONTAGUE BUTLER. 1918. Pp. 546. 4½ x 7 ..... 8.50

The Colloid Chemistry of the Silicate Minerals. By C. EDMUND MARSHALL. 1953. Pp. 195. Illus. 6.80

Colorimetric Determination of Traces of Metals. By ERNEST B. SANDELL. 1959. 3rd Ed. Revised. Pp. 1054. Illus. 110. Tables 123 ..... 24.00

How to Know Minerals and Rocks. By RICHARD M. PEARL. 1955. Pp. 192. Figs., Keys 3.75

Minerals and Rocks. By RUSSELL D. GEORGE. 1943. Pp. 595. Figs. 150. Pls. 48 ..... 6.00

Quartz Family Minerals. By H. C. DAKE, F. L. FLEENER, and B. H. WILSON. 1938. Pp. 304 .... 4.75

Gemstones. By G. F. HERBERT SMITH. 13th Ed. 1958. Pp. 560. Plates 27 ..... 7.00

A Handbook of Gem Identification. 5th Ed. By RICHARD T. LIDDICOAT, JR. 1957. Pp. 349. Illus. 117 ..... 6.00

Jewelry, Gem Cutting, and Metalcraft. 3rd Ed. By WILLIAM T. BAXTER. 1950. Pp. 360. Illus. 175 ..... 5.75

The Art of the Lapidary. By F. J. SPERISEN. 1950. P. 278. Illus. 406 ..... 7.00

Gem Testing. 1st Ed. By B. W. ANDERSON. 1948. Pp. 256. Illus. 55 ..... 5.00

Gem Testing. 2nd Ed. Revised, Expanded, and Reset. By B. W. ANDERSON. 1959. Pp. 324. Illus. 95 ..... 11.50

Dictionary of Gems and Gemology. 4th Ed. By R. M. SHIPLEY. 1951. Pp. 260 ..... 5.50

A Key to Precious Stones. 2nd Ed. By L. J. SPENCER. 1946. Pp. 237. 57 Illus. 8 pp. pls. 3.95

Gems and Gem Materials. 5th Ed. By EDWARD H. KRAUS and C. B. SLAWSON. 1947. Pp. 332. Illus. 6.75

Colorado Gem Trails. By R. M. PEARL. 3rd Ed. 1953. Pp. 128. Photos; Sketch maps 2.95

Popular Gemology. By RICHARD M. PEARL. 1948. Pp. 316. Figs. 115 ..... 4.00

A Handbook of Precious Stones. By WAO BAHADUR DR. L. A. N. IYER. 1948. Pp. 188. Figs. 39. 3.15

A Roman Book on Precious Stones. By SYDNEY H. BALL. 1950. Pp. 360 ..... 6.75

ECONOMIC GEOGRAPHY

Geography in the Twentieth Century. Edited by GRIFFITH TAYLOR. 1951. Pp. 630. Figs. 56 .... 10.00

Economic Geography of Industrial Materials. By ALBERT S. CARLSON, Ed. 1956. Pp. 494 ..... 15.00

The Nation Looks at its Resources. By HENRY JARRET. 1954. Pp. 417 ..... 5.00

Geography of North America. By GEORGE J. MILLER, ALMON E. PARKINS and BERT HUDGINS. 1954. 3rd Ed. Pp. xi + 664. Figs. 290, tbls. 25 ..... 7.50

California and the Southwest. Ed. by CLIFFORD M. ZIERER. 1956. Pp. 376: Illus. 11.25

Mineral Commodities of California. Prepared under direction of OLAF P. KENKINS. Edited by LAUREN A. WRIGHT. 1957. Pp. 736. Figs. 130 Maps and Cross-sections. Photographs. 239 .. 7.50

The Polar Regions in Their Relation to Human Affairs. By L. M. GOULD. 1958. Pp. iv + 54 .... 3.50

The Canadian Northwest: Its Potentialities. By FRANK H. UNDERHILL. 1959. Pp. viii + 104 ..... 4.00

Geography of the Northlands. By GEORGE H. T. KIMBLE and DOROTHY GOOK. 1955. Pp. 534, Illus. 10.50

Industrial and Commercial Geography. 4th Ed. By J. RUSSELL SMITH, M. O. PHILLIPS, and T. R. SMITH. 1955. Pp. 768 ..... 8.25

Economic Geography: New Edition. By CHARLES C. COLBY and ALICE FOSTER. 1954. Pp. 685 ... 4.88

World Economic Geography. By EARL B. SHAW. 1955. Pp. 582. Figs. 339. Tables 12 ..... 6.75

World Commerce and Governments. By W. S. WOYTINSKY and E. S. WOYTINSKY. 1955. Pp. 907. Figs. 166. Tables 291 ..... 10.00 Special price for 2 volumes 20.00

World Population and Production. By W. S. WOYTINSKY and E. S. WOYTINSKY. 1953. Pp. 1268, tbls. 497, figs. 338 ..... 12.00 Special price for 2 volumes 20.00

Geography of Living Things. By M. S. ANDERSON. 1952. Pp. 202. Figs. 5 ..... 2.75

Fundamentals of Economic Geography. 4th Ed. Rev. Ed. by NELS A. BENGSTON and W. VAN ROYEN. 1950. Pp. 574. Phots. 142. Maps 76. Charts, etc. 150 ..... 10.65

Principles of Economic Geography. 6th Ed. By ELLSWORTH HUNTINGTON assisted by FRANK E. WILLIAMS, SAMUEL VAN VALKENBERG, and STEPHEN S. VISHER. 1951. Pp. 806. Illus. 7.50

General Geography for Colleges. By O. D. VON ENGELN. 1957. Pp. 681. Illus. 7.50

Physical Elements of Geography. 3rd Ed. By V. C. FINCH and G. T. TREWARTHA. 1957. 4th Ed. Pp. 696. Illus. 6.95

(*Continued on Page xi*)

(*Continued from Page x*)

BOOKS IN GEOLOGICAL SCIENCE

ECONOMIC GEOGRAPHY (Continued)

Advanced Atlas of Modern Geography. 3rd Ed. By JOHN BARTHOLOMEW. 1956. Pp. 306, 160 of which are maps. Printed in Great Britain at the Geographical Institute 8.00

Principles of Human Geography. Rev. Ed. By ELLSWORTH HUNTINGTON and EARL B. SHAW. 1951. Pp. 805. Illus. including black and white maps 7.50

The Prentice-Hall World Atlas. Edited by JOSEPH WILLIAMS. 1958. Pp. 26 ..... 7.95

Europe. 2nd Ed. By PROF. VAN VALKENBURG and COLBERT C. HELD. 1952. Pp. 826 ..... 7.50

Southeast Asia. By E. G. H. DOBBY. 1950. Pp. 415 ..... 5.00

The Pattern of Asia. By BRUSH, MCCUNE, PHILBRICK, RANDALL, WIENS, and GINSBURG. 1958. Pp. 929. Illus. 11.65

Asia, East by South. By J. E. SPENCER. 1954. Pp. 453. Figs. 136 ..... 8.95

Conserving Natural Resources—Principles and Practice in a Democracy. By SHIRLEY W. ALLEN. 1955. Pp. 347, Figs. 168 ..... 6.50

Conservation in the United States. 3rd Ed. By AXEL F. GUSTAFSON, C. H. GUISE, W. J. HAMILTON, JR., and H. RIES (Members of the faculty of Cornell University). 1949. Pp. 544. Illus. 254 .. 5.00

The Pacific Northwest. By O. W. FREEMAN, H. H. MARTIN, and others. 2nd Ed. 1954. Pp. 540. Illus. 8.50

ECONOMIC GEOLOGY

The Formation of Mineral Deposits. By ALAN M. BATEMAN. 1951. Pp. 371. Illus. 6.25

Mining Geology. By HUGH E. MCKINSTRY. 1948. Pp. 680 ..... 12.35

Principles of Field and Mining Geology. By J. DONALD FORRESTER. 1946. Pp. 647. Illus. 316 ... 10.50

Economic Mineral Deposits. 2nd Ed. By ALAN M. BATEMAN. 1950. Pp. 918. Illus. 308 ..... 8.75

Textures of the Ore Minerals and their Significance. By A. B. EDWARDS. 2nd Ed. 1954. Pp. 242. 204 Illus. 14.00

Flotation. By A. M. GAUDIN. 3rd Ed. 1957. Pp. 554. Illus. 243 ..... 13.50

Non-Metallic Minerals. 2nd Ed. By RAYMOND B. LADOO and W. M. MYERS. 1951. Pp. 605 .... 12.00

Minerals and Mineral Deposits. By W. R. JONES and D. WILLIAMS. 1948. Pp. 255. Figs. 36. Maps. Bibliography. Tables 1.20

Mineral Deposits. 4th revised Ed. By WALDEMAR LINDGREN. 1953. Pp. 930 ..... 12.75

Minerals for Atomic Energy. 2nd Ed. By ROBERT D. NININGER. 1956. Pp. 399. Illus. 8.50

Ore Genesis. By J. S. BROWN. 1948. Pp. 204. Illus. 4 ..... 3.50

Structural Geology of Canadian Ore Deposits (Symposium volume published in commemoration of 50th Anniversary of the Canadian Institute of Mining and Metallurgy). 1951. Pp. 930 (132 separate papers as written by over 100 Canadian mining executives). Illus. 300 ..... 10.00
Price to qualified students 8.00

The Geology of Uranium. Soviet Journal of Atomic Energy, Supplement No. 6. 1957. Pp. 128 .... 6.00

Geologie de L'Uranium. By MARCEL ROUBAULT. 1958. Pp. 462. Figs. 205 ..... 17.40

Bibliography and Index of Literature on Uranium and Radio-Active Occurrences in the United States Special Paper No. 67. By MARGARET COOPER. 1958. Pp. 472 ..... 6.75

Mineralogy and Geology of Radioactive Raw Materials. By E. WM. HEINRICH. 1958. Pp. xiv + 654. Illus. 14.50

Geologie De L'Uranium. (In French) By MARCEL ROUBAULT. 1958. Pp. 462. Illus. 13.00

Exploration for Nuclear Raw Materials. By ROBERT D. NININGER. 1956. Pp. 293 ..... 8.50

Uranium (Where it is and how to find it). By P. D. PROCTOR, E. P. HYATT, and K. C. BULLOCK. 1954. Pp. 96. 18 full pages maps. Illus. ..... Cloth 2.50

Minerals, for the Chemical and Allied Industries. By SIDNEY J. JOHNSTONE. 1954. Pp. 692 ..... 12.50

Copper Venture. By KENNETH BRADLEY. 1952. Pp. 112. Illus. and Maps 3.00

Tin 1954: A Review of the World Tin Industry. By INTERNATIONAL TIN STUDY GROUP. 1955. Pp. 56. Charts 23 ..... 1.00

Lazarus Erker's Treatise on Ores and Assaying. By A. G. SISCO and C. S. SMITH. 1951. Pp. 360. Illus. 41 ..... 10.00

Occurrence and Production of Molybdenum. By J. W. VANDERWILT. 1942. Pp. 78. Paper 1.50

Mineral Resources of China. By V. C. JUAN. 1946. Pp. 75. Illus. Paper ..... .75

The Coalfields of Great Britain. By SIR ARTHUR TRUEMAN. 1954. Pp. xi + 396, pls. 7, figs. 106, tbls. 5 ..... 17.50

Coal: Its Formation and Composition. By WILFRED FRANCIS. 1954. Pp. 567 ..... 22.50

Coals and Bitumens. By S. I. TOMKEIEFF. 1954. Pp. 122. Illus. 4 ..... 3.00

Progress in Coal Science. Vol. I. By D. H. BANGHAM (ed.). 1950. Pp. 469. Illus. 32. Tables 29, Pl. 12 ..... 7.00

The Nature and Origin of Coal and Coal Seams. 3rd Ed. By ARTHUR RAISTRICK and C. E. MARSHALL. 1952. Pp. 316. Illus. 2.60

Coal Through the Ages. By H. N. EAVENSON. 1939. Pp. 123 ..... 1.80

Geochemical Prospecting. By NALIN R. MUKHERJEE and LEO MARK ANTHONY. 1957. Pp. 81. Illus. 2.00

Coalmining. By I. C. F. STATHAM. 1951. Pp. 564. Illus. 15.00

Geology of Petroleum. By A. I. LEVORSEN. 1954. Pp. 720, illus. 327. Tables 47 ..... 9.00

North American Petroleum. 3rd Ed. 1958. Rev. Ed. 1952. By W. A. VER WIEBE. Pp. 461. Illus. 398 ..... 12.00

(*Continued on Page xii*)

(*Continued from Page xi*)

BOOKS IN GEOLOGICAL SCIENCE

ECONOMIC GEOLOGY (Continued)

The Sea Off Southern California: A Modern Habitat of Petroleum. By K. O. Emery. 1960. Pp. 336 14.00

Graphic Problems in Petroleum Geology. By L. W. LeRoy and Julian W. Low. 1954. Pp. 238. 4.50

Principles of Petroleum Geology. By Cecil G. Lalicker. 1949. Pp. 377. Illus. Pl. Maps.... 5.00

Petroleum Geology. By Kenneth K. Landes. 2nd Ed. Pp. 444. Illus.... 9.50

Principles of Petroleum Geology. By W. L. Russell. 2nd Ed. 1960. Pp. 508.... 9.50

Some Fundamentals of Petroleum Geology. By G. D. Hobson. 1954. Pp. 139. Figs. 41.... 2.90

Subsurface Geology in Petroleum Exploration. Edited by John D. Haun and L. W. LeRoy.... 10.00

Geochemical Methods of Prospecting and Exploration for Petroleum and Natural Gas. By A. A. Kartsev, Z. A. Tabasaranskii, M. I. Subbota, and G. A. Mogilevskii. 1959. Pp. 349. Figs. 151.... 12.50

How Oil is Found. 3rd Ed. By W. A. Ver Wiebe. 1959. Pp. 254. Illus. 312.... 8.50

Fundamental Research on Occurrence and Recovery of Petroleum, 1950-51. By Lloyd E. Elkins. 1953. Pp. 263.... 12.00

Petroleum Geology. By E. N. Tiratsoo. 1952. Pp. 449.... 8.50

Practical Oil Geology. 6th Ed. By Dorsey Hager. 1951. Pp. 466. 5½ x 7½. Illus.... 9.00

Fundamentals of Logging. 1957. Pp. 169.... 3.00

Structure of Typical American Oil Fields. Vol. III. 1948. Pp. 516. Illus. 219.... 4.50

Petroleum Microbiology. By Ernest Beerstecher, Jr. 1954. Pp. 391; figs. 71.... 8.50

Oil Property Valuation. By Paul Paine. 1942. Pp. 204.... 5.50

Properties of Petroleum Reservoir Fluids. By Emil Burcik. 1957. Pp. 190.... 7.50

Physical Principles of Oil Production. By Morris Muskat. 1949. Pp. 937. Illus.... 17.50

Oil and Gas Production. By the Engineering Committee of the Interstate Oil Compact Commission. Pp. 140. Illus. with charts, graphs, and tables.... 2.75

Practical Petroleum Engineers Handbook. 4th Ed. 1956. Pp. 654. Illus. by Joseph Zaba and W. T. Doherty.... 14.00

Elements of Petroleum Subsurface Engineering. By Harold Vance. 1950. Pp. 168. Illus. 108.. 4.25

Oil Reservoir Engineering, 2nd Edit. By Sylvain J. Pirson. 1958. Pp. 735.... 15.00

Oil Well Drainage. By S. C. Herold. 1941. Pp. 407. Figs. 15.... 5.00

World Geography of Petroleum. Edited by W. E. Pratt and Dorothy Good. 1950. Pp. 482. Illus. 9.00

Early Days of Oil. By P. H. Giddens. 1948. Pp. 160. Illus.... 6.00

Oil in the Soviet Union: History, Geography, Problems. By Heinrich Hassmann. Translated from the German with the addition of much new information, by Alfred M. Leeston. 1953. Pp. 173. Figs. 19 (maps and charts). Tables 43.... 3.75

Petroleum Production Engineering. By Lester C. Uren.

Vol. I. Oil Field Development. 4th Ed. 1956. Pp. 764.... 13.50

Vol. II. Oil Field Exploitation. 3rd Ed. 1953. Pp. 807. Illus. 367.... 12.50

Vol. III. Petroleum Production Economics. 6th Ed. 1956. Pp. 792. Figs. 117. Tables 74. 10.00

Science and Petroleum. By A. E. Dunstan, et al.

Vol. IV. 1938. Pp. 3192. Illus. Figs. Available as a set @ $60.00 (Vols. I-IV)

Vol. V. 1950. Pp. 200. Illus. Part I is available separately.... 11.00

Natural Gas and Natural Gasoline. By R. L. Huntington. 1950. Pp. 598. 6 x 9. Illus. 267.... 13.50

Encyclopedia of Hydrocarbon Compounds.

Vol. X. $C_{21}H_8$ to $C_{21}H_{32}$. By Joseph E. Faraday. 1951. Pp. 270.... 15.50

Vol. XI. $C_{21}H_{34}$ to $C_{21}H_{56}$. 1952. Pp. 325.... 18.50

Vol. XII. C_{22}. 1953. Pp. 417.... 21.50

Vol. XIII. $C_{22}H_8$ to $C_{22}H_{32}$. 1954. Pp. 334.... 20.00

Petroleum Conservation. Edited by Stuart E. Buckley. 1951. Pp. 300. Illus.... 6.00

The Uranium Prospector's Guide. By Thomas J. Ballard and Quentin E. Conklin. 1955. Pp. 251. Illus.... 3.50

Exploration for Nuclear Raw Materials. By Robert D. Nininger. 1956. Pp. 293.... 8.50

Regional Tectonics of the Colorado Plateau and Relationship to the Origin and Distribution of Uranium. By V. C. Kelley. 1955. Pp. 120. Figs. 17. Pls. 8.... 2.00

The Conservation of Ground Water. By Harold E. Thomas. 1951. Pp. 321. Illus.... 8.00

Soil and Water Conservation Engineering. By Richard K. Frevert, Glenn O. Schwab, Talcott W. Edminster and Kenneth K. Barnes. 1955. Pp. 479. Illus.... 8.00

Realms of Water. (Some Aspects of Its Cycle in Nature). By P. H. Kuenen. 1955. Pp. 327.... 7.00

Groundwater. By Cyrus F. Tolman. 1937. Pp. 593. Illus. 189.... 10.00

The Geology of Water Supply. By Cyril S. Fox. 1949. Pp. 209. Profusely illustrated. Cloth.. 7.75

Applied Hydrology. By R. K. Linsley, Jr., Max A. Kohler, and J. L. H. Paulhus. 1949. Pp. 689. Illus. 328.... 11.00

Hydrology. By Oscar E. Meinzer. 1949. Pp. 723. Illus. 165.... 4.95

Hydrology. By C. O. Wisler and E. F. Brater. 1959. Pp. 408. Illus.... 9.25

Ground Water Hydrology. By David K. Todd. 1959. Pp. 336. Illus.... 10.75

Elements of Applied Hydrology. By D. Johnstone and W. P. Cross. 1949. Pp. 276. Illus. 109. Tables 32.... 6.00

(*Continued on Page xiii*)

(*Continued from Page xii*)

BOOKS IN GEOLOGICAL SCIENCE

ECONOMIC GEOLOGY (Continued)

Hydrogeologie: P. Fourmarier. 1958. 2nd Ed. Pp. 294. Illus. 8.70

A Practical Handbook of Water Supply. By Frank Dixey. 1950. Pp. 573; maps 6; figs. 133. 35s

The Law of Water Allocation in the Eastern United States. Edited by David Haber and Stephen Bergen. 1958. Pp. 643. 7.50

Water Supply and Waste-Water Disposal. By Gordon Maskew Fair and John Charles Geyer. With a chapter (on water chemistry) by John Carrell Morris. 1954. Pp. 973. Illus. 16.00

The Flood Control Controversy. By Luna B. Leopold and Thomas Maddock, Jr. 1954. Pp. 278. 5.00

Principles of Engineering Geology and Geotechnics. By D. P. Krynine and W. R. Judd. 1957. Pp. 736. 10.50

Geology in Engineering. By John R. Schultz and Arthur B. Cleaves. 1955. Pp. 592. Illus. 214. 8.75

Geology and Engineering. By Robt. F. Legget. 1939. Pp. 650. Illus. Cloth, 6 x 9. 9.25

Geology for Engineers. By J. M. Treffethen. 1949. Pp. 620. Illus. 7.00

Geology for Engineers. 3rd Ed. By Francis G. Blyth. 1952. Pp. 336. Illus. 6.25

Basic Geology for Science and Engineering. By Edward C. Dapples. 1959. Pp. 609. Illus. Paper 9.50

Geology Applied to Building and Engineering. By Arthur Bray. 1948. Pp. 196. 6.25

Heat Conduction, with Engineering, Geological, and Other Applications. By L. R. Ingersoll, O. J. Zobel, and A. C. Ingersoll. 1954. Pp. 325. Figs. 53. 5.00

Applied Geology, a Symposium. By F. M. Van Tuyl and Truman H. Kuhn. Vol. 45, No. 1-B. 1950. Pp. 343. 3.00

Our Mineral Resources: An Elementary Textbook in Economic Geology. By Charles M. Riley. 1959. Pp. 338. Illus. 7.50

Mineral Resources of the United States. By the Staffs of the U. S. Bureau of Mines and the Geological Survey. 1948. Pp. 212. 5.00

Industrial Minerals and Rocks. Editor-in-chief Joseph L. Gillson. 1960. Pp. 934. 3rd Ed. Illus. 12.00

Geology of the Industrial Rocks and Minerals. By Robert L. Bates. 1960. 10.00

The Chemistry of Portland Cement. 2nd Ed. By Robert Herman Bogue. 1955. Pp. 793. Illus. 16.50

Conditions de Formation des Gisements de Minerals. By P. M. Tatarinov. 1959. Pp. 215. Figs. 77. 11.60

Refractories. 3rd Ed. By F. H. Norton. 1949. 782 Pp. 419 Illus. 14.00

The Chemistry and Physics of Clays and Other Ceramic Materials. By Alfred B. Searle and Rex W. Gromshaw. 1959. Pp. 95. Illus. 16.25

Microscopy of Ceramics and Cements. Including glasses, slags, and foundry sands. By Herbert Insley and Van Derck Frechette. 1955. Pp. 286. Illus. 7.50

The Vermiculites and Their Utilization. By August Goldstein, Jr. 1946. Pp. 64. 1.00

The Occurrence and Production of Vanadium. By G. O. Argall, Jr. 1943. Pp. 56. 1.00

Crushing and Grinding: A Bibliography. 1960. Pp. 425. 10.50

Foundation Engineering. By Peck, Hanson, and Thornburn. 1953. Pp. 410. 8.00

Landslides in Clays. By Alexandre Collin. 1956. Pp. 261. Illus. and plates. 6.50

Geologie Applicata Alla Ingegneria. 2nd Ed. By Ardito Desio. 1959. Pp. 1058. 13.60

Landslides and Engineering Practice HRB Special Report 29. Edited by Edwin B. Eckel, Chairman. Prepared by the Committee on Landslide Investigations. 126 Illus. 6 tables. 1 plate. Pp. 232 6.00

Soil Mechanics in Engineering Practice. By Karl Terzaghi and Ralph B. Peck. 1948. Pp. 566. 7.50

Soil Mechanics. 2nd Ed. By D. P. Krynine. 1947. Pp. 450. Illus. 7.75

Fundamentals of Soil Mechanics. By Donald W. Taylor. 1948. Pp. 700. Illus. 239. 7.50

New Instruments and Methods of Engineering Geology. By N. V. Glazov, and A. N. Glazov. 1959. Pp. 69. Illus. 3.25

Subsurface Exploration and Sampling of Soils for Civil Engineering Purposes. By M. Juul Hvorslev. 1949. Pp. 521. Illus. 450. 6.00

Introduction to Mine Surveying. By W. W. Staley. 1939. Pp. 275. Illus. 3.75

A Mining Engineer's Survey Manual. By J. E. Metcalfe. 1951. Pp. 341. 30s

Mines Register. Revised New 1956 edition. 25.00

Manual of Oil and Gas Terms, Annotated. By Howard Williams and Charles Meyers. 10.00

The Law of Oil and Gas Leases. By Earl A. Brown. 25.00

Petroleum Sourcebook. Edited by Curtis Stevens. 1958. Pp. 179. 6.00

The Law of Pooling and Unitization, Voluntary-Compulsory. 1958. By Raymond Myers. 25.00

GEOCHEMISTRY, CHEMICAL GEOLOGY

Geochemistry. By V. M. Goldschmidt edited by Alex Muir. 1954. Pp. 730, tbls. 96. 11.20

Principles of Geochemistry. 2nd Ed. By Brian Mason. 1958. Pp. 310. Illus. 8.50

Researches in Geochemistry. Edited by P. H. Abelson. 1959. Pp. 511. Illus. 11.00

Isotope Geology. By Kalervo Rankama. 1955. Pp. 550. 12.00

Nuclear Geology. By Henry Faul. 1954. Pp. 414. 7.00

The Atom and the Energy Revolution. By Norman Lansdell. 1958. Pp. 200. Pl. 32. 6.00

(*Continued on Page xiv*)

(*Continued from Page xiii*)

BOOKS IN GEOLOGICAL SCIENCE

GEOCHEMISTRY, CHEMICAL GEOLOGY (Continued)

Geochemistry. By KALERVO RANKAMA and TH. G. SAHAMA. 1950. Pp. 912. Illus. 60 ..... 15.00

Growth and Perfection of Crystals. By R. H. DOREMUS, B. W. ROBERTS and DAVID TURNBULL, editors. 1958. Pp. 609 ..... 12.50

Physics and Chemistry of the Earth. Vol. 1. By L. H. AHRENS, KALERVO RANKAMA, S. K. RUNCORN Eds. 1956. Pp. 317 ..... 15.00

The Principles of Chemical Weathering. By W. D. KELLER. 1957. Pp. 111. Figs. 21 ..... 3.25

General Chemistry. 2nd Ed. By LINUS PAULING. 1953. Pp. 722. Illus. 193 including 2 color plates. Tables 33 ..... 6.75

The Physical Chemistry of the Silicates. By WILHELM EITEL. 1954. Pp. 1592, figs. 952 ..... 45.00

The Geochemistry of Rate and Widely Scattered Chemical Elements in Soils. By A. P. VINOGRADOV. 1959. Illus. Pp. 249 ..... 9.50

Silicate Analysis: A Manual for Geologists and Chemists, with Chapters on Check Calculations and Geo-Chemical Data. 2nd Ed. By A. W. GROVES and Foreword by ARTHUR HOLMES. 1951. Pp. 359 ..... 5.50

Differential Thermal Analysis. By W. J. SMOTHERS and YAO CHIANG. 1958. Pp. 444. Illus. 16.00

Radiocarbon Dating. By WILLARD F. LIBBY. Revised 1955. Pp. 175. Illus. 4.50

Wavelength Tables of Sensitive Lines. By L. H. AHRENS. 1st Ed. 2nd ptg. 1954. Pp. 86 ..... 2.50

GEOPHYSICS, GEOPHYSICAL EXPLORATION

Introduction to Geophysics. By BENJAMIN F. HOWELL, JR. 1959. Pp. 399. Illus. 9.00

Geophysics and the IGY. By HUGH ODISHAW and S. RUTTENBERG, Editors. 1958. Pp. 210 ..... 8.00

Advances in Geophysics. Volume I. By H. W. LANDSBERG. 1952. Pp. 362. XII. Illus. 9.00

Advances in Geophysics. Vol. 3. By H. E. LANDSBERG, Ed. 1956. Pp. 378 ..... 9.00

Advances in Geophysics. Vol. 4. Edited by H. E. LANDSBERG and J. VAN MIEGHEM. 1958. Pp. 456 ..... 12.00

The Earth and its Gravity Field. By W. A. HEISKANEN and F. A. VENING MEINESZ. 1958. Pp. x + 470. Illus. 12.50

Fundamentals of Physical Science. By KONRAD B. KRAUSKOPF. 4th Ed. 1959. Pp. 694 ..... 6.95

Lectures on Rock Magnetism. By P. M. S. BLACKETT. 1954. Pp. 131 ..... 5.00

The Atomic Nucleus. By ROBLEY D. EVANS. 1955. Pp. 972. Illus. 15.50

The Geometry of Geodesics. By HERBERT BUSEMANN. 1955. Pp. 422 ..... 9.00

An Introduction to the Theory of Seismology. By K. E. BULLEN. 2nd Ed. 1953. Pp. 296. Figs. 42 ..... 7.50

Elementary Seismology. By CHARLES F. RICHTER. 1958. Pp. 768. 205 figures and 47 tables 12.00

Seismicity of the Earth and Associated Phenomena. By B. GUTENBERG and C. F. RICHTER. Revised 1954. Pp. 277. Maps. 154 pages of tables 10.00

Elastic Waves in Layered Media. By W. M. EWING, F. PRESS, W. S. JARDETZKY. 1957. Pp. 375 .. 10.75

Internal Constitution of the Earth. Edited by B. GUTENBERG. 1951. Pp. 439. Tables 88. Illus. 43 2.45

Seismic Prospecting for Oil. By CHARLES HEWITT DIX. 1952. Pp. 414. Illus. 175 ..... 8.00
Textbook edition available for classroom use 6.00

Introduction to Geophysical Prospecting. By M. B. DOBRIN. 2nd Ed. 1960. Pp. 435. Illus. 265 9.50

Geophysical Surveys in Mining, Hydrological and Engineering Projects. By GEORGE R. ROGERS and DART WANTLAND. Pp. 270 ..... To EAEG and SEG members 3.25
To all others 4.50

Exploration Geophysics. By J. JAY JAKOSKY. 1957. Revised and Reprinted. Pp. 1200 ..... 12.50

Manual on Geophysical Prospecting with the Magnetometer. 2nd. Ed. By JAMES WALLACE JOYCE. 1948. Pp. 137 ..... 6.00

Applied Geophysics in the Search for Minerals. 4th Ed. By A. S. EVE and D. A. KEYS. 1954. Pp. 382. 160 text-figures 9.50

The Fundamentals of Electric Log Interpretation. By M. R. J. WYLLIE. 1957. Pp. 176. Illus. Ed. 2. 4.50

Geophysical Prospecting for Oil. By LEWIS L. NETTLETON. 1940. Pp. 444 ..... 9.00

Earth Waves. By L. DON LEET. 1950. Pp. 122. Illus. 69 ..... 3.90

Sonics. By THEODOR F. HUETER and RICHARD H. BOLT. 1955. Pp. 456. Illus. 231 ..... 10.00

The New Physics. By SIR C. V. RAMAN. 1951. Pp. 144 ..... 3.75

GEOMORPHOLOGY, PHYSICAL GEOLOGY, PHYSIOGRAPHY

Geology of the Great Lakes. By JACK L. HOUGH. 1958. Pp. 313. Illus., maps and diagrams 8.50

Geographical Essays. By W. M. DAVIS. 1909. Republished unabridged, 1954. Pp. 777. Figs. 130 2.95

Physical Geology. By L. DON LEET and SHELDON JUDSON. 1954. Pp. 466 ..... 10.35

Physical Geology. 3rd Ed. By CHESTER R. LONGWELL, ADOLPH KNOPF, and RICHARD F. FLINT. 1948. Pp. 602. Illus. 365 ..... 6.50
Visual Aids Kit 85.00

Introduction to Physical Geology. By C. R. LONGWELL and R. F. FLINT. Pp. 432. Figs. 308, Tbl. 12, Pls. 2 ..... 5.50

A Textbook of Geology. By R. M. GARRELS. 1951. Pp. 511. Figs. 200. Illus. 100 ..... 6.00

Principles of Geomorphology. By WILLIAM D. THORNBURY. 1954. Pp. 618. Figs. 275 ..... 8.00

Principles of Geology. By JAMES GILLULY, AARON C. WATERS, and A. O. WOODFORD. 2nd Ed. 1959. Pp. 534. Illus. 320 ..... 7.50

(*Continued on Page xv*)

(*Continued from Page xiv*)

BOOKS IN GEOLOGICAL SCIENCE

GEOMORPHOLOGY, PHYSICAL GEOLOGY, PHYSIOGRAPHY (Continued)

Elements of Geology. By JAMES ZUMBERGE. 1958. Pp. 368 ..... 5.50

General Principles of Geology. By J. F. KIRKLADY. 1955. Pp. 327. Pls. 6, Figs. 84 ..... 10.00

The Principles of Physical Geology. By V. E. MONNETT and H. E. BROWN. 1950. Pp. 450. Illus. 265 plus 16 topographic maps 5.75

Physical Geography. By A. H. STRAHLER. 1951. Pp. 442 ..... 7.25

Introduction to Geology. By HOWARD E. BROWN, VICTOR E. MONNETT and J. WILLIS STOVALL. 1958. Pp. 644 ..... 7.25

Introduction to Geology. 3rd Ed. By E. B. BRANSON, W. D. KELLER, and W. A. TARR. 1952. Pp. 482. Illus. 6.75

Geology: Principles and Processes. By WM. H. EMMONS, GEO. A. THIEL, CLINTON STAUFFER, IRA S. ALLISON. 4th Ed. 1955. Pp. 642 ..... 7.50

Principles of Physical Geology. By ARTHUR HOLMES. 1945. Pp. 532. Pls. 95. Figs. 262 ..... 6.00

Down to Earth. 2nd Rev. Ed. By C. CRONEIS and W. C. KRUMBEIN. 1947. Pp. 501. Pl. 64. Figs. 344 ..... 5.50

Geomorphology. By C. A. COTTON. 7th Ed. 1958. Pp. 505. Illus. 8.75

Textbook of Geomorphology. 2nd Ed. By PHILLIP G. WORCESTER. 1948. Pp. 584. Illus. Maps. 6.50

Outlines of Physical Geology. 2nd Ed. By CHESTER R. LONGWELL, ADOLPH KNOPF, and R. F. FLINT. 1941. Pp. 387. Illus. 281 ..... 5.95

Morphological Analysis of Land Forms. By WALTHER PENCK. (Translated by HELLA CZECH and KATHERIN C. BOSWELL). 1953. Pp. 429. Figs. 21. Pls. 12 ..... 8.50

Morphological Integration. By EVERETT C. OLSON and ROBERT L. MILLER. 1958. Pp. 317 ..... 10.00

This Sculptured Earth. By JOHN A. SHIMER. 1959. Pp. 255. Illus. 7.50

Physics and Geology. By J. A. JACOBS, R. D. RUSSELL, and J. TUZO WILSON. 1959. Pp. 424. Illus. 9.75

Geology. 5th Ed. By P. LAKE and R. H. RASTALL. 1941. Pp. 491. Figs. 129 ..... 7.00

Geomorphology. By A. K. LOBECK. 1939. Pp. 731. Fully Illus. 9.50

Block Diagrams, and Other Graphic Methods Used in Geology and Geography. 2nd Edition 1958. By A. K. LOBECK. Pp. 212. Figs. 288 ..... 6.00

Introduction to Physical Geology. 5th Ed. Revised by W. J. MILLER. 1949. Pp. 482. Illus. Maps 5.95

Outlines of Geology. 2nd Ed. Contains Outlines of Physical Geology. By CHESTER R. LONGWELL, ADOLPH KNOPF, and RICHARD FLINT; and Outlines of Historical Geology by CHARLES SCHUCHERT and CARL O. DUNBAR. 1941. Pp. 672. Illus. 431 ..... 7.95

Laboratory Manual for Geology. By K. F. MATHER, C. J. ROY and L. R. THIESMEYER

Part I. Physical Geology (Revised). 1950. Pp. 165. Illus. 25 Line, 4 HT ..... Paper 2.75

Part II. Historical Geology. 1952. Pp. 252. Illus. 80 Line, 1 HT ..... Paper 2.75

Physical Geology in the Laboratory. By J. P. MILLER and ROBERT SCHOLTEN. 1957. Pp. 312 ..... 4.00

General Geology Laboratory Work Book. By SAMUEL P. ELLISON, JR. 1958. Pp. 285 ..... 3.57

Earth Science: The World We Live In. By SAMUEL N. NAMOWITZ and DONALD B. STONE. 1953. Pp. 448 ..... 4.48

Coastal and Submarine Morphology. By ANDRE GUILCHER, translated by B. W. SPARKS and R. H. W. KNEESE. 1958. Pp. 274. Illus. 6.50

The Sea Coast. By J. A. STEERS. "New Naturalist Series". 1951. Pp. 276. Figs. 52 ..... 6.25

Landscapes of Alaska—Their Geologic Evolution. By HOWELL WILLIAMS, Editor. 1958. Pp. 148. Plates 23. Figs. 3. Maps 5 ..... 5.00

The Galathea Deep Sea Expedition 1950-52. By ANTON F. BRUUN, SV. GREVE, HAKON MIELCHE, RAGNAR SPARCK. Translated from Danish by R. SPINK. 1957. Pp. 296, Illus. 8.00

The Incomparable Valley—A Geologic Interpretation of the Yosemite. By FRANCOIS E. MATTHES; edited by FRITIOF FRYXELL. 1950. Pp. 176. Frontis. 50 Illus. 11 Figs. 2 maps 3.75

Crater Lake (The Story of Its Origin). By HOWELL WILLIAMS, 3rd printing. 1954. 114 Pp., 25 Illus. 2.00

South African Scenery, A Textbook of Geomorphology. 2nd Rev. and Enlarged Edition. By L. C. KING. 1951. Pp. 412. Illus. 267, 79 text figures, 1 folding map, 1 colored erosion map 6.37

Manual for Physical Geology. By PERCIVAL ROBERTSON. 3rd Ed. 1957. Pp. 108 ..... 2.75

Physiography of Eastern United States. By NEVIN M. FENNEMAN. 1938. Pp. 714. Illus. Cloth .. 12.00

Physiography of Western United States. By NEVIN M. FENNEMAN. 1931. Pp. 534 ..... 10.00

The Physiography of Southern Ontario. By L. J. CHAPMAN and D. F. PUTNAM. 1951. Pp. xxii + 284. 81 photographs, maps, diagrams (Large maps in slip case) 4.00

The Physiographic Provinces of North America. By W. W. ATWOOD. 1940. Pp. 536. Illus. 281 .. 7.80

The Oceans: Their Physics, Chemistry, and General Biology. By H. U. SVERDRUP, M. W. JOHNSON, and R. H. FLEMING. 1942. Pp. 1087 ..... 16.65

The Ocean. By F. D. OMMANNEY. 1949. Pp. 238. Pl. 4. Figs. 12. Bibliography Maps. 1.20

Submarine Geology. By FRANCIS P. SHEPARD. 1948. Pp. 348. Illus. 6.00

Marine Geology. By PH. H. KUENEN. 1950. Pp. 568. Illus. 250 ..... 9.50

The Earth Beneath the Sea. By FRANCIS P. SHEPARD. 1959. Pp. 275. Illus. 5.00

The Ocean Floor. By HANS PETTERSSON. 1954. Pp. 181. Figs. 48 ..... 3.75

Handbuch der Gletscherkunde und Glazialgeologie. By KLEBELSBERG. PROF. DR. R. 1948-49. 2 Bde. 40.00

(*Continued on Page xvi*)

(*Continued from Page xv*)

BOOKS IN GEOLOGICAL SCIENCE

GEOMORPHOLOGY, PHYSICAL GEOLOGY, PHYSIOGRAPHY (Continued)

Origin and Development of Craters. By THOMAS A. JAGGAR. 1947. Pp. 508. Pls. 87. Figs. 14.. 8.00

Steam Blast Volcanic Eruptions. A Study of Mount Pelee in Martinique as Type Volcano. By THOMAS A. JAGGAR. 1949. Figs. 41. 137 pp. 4.00

Catalogue of the Active Volcanoes of the World Including Solfatara Fields. Part I. Indonesia. By M. NEUMANN VAN PADANG. Ed. by the International Volcanological Assoc. 1951. Pp. 271. Figs. 117. 5.00

Our Amazing Earth. By C. L. FENTON. Reissue 1945. Pp. 348. 39 pages halftones. 59 line drawings 4.75

Earth Sciences. By J. HARLEN BRETZ. 1940. Pp. 260. Illus. 122. 3.00

METAMORPHIC, STRUCTURAL AND FIELD GEOLOGY

Metamorphism. A Study of the Transformation of Rock-Masses. 3rd Ed. By ALFRED HARKER. 1950. Pp. 362. Figs. 185. Cloth, 6 x 9. 5.50

The Origin of Metamorphic and Metasomatic Rocks. By HANS RAMBERG. 1952. Pp. 317. Illus.. 10.00

Deformation of the Earth's Crust. By WALTER H. BUCHER. 1957. Pp. 578. 10.00

Structural Geology. By L. U. DE SITTER. 1956. Pp. 552. Figs. 309. Tables 15. 11.50

The Earth's Shifting Crust. 1st Ed. By CHARLES H. HAPGOOD with the collaboration of J. H. CAMPBELL. 1958. Pp. 438. Illus. 6.50

Our Wandering Continents. By A. L. DU TOIT. 1957. Pp. 379. Diagr. Maps. Glossary. 5.50

Graphic Methods in Structural Geology. By WM. L. DONN and J. A. SHIMER. 1958. Pp. 180. Figs. 104. 4.00

Structural Geology Manual. By JOHN C LUDLUM and JOHN M. DENNISON. 1957. Pp. 115. Figs. 47 3.00

Principles of Structural Geology. 4th Ed. By C. M. NEVIN. 1949. Pp. 410. Illus. 250. 7.00

Principles of Geodynamics. By ADRIAN E. SCHEIDEGGER. 1958. Pp. 280. Figs. 86. 12.00

Structural Methods for the Exploration Geologist. By PETER C. BADGLEY. 1959. Pp. 275. Illus.. 7.50

Structural Geology. By MARLAND P. BILLINGS. 2nd Ed. 1954. Pp. 473. Figs. 336. Pls. 19. 11.65

Mountain Building. By REIN W. VAN BEMMELEN. 1954. Pp. 189, figs. 51. 4.00

Structural Geology of North America. By A. J. EARDLEY. 1951. Pp. 624. Illus. 776. 13.50

The Tectonics of Middle North America. By PHILIP B. KING. 1951. Pp. 224. 52 Maps. 3.75

Outline of Structural Geology. 3rd Ed. By E. S. HILLS. 1953. Pp.182. 3.50

The Dynamics of Faulting and Dyke Formation with Applications. 2nd Ed. By ERNEST M. ANDERSON. 1951. Pp. 216. Figs. 39. 4.00

Field Geology. 5th Ed. By F. H. LAHEE. 1952. Pp. 853. Illus. 5 x 7½. 9.95
Textbook edition available for classroom use 4.50

Geologic Field Methods. By JULIAN W. LOW. 1957. Pp. 489. Line Drawings 214 6.00

Structural Geology for Petroleum Geologists. By WILLAIM L. RUSSELL. 1955. Pp. 427. Figs. 159. Tables 7. 8.50

Principles of Field and Mining Geology. By JAMES D. FORRESTER. 1946. Pp. 647. Illus. 316. 8.75

Aerial Photographic Interpretation. By DONALD R. LUEDER. 1959. Pp. 452. Illus. 17.50

The Use of Stereographic Projection in Structural Geology. By F. C. PHILLIPS. 1954. Pp. 86. Figs. 86. 3.75

METEOROLOGY AND CLIMATE

Climatic Atlas of the United States. By STEPHEN SARGENT VISHER. 1954. Pp. 403. Illus. 9.00

Climatic Change: Evidence, Causes, and Effects. Ed. by HARLOW SHAPLEY. 1953. P. 318. Figs. 58 7.00

The Climate Near the Ground. By R. GEIGER. 1950. Pp. 482. Figs. 181. Tables 63. 6.00

The Atmospheres of the Earth and Planets. Rev. Ed. By GERARD P. KUIPER. 1952. Pp. 434 Cloth 8.50

Cloud Physics. By D. W. PERRIE. 1950. Pp. 119. Pls. 5.50

Weather Elements. 4th Ed. By T. A. BLAIR. 1948. Pp. 373. 6.95

Descriptive Meteorology. By HURD C. WILLETT. 1952. Pp. 310. VIII. 7.50

Dynamic Meteorology. By HOLMBOE, FORSYTHE and GUSTIN. 1945. Pp. 378. Illus. 222. 7.00

General Meteorology. By HORACE R. BYERS. 1944. Pp. 645. Illus. 284. Tables 27. 9.00

Handbook of Meteorology. By FREDERIC A. BERRY, E. BOLLAY and N. R. BEERS. 1945. Pp. 1116 15.00

Climatology. By BERNARD HAURWITZ and JAMES M. AUSTIN. 1944. Pp. 410. 8.50

Techniques of Observing the Weather. By BENARTHUR C. HAYNES. 1947. Pp. 272. Illus. 98. 5.90

MINERAL ECONOMICS, GEOPOLITICS

Economics of Atomic Energy. By MARY S. GOLDRING. 1957. Pp. 179. 6.00

Facing the Atomic Future. By E. W. TITTERTON. 1956. Pp. 379. 5.00

Minerals in World Industry. By WALTER H. VOSKUIL. 1955. Pp. 316. Tables 38. Figs. 26. 6.00

(*Continued on Page xvii*)

(*Continued from Page xvi*)

BOOKS IN GEOLOGICAL SCIENCE

MINERAL ECONOMICS, GEOPOLITICS (Continued)

An Encyclopedia of the Iron and Steel Industry. By A. K. Osborne. Pp. 558. Pls. 16. Figs. 9. 1956 ..... 25.00

Conservation of Natural Resources. 2nd Ed. Ed. by Guy-Harold Smith. 1958. Pp. 474. Illus. 8.50

The Future of Our Natural Resources. Volume 281 of The Annals of the American Academy of Political and Social Science. By Stephen Raushenbush. May, 1952. Pp. 275 ..... 2.00

The Earth and Its Resources. 2nd Ed. By V. C. Finch, M. T. Trewartha, and M. H. Shearer. 1948. Pp. 584. Illus. 463 ..... 6.00

Out of the Earth. By G. B. Langford. 1954. Pp. 140, pls. 14, figs. 28 ..... 3.50

Science and Economic Development: New Patterns of Living. By Richard L. Meier. 1956. Pp. 266. Tbls. 22. Figs. 28 ..... 6.00

Natural Resources Utilization in a Background of Science and Technology. Vol. 1: Geology and Geography. By James C. Malin. 1950. Pp. 377. Illus. 5. Lithoprint from typescript, paper cover 2.50

The Agricultural Resources of the World. By Wm. Van Royen. 1954. Pp. 258. Figs. 338 (Vol. I of Atlas of World Mineral Resources) 13.35

Resource Conservation: Economics and Policies. By Ciriacy-Wantrup. 1952. Pp. 396 ..... 6.50

World Population and Future Resources. The Proceedings of the Second Centennial Academy Conference of Northwestern University, Evanston, Ill. By P. K. Hatt. 1952. Pp. 280 ..... 5.00

Conservation in the United States. 3rd Ed. By Gustafson, Guise, Hamilton, Jr., and Ries (Members of the faculty of Cornell University). 1949. Pp. 543. Tables 21 ..... 5.00

A Conservation Handbook. By Samuel H. Ordway, Jr. 1949. Pp. 76. Available only in the paperbound edition ..... .50

Petroleum: Prehistoric to Petrochemicals. By G. A. Purdy. 1958. Pp. 492. 454 Illus. 15.00

Arabian Oil—America's Stake in the Middle East. By Raymond F. Mikesell and Hollis B. Chenery. 1949. Pp. 216. 19 tables 3.50

The Future Supply of Oil and Gas. By Bruce C. Netschert. 1958. Pp. 134 ..... 3.00

Oil: From Prospect to Pipeline. By Robert Wheeler and Maurine Whited. 1958. Pp. 115. Illus. 2.95

Energy Sources—The Wealth of the World. By Eugene Ayres and Charles A. Scarlott. 1952. Pp. 344 ..... 6.00

World Minerals and World Peace. By Charles K. Leith, J. W. Furness and Cleona Lewis. 1943. Pp. 253. Pls. 15. Tables 41 ..... 2.50

The Porphyry Coppers in 1956. By A. B. Parsons. 1957. Pp. 270 ..... 5.00

Minerals—A Key to Soviet Power. By Demitri B. Shimkin. 1953. Pp. 452. Figs. 8. Tables 101 9.00

Seventy-five Years of Progress in the Mineral Industry (1871-1946) American Institute of Mining and Metallurgical Engineers. By A. B. Parsons, *Editor*. 1947. Pp. 817 ..... 5.00

MINING

Elements of Mining. 4th Ed. By G. J. Young. 1946. Pp. 755. Illus. 382 ..... 9.50

The Basis of Mine Surveying. By M. H. Haddock. 1952. Pp. 301. Fig. 246 ..... 5.00

Mining Year Book. By Walter E. Skinner. 1953. Pp. 856 ..... 7.00

Mines Register, 1952 Rev. Ed. Successor to **The Mines Handbook (Descriptions of mines and mining companies).** Pp. 730 ..... 25.00

Introductory Prospecting and Mining. By Leo Mark Anthony. 1958. Pp. 88. Illus. 2.50

Handbook for Prospectors and Operators of Small Mines. 4th Ed. By Max W. von Bernewitz—Revised by Harry C. Chellson. 1943. Pp. 547. Illus. 161. 5 x 7½ 9.00

Mining Engineer's Handbook. By Robert Peele, *Editor*. 3rd Ed. 1941. 2 Vols. 18.75

Examination and Valuation of Mineral Property. By Roland D. Parks. 4th Ed. 1957. Pp. 507. Illus. 9.75

PALEONTOLOGY, STRATIGRAPHY, HISTORICAL GEOLOGY

The Evolution of North America. By Philip B. King. 1959. Pp. 200. Over 100 plates, plus large 20¼ x 21½ tectonic map bound in at back 7.50

The Geological Evolution of North America. By Thomas H. Clark and Colin W. Stearn. 1960. Pp. 434. Illus. tables 7.50

Historical Geology. By Carl O. Dunbar. 1949. Pp. 567. Illus. 380 ..... 7.25

Introduction to Historical Geology. By Raymond C. Moore. 2nd Ed. 1958. Pp. 582. Illus. Maps 7.95

Historical Geology. By Raymond C. Moore. 1933. Pp. 673. Figs. 413 ..... 10.00

Historical Geology—The Geologic History of North America. 2nd Ed. By Russell C. Hussey. 1947. Pp. 465. Illus. 344 ..... 6.90

Geology: An Introduction to Earth History. By H. H. Read. 1949. Pp. 248. Illus. 30. Maps ... 1.20

Principles of Earth History. By William Lee Stokes. 1960. Pp. 576. Illus. 8.75

The Principles of Historical Geology. By J. Willis Stovall and H. E. Brown. 1954. Pp. 472. Illus. 200 ..... 6.50

An Introduction to Historical Geology. 6th Ed. By W. J. Miller. 1951. Pp. 555. Illus. 6.75

Outline of Historical Geology. By A. K. Wells. 1959 ..... 4.48

(*Continued on Page xviii*)

(*Continued from Page xvii*)

BOOKS IN GEOLOGICAL SCIENCE

PALEONTOLOGY, STRATIGRAPHY, HISTORICAL GEOLOGY (Continued)

The Origin and History of the Earth. By ROBERT TUNSTALL WALKER and WOODVILLE JOSEPH WALKER. 1954. Pp. 244. Illus., Figs. . . . U.S., 5.00; Canada & Mexico, 5.25; Other Countries 5.50

The Planets: Their Origin and Development. By HAROLD C. UREY. 1952 5.00

The Origin of the Earth. 2nd Ed. By W. M. SMART. 1951. Pp. 240, 8 plates, 42 text-figs. 3.50

Geology and Man. By KENNETH K. LANDES and RUSSELL C. HUSSEY. 1948. Pp. 518. Figs. 188. 10.35

Introduction to College Geology. By CHAUNCEY D. HOLMES. 1949. Pp. 429; figs. 312; tables. 5.90

The Pleistocene Period: Its Climate, Chronology and Faunal Successions. By FREDERICK E. ZEUNER. 1959. Pp. 447 6.50

Glacial and Pleistocene Geology. By R. F. FLINT. 1957. Pp. 553. 12.50

Glacial Geology and the Pleistocene Epoch. By RICHARD F. FLINT. 1947. Pp. 589. Illus. 94. 9.00

The Last Million Years. By A. P. COLEMAN. 1941. Pp. xii + 216 3.75

Prehistory and Pleistocene Geology in Cyrenaican Libya. By C. B. M. MCBURNEY and R. W. HEY. 1955. Pp. 316. Figs. 40. Pls. 16. Tables 5 12.50

Outlines of Historical Geology. 4th Ed. By CARL O. DUNBAR and CHARLES SCHUCHERT. 1941. Pp. 291. Illus. 176 4.50

Atlas of Paleographic Maps of North America. By CHARLES SCHUCHERT. 1955. Pp. 177 4.75

Jurassic Geology of the World. By W. J. ARKELL. 1956. Pp. 806. Figs. 102. Pls. 16. Correlation Tables 28 16.00

The Grenville Problem. By J. E. THOMPSON. 1956. Pp. viii + 119. Figures and Tables. 3.95

Record of the Rocks. By HORACE G. RICHARDS. 1953. Pp. 413. Figs. 294 6.50

An Introduction to Stratigraphy. 2nd Edition, revised. By L. D. Stamp. 3rd Ed. 1957. Pp. 381 3.25

The Proterozoic in Canada. Edited by J. E. GILL. 1957. Pp. x + 191. 5 phot., maps, figures, and 1 folding chart 5.95

Principles of Stratigraphy. By C. O. DUNBAR and J. RODGERS. 1957. Pp. 356. 10.00

Stratigraphic Geology. By MAURICE GIGNOUX. 1955. Pp. 830. Fig. 155 9.50

Stratigraphic Principles and Practice. By MARVIN WELLER. 1960. Pp. 679. Figs. 273. Illus. 10.00

Invertebrate Paleontology. By WILLIAM H. EASTON. 1960. 10.00

Stratigraphical Paleontology—a Study of Ancient Life-Provinces. By E. NEAVERSON. 2nd Ed. 1955. Pp. 806. Figs. 90 16.80

Principles of Invertebrate Paleontology. By R. P. SHROCK and W. H. TWENHOFEL. 2nd Ed. 1953. Illus. 488. Pp. 816 13.00

Search for the Past: An Introduction to Paleontology. By JAMES R. BEERBOWER. 1960. Pp. 544. Illus. 7.50

The Fossil Book. By CARROLL LANE FENTON and MILDRED ADAMS FENTON. 1958. Pp. 348 15.00

Outlines of Paleontology. 3rd Ed. By H. H. SWINNERTON. 1947. Pp. 385. Figs. 368. 6.50

Index Fossils of North America. By HERVEY W. SHIMER and ROBERT P. SHROCK. 1944. Pp. 837. Illus. 8,000. Pls. 303 22.00

Invertebrate Fossils. By R. MOORE, C. LALICKER and A. FISCHER. 1952. Illus. 454. Pp. 738. 13.00

Palaeontology—Invertebrate. 8th Ed. Rev. and Enl. By HENRY WOODS. 1946. Pp. 477. Figs. 221 3.75

Echinodermata. Vol. IV of The Invertebrates. The coelomate bilateria. By LIBBIE HENRIETTA HYMAN. 1955. Pp. 763. Illus. 13.50

Evolution of the Vertebrates. By EDWIN H. COLBERT. 1955. Pp. 479. 125 Illus. 8.95

Paleontology and Modern Biology. By D. M. S. WATSON. 1951. Pp. 216. Figs. 77 4.00

Marine Ecology. By HILARY B. MOORE. 1958. Pp. 493 9.50

Natural History of Marine Animals. By MACGINITIE and MACGINITIE. 1949. 473 Pp., 282 Illus. 8.95

Introduction to Microfossils. By DANIEL J. JONES. 1956. Pp. 406. Illus. 7.00

Foraminifera: Their Classification and Economic Use. 4th Ed., Revised and Enlarged. By JOSEPH A. CUSHMAN. 1948. Pp. 605. Figs. 9. 31 Text Pls. 55 Key Pls. 12.50

The Invertebrates: Platyhelminthes and Rhynchocoela. The Acoelomate Bilateria, Vol. II. By LIBBIE HENRIETTA HYMAN. 1951. Pp. 550. 208 figs. 11.50

A Textbook of Evolution. By EDWARD O. DODSON. 1952. Pp. 419. Illus. 101 5.00

Evolution Emerging. By W. K. GREGORY. 1951.
Vol. I. Pp. 736. Vol. II. Pp. 1013. Boxed set of two volumes 25.00

The Meaning of Evolution, A Study of the History of Life and its Significance for Man. By G. G. SIMPSON. 1950. Pp. 364. Illus. 4.00

The Origin of Vertebrates. By N. J. BERRILL. 1955. Pp. 257. Illus. 4.00

The Principles of Classification and a Classification of Mammals. By G. G. SIMPSON. 1945. Vol. 85. Pp. 350. Illus. 3.50

Horses: the Story of the Horse Family in the Modern World Through Sixty Million Years of History. By G. G. SIMPSON. 1951. Pp. 247. Illus. 32. 6.50

Time's Arrow and Evolution. By HAROLD F. BLUM. 1959. Pp. 236. Paperback Ed. 1.75

History of the Primates. 2nd Ed. By W. E. LE GROS CLARK, F.R.S. 1950. Pp. 118. 40 text-figures 1.25

The Dinosaur Book: The Ruling Reptiles and Their Relatives. By E. H. COLBERT. 1951. Pp. 156. Illus. 5.95

On the Origin of Species. By CHARLES DARWIN. Reprinted 1951 of 1859 Edition. Pp. 426. 3.75

(*Continued on Page xix*)

(*Continued from Page xviii*)

BOOKS IN GEOLOGICAL SCIENCE

PALEONTOLOGY, STRATIGRAPHY, HISTORICAL GEOLOGY (Continued)

The Fossil Evidence for Human Evolution. By W. E. Le Gros Clark. 1955. Pp. 181 ..... 6.00

Time, Life and Man: The Fossil Record. By Dr. R. A. Stirton. 1959. Pp. 559 ..... 9.00

Finding Fossil Man. By Robin Place. 1957. Pp. 126. Figs. 46. Pl. 63 ..... 7.50

Man, the Tool-Maker. 2nd Ed. By K. P. Oakley. 1950. Pp. 98. 41 text-figures 1.00

Ancient Man in North America. 4th Ed. 1957. By H. M. Wormington. Pp. 322. 71 Illus. Cloth 5.20 Paper 3.65

Man in the Primitive World. 2nd Ed. By E. Adamson Hoebel. 1958. Pp. 678. Illus. Ed. ..... 9.00 Text Ed. 6.95

Strange Story of our Earth. By A. H. Verrill. 1952. Pp. 255. Illus. 72 ..... 3.75

The Story of Life. By H. E. L. Mellersh. 1958. American Edition 1. Pp. 263. Illus. 3.95

The Succession of Life through Geological Time. By K. P. Oakley and H. M. Muir-Wood. 2nd Ed. 1949. Pp. 92. Pls. 12 and 4 maps 2s 6d

Life Through the Ages. By Charles R. Knight. 1946. Pp. 66 ..... 3.00

Life Through the Ages. By R. W. Burnett. 1947. Pp. 48. Illus. 1.00

The Living Rocks. Translated by Joyce Emerson and Stanley A. Pacock. Photographs by S. Celebonovic with a commentary by Geoffrey Grigson and a preface by Andre Maurois. 1957. Pp. 94 ..... 6.00

The Search Beneath the Sea. By J. L. B. Smith. 1956. Pp. 260. Illus. 3.95

American Seashells. By R. Rucker Abbott. 1954. Pp. 560. Figs. 100. Pls. 40 ..... 13.75

Principles of Paleobotany. By William C. Darrah. 2nd Ed. 1960. Pp. 295. 75 Illus. Tables 6.50

Introduction to Paleobotany. By Chester A. Arnold. 1947. Pp. 433 ..... 9.00

An Introduction to the Study of Fossil Plants. By John Walton. 1940. Pp. 188. Illus. 4.75

Procedure in Taxonomy. By E. T. Schenk and J. H. McMasters. Revised Ed. 1956. Pp. 119. 4.00

Examination of Well Cuttings. By Julian W. Low. 48 Pp. 13 schematic illustrations. 1952 ..... 1.50

Subsurface Mapping. By Margaret S. Bishop. 1960. Pp. 198. Illus. 5.75

PETROLOGY, SEDIMENTATION

The Evolution of the Igneous Rocks. By N. L. Bowen. With a new introduction by J. F. Schairer. 1956. Pp. 332 ..... 1.85

Petrology for Students. 8th Ed. By Alfred Harker; revised by C. E. Tilley, S. R. Nockolds, and M. Black. 1954. Pp. 284. 99 text-figures 3.75

Guide to the Study of Rocks. A part of the Harpers Geoscience Series. By L. E. Spock. 1953. Pp. 256. Line cuts 34 ..... 4.50

A Descriptive Petrography of the Igneous Rocks. 1931–38. By A. Johannsen.

Vol. I—Introduction, Textures, Classifications, and Glossary. Rev. Ed. 1939. Pp. 318 ..... 7.50

Vol. II—The Quartz-Bearing Rocks. 1932. Pp. 438. Diagrams 9. Photographs 16. Photomicrographs 66. Portraits 32. Tables 209 ..... 8.00

Vol. III—The Intermediate Rocks. 1937. Pp. 360. Diagrams 4. Photographs 18. Photomicrographs 114. Portraits 47. Tables 108 ..... 7.00

Vol. IV—Part I. The Feldspathoid Rocks; and Part II. The Peridotites and Perknites. 1938. Pp. 551. Diagram 8. Photographs 9. Photomicrographs 95. Portraits 77. Tables 159 .. 10.00

Textbook of Petrology.

Vol. 1: The Petrology of the Igneous Rocks. 10th Ed. By F. H. Hatch, A. K. Wells, and M. K. Wells. 1950. Pp. 469 ..... 5.25

Vol. 2: The Petrology of the Sedimentary Rocks. 3rd Ed. revised by Maurice Black. 1938. By F. H. Hatch and R. H. Rastall. 1913. Reprinted 1950. Pp. 383. Illus. 75. Tables 15 6.75

Petrography. Part I—Igneous Rocks; Part II—Metamorphic Rocks; Part III—Sedimentary Rocks. By Howel Williams, Francis J. Turner and Charles M. Gilbert. 1954. Pp. 416. 133 Illus. 6.50

Microscopic Petrography. By E. William Heinrich. 1956. Pp. 296. Illus. 70 ..... 6.95

Gesteine und Minerallagerstatten, Allgemeine Lehre von den Gesteinen und Mineralliagerstaatten. By Paul Niggli. 1952. Pp. 554. Figs. 181

Vol. I 12.00

Vol. II 12.00

Einfuhrung in die gesteinkunde. By H. Leitmeier. 1950. Pp. 275 ..... 5.00

Igneous and Metamorphic Petrology. By F. J. Turner and J. Verhoogen. 2nd Ed. 1960. Pp. 694 12.00

Theoretical Petrology. By T. F. W. Barth. 1952. Pp. 387. Illus. 6 x 9½ 7.75

Introduction to Theoretical Igneous Petrology. By Ernest E. Wahlstrom. 1950. Pp. 365; numerous figs. and tables 7.95

Petrographic Modal Analysis. By Felix Chayes. 1956. Pp. 113. Figs. 14 ..... 5.50

A Historical Survey of Petrology. By F. J. Loewinson-Lessing translated by S. I. Tomkieff. 1954. Pp. 112 ..... 2.25

Petrographic Mineralogy. By Ernest E. Wahlstrom. 1955. Pp. 408 ..... 7.75

The Study of Rocks in Thin Section. By W. W. Moorhouse. 1959. Pp. 514. Illus. 8.00

Rocks and Rock Minerals. 3rd Ed. By Louis V. Pirsson and Adolph Knopf. 1947. Pp. 349. Pls. 36. Figs. 72 ..... 6.00

(*Continued on Page xx*)

(*Continued from Page xix*)

BOOKS IN GEOLOGICAL SCIENCE

PETROLOGY, SEDIMENTATION (Continued)

Rocks and Minerals. By RICHARD M. PEARL. 1956. Pp. 275. Pls. 12. Figs. 35 ..... 1.95

Rocks and Mineral Deposits. By PAUL NIGGLI (English Translation by ROBERT L. PARKER). 1954. Pp. 572. Figs. 351, tbls. 73 ..... 12.00

Les Pegmatites—Les Pegmatites Granitiques. By A. E. FERSMAN. 1951. Pp. 675.

Vol. I—Partie Preliminaire. Chaps. 1–10 (French translation with Illus. from the Russian Ed. 1931)

Vol. II—Partie Descriptive. Chaps. 11–18

Vol. III—Partie Generale. Chaps. 19–25 ..... 18.00

The Physics of Flow Through Porous Media. By A. E. SCHEIDEGGER. 1957. Pp. xii + 236. 26 drawings 14.00

The Study of Rocks. 4th Ed. By S. J. SHAND. 1951. Pp. 236 ..... 2.25

Igneous Minerals and Rocks. By ERNEST E. WAHLSTROM. 1947. Pp. 367. Illus. 7.00

Structural Petrology of Deformed Rocks. 2nd Ed. 2nd Ptg. By HAROLD W. FAIRBAIRN and FELIX CHAYS. 1949. Pp. 344; numerous figs. and tables 12.50

Petrography and Petrology. By FRANK F. GROUT. 1932. Pp. 522 ..... 9.00

Microscopic Sedimentary Petrography. By ALBERT V. CAROZZI. 1960. Pp. 464 ..... 11.50

Photomicrography. By CHARLES P. SHILLABER. 1944. Pp. 773. Illus. 291 ..... 16.50

Applied Sedimentation. A Symposium edited by PARKER D. TRASK. 1950. Pp. 707. Illus. 134 ... 8.00

Principles of Sedimentation. 2nd Ed. By W. H. TWENHOFEL. 1950. Pp. 673. Figs. 81 ..... 10.00

Methods of Study of Sediments. By W. H. TWENHOFEL and S. A. TYLER. 1941. Pp. 183. Illus. 5.00

Sedimentary Rocks. 2nd Ed. By F. J. PETTIJOHN. 1957. Pp. 718. Line drawings 173. Pls. 40. Photomicrographs 100 ..... 12.00
Textbook edition available for classroom use 9.00

Methodes d'Etude des Roches Sedimentaires. By N. M. STRAKHOV, editor. 1958. Vol. 1—Pp. 543. Vol. 2—Pp. 535 ..... 46.40

Stratigraphy and Sedimentation. By W. C. KRUMBEIN and L. O. SLOSS. 1951. Pp. 507. Illus. 123. Line Drawing 6.50

Grundzuge der Lithologie. By L. B. RUCHIN. 1958. Pp. 806. Figs. 304 ..... 13.36

The Composition and Origin of the Antrim Laterites and Bauxites. By V. A. EYLES. 1952. Pp. 90, pls. 2, tbls. 10 ..... 12s6d

Problems of Clay and Laterite Genesis. By AIME. 1952. Pp. 252. AIME Members 4.20
Nonmembers 6.00

Abrasion Hardness. By THOMAS A. JAGGAR. 1950. Pp. 43. Pl. 6. Figs. 5. Tables 7 ..... 3.00

An Introduction to the Study of Organic Limestones. By J. HARLAN JOHNSON. Rev. Ed. 1951. Pp. 185. Illus. 104 ..... 2.00

Recent Sediments of the Gulf of Paria, Reports of the Orinoco Shelf Expedition. Vol. I. By TJ. VAN ANDEL and H. POSTMA. 1954. Pp. 245. Figs. 78. Append. 11. Pls. 7. Maps 4 ..... 6.00

Sequence in Layered Rocks. By ROBERT R. SHROCK. 1948. Pp. 507 ..... 9.50

Manual of Sedimentary Petrography. By KRUMBEIN and PETTIJOHN. 1938. Pp. 549. Figs. 262 .. 6.50

The Examination of Fragmental Rocks. By F. G. TICKELL. New Ed. 1947. Pp. 154. Line Drawings 5.00

Micromeritics, The Technology of Fine Particles. 2nd Ed. By JOSEPH M. DALLA VALLE. 1948. Pp. 555. Figs. 131 ..... 10.00

The Rock Book. By C. L. FENTON and M. A. FENTON. 1940. Pp. 376. 48 pp. Photo. 40 figs. ... 7.50

The Rock-Hunter's Field Manual: A Guide to Identification of Rocks and Minerals. By D. K. FRITZEN. 1959. Pp. 200 ..... 3.50
Textbook Edition 2.75

Soil. By G. V. JACKS. 1955. Pp. 221. Pls. 10. Figs. 5 ..... 5.00

Factors of Soil Formation. By HANS JENNY. 1941. Pp. 281. 6 x 9 Illus. 6.50

A Bibliography on Meteorites. By HARRISON BROWN, Editor. 1953. Pp. 686 ..... 12.50

HISTORICAL AND BIOGRAPHICAL

Sir James Jeans. A Biography. By E. A. MILNE. 1952. Pp. 176 ..... 4.00

The Life and Times of Alexander von Humboldt, 1769–1859. By HELMUT DE TERRA. 1955 ..... 5.75

The Birth and Development of the Geological Sciences. By F. D. ADAMS. 1955. Pp. 511. Illus. 91 2.00

Blazing Alaska's Trails. By ALFRED H. BROOKS. 1953. Pp. 528. Illus. 50 ..... 4.50

Life and Letters of R. A. F. Penrose, Jr. By HELEN R. FAIRBANKS and CHARLES P. BERKEY. 1952. Pp. 765 ..... 4.00

Giants of Geology. By CARROLL and MILDRED FENTON. 1952. Pp. 333. Illus. 4.00

(*Continued on Page xxi*)

(*Continued from Page xx*)

BOOKS IN GEOLOGICAL SCIENCE

HISTORICAL AND BIOGRAPHICAL (Continued)

The Growth of Physical Science. 2nd Ed. By SIR JAMES JEANS. 1951. Pp. 364. Pls. 12 ..... 3.75

Giordano Bruno—His Life and Thought. With Annotated Translation of his Work on the Infinite Universe and Worlds. By DOROTHEA WALEY SINGER. 1950. Pp. 404. Illus. 6.00

Benjamin Silliman, Pathfinder in American Science. By JOHN F. FULTON and ELIZABETH H. THOMSON. 1947. Pp. 312 ..... 4.00

Journal of Researches into the Geology and Natural History of the Various Countries Visited by H.M.S. Beagle. 1952. Pp. 615; pls. 16 (reprint of first edition, 1839) 7.50

Powell of the Colorado. By W. C. DARRAH. 1951. Pp. 426 ..... 6.00

The Lost Villages of England. By MAURICE BERESFORD. 1954. Pp. 445. Figs. 13. Pls. 16. Tables 18 ..... 12.00

The Bonanza Trail, Ghost Towns and Mining Camps of the West. By MURIEL SIBELL WOLLE. 1953. Pp. 476, figs. 108, maps 14 ..... 8.50

PHOTOGRAMMETRY, TOPOGRAPHY

Elements of Cartography. By ARTHUR H. ROBINSON. 1953. Pp. 254. Figs. 186. Tables 38 ..... 7.50

Plane Table Mapping. By J. W. LOW. 1952. Pp. 365. Illus. 148 ..... 6.00
Textbook edition available for classroom use 4.50

Handbook of Aerial Mapping and Photogrammetry. By L. G. TROREY. 1952. 2nd ed. rev. Pp. 180. Illus. 6.50

Manual of Photogrammetry. 2nd Ed. 1952. Pp. 876. Illus. ..... Members 7.50
Non-members 12.50

Aerial Photographs and Their Application. By HAROLD T. U. SMITH. 1943. Pp. 372. Figs. 61 ..... 5.00

Military Maps and Air Photographs. By ARMIN K. LOBECK and W. J. TELLINGTON. 1944. Pp. 256. Illus. 8½ x 11 ..... 9.00

TECHNICAL DICTIONARY, TERMINOLOGY, THESAURUS

Geological Nomenclature. Edited by A. A. G. SCHIEFERDECKER. 1959. Pp. 523 ..... 12.50

Concise Dictionary of Science. By FRANK GAYNOR. 1959. Pp. 546 ..... 10.00

Composition of Scientific Words. By WILBUR BROWN. 1954. Pp. 882 ..... 8.00

Multilingual Mining—Metallurgical—Geological—Mineralogical—Petrographical and Petroleum Dictionary. English-Spanish, French, German, and Russian. By ALEJANDRO NOVITZKY. 1951. Pp. 369. Sold with Alphabetical Index only 12.00

Alphabetical Index for Mining Dictionary. Spanish, French, German, and Russian. 1958 ..... 12.00

German-English and English-German Dictionary for Scientists. By O. W. LEIBIGER and I. S. LEIBIGER. 1950. Pp. 752 ..... 12.00

German-English Technical and Engineering Dictionary. By LOUIS DEVRIES. 2nd Ed. 1950. Pp. 940 ..... 25.00

German-English Technical Dictionary. 2 Volumes. By KURT F. LEIDECKER (ed.), Compiled by U. S. Air Force. 100,000 terms 35.00

English-French and French-English Technical Dictionary. By FRANCIS CUSSET. Rev. Ed. 1957. Pp. 663 ..... 8.00

Geology and Allied Sciences. A thesaurus and coordination of English and German terms. Pt. I. German-English. WALTER HUEBNER, Ed. Pp. 424. 1939. Cloth, 5½ x 8½ 7.50

Dictionary of Scientific Terms. 6th Ed. By I. F. HENDERSON. 1957. Pp. 532 ..... 12.50

Chambers Mineralogical Dictionary. 1948. Pp. 87. Col. Pls. 40 ..... 4.75

The Russian-English Technical and Chemical Dictionary. By LUDMILLA I. CALLAHAM. 1947. Pp. 794 ..... 16.50

Scientific German. By G. E. CONDOYANNIS. 1957. Pp. 164 ..... 2.50

Scientific French. By WILLIAM J. LOCKE. Pp. 112. 1957 ..... 2.25

Scientific Russian. By J. W. PERRY. 1951. Pp. 845 ..... 8.50

Scientific Russian. By GEORGE E. CONDOYANNIS. 1959. Pp. 256 ..... 3.50

Elementary Scientific Russian Reader. By G. A. ZNAMENSKY. 1944. Pp. 107 ..... 1.75

The International Dictionary of Physics and Electronics. By WALTER C. MICHELS. 1956. Pp. 1004 ..... 20.00

Van Nostrand's Scientific Encyclopedia. By VAN NOSTRAND. 3rd Edition. 1958. Pp. 1,839 ..... 29.75

Webster's Geographical Dictionary. 1949. Pp. 1352. 177 maps, 24 color plates 8.50

Pocket Dictionary of Meteorology. By DR. KARL KEIL. 1950. Pp. 604 with numerous Illus. 7.00

(*Continued on Page xxii*)

(*Continued from Page xxi*)

BOOKS IN GEOLOGICAL SCIENCE

MISCELLANEOUS

Beyond the Hundredth Meridian—John Wesley Powell and the Second Opening of the West. By WALLACE STEGNER. 1954. Pp. 438. Figs. 12. Maps 7 ..... 6.00

Man's Nature and Nature's Man. By LEE R. DICE. 1955. Pp. 329 ..... 5.00

Explorations East of the High Andes (from Patagonia to the Amazon). By VICTOR OPPENHEIM. 1958. Pp. 267 ..... 5.00

Men to Match My Mountains: The Opening of the Far West 1840-1900. By IRVING STONE. 1956. Pp. 495. Index 5.95

Quest for a Continent. By WALTER SULLIVAN. 1957. Pp. 372 ..... 5.95

Man's Role in Changing the Face of the Earth. Ed. by WM. L. THOMAS. 1956. Pp. 1230. Illus. .. 12.50

Man's Emerging Mind. By N. J. BERRILL. 1955. Pp. 308 ..... 4.00

Conversation with the Earth. By HANS CLOOS. 1953. Pp. 413. Pls. 53. Tables 26 ..... 5.75

Man, Time and Fossils. By RUTH MOORE. 1953. Pp. 411, figs. 71, pls. 62 ..... 6.50

The Prehistoric Cultures of the Horn of Africa. By J. DESMOND CLARK. 1954. Pp. 386. Figs. 36. Pls. 52 ..... 22.50

Man and His Physical Universe. By RICHARD WISTAR. 1953. Pp. 488. Illus. 300 ..... 5.00

The Philosophy of Science (the link between science—philosophy). By PHILIPP FRANK. 1957. Pp. 394 ..... 8.65

Psychical Physics. By S. W. TROMP. 1949. Pp. 534. Illus. 153 ..... 12.00

Guide to Geologic Literature. By RICHARD M. PEARL. 1951. Pp. 239 ..... 5.75

Fundamentals of Earth Science. By HENRY D. THOMPSON. 1947. Pp. 420 ..... 4.50

The Earth We Live On. By RUTH MOORE. 1956. Pp. 416 ..... 6.00

How to Collect Mountains. By CHARLES B. HUNT. 1958. Illus. by author 1.25

Down to Earth, a Practical Guide to Archaeology. By ROBIN PLACE. Pp. 173. Figs. 88 ..... 7.50

The Earth Beneath Us. By H. H. SWINNERTON. 1956. Pp. 335 ..... 5.00

Geology and Ourselves. By F. H. EDMUNDS. 1956. Pp. 256. Pls. 12. Line drawings 15 ..... 10.00

Readings in Anthropology. E. ADAMSON HOEBEL, JESSE D. JENNINGS, and ELMER R. SMITH. 1955. Pp. 417 ..... 5.25

Symphony of the Earth. By J. H. F. UMBGROVE. 1951. Pp. 220. Pls. 10. Figs. 123 ..... 5.00

Readings in the Physical Sciences. By HARLOW SHAPLEY (ed.). 1948. Pp. 501 ..... 3.00

The Sea Around Us. By R. L. CARSON. 1951. Pp. 230. Figs. 4. Chart 1 ..... 3.50

This Great and Wide Sea. Rev. Ed. By R. E. COKER. 1949. Pp. 344. Pl. 91. Figs. 23 ..... 6.00

Volcanoes Declare War. By THOMAS A. JAGGAR. 1945. Pp. 166. Pl. 32. Figs. 34 ..... 4.85

Volcanoes New and Old. By MRS. SATIS N. COLEMAN. 1946. Pp. 234 ..... 4.00

Rocks and Rivers of North America. By ELLIS W. SHULER. 1945. Pp. 300 ..... 5.00

Engineering in History. By RICHARD S. KRIBY, SIDNEY WITHINGTON, ARTHUR B. DARLING, FREDERICK G. KILGOUR. 1956. Pp. 530 ..... 8.50

The Caves Beyond: The Story of the Floyd Collins' Crystal Expedition. By JOE LAWRENCE, JR., and ROGER W. BRUCKER. 1955. Pp. 283. Illus. 4.75

This Earth of Ours—Past and Present. By CALEB W. WOLFE. 1950. Pp. 384. Illus. 5.00

The Face of the Moon. By R. B. BALDWIN. 1949. Pp. 239. Illus. 5.00

Relativity for the Layman. 2nd Ed. By JAMES A. COLEMAN. 1958. Pp. 131. Figs. 24. Illus. ..... Cloth-bound 2.75

Measuring Our Universe. By O. J. LEE. 1950. Pp. 170. Illus. 45 ..... 4.00

Writing Useful Reports. Principles and Applications. By ROBERT E. TUTTLE and C. A. BROWN. 1956. Pp. 635 ..... 4.50

Writing the Technical Report. 3rd Ed. By J. R. NELSON. 1952. Pp. 388 ..... 5.50

French Bibliographic Digest: Science, Geology (2). Bibliographical Digest of French geological books and articles published from 1948 to 1954. Pp. 102 (The Cultural Division of the French Embassy, 972 Fifth Avenue, New York 21, N. Y. free of charge) ..... free

---

Address ECONOMIC GEOLOGY, Urbana, Ill. Books not in this list (except the publications of official Surveys and those of the Geological Society of America) will be furnished at Publisher's prices. Also consult more extended lists in volume 50.

Economic Geology Publishing Company will also attempt to secure past volumes of domestic and foreign geological journals and similar publications when contained in our file listings of secondhand book dealers. Special correspondence in search of material however can not be undertaken.